2019

Innovative studies on reinforced concrete panel structures through experimental testing and finite element modeling; and teaching structural engineering courses using augmented reality

Elizabeth Miller
Iowa State University

Innovative studies on reinforced concrete panel structures through experimental testing and finite element modeling; and teaching structural engineering courses using augmented reality

by

Elizabeth Miller

A thesis submitted to the graduate faculty

in partial fulfillment of the requirements for the degree of

MASTER OF SCIENCE

Major: Civil Engineering (Structural Engineering)

Program of Study Committee:
An Chen, Major Professor
In-Ho Cho
Jennifer Shane

The student author, whose presentation of the scholarship herein was approved by the program of study committee, is solely responsible for the content of this thesis. The Graduate College will ensure this thesis is globally accessible and will not permit alterations after a degree is conferred.

Iowa State University

Ames, Iowa

2019

TABLE OF CONTENTS

Page

LIST OF FIGURES

Page

LIST OF TABLES

Page

ACKNOWLEDGMENTS

I would like to thank my committee chair, Dr. An Chen, and my committee members, Dr. In-Ho Cho and Dr. Jennifer Shane, for their willingness to serve on my POSC. Additionally, I would like to thank the civil engineering department faculty at Iowa State University for enriching my knowledge of structural engineering throughout my time here.

Research on iStructAR would not have been possible without the support of the Miller Grant, as well as the National Science Foundation. Research on the deck over backwall detail would not have been possible without the support of Iowa Department of Transportation. Any opinions, findings, and conclusions or recommendations expressed in this material are those of the authors and do not necessarily reflect the views of the National Science Foundation, Iowa Department of Transportation, or the Miller Grant.

Additionally, I would like to thank Doug Wood and Owen Steffens for their never-ending help and willingness to answer questions, regardless of scope. Their expertise and assistance cannot be overstated.

I would like to thank my friends and colleagues at Iowa State University, who made this two-year journey much more enjoyable. Thank you to Andrew Mock, Austin DeJong, Doug Krapf, and Rizwan Karim. Additionally, thank you to my fellow research group members Jin Yan, Kara Korthals, Hanming Zhang, Zhe Wang, Mohammed Bazroun, and Zac Dietrich. You all have bright futures ahead of you. Special thanks to Zhe for assisting me in the development of the FE models.

I would like to thank my friends for cheering me on from afar. A very special thank you to Brad for the never-ending support, copious amounts of coffee, and limitless memories in Iowa.

Lastly, and most importantly, I would like to thank my parents. Thank you for teaching me to always hold myself, and others, to a high standard.

ABSTRACT

This thesis presents the results of four studies conducted within the field of structural engineering during completion of a master's thesis. The first two studies report on the results of experimental testing and finite element modeling in reinforced concrete structures. Both structures can be thought to be composed of concrete panels. The third and fourth study, while not related to experimental work, details results of an in-classroom experiment utilizing an application developed to transform typical teaching pedagogy utilizing augmented reality.

The first study focuses on a particular detail utilized within the connection of an approach slab to bridge deck. Known as the deck over backwall detail, the concept gets rid of the typical expansion joint at the interface, extending the bridge deck to the approach slab, allowing them to act as one continuous piece. Within the study, two different reinforcing options are analyzed through both laboratory testing and validation with finite element modeling. Findings indicate that detailing of reinforcing through the joint has a large impact on the cracking that could occur on top of the bridge deck.

The second study focused on the performance of concrete walls with openings, subjected to different loading conditions. The walls, envisioned as being a part of a tuned liquid wall damper system, are testing for their axial, weak-axis bending, strong-axis bending, and shear strengths. Results of testing are compared to walls of the same geometry without openings, as well as developed finite element models. Results indicate that as expected, walls with openings do contain a strength reduction. However, strength reductions are not too large to prevent use of walls with openings in tuned liquid wall damping systems, and present a viable option for increasing the damping of a system.

The last two studies focused on the development and implementation of an augmented reality application aimed at transforming the existing teaching pedagogy within a structural analysis classroom setting. Results from initial usability testing are presented, including educational design and user interface decisions. Additionally, both quantitative and qualitative results from utilizing the application within two structural analysis classes over a semester are presented. Results indicate that while the application may not have a statistically significant effect on student's learning, student engagement and understanding of broader concepts increases, showing the potential to increase student learning in the future.

CHAPTER 1. GENERAL INTRODUCTION

Four studies are presented within this thesis. The first two studies are linked by their nature; both involve experimental testing and development of finite element models surrounding structures that include reinforced concrete panels. In particular, the first study notates the experimental results of a deck over backwall detail, utilized in highway bridges to mitigate problems caused by traditional placement of an expansion joints. Finite element models were also developed to correlate with results, in order to draw additional conclusions. The second study was similar in nature to the first, however, focused on testing and modeling of reinforced concrete walls with holes. The third and fourth study included a similar dependency on technology as the first and second, however, were very different in nature. Both studies focus on the development and use of an augmented reality application to teach structural analysis.

1.1 Objectives

Objectives were specific to each study completed, and are as follows:

- Study 1:
    1. Study the performance of the deck over backwall detail through experimental testing and finite element modeling.
    2. Observe the difference in performance of the detail within two different longitudinal options. Conclude if one option minimizes cracking and maximizes strength.
- Study 2:
    1. Study the performance of walls with holes in three different loading scenarios through experimental testing and finite element modeling.

2. Observe the failure mode of the walls with holes, and compare to solid reinforced concrete walls.
3. Compare the failure load of walls with holes to solid reinforcing concrete walls.

- Study 3:
  1. Refine AR application through usability testing, using iterative process.
  2. Implement improvements to application. Develop remainder of application utilizing improved user interface.
- Study 4:
  1. Construct lesson plans incorporating AR application into the structural analysis classroom setting; construct testing devices and surveys.
  2. Utilize application in classroom following the lesson plans developed.
  3. Study the difference between control class and experimental class in terms of test scores, cognitive engagement, and survey results.

1.2 Thesis Organization

This thesis is organized as follows: Chapter 2 reports the results of the first study, focusing on a deck extension detail, as part of a larger Iowa DOT project. Chapter 3 reports the results of the second study, focusing on strength reduction in walls with holes. Chapter 4 reports the process and resulting improvements associated with usability testing in an augmented reality application. Chapter 5 studies the implementation of the application into a structural analysis classroom, documenting data sources, analyses, and results. Because of the distinctness of each study, each chapter provides a separate abstract, introduction, and

conclusion and future work section. However, Chapter 6 provides a general overview of the conclusions and future work drawn from each study.

CHAPTER 2. INNOVATIVE STUDIES ON REPAIR OF BRIDGE DECK EXPANSION JOINT USING SLAB-OVER-BACKWALL CONCEPT

A paper to be submitted to Journal of Bridge Engineering, ASCE

Elizabeth Miller, David Morandeira[1], Dr. An Chen, Dr. Charles Jahren

Abstract

Iowa DOT funded a three phase research project focusing on Rapid Bridge Deck Joint Repair Investigation. Phase I focused on the documentation of current means and methods of bridge expansion joint maintenance and replacement. Within Phase II, a workshop with DOT personnel, engineers, and researchers identified possible improvements to traditional expansion joint options. From the workshop, a deck over backwall detail was developed that moved the expansion joint away from the bridge deck, instead placing it on the approach slab. This would not only minimize the concrete removal needed for a rehabilitation, but in turn mitigate deicing chemicals from leaking onto the bridge substructure.

This particular research focused in depth on the detailing of the deck over backwall concept. Through experimental testing and the development of finite element models, two reinforcing options within the approach slab and diaphragm sections were considered. Results showed that when the both the top and bottom longitudinal reinforcing was kept continuous through the approach slab and diaphragm section, negative moment was transferred to the bridge deck. This transfer of stress through the top reinforcing caused cracking to occur on the top of the bridge deck that could lead to leaking of harmful chemicals to the substructure. Conversely, experimental testing showed that these stresses

[1] Completed literature review, and worked with Iowa DOT to come up with preliminary deck over backwall detail. Additionally, performed parametric study of detail using finite element analysis, performed cost analysis of joint options, and completed construction observation and post-construction testing plan. Completed preliminary plans for laboratory testing.

could be eliminated if the top longitudinal reinforcing and concrete cover was saw cut. Results from the study indicate that designs should cut the top longitudinal reinforcing, as cracking on the bottom of the approach slab and bridge deck is preferable to cracking on the top. If the decision is made to saw cut the top reinforcing, special care should be taken in choosing an appropriate filler material able to withstand deformation both translationally and rotationally.

This study could not have been possible without financial support from Iowa DOT.

2.1 Background

Iowa DOT funded a three phase research project focusing on Rapid Bridge Deck Joint Repair Investigation. Phase I of the project focused on documenting the current means and methods of bridge expansion joint maintenance and replacement. Then, through a workshop with Iowa DOT personnel, engineers, and researchers, possible improvements to traditional expansion joint options were identified. Phase II of the project completed a literature review of a wide range of related topics, including types of joints used in other states, common reported failure modes of joints in other states, integral abutment use throughout the country, and any other methods of eliminating deck joints from existing bridges. Additionally, a survey was completed by DOT personnel to identify the average life span of different types of expansion joints. From the workshops and survey, two key needs rose to the surface. First, the amount of concrete removal for the replacement of the expansion joint should be minimized. Minimizing the concrete removal in turn minimizes the overall construction time needed for the project. Secondly, the joint should be moved away from the bridge deck at the abutment interface, and instead placed on the approach slab. Moving the joint away from the abutment interface would mitigate deicing chemicals from leaking onto the substructure, limiting deterioration over time. From both of these key needs,

a concept referred to as the “deck over backwall” concept arose. Phase III of the project focused on developing this deck over backwall concept.

This particular research focused more in detail on this deck over backwall concept, including the completion of an experimental study, using two distinct reinforcing options. Results from the study were analyzed, and then correlated with finite element models.

2.1.1 Joint Detailing

In Phases I, II and III, researchers worked with engineers from Iowa DOT to develop an appropriate detail for the deck over backwall concept that would perform well under DOT standards. Researchers presented various detailing options including a cast-in-place approach slab, precast slab, sleeper slab, and micropiles. Using the various options presented, the following detail was developed by Iowa DOT engineers considering construction practices and preferences.

A section view of the preliminary detail developed is shown in Figure 2-1. As seen, the initial detailing of the approach slab contains both top and bottom longitudinal reinforcing, continuous through the diaphragm and into the bridge deck. Additionally, reinforcing hoops are provided within the concrete diaphragm. The approach slab is not connected to the backwall, and can freely slide over the element.

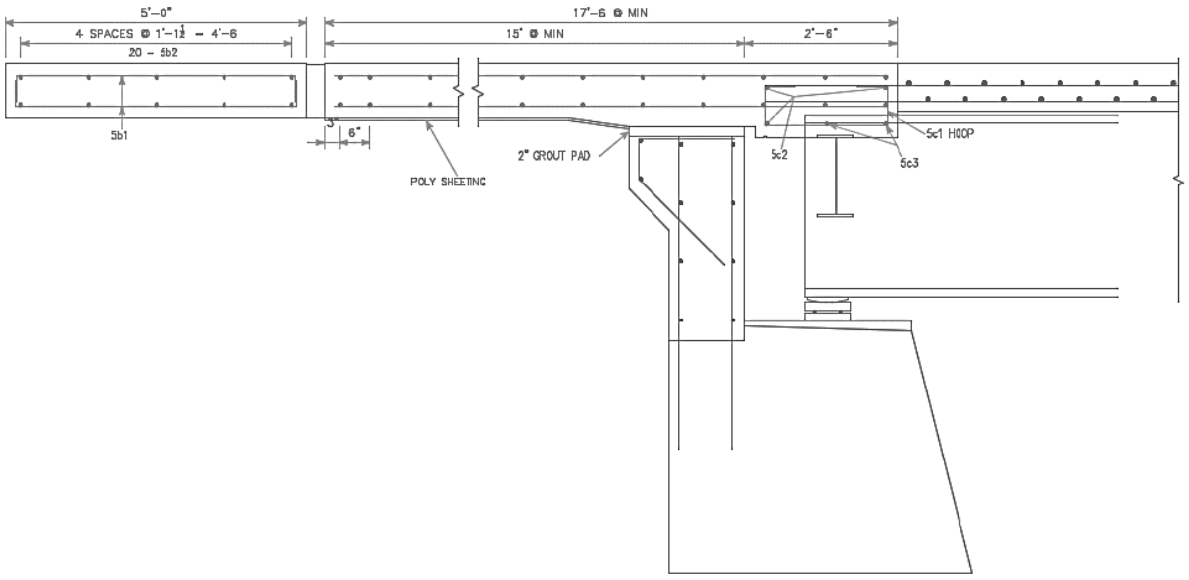

Figure 2-1. *Preliminary approach slab detail developed by IowaDOT. Source: Iowa DOT.*

While both the top and bottom reinforcing are shown as continuous in Figure 2-1, the DOT provided the option of saw cutting either one, or both, of these longitudinal reinforcing elements. This is shown below in Figure 2-2. In this figure, both the top and the bottom reinforcing are shown as being cut. The detail identifies that after saw cutting, the joint should be sealed. The type of joint would aid the performance of the deck, should the approach slab deflect a considerable amount. With considerable deflection, the rotation of the approach slab would cause negative moment to be transferred into the existing bridge deck. The saw cut and seal joint would prevent these moments and additional stresses from fully transferring to the existing bridge deck. This would mitigate any extra cracking that may occur, while also preventing rotation of the deck that might affect driver comfort.

Figure 2-1 also shows that a joint is to be provided a minimum of 17'-6" from the existing bridge deck in the approach slab. Possible options for this joint could include a

sleeper slab, a subdrain, or Iowa DOT's EF, CF, or CD joints. A combination of these could also be implemented.

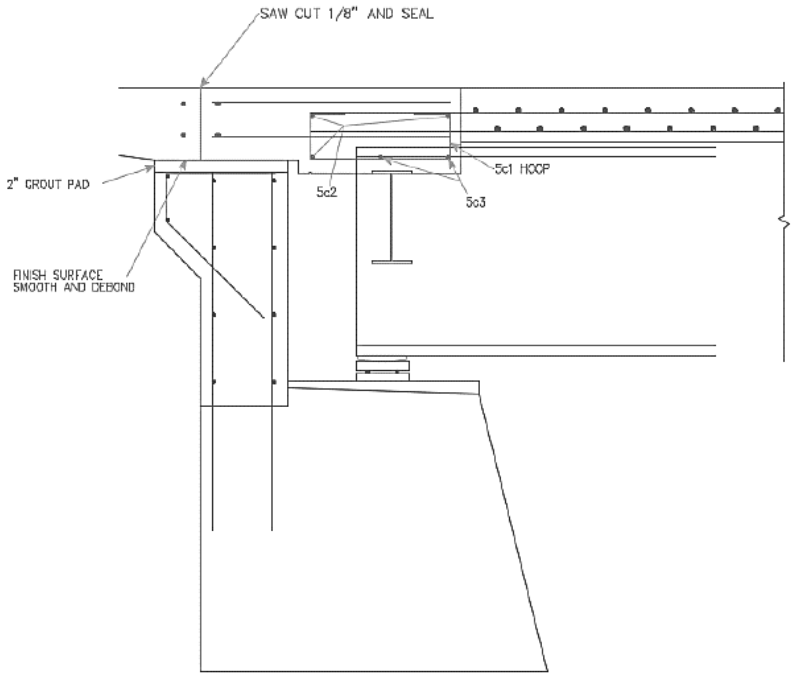

Figure 2-2. *Preliminary approach slab detail with option of saw cut and seal. Source: Iowa DOT.*

Figure 2-3 details the concrete removal process that should occur to attain the detail outlined in the previous figures. Several important aspects critical to the performance of the joint are detailed. First, the figure identifies that both the top and bottom longitudinal bars from the bridge deck should be protected during the removal process. Keeping these bars ensures that they can be fully incorporated into the new approach slab section. Secondly, the detail identifies that the minimum removal limit of the bridge deck can be no less than 2'-6". Finally, the removal limits for the approach slab should be approximately twenty feet, corresponding to the length of an Iowa DOT approach slab section. Depths of the previously

existing bridge deck, concrete above the steel diaphragm girders, and new approach slab sections vary.

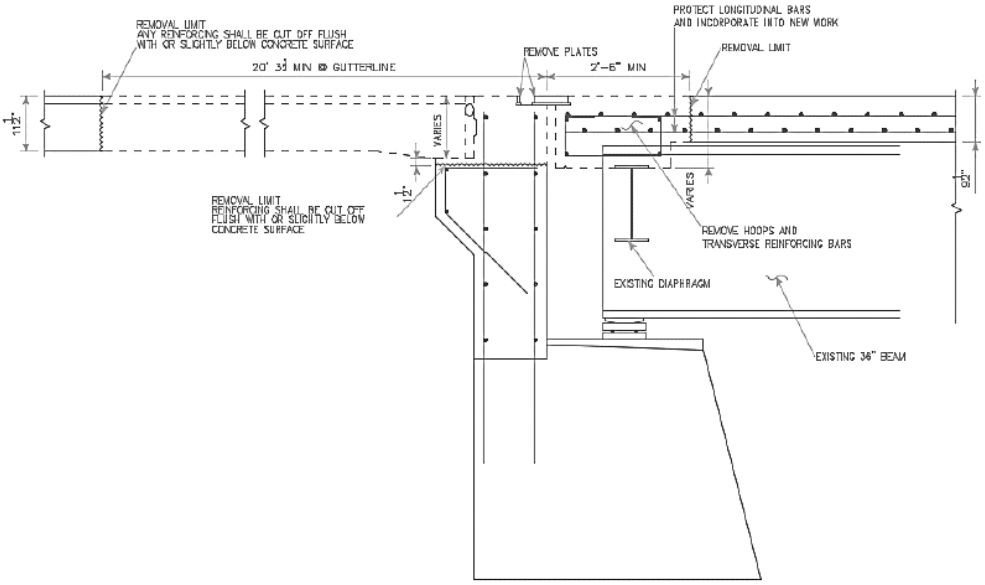

Figure 2-3. *Concrete removal process for Iowa DOT joint. Source: Iowa DOT.*

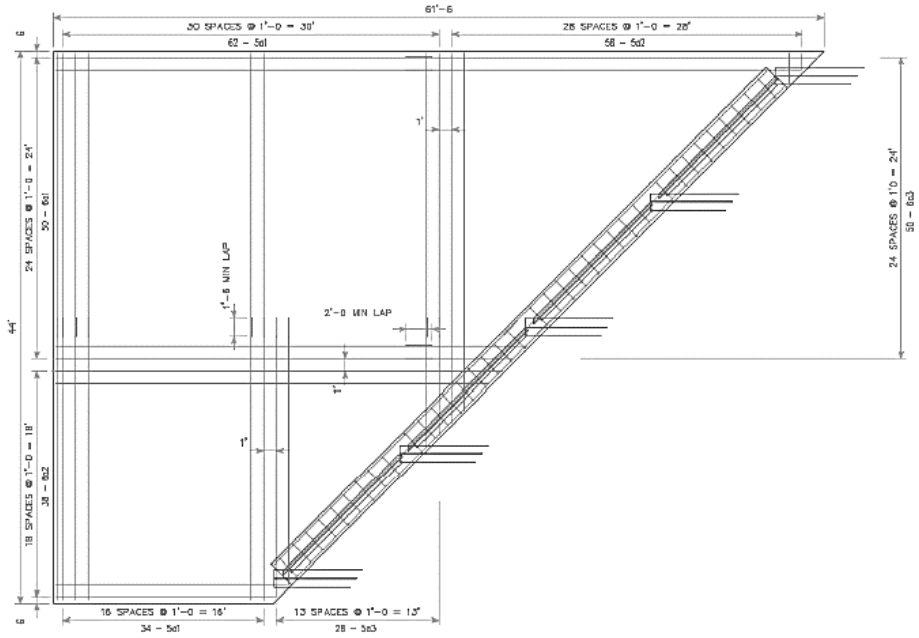

Figure 2-4. *Section view of Iowa DOT joint. Source: Iowa DOT.*

Figure 2-4 above shows an example plan view of the joint developed by the Iowa DOT. It can be see that the example plan view is provided for a skewed bridge. The reinforcing in both the longitudinal and transverse directions for the approach slab are shown. Spacing for these bars is one foot in all directions. Additionally, splice lengths for these bars are also provided.

2.2 Objectives

The objectives of this research are to:

1. Assess the overall performance of the deck over backwall concept through laboratory testing.
2. Compare two different reinforcing options within the approach slab through laboratory testing.
3. Compare the results of laboratory testing to finite element models, and use developed models to draw additional conclusions related to the performance of the detail.

By achieving these three specific goals, the deck over backwall concept can be further defined, allowing the Iowa Department of Transportation (DOT) to confidently design future bridges using the detail.

2.3 Literature Review

2.3.1 Literature Review Objectives

A literature review was conducted to review and synthesize information from previous research completed related to the deck over backwall concept. It should be noted that more intensive literature reviews were completed in Phase I and II of the project related to expansion joint replacement and repairs, completed by Miller and Jahren (2015, 2016). Therefore, this review summarized jointless bridge types, the behavior of bridges using the

deck over backwall design, use of approach slabs in bridges with the deck over backwall, and comparison of deck over backwall reinforcing detailing.

2.3.2 Jointless Bridge Types

Jointless bridges have grown in popularity in more recent years. Joints on bridges not only lead to corroding of substructure elements, but can also cause bumps in transitional pavement. Therefore, jointless bridges not only reduce spending on maintenance, but enhance the quality of the ride of the traveling public (Hoppe et al., 2016). There are three main types of jointless bridges currently used in the United States: the integral abutment, the semi-integral abutment, and the deck over backwall.

2.3.2.1 Integral Abutment

A full integral abutment bridge has both the steel girders and the deck slab fully integrated into the abutment. The superstructure and substructure move as one to allow required rotation and translation. A full integral abutment bridge allows displacements of the bridge deck due to thermal expansion and contraction to be transferred into pile caps and foundation piles (Hoppe et al., 2016). There are no expansion joints, and no bearings. An example of a full integral abutment bridge detail can be seen in Figure 2-5. This particular detail is one utilized by New York State DOT. As shown, the steel beam is fully encased into the abutment. Additionally, the reinforcing in the superstructure slab is tied to the abutment, forcing the two components to act as one. The abutment sits on piles.

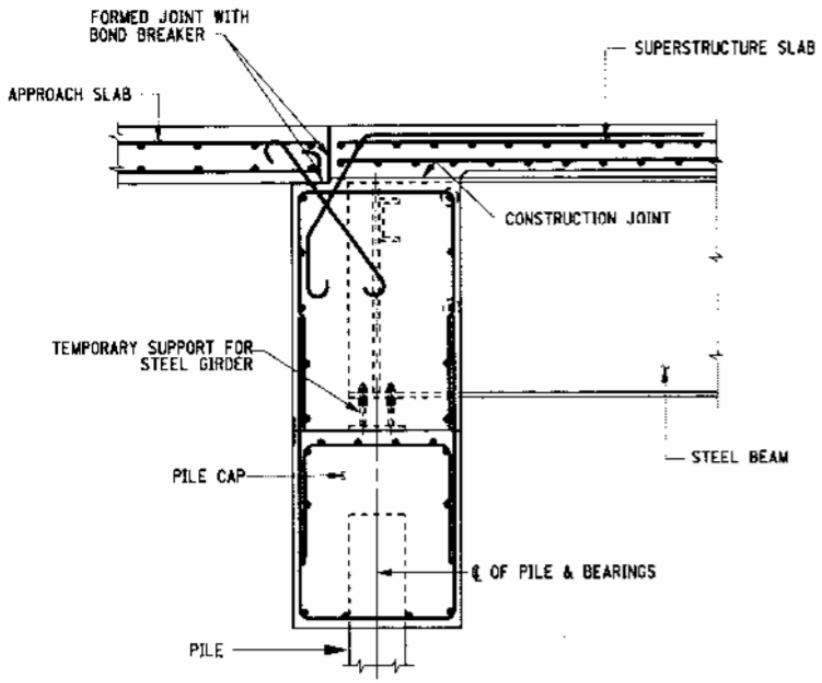

Figure 2-5. *Integral abutment bridge detail in New York State DOT. Source: Hoppe et al, 2016, courtesy of NYSDOT.*

2.3.2.2 Semi-Integral Abutment

Semi-integral abutments are similar to full integral abutments, however, the superstructure and substructure elements are not interconnected. Only the backwall is connected with the superstructure, preventing the backwall from providing any moment transfer to the underlying abutment (Hoppe et al., 2016). An example of a semi-integral abutment can be seen in Figure 2-6. As seen, the bridge deck, backwall, and steel beams act together rigidly, separated from the abutment (White, 2007). Bearings on top of the abutment allow for horizontal movement of the superstructure. In semi-integral abutments, there are no expansion joints provided at the end of the deck, however, a control joint is provided at the end of the approach slab (Semi-Integral, 1999). The semi-integral detail may be utilized in situations where the fully integral abutment cannot be used, perhaps due to pile and

foundational constraints. However, the semi-integral abutment detail requires an increased complexity in joint, foundation, and bearing design, often resulting in an increased cost.

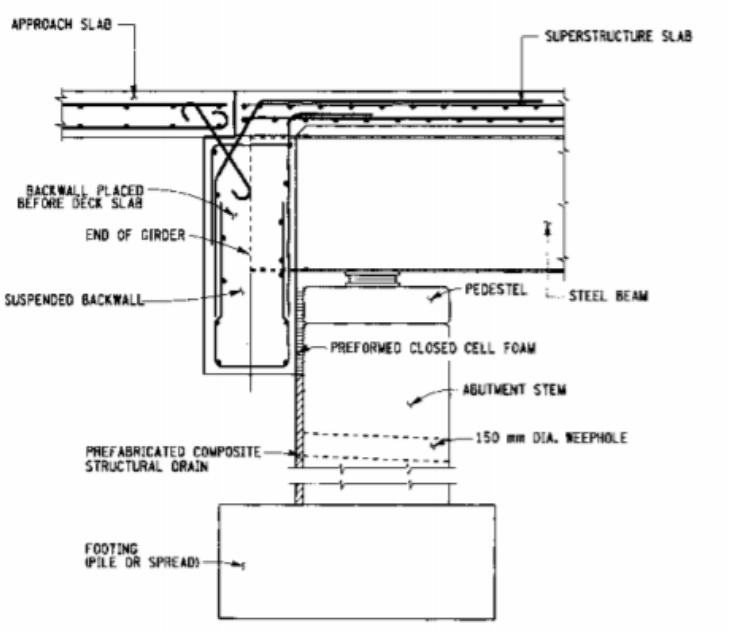

Figure 2-6. *Semi-integral abutment bridge detail. Source: Hoppe et al, 2016.*

2.3.2.3 Deck over Backwall Concept

Deck extensions have been utilized within the United States before, and are particularly prominent in the Northeast region of the country (Miller and Jahren, 2015). Deck extensions allow decks to slide over a backwall, eliminating the need for expansion joints over the abutments. The deck and backwall acts as a combined system, transferring the movement of the superstructure to the end of the approach slab (Aktan et al., 2008). Because the joint is not located above the superstructure of the bridge, harmful chemicals cannot leak below and cause deterioration, altering the structural integrity. Deck extensions are similar to semi-integral abutment designs, however, the steel girder ends are not embedded into the

backwall, and are as found in a typical gravity-carrying bridge. This can be seen in Figure 2-7, which shows a typical deck over backwall detail.

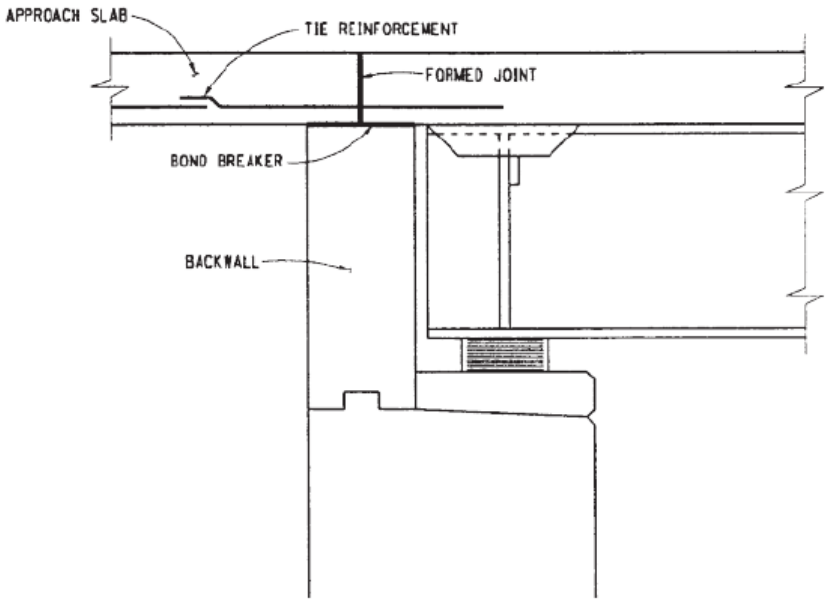

Figure 2-7. *Deck extension detail in NYSDOT. Source: Miller and Jahren, 2015.*

According to a survey completed in 2004, approximately 3900 bridges in the United States have deck extensions. Deck extensions are more prominent in the Northeast region of the United States (Miller and Jahren, 2015). In particular, New York State DOT (NYSDOT), Michigan DOT (MDOT), and Virginia DOT (VDOT) have incorporated deck extensions into their bridges, and notated performance results.

Within New York State DOT, a research team analyzed over 105 bridges with deck extensions. Of these bridges, all were found to be performing as expecting. There was minor deck cracking, the only significant problem listed (Miller and Jahren, 2015). As with some other bridge design types, the performance of the deck extensions was found to worsen with an increase skew or increased span length. Overall, Miller and Jahren found that jointless

bridges performed better than bridges with other types of common joints, such as compression seals.

2.3.3 Approach Slabs

Approach slabs have been incorporated into bridges using the deck over backwall detail, in order to minimize differential settlement effects and provide a transition from the roadway pavement to the bridge deck (Faris, 2009). Approach slab performance is impacted by dimensions, reinforcement detailing, use of a sleeper slab, and the connection between the bridge deck and approach slab.

Approach slabs can range in feet from five feet (utilized by MDOT) to twenty feet long (utilized by NYSDOT and Iowa DOT). A nationwide survey was completed in 2004, notating the use, design, and performance of jointless bridges within the country. While details of the approach slab varied from state to state within jointless bridges, 84% of states that responded said that the most encountered issue with jointless bridges was settling of the approach slab. Miller and Jahren made direct contact with MDOT and found that they too had settlement issues with their sleeper slab, allowing settling of the approach slab. This caused a bump in the driving conditions when transitioning from the approach slab to the highway pavement (Miller and Jahren, 2015). To counteract settling, 31% of states responded that they used a sleeper slab at the end of the approach slab, 26% used fill material to “float” the slab, and 30% of states utilized a combination of both designs (Aktan et al., 2008).

When utilized with deck extensions, reinforcement from the approach slab is directly connected to the bridge deck. This differs from approach slab connections to abutments, as used in integral abutments, or no connections (Faris, 2009). Currently, AASHTO has no guidelines for designing approach slabs (Faris, 2009).

2.3.4 Deck over Backwall Detailing

Many other states have used a deck extension detail similar to the one shown in Figure 2-7. However, between state details, differences could include location of the construction joint, location of the continuous longitudinal reinforcing, and incorporation of a sleeper slab.

The detail in Figure 2-7, as previously stated, is utilized by NYSDOT. The detail identifies a “formed joint” over the center of the backwall. The intention of this joint is to allow rotation of the superstructure, while still keeping the two slabs connected via longitudinal steel. In the particular extension detail shown, the deck and the approach slab were poured continuously, and then a formed joint was saw cut after the pour. The joint was formed to encourage cracking at the correct location. In more recent details developed, the approach slab and deck are poured separately (Alampalli and Yannotti, 1998).

Figure 2-8 below shows another example of a deck extension detail, this one from Michigan DOT. In comparing Figure 2-7 and Figure 2-8, one can observe several differences. First, the MDOT detail places the construction joint in line with the inside edge of the backwall, rather than in line with the center of the backwall, as done in NYSDOT. Secondly, specification of the continuity of the longitudinal reinforcing differs. In the NYSDOT detail, only bottom longitudinal reinforcing is provided. However, in the MDOT detail, the top longitudinal reinforcing is specified as continuous. Not shown in the detail, MDOT also states that a sleeper slab should be incorporated at the end of the approach slab.

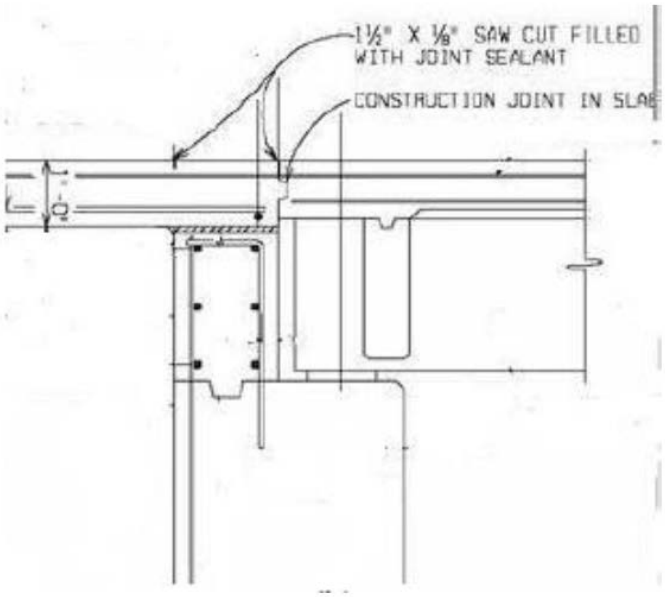

Figure 2-8. *Deck extension detail in MDOT. Source: Miller and Jahren, 2015.*

The continuity of the longitudinal reinforcing from the approach slab to the bridge deck affects the stresses that could transfer into the bridge deck. A study completed by Western Michigan University studied the differences between continuity of top versus bottom reinforcing in the approach slab. Their developed finite element models showed that when continuing the top reinforcing, negative moment (and therefore, tensile stress) was transferred through the joint. Conversely, only continuing the bottom layer of longitudinal reinforcement increased the positive moment at the midpoint of the approach slab. Additionally, continuity of bottom reinforcement only allowed the joint to act like a hinge, eliminating those stresses that were transferred with continuity of top reinforcing (Aktan et al., 2008).

Miller and Jahren (2015) agreed with these conclusions, and noted that continuing the top longitudinal reinforcing layer through the joint should allow negative moment transfer. This would not then, allow the joint to act as a hinge. Because cracking was preferred on the

bottom of the slab as opposed to the top surface, bottom reinforcement only was preferred. While the midspan moment capacity would be reduced, the design for additional midspan moment is more achievable and preferable than designing for a negative moment capacity to prevent top cracking (Miller and Jahren, 2015).

2.4 Experimental Testing Plan

2.4.1 Introduction

Experimental testing was completed to not only assess the performance of the deck over backwall concept, but understand the performance of the detail when different design decisions were made. The displacement of various sections of the specimen, along with cracking patterns and stress concentrations, were analyzed.

2.4.2 Testing Objectives

Testing was completed to satisfy several objectives pertaining to the performance of the deck over backwall concept. These objectives included:

1. Understanding of interaction between “existing” concrete bridge deck and newly poured approach slab section using typical DOT construction practices.
2. Understanding of cracking underneath the bottom of the approach slab.
3. Understanding of how detailing of longitudinal reinforcing in approach slab affects the performance of the joint.
4. Understanding of how the presence of a backwall support could affect the performance of the joint.

To achieve the objectives outlined above, it was decided that two tests would be performed on the same lab specimen. Two distinct differences existed between these two tests. First, the continuity of the top reinforcing was altered. In Test 1, both the top and bottom longitudinal reinforcing in the approach slab would be continuous. However, in Test

2, the top reinforcing would be cut, similar to the detail outlined in Figure 2-2. Secondly, the existence of a hard support, representative of an abutment stud wall and backwall, would change from Test 1 to Test 2. In Test 1, no support would exist. Because the deck slides over the backwall, it is possible that a full reaction force is not provided by this support. For this reason, the backwall was neglected in Test 1. This was an extremely conservative approach. In Test 2, a hard support was provided to simulate this backwall. The top reinforcing would be cut over the center of this backwall, again corresponding to the detail provided in Figure 2-2. Details surrounding testing setup, specimen geometry, loading, and instrumentation will be discussed in the following sections.

2.4.3 Testing Plan

2.4.3.1 Geometry

Simplifications to the joint detail developed by the Iowa DOT were made in order to facilitate both framework and construction. Simplifications did not impact the pertinent results that the experimental investigation produced.

Overall dimensions of the cast-in-place specimen can be seen in Figure 2-9 below. The lab specimen consisted of three main sections, corresponding to the main structural components of the Iowa DOT detail. The sections will be referred to as “existing bridge deck”, “concrete diaphragm”, and “approach slab” throughout this paper. The existing bridge deck section was 9.5” thick, corresponding to the thickness provided by Iowa DOT for a typical bridge deck. This section was three feet in length. Next, the concrete diaphragm served as the main structural diaphragm for the specimen. The diaphragm was 14.5” thick, and contained the reinforcing hoops as seen in Figure 2-1 and Figure 2-2. Finally, the approach slab section was 20’-0” in length, corresponding to the minimal removal limit as shown in Figure 2-3. The thickness of the approach slab section was 11.5”. The entire

laboratory specimen was 10’ wide, corresponding to the spacing of typical girders on an Iowa DOT bridge, as well as lane load corresponding to AASHTO Specifications (American Association of State Highway and Transportation Officials, 2014).

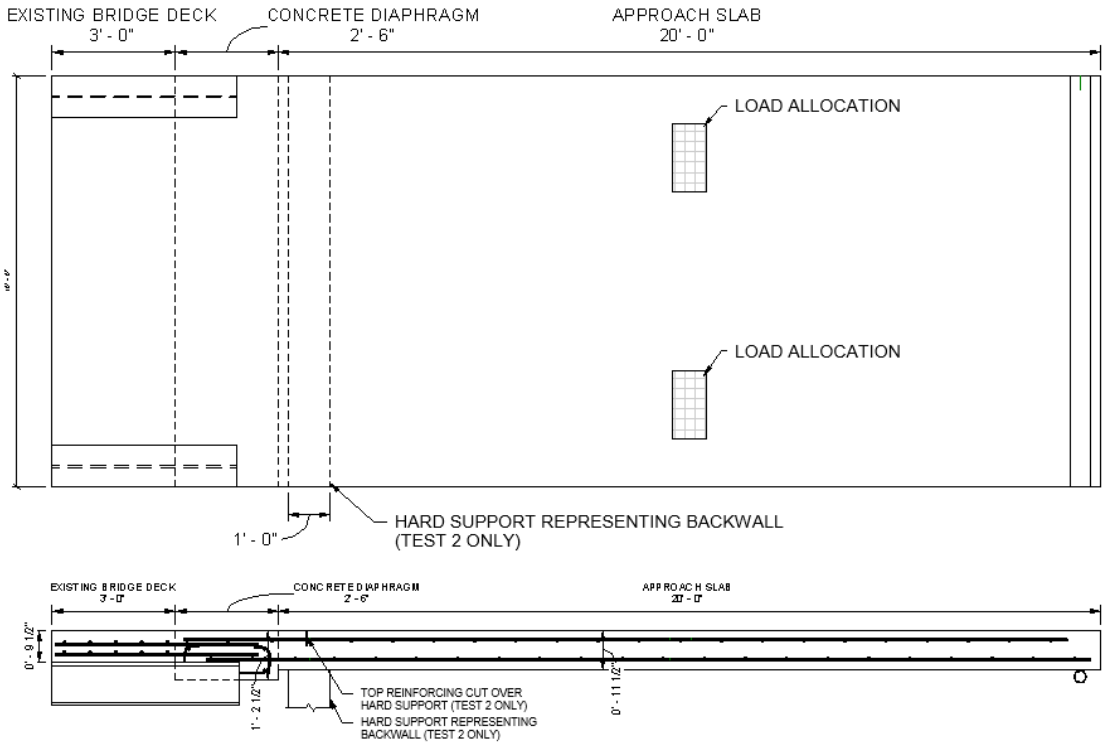

Figure 2-9. *Laboratory test setup for Test 1 and Test 2.*

In both the plan and profile view provided in Figure 2-9 above, the location of the hard support utilized for Test 2 is shown. Above the hard support, the top reinforcing was cut for Test 2, as shown by the indicated note.

Similar to field conditions for a removal and rehabilitation project, the existing bridge deck was poured at a separate time than the concrete diaphragm and approach slab. Because the bridge deck would not be demolished during the concrete removal process, it was poured first and allowed to fully cure before pouring the remainder of the specimen monolithically.

Therefore, a cold joint (also referred to as a construction joint) existed between the existing bridge deck and concrete diaphragm sections.

2.4.3.2 Boundary Conditions

The specimen was supported on one end by two steel beams, simulating the girders in a full bridge. The two steel beams extended under the bridge deck section and into the concrete diaphragm. As noted previously, the spacing of the two beams mimicked that of typical spacing of girders on an Iowa DOT bridge. The beams were 4'-6" long, and had shear studs on the top flanges embedded into the concrete of the bridge deck. The end of the existing bridge deck section was tied down to the strong floor of the laboratory.

A steel pipe filled with concrete acted as a roller on the other end of the specimen. The roller was located six inches in from the edge of the specimen, allowing the slab to move horizontally during loading. The roller was supported by steel sections in order to make the support level with the remainder of the specimen.

Normally, soil would be present under a portion of the approach slab. However, soil was not added to the laboratory testing. This was a conservative approach, as soil could compact over time, moving away from the bottom of the approach slab and no longer providing support.

2.4.3.3 Reinforcing

Reinforcing for the lab specimen followed that of a typical Iowa DOT bridge project. Reinforcing bars in the existing bridge deck were not epoxy-coated, while the reinforcing throughout the rest of the specimen was epoxy coated. Details of reinforcing are sorted by section of specimen, and are as follows:

- Existing Bridge Deck:

- Top Longitudinal Bars: #6 bars at varied spacing, extend into concrete diaphragm section 2’-0”
- Bottom Longitudinal Bars: #6 bars at varied spacing, extend into concrete diaphragm 2’-0”; 2” cover
- Transverse Top Bars: #7 bars at 7.5” spacing; 3.5” cover
- Transverse Bottom Bars: #7 bars at 7.5” spacing

- Concrete Diaphragm:
  - Hoop: #5 hoop with (4) #5 bars at the corners and (1) #5 bar at the bottom middle; 2” cover on bottom; hoops tied with top bars of approach slab

- Concrete Diaphragm:
  - Top Longitudinal Bars: #5 at 12” on center; 2.5” cover
  - Bottom Longitudinal Bar: #6 at 12” on center; 2.5” cover
  - Top Transverse Bars: #5 at 12” on center
  - Bottom Transverse Bars: #5 at 12” on center

Table 2-1 summarizes all reinforcing bars, their lengths, and pertaining characteristics.

Table 2-1. *Reinforcing bar list.*

Reinforcing Bar List						
Part	**Bar**	**Location/Type**	**Number**	**Length**	**Spacing**	**Epoxy**
Existing Bridge Deck	#6	Top, Long	15	4’-11”	Varied, See Plan View	No
	#6	Bottom, Long	14	4’-11”	Varied, See Plan View	
	#7	Top, Transverse	5	9-6”	7.5”	
	#7	Bottom, Transverse	5	9-6”	7.5”	
Diaphragm	#5	Hoop	9	4’-4”	1’, w/ approach top bars	Yes
Approach Slab	#5	Transverse	5	6’-6”	Around hoop	Yes
	#5	Top, Long	9	21’-6”	12”	
	#6	Bottom, Long	9	21’-6”	12”	
	#5	Top, Transverse	24	9’-6”	12”	
	#5	Bottom, Transverse	24	9’-6”	12”	

2.4.3.4 Concrete

Typical concrete strengths were utilized, with all concrete specified as C4 mix. Two distinct pours were completed. The first pour, used for the existing bridge deck section of the specimen, had an average 28 day compressive strength of 6505 psi. The second pour, utilized for the remainder of the lab specimen, had an average 28 day compressive strength of 5116 psi at the time of testing. These results are shown below in Table 2-2.

Table 2-2. *Compressive strength of concrete cylinders.*

Cylinder #	Existing Bridge Deck Section	Concrete Diaphragm/Approach Slab Sections
1	6531	5205
2	6372	4830
3	6612	5313
Average	**6505**	**5116**
St. Deviation	122	254

Per typical Iowa DOT construction practices, the lateral surface of the existing concrete deck was roughened using a jack hammer. This promoted additional bonding between the two pours. This can be seen in Figure 2-13.

2.4.3.5 Loading

Loading conditions were the same for Test 1 and Test 2. Loading corresponded to that of the rear axle of an HS-20-44 truck. To mimic this load, loading areas were 10”x20”, spaced six feet apart. Load was applied to the specimen via actuators pushing onto loading pads anchored to the specimen. The specimen was loaded until there was 16 kips on each loading area, corresponding to the weight of the rear axle of the truck. Test 2 was loaded to this point, however then loaded until failure. During Test 2 loading, force displacement was used until 20 kips was on each loading area; after this point, deflection control was used until failure.

2.4.3.6 Instrumentation

2.4.3.6.1 Strain Gages

Strain gages were one of two main instruments utilized to collect data during testing. A total of 23 strain gages were installed into the reinforcing of the lab specimen. Strain gage locations on reinforcing can be seen in Figure 2-10. Strain gages were placed in positions that would aid in collecting data corresponding to the objectives of testing outlined previously. In particular, reinforcing strain gages were placed on the reinforcing near the location of the hard support in Test 2. All strain gages in this area were placed past the development length of the reinforcing, ensuring that a full bond existed between the reinforcing and concrete. Additionally, strain gages were placed near the loading areas. It was expected that the midspan of the approach span would experience the largest strains due to the positive moment incurred by loading. Therefore, the strain gages near the loading areas would be able to capture the maximum strains that occurred during Test 1 and Test 2.

Concrete strain gages, referred to as BDIs, were placed on the surface of the specimen to capture the stresses that occurred in the concrete during loading in Test 1 and Test 2. The placement of these gages mirrored that of the reinforcing strain gages, so that results from both could be directly compared. There were 13 concrete strain gages in total. Figure 2-11 shows the location of these gages. Gages 9, 11, and 13 were placed on the underside of the specimen, in the concrete diaphragm section.

2.4.3.6.2 String Pots

String pots were placed in several locations on the specimen to record the displacement that occurred during testing. Figure 2-12 shows the location of these displacement meters. In total, there were eight string pots. String pots D1 and D8 were placed on opposing ends of the specimen. These meters would record how the specimen deflected at

the supports during tests. D3 through D7 were placed on the main body of the approach slab. Three string pots were placed perpendicular to the plane of loading. D4 and D6 captured any unsymmetrical twisting that the approach slab experienced during loading, if loading was not completed symmetrical. Finally, D2 was placed at the end of the steel girders in the diaphragm section.

2.4.3.6.3 Linear Velocity Displacement Transducers (LVDTs)

Three LVDTs were utilized to measure the horizontal growth of the saw cut made through the top of the approach slab and reinforcing during Test 2. These LVDTs were placed along the length of the cut, with one LVDT measuring displacement at the center, and two measuring displacement at the outer edges of the width of the specimen.

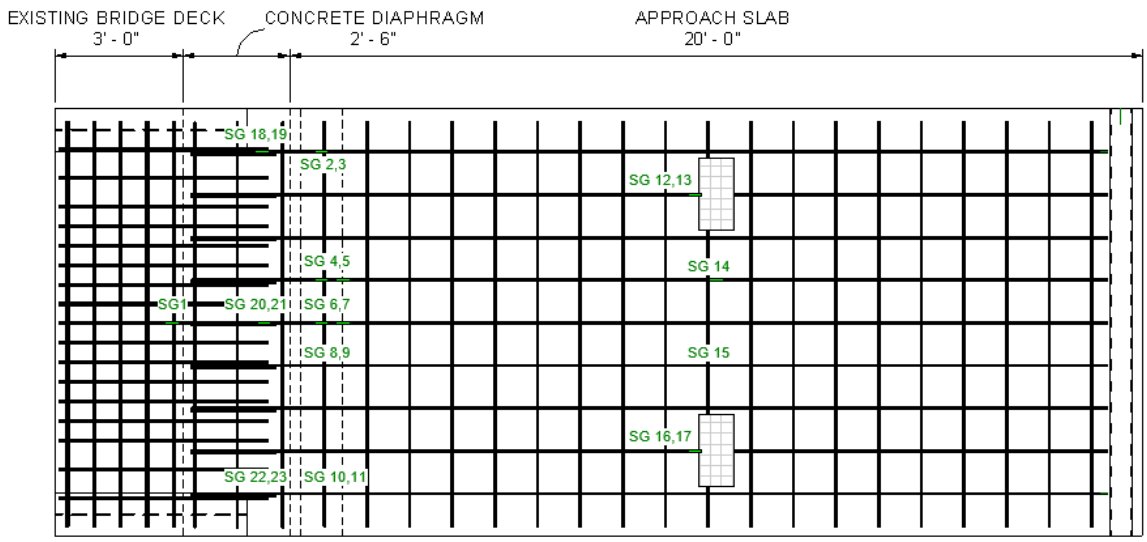

Figure 2-10. *Reinforcing strain gage layout.*

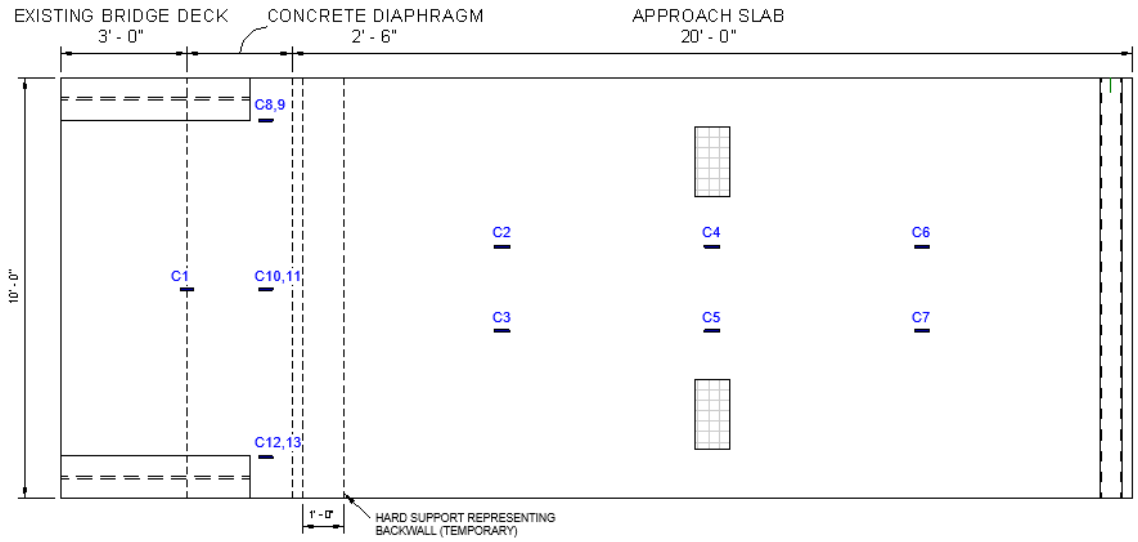

Figure 2-11. *Concrete strain gage (BDI) layout.*

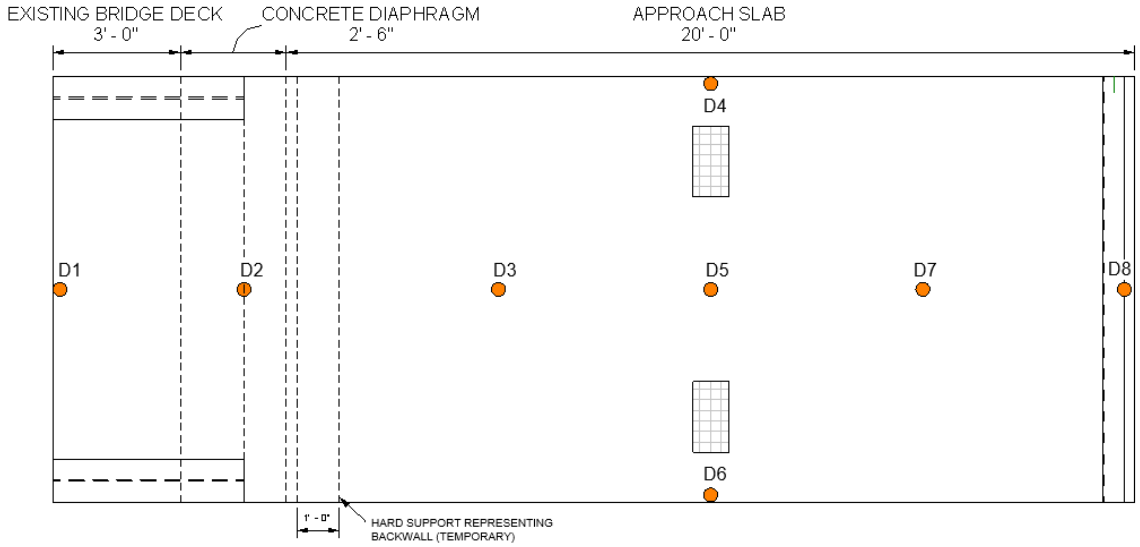

Figure 2-12. *String pot (displacement meter) layout.*

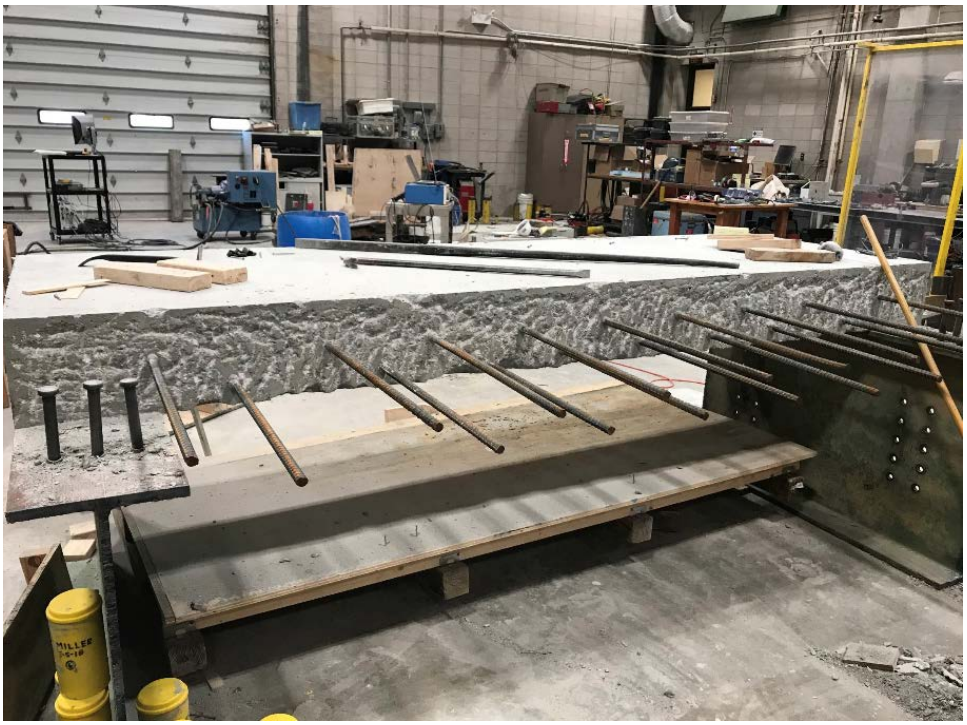

Figure 2-13. C*onstruction joint at interface of existing bridge deck and concrete diaphragm sections.*

Figure 2-14. *Jack hammering performed on construction joint to increase bond strength.*

Figure 2-15. *Laboratory specimen when approach slab and diaphragm sections are poured; view of steel girders.*

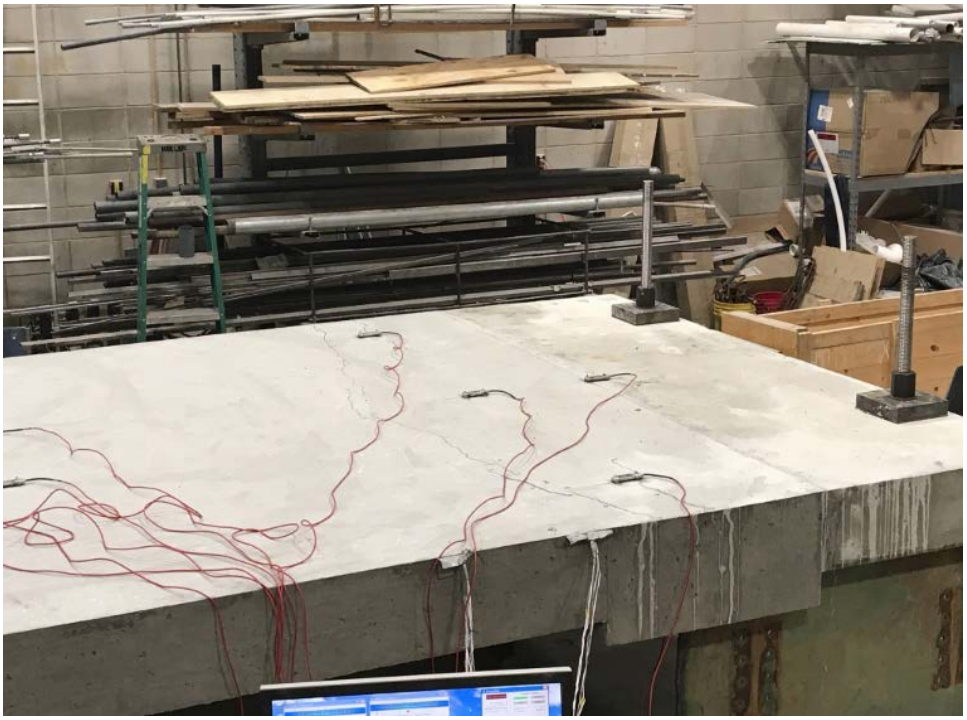

Figure 2-16. *BDIs on laboratory specimen.*

2.5 Experimental Testing Results

2.5.1 Introduction

Testing results were gathered from Test 1 and Test 2. Results for each test will first be presented independently. Then, comparisons between the two tests will be made. While Test 2 results were altered by effects that Test 1 had on the specimen, such as cracking, general trends between the two tests can still be compared. Additionally, utilizing finite element analysis, Test 2 results for an untested specimen could be generated. These results will be presented in the next section of this paper.

2.5.2 Test 1 Results

During Test 1, both the top and the bottom longitudinal reinforcing was continuous through the concrete diaphragm section. The specimen was loaded until there was 16 kips on each loading area, corresponding to the full load of the rear axle of the truck chosen. Figure 2-17 shows the general loading pattern used during Test 1. Load was applied incrementally, and then halted as the specimen was checked for cracking and strains were monitored. This pattern continued until 16 kips was reached on each loading area.

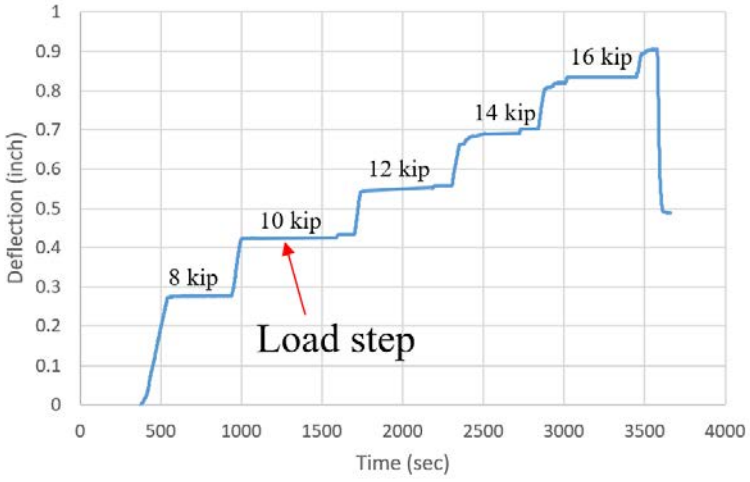

Figure 2-17. *General loading with load steps for Test 1.*

2.5.2.1 Cracking Patterns

Cracks were monitored on the top, bottom, and sides of the specimen during the entirety of Test 1. Particular attention was paid to the areas near the concrete diaphragm, where the cut would be made in Test 2, as well as the bottom of the approach slab where the largest positive moment (and therefore, largest strains) would be.

In order to accurately record cracking, a grid was created on all surfaces of the test specimen, subdividing the specimen into a 1' by 1' grid. Figure 2-18 shows the pattern for labelling the gridded sections of the specimen. During testing, cracks were marked incrementally, and at the end of testing, photos were taken of each individual grid section in order to create an overall cracking pattern map for the different surfaces of the specimen.

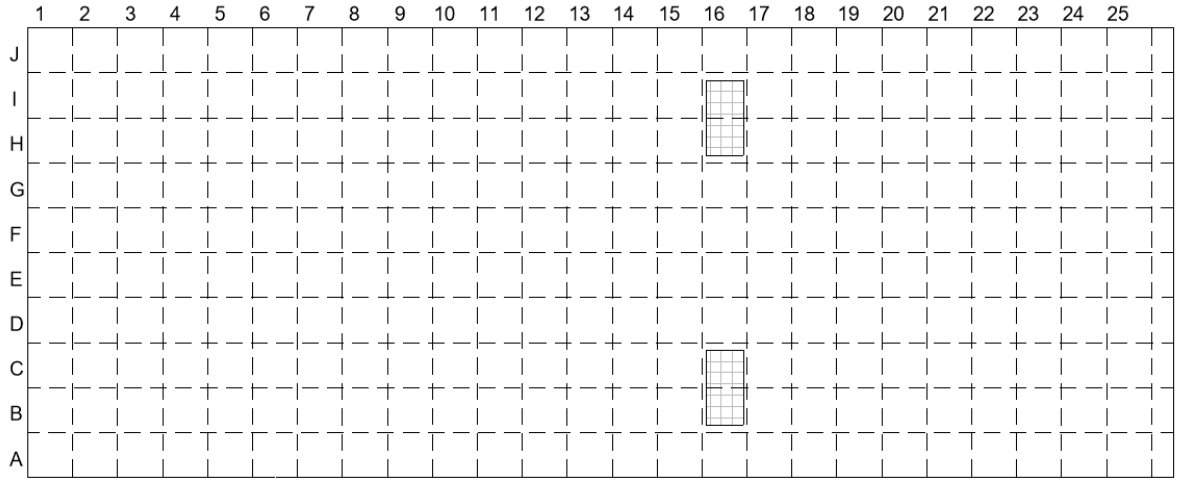

Figure 2-18. *Gridded laboratory specimen for cracking documentation.*

Figure 2-19 shows the cracking that occurred on the top of the slab during Test 1. Cracks are color coded by which load they occurred at. As seen, the majority of cracking on the top of the specimen occurred near the interface of the concrete diaphragm and existing bridge deck. The first crack to appear was at the cold joint between the concrete diaphragm and existing bridge deck. Even though the surface of this joint was roughened, the concrete

bond at this surface was not as strong as the remainder of the specimen. This large, horizontal crack at the joint can be seen in Figure 2-20, and formed near a loading condition of 7.5 kips on each tire area. In looking at the remainder of the cracks on the top of the specimen, it can be seen that the continuity of the top reinforcing caused stress to be transferred from the approach slab to the concrete diaphragm.

Figure 2-21 shows the cracking that occurred on the bottom of the slab during Test 1. Similar to Figure 2-19 , cracks are color coded by which load they occurred at. All of the cracks that formed on the bottom of the slab extended across the width of the slab, and were primarily concentrated under the application of the load where the largest tensile stresses existed. As load was applied, cracks formed on either side of the width of the specimen; as the load increased, the cracks propagated until coming together and forming one crack along the full width of the slab. Those cracks that were formed earlier in the loading stage (i.e. cracks shown in yellow, corresponding to 10 kips per loading area) began to experience hairline cracks branching off at later loading stages. To summarize, those cracks on the bottom of the slab extended a total length of 10 feet, and were located approximately one foot apart.

Figure 2-22 and Figure 2-23 show the cracking that occurred on the sides of the slab. The sides of the specimens are separated by North and South directions, or by direction when looking at the roller. As seen, the majority of the cracks on both sides were flexural cracks that propagated from the bottom of the slab, concentrated at the middle of the approach slab. Additional cracks formed in the concrete that was surrounding the steel girder. A close up of this cracking area can be seen in Figure 2-24. Cracks from the top of the slab near the concrete diaphragm section also grew towards the side of the specimen.

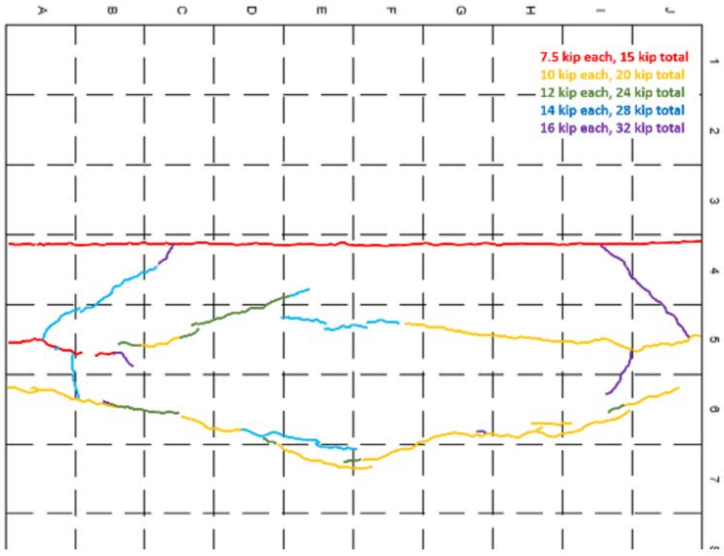

Figure 2-19. *Cracking on top of slab, Test 1.*

Figure 2-20. *Crack at construction joint.*

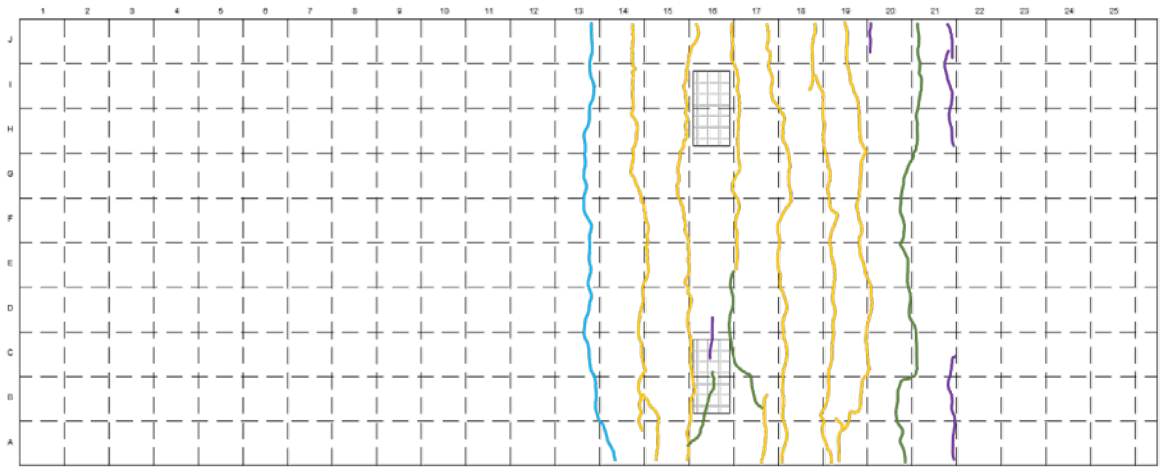

Figure 2-21. *Cracking on bottom of slab, Test 1.*

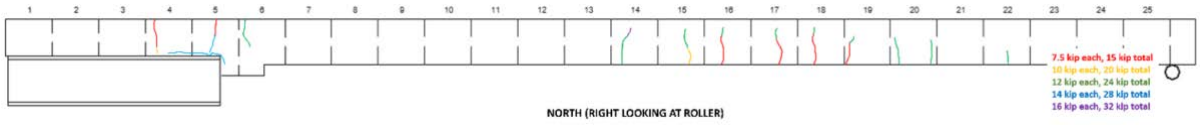

Figure 2-22. *Cracking on north side of slab, Test 1.*

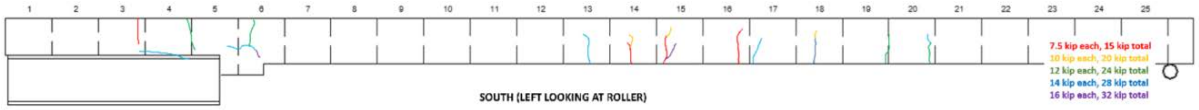

Figure 2-23. *Cracking on south side of slab, Test 1.*

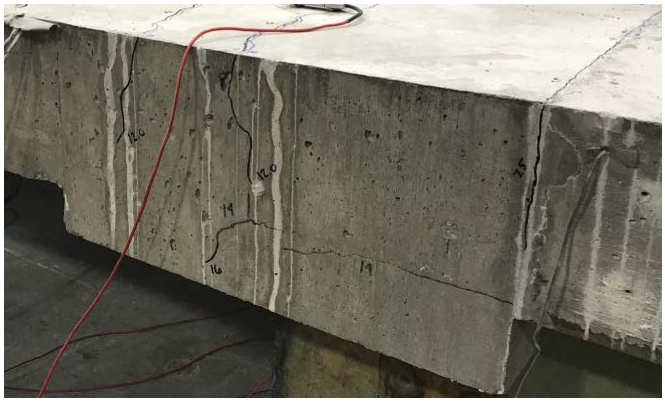

Figure 2-24. *Cracking occurring in concrete diaphragm section at intersection with steel girder, Test 1.*

2.5.2.2 Deflection

The load-displacement curve for the center of the approach slab, where the maximum moment occurred, can be seen in Figure 2-25. As shown, the deflection becomes nonlinear after a loading condition of approximately four kips per tire area. While the first visible crack occurred at the construction joint at 7.5 kips per loading area, the load-displacement curve becomes nonlinear before this point, at approximately four kips per loading area. This could be due to micro-cracking that was unable to be seen. This statement is supported in looking at strain data from BDIs located in the area. At truck loading condition, the maximum deflection experienced by the slab at midspan was approximately 0.8". It should be noted that the load-displacement curve is not smooth due to small jolting of loading equipment when cracking occurred underneath in the approach slab.

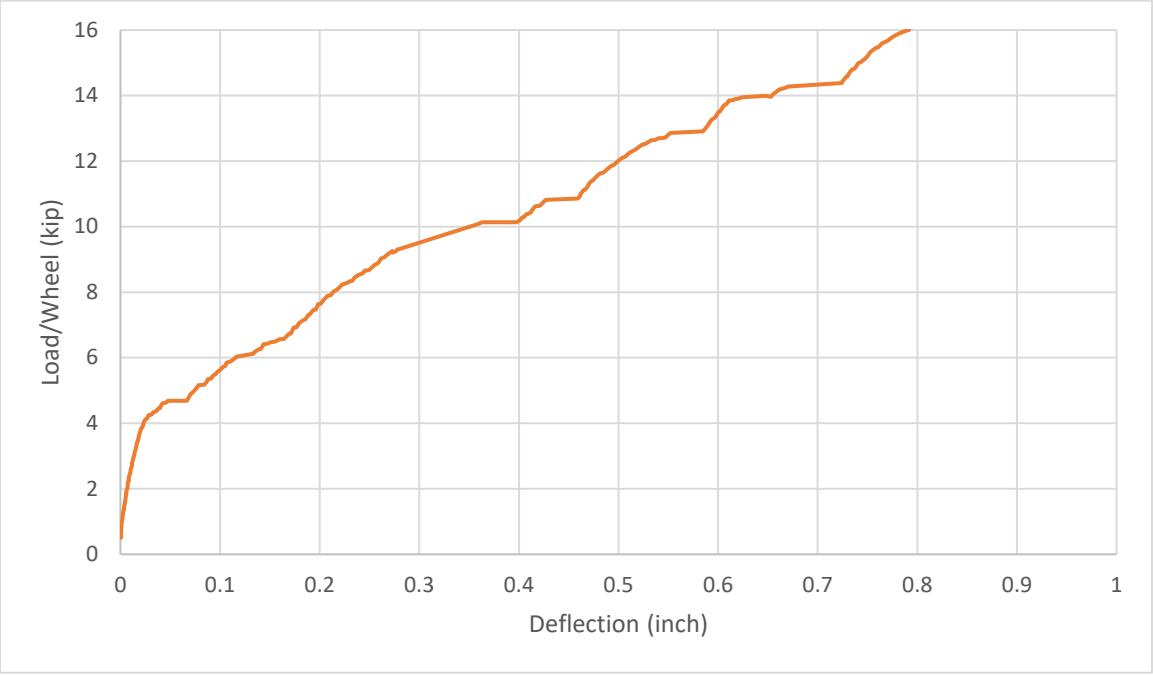

Figure 2-25. *Load-deflection curve at midspan of approach slab, Test 1.*

Table 2-3 presents the deflection occurring along the specimen at the standard truck loading condition. The locations are specified by distance from the end of the steel girders.

As expected, those meters at the ends of the specimen experienced very small deflection as compared to the rest of the specimen. However, there was a small rotation of the approach slab occurring at the roller support. At the third points of the approach slab, the specimen experienced approximately 0.5” of deflection, shown by D3 and D7. Comparing the deflection along the width of the approach slab at midspan, one can see that the deflections are reasonably similar, indicating that loading was approximately symmetric.

Table 2-3. *Deflection along length of specimen at 16 kips per loading area, Test 1.*

Location, x (ft)	0	4’-0”	10’-6”	15’-6”L	15’-6”R	15’-6”M	20’-6”	25’-0”
Meter	D1	D2	D3	D4	D5	D6	D7	D8
Deflection (in)	0.00	0.06	0.50	0.79	0.81	0.81	0.51	0.04

The two main areas of interest within the specimen were near the concrete diaphragm and the approach slab, where the largest deflection and strains occurred. Therefore, the following two sections will present patterns of strain in these two areas

2.5.2.3 Near Concrete Diaphragm

Figure 2-26 below shows the magnitudes of strains existing within the reinforcing at standard truck loading. The simple bar chart allows a direct comparison between locations of gages, and allows patterns to be detected easily. Strain gages SG4, SG6, and SG8 were located on the top reinforcing in the concrete diaphragm, and are highlighted in green. Strain gages SG5, SG7, and SG9 were in the same location, however, placed on the bottom reinforcing. These gages are highlighted in purple. One can easily see that the strain experienced by the top reinforcing in the diaphragm is substantially higher than the strain experienced by the bottom reinforcing. Strain gages SG2 and SG10 were also located in the concrete diaphragm on the top reinforcing, however were on the outer longitudinal bars. One

can see that strain in these two areas was much smaller in comparison, perhaps due to the stiffness provided by the steel girders.

Figure 2-27 presents the strain experienced by the concrete gages on the top of the concrete diaphragm, and Figure 2-28 presents the strain experienced by the concrete gages on the bottom of the concrete diaphragm. The "x" markings in the figures indicate that cracking occurred near or underneath the gages. Therefore, the rest of the data from the gage is not accurate. One can see that cracking was experienced by those gages on the top of the concrete diaphragm, coinciding with the cracking pattern data. The majority of cracks occurred on the top of the deck around eight to ten kips per wheel area. One can also see that the top concrete, similar to the top reinforcing gages, experienced tension, shown by the positive microstrain values. Conversely, the bottom concrete gages experienced compression, as shown by the negative microstrain values. This indicates that the concrete diaphragm was experienced negative moment, as the approach slab was rotating into the steel girders.

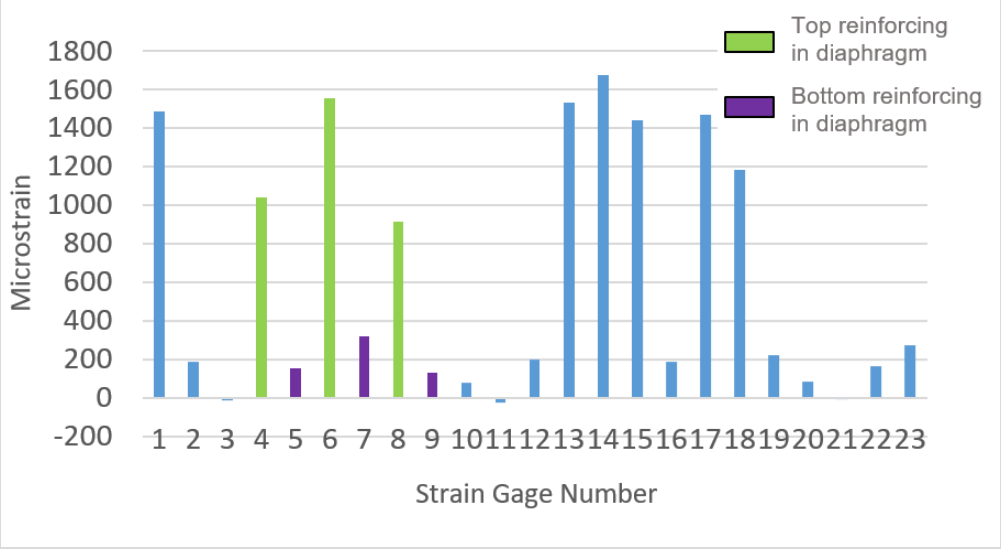

Figure 2-26. *Magnitude of strain in reinforcing at 16 kips per loading area, with focus on gages in concrete diaphragm, Test 1.*

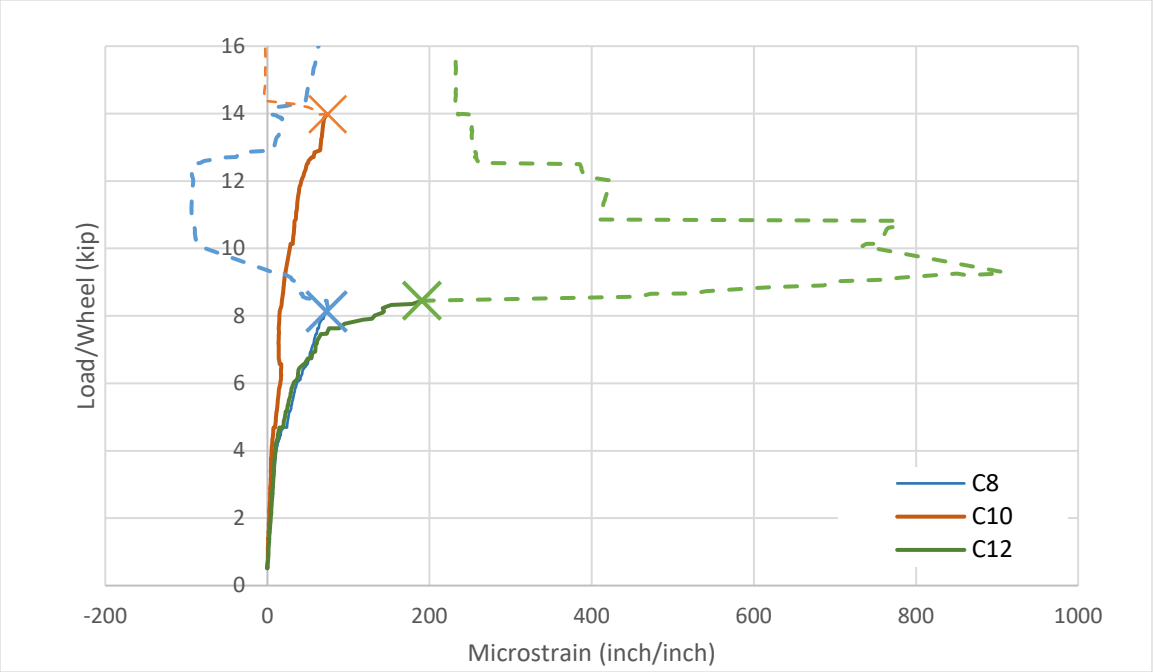

Figure 2-27. *Load vs. strain curve for BDIs on top surface of concrete diaphragm, Test 1.*

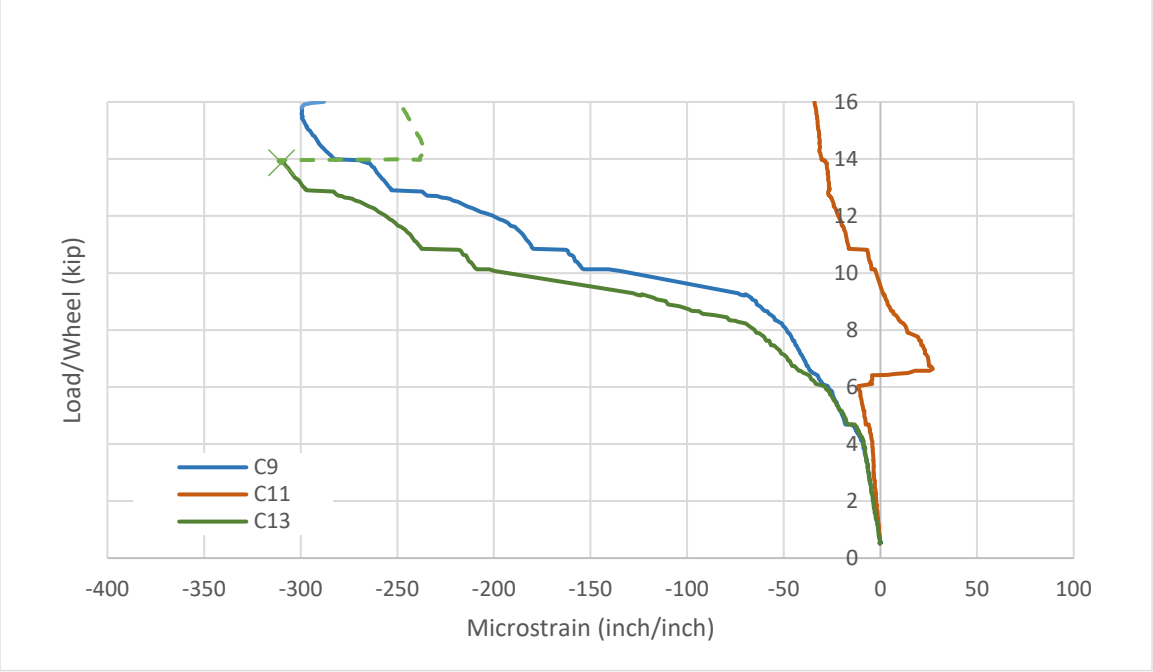

Figure 2-28. *Load vs. strain curve for BDIs on bottom surface of concrete diaphragm, Test 2.*

2.5.2.4 Midspan of Approach Slab

Figure 2-29 presents the magnitude of strain in the reinforcing at 16 kips/wheel. Those bars shown in purple represent the magnitude of strain on the bottom reinforcing, and those shown in green represent the strain on the top reinforcing. One can see that with the large positive moment, the top reinforcing was engaged in tension at the midspan. Overall, in comparing the strains at this location to all other locations, it is easy to see that the midspan of the approach slab experiences the largest strains, as expected.

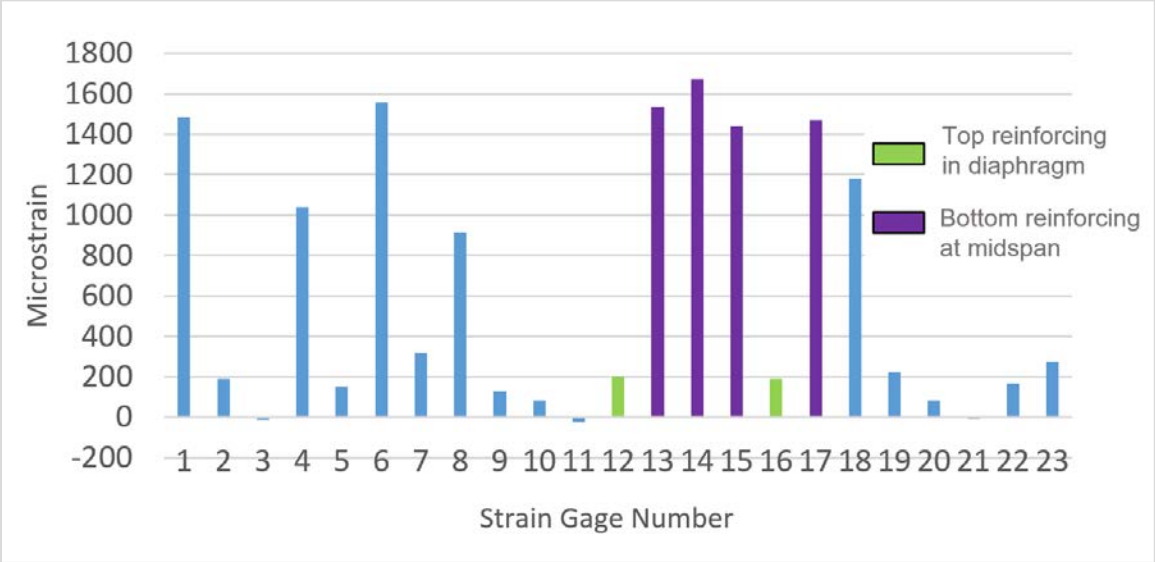

Figure 2-29. *Magnitude of strain in reinforcing at 16 kips per loading area, with focus on gages at midspan of approach slab, Test 1.*

Those concrete gages at the midspan and second third point of the approach slab experienced compression for the duration of loading in Test 1. However, the first third point of the approach slab switched from feeling compression to feeling tension on the top, although very minor. This correlates with a switch from a region of positive moment to negative moment, and correlates with previously presented data. Figure 2-30, Figure 2-31, and Figure 2-32 present the data for these strain gages.

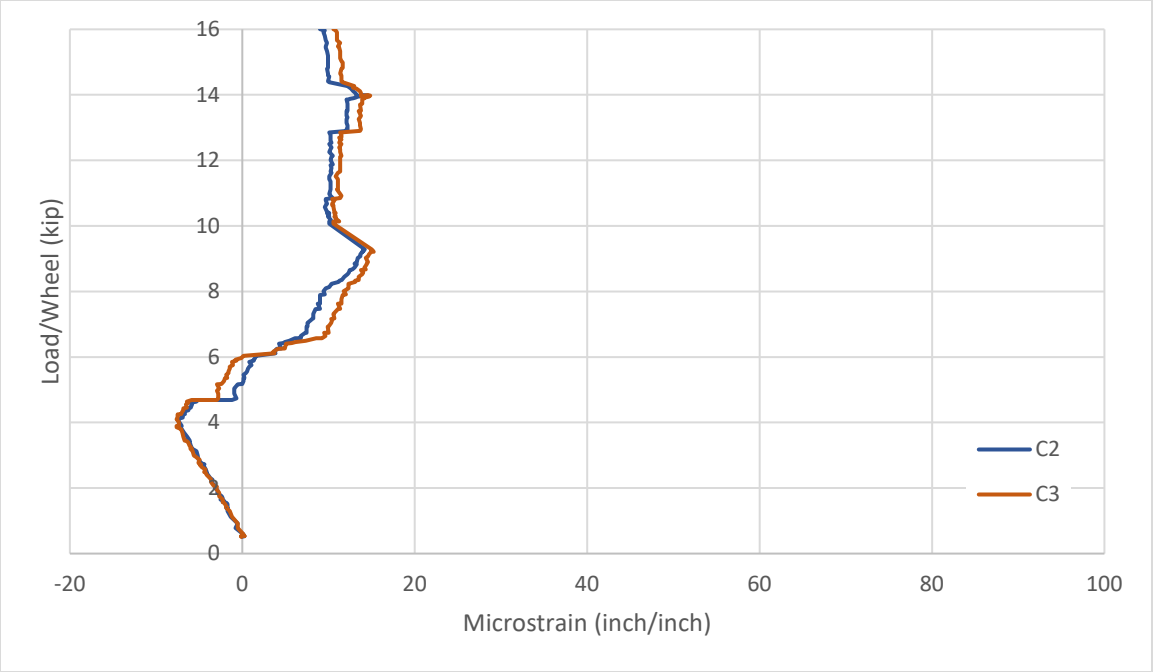

Figure 2-30. *Load vs. strain for BDIs at first third point on approach slab, Test 1.*

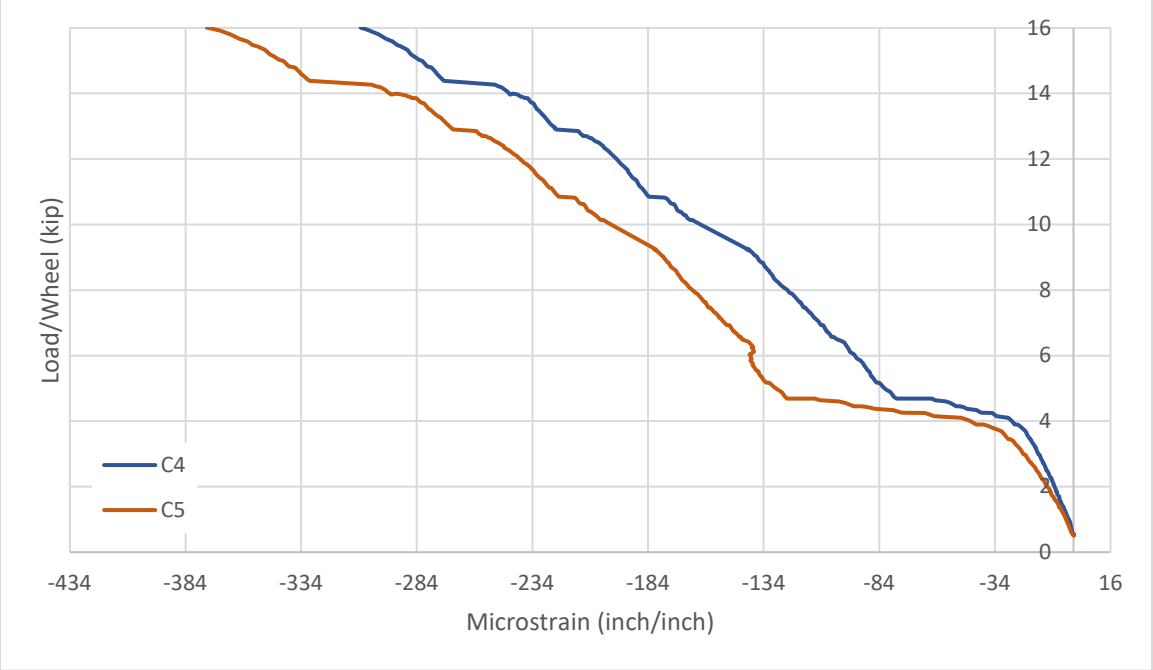

Figure 2-31. *Load vs. strain for BDIs at midspan on approach slab, Test 1.*

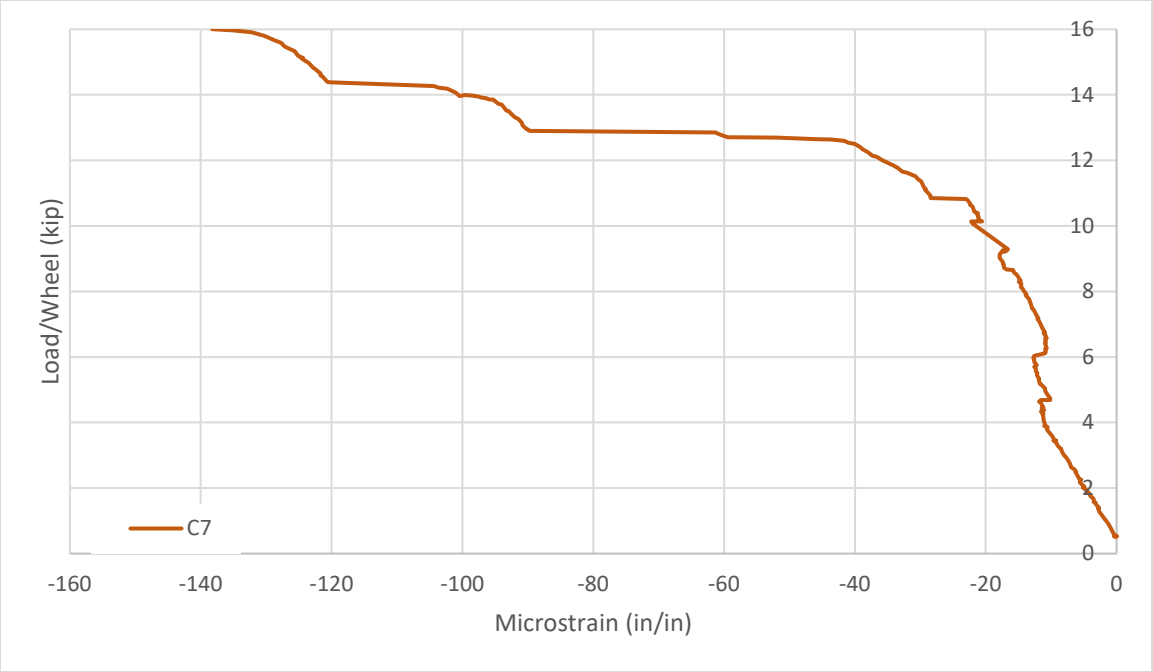

Figure 2-32. *Load vs. strain for BDIs at second third point on approach slab, Test 1.*

2.5.3 Test 2 Results

In Test 2, a hard support representing the backwall was inserted approximately three inches from the end of the diaphragm section. Above the middle of this backwall, the top longitudinal reinforcing was cut. Additionally, during Test 2, the specimen was loaded until failure. The loading pattern was similar in nature to that utilized in Test 1, and is shown in Figure 2-33. Towards the end of testing, deflection control was utilized, as pointed out on the figure. Because Test 2 was completed on an already tested and cracked specimen, it is important to note that Test 2 values cannot be directly compared to those values obtained from Test 1. It would not make sense to compare strain values directly, as residual stress could have been left in bars after Test 1 was complete, even if bars did not yield. However, one can compare patterns between the two tests, and draw conclusions thereafter.

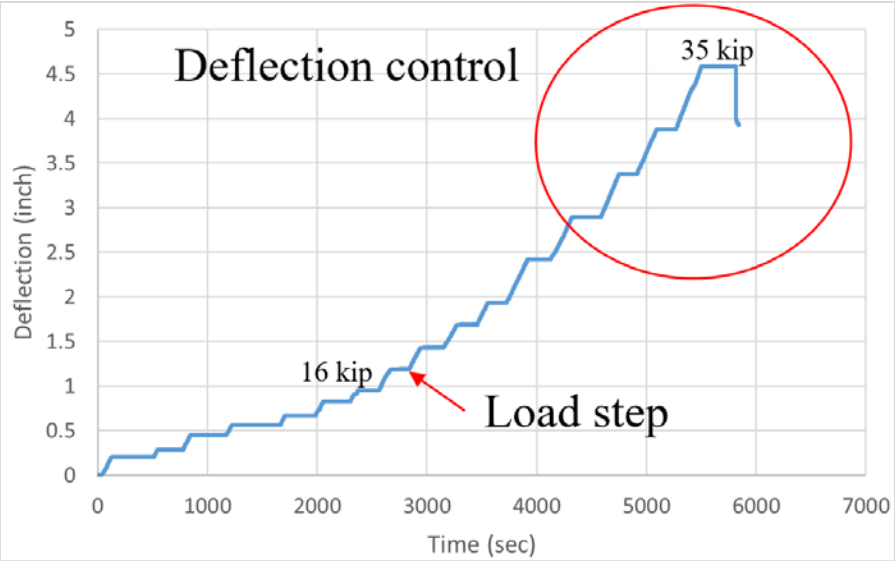

Figure 2-33. *General loading with load steps for Test 2.*

2.5.3.1 Cracking Patterns

During Test 2, no new cracks formed on the top of the specimen. While cracking was already present in the diaphragm and bridge deck sections from Test 1, it is presumed that the presence of the saw cut created a release for the stress from the negative moment. Therefore, if Test 2 were completed on a specimen that had not been previously tested, it is assumed that cracking would still not occur on the top of the specimen. This assumption is checked with the use of finite element software, presented in the following section.

Because the specimen was tested until failure during Test 2, and already had cracks present from Test 1, cracking patterns were not recorded underneath the slab due to the safety risks posed. However, from both visual and audible inspection near the specimen, it was clear that additional cracking occurred on the bottom of the approach slab. Cracks formed during Test 2 could have formed from either opening, propagation, or branching of cracks formed during Test 1, or from development of new stress areas. A better understanding of cracks that formed on the bottom of the approach slab during Test 2 can be achieved by

examining those cracks that occurred on the sides of the specimens, shown in Figure 2-35 and Figure 2-36. Those cracks that already existed from Test 1 are shown in gray. Those cracks that formed before or at 16 kips per loading area are shown in blue, and those cracks that occurred after this loading condition until failure are shown in orange. Shaded, circled, orange areas imply that the area experienced significant crushing or spalling of concrete.

As seen, many of the cracks that formed on the side of the slab during Test 1 propagated during Test 2, specifically occurring from grid lines 14 to 20. Cracks that had previously extended approximately half of the thickness of the approach slab grew very close to the top of the slab. An example of this behavior can be seen in Figure 2-37. Additional cracks that were formed during Test 2 near this area mainly occurred at higher loads. However, it can be seen that on both sides of the slab, additional cracks formed at or prior to the standard truck load within gridline 12. New cracks were also formed on the other side of the loading area, in gridlines 20 to 22. However, these cracks formed after the standard truck load. Similar to those cracks formed during Test 1, it can be assumed that the new cracks formed during Test 2 on the side of the specimen at midspan of the approach slab exist on the bottom of the approach slab, across the width of the specimen.

From gridlines 15 to 17, one can see that the concrete experienced significant damage. At failure, the entire width of the approach slab experienced crushing. This can be seen in Figure 2-38. Before failure, several cracks grew towards this location as the load increased. However, as failure during Test 2 occurred at approximately 35 kips on each loading area, there is no concern that this type of crushing would occur on real bridge structures.

The most significant cracking, other than cracking experienced at the midspan of the approach slab, occurred underneath the saw cut made above the hard support. Looking at Figure 2-35 and Figure 2-36, this saw cut occurs approximately in the middle of grid 7. Cracks started forming underneath this saw cut at 7.5 kips per loading area, less than half of the standard truck load. Figure 2-39 shows the progression of cracks in this area as load was applied. As seen, cracks developed on either side of the joint, progressing towards the bottom of the slab. While the length of these cracks was significant, the width was also significant. Throughout loading, some cracks opened up more than one quarter of an inch. This area could be a point of concern when using this design in future details.

Figure 2-34. *Saw cut at top of approach slab through top reinforcing for preparation of Test 2.*

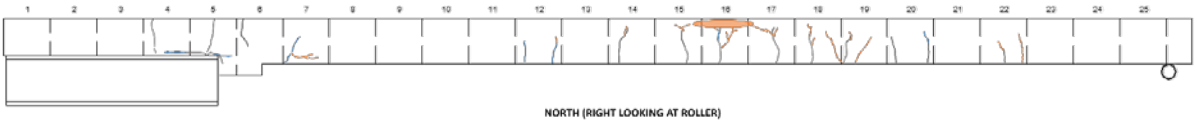

Figure 2-35. *Cracking on north side of slab, Test 2.*

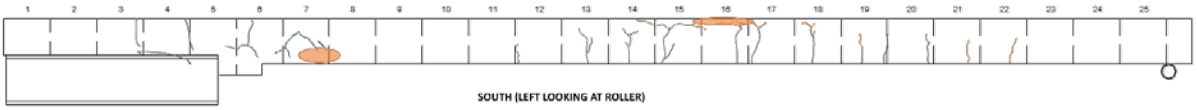

Figure 2-36. *Cracking on south side of slab, Test 2.*

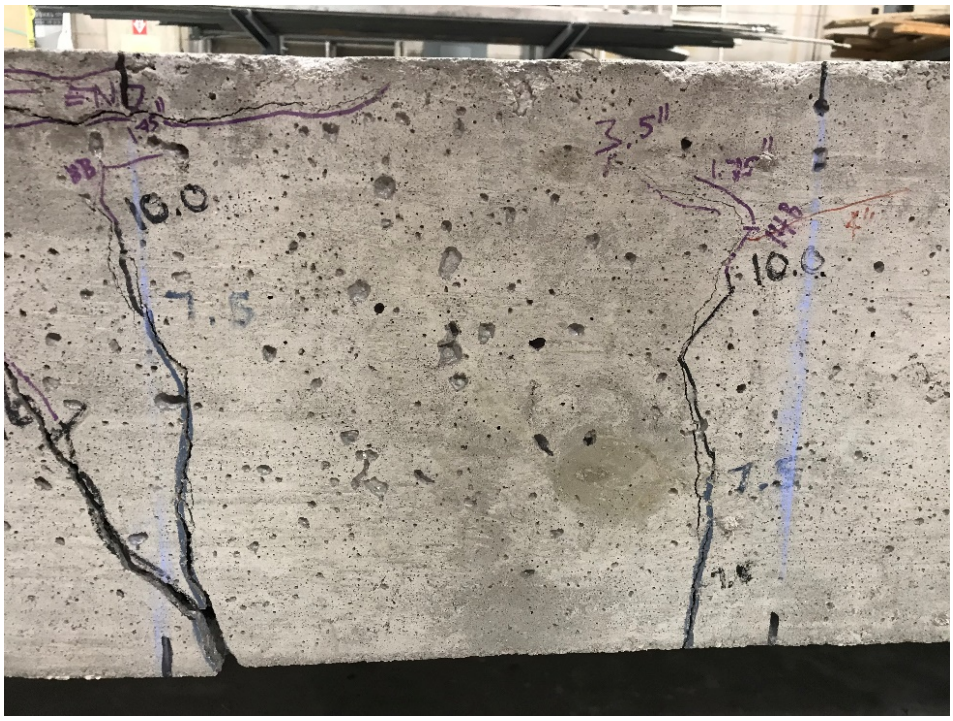

Figure 2-37. *Propagation of cracks occurring near midspan of approach slab, Test 2.*

Figure 2-38. *Crushing occurring at midspan of approach slab at failure, Test 2.*

Figure 2-39. *Sequence showing propagation of cracking occurring above hard support until failure, Test 2.*

2.5.3.2 Deflection

Figure 2-40 shows the load-deflection curve for the specimen during Test 2. As shown, the deflection until standard truck loading is fairly linear, due to the cracking already present from Test 1.

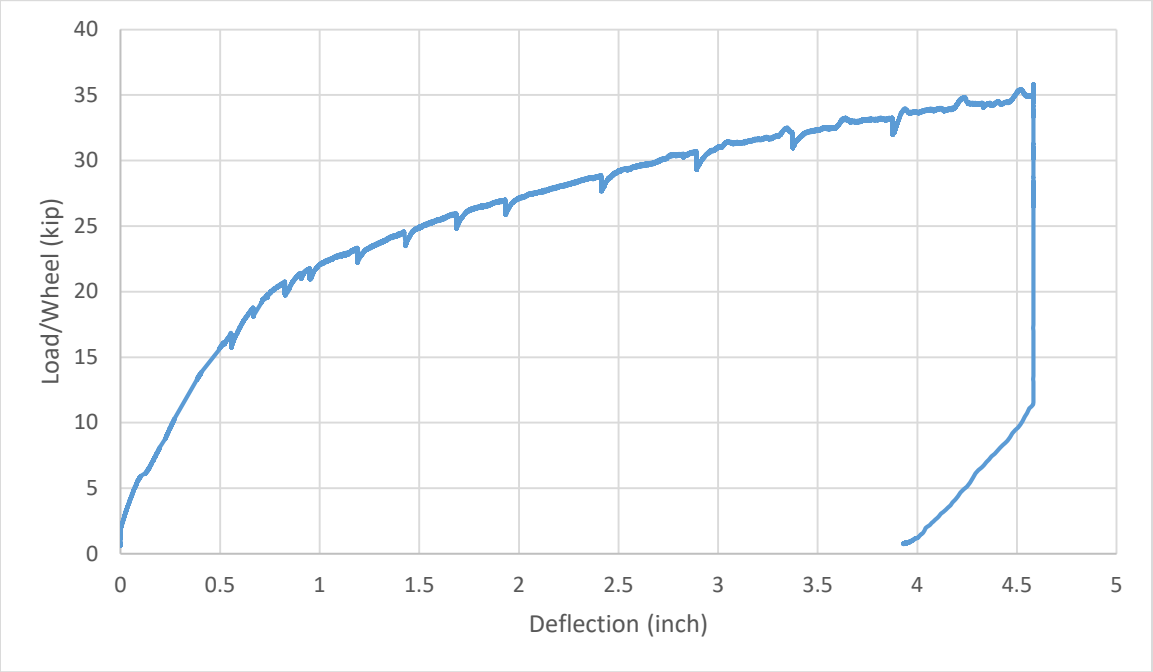

Figure 2-40. *Load-deflection curve at midspan of approach slab for Test 2.*

Figure 2-41 shows the deflection along the length of the curve at both standard truck loading condition, as well as at failure. As expected, in both conditions, the largest deflection occurred at midspan of the approach slab where the load was being applied. The largest deflection that occurred is approximately a half inch during standard truck loading. Similar to Test 1, the end of the approach slab resting on the roller support experienced upwards displacement due to the curvature of the specimen.

At failure, the deflection encountered at the midspan of the approach slab increased dramatically to more than four and a half inches. Due to this large deflection, the approach

slab end rotated an additional amount, and the end with the roller experienced a horizontal displacement of more than a quarter inch. The horizontal movement associated with the slab deflecting on the roller can be seen in Figure 2-42.

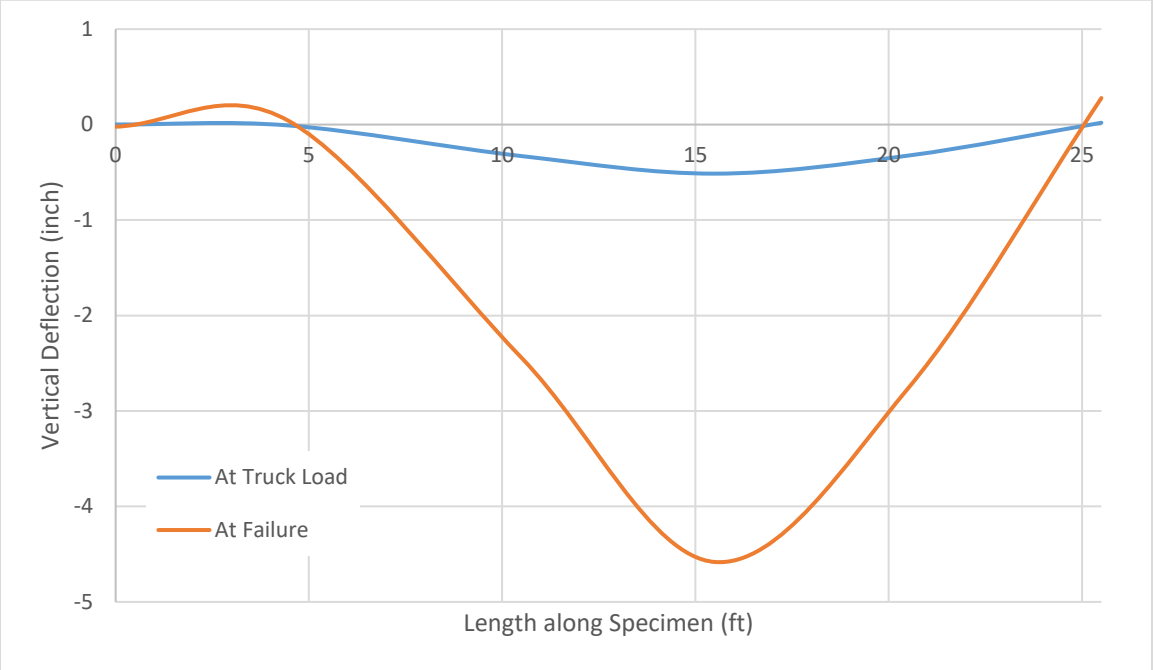

Figure 2-41. *Deflection along length of specimen at truck loading condition and failure, Test 2.*

Figure 2-42. *Horizontal movement of slab at roller support, Test 2.*

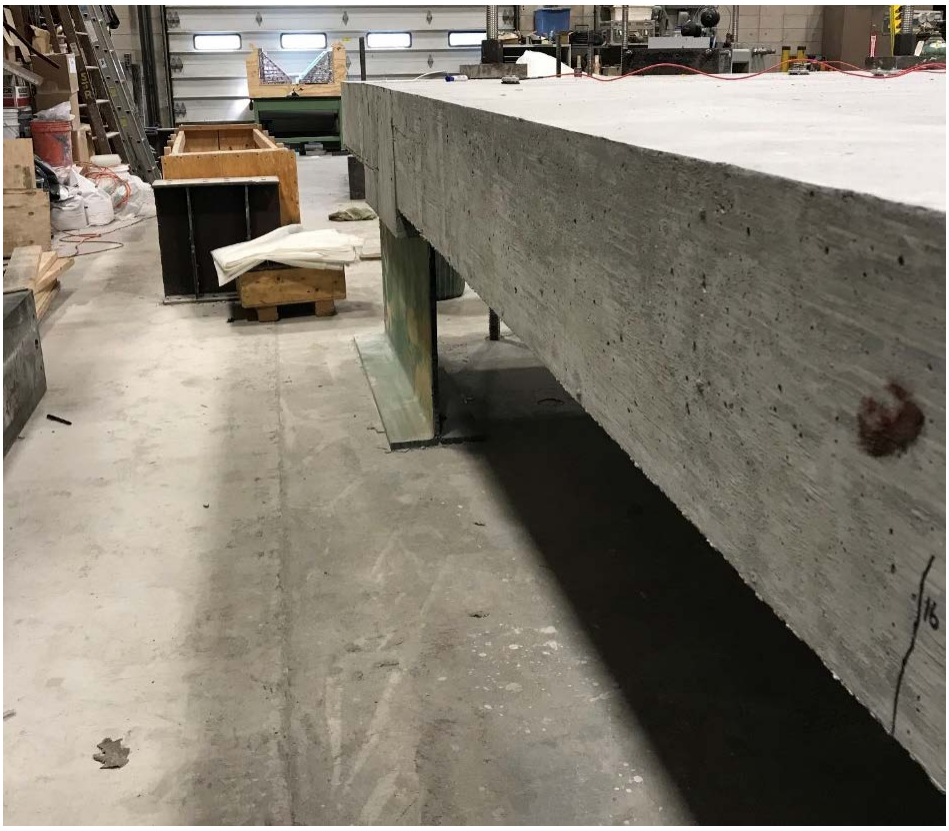

Figure 2-43. *Side view of deflection of lab specimen and rotation at beginning of approach slab, Test 2.*

2.5.3.3 LVDTs

LVDTs were utilized during Test 2 to monitor how far the saw cut opened during loading. Three displacement meters were placed along the width of the crack: two were placed on the outer edges, and one was placed at the center. At standard truck loading of 16 kips/wheel, the saw cut at the center of the width of the specimen had widened by 0.03”, and the outer edges of the saw cut widened by an average of approximately 0.06”. When the slab failed at more than 35 kips per loading area, the middle of the cut had widened by approximately 0.28”, and the two sides had widened by more than 0.64”.

2.5.3.4 Near Concrete Diaphragm

Because the top reinforcing was cut in Test 2, strain gages SG2, SG4, SG6, SG8, and SG10 were removed, as these gages existed at the location of the cut. Figure 2-44 shows the magnitudes of the strain gages existing in the concrete diaphragm. The bottom reinforcing gages are highlighted. As shown, the bottom reinforcing in the diaphragm experiences the largest tensile strain in the specimen during Test 2. Because the top reinforcing was cut, the bottom reinforcing was forced to take additional stress.

Figure 2-45 and Figure 2-46 show the strain experienced by the concrete in the diaphragm during loading until 16 kips per loading area. As shown, very little strain is experienced by the concrete on either the top or the bottom. Unlike Test 1, due to the presence of the saw cut, very little strain is felt in the diaphragm section past the cut reinforcing. This is also shown in Table 2-4, which presents the strain felt by reinforcing gages at 16 kips per loading area during Test 1 and Test 2. Gages 2, 6 and 22 existed above the hard support during Test 1, and therefore were cut during Test 2. Gages 18, 20, and 22 existed on the same reinforcing bar past the hard support. Therefore, by comparing gages 2 and 18, 6 and 20, and 10 and 22, one can see the continuity of strain in the two tests. As shown, the reinforcing past the hard support experiences very little strain in Test 2, as compared to Test 1.

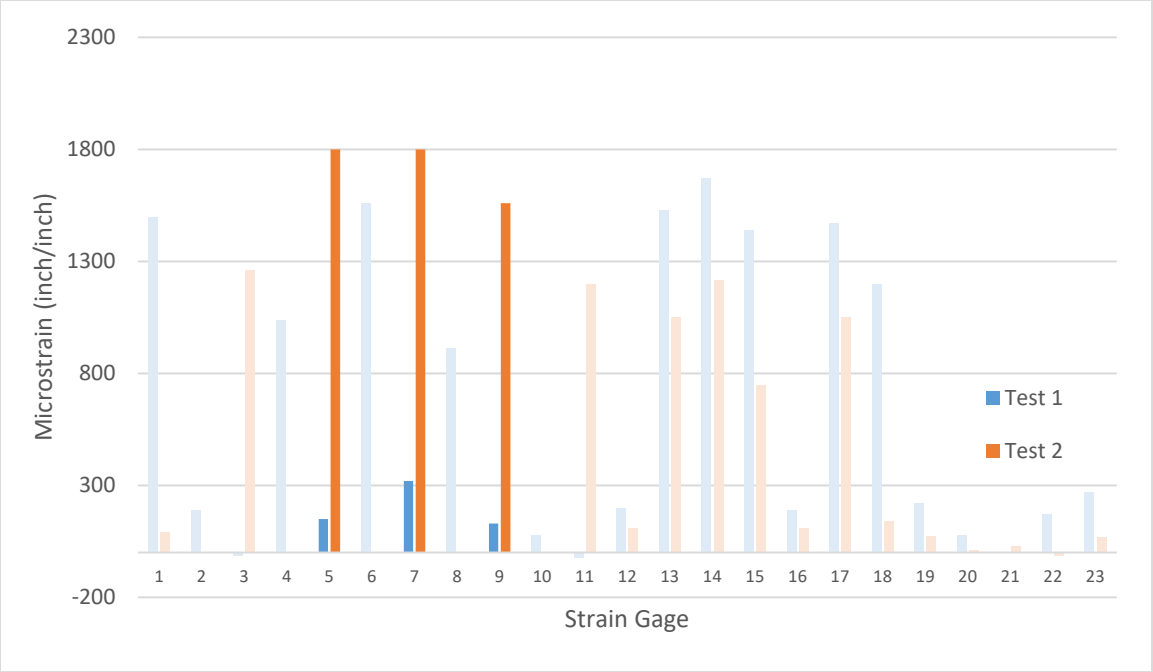

Figure 2-44. *Reinforcing strain gage magnitudes at 16 kips per loading area.*

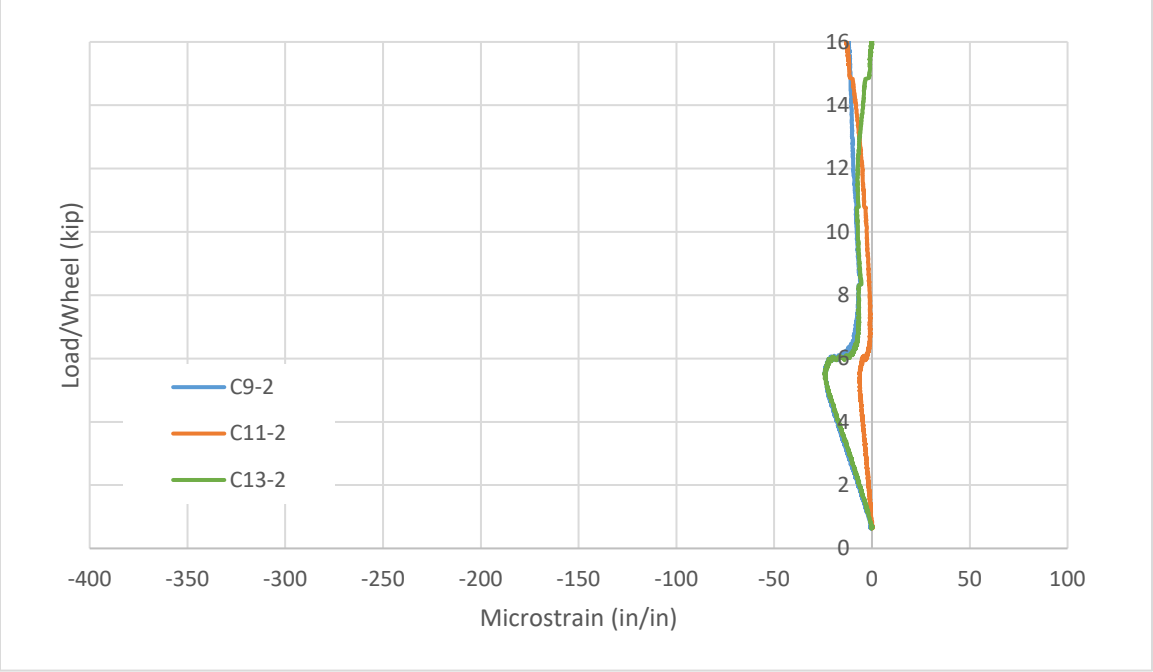

Figure 2-45. *Load-strain diaphragm for BDIs on bottom surface of concrete diaphragm, Test 2.*

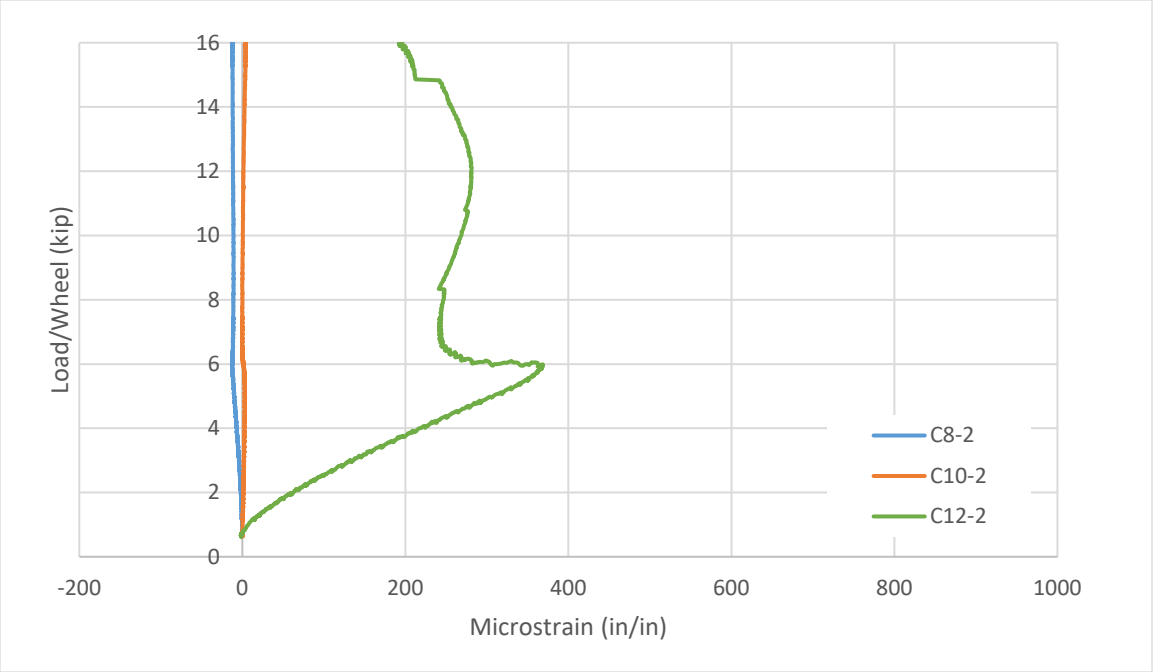

Figure 2-46. *Load-strain diaphragm for BDIs on top surface of concrete diaphragm, Test 2.*

Table 2-4. *Comparison of continuity of strain in reinforcing in Test 1 and Test 2 in concrete diaphragm section.*

Reinforcing Gage	Location	Test 1 Microstrain	Test 2 Microstrain
2	Outer reinforcing, above support	200	-
18	Outer reinforcing, past support	1560	140
6	Middle reinforcing, above support	1640	-
20	Middle reinforcing, past support	100	10
10	Outer reinforcing, above support	100	-
22	Outer reinforcing, past support	400	-10

2.5.3.5 Midspan of Approach Slab

The second area of interest, due to high strain values, is at the middle of the approach slab. As expected, those reinforcing strain gages at the midspan of the approach slab experienced less strain during Test 2 than Test 1, due to the shortened effective length of the approach slab with the presence of the hard support. With the shortened length, the positive moment caused by the load at midspan was minimized. At standard truck loading, SG14 and SG15, the gages in the center of the slab, experienced an average of 1555 microstrain.

The concrete gages on the top of the approach slab at midspan experienced similar compressive strains to those from Test 1. However, one can see a difference in the concrete strain at the third points when referencing both Test 1 and Test 2. Table 2-5 presents these differences. As shown, the first third point of the approach slab is in tension due to the negative moment in Test 1. However, because of the present of the hard support and cut top reinforcing, the entirety of the approach slab is in positive moment in Test 2, causing the first third point to experience compression.

Table 2-5. *Concrete strain along approach slab at standard truck loading, Test 1 and Test 2.*

Concrete Gage	Location	Test 1 Microstrain	Test 2 Microstrain
2/3	First third point	10	-150
4/5	Midspan	-210	-260
6/7	Second third point	0	0

2.6 Finite Element Modeling

2.6.1 Introduction

Two finite element models were developed to compare laboratory results with, each model corresponding to either Test 1 or Test 2 conditions. A brief overview pertaining to the characteristics of the finite element model is provided next.

2.6.2 Finite Element Model Characteristics

2.6.2.1 Element Type

To model the geometry, three-dimensional solid shapes were used for the concrete slab and steel girders. The steel reinforcing was modeled using wire shapes, with an associated cross sectional area that matched that of #5 and #6 reinforcing steel bars where each was applicable. Hex elements were utilized for the three-dimensional shapes, in order to yield accurate results and reduce computational time. A linear 3D truss element was utilized to model the wire elements. A mesh size of two inches was utilized to model all parts.

2.6.2.2 Material Properties

2.6.2.2.1 Concrete

Elastic material properties for concrete included the mass density, poisson's ratio, and modulus of elasticity. The mass density was based on a typical density of 150 lb/ft^3. The modulus of elasticity was based on an average compressive strength of 5.2 ksi, gained from cylinder tests completed at the time of testing. The lower of the strengths from the bridge deck and the approach slab was used. Hsu and Hsu (1994) stated that ACI 318-14 Building Code overestimates the modulus of elasticity with the typical equation $57{,}000\sqrt{f'_c}$. Therefore, an adjusted modulus of elasticity, Equation 2-1 calculated using was used.

$$E_0 = 1.2431 * 10^2 f'_c + 3.28312 * 10^3$$

Equation 2-1

Using this equation, the modulus of elasticity utilized in the model was 3919.1 ksi. The poisson's ratio was taken as 0.15.

Hsu and Hsu's model (1994) was used to generate the nonlinear stress-strain behavior for concrete. Unlike other models developed, Hsu and Hsu's model only relies on the compressive strength of the concrete. As shown in Figure 2-47, the concrete follows a linear stress-strain relationship corresponding to the maximum compressive strength, f'_c. Hsu and Hsu's model begins at $0.5f'_c$, and ends when the stress descends to $0.3f'_c$. Between these points, Equation 1-2 below describes the compressive stress values:

$$f_c = \left(\frac{\beta\left(\varepsilon_c/\varepsilon_o\right)}{\beta - 1 + \left(\varepsilon_c/\varepsilon_o\right)}\right) f'_c$$

Equation 2-2

where

$$\beta = \frac{1}{1-\left[f'_c/\varepsilon_o E_o\right]}$$

Equation 2-3

and $\varepsilon_o = 8.9 * 10^{-5} f'_c + 2.114 * 10^{-3}$

Equation 2-4

The inelastic strain of the concrete, ε_c^{in}, is equivalent to the total strain, ε_c, minus the elastic strain, dictated as:

$$\varepsilon_c^{in} = \varepsilon_c - \frac{f'_c}{E_o}$$

A damage factor was be used to represent the degradation of the elastic stiffness of the system, and can be calculated using the following equation:

$$d = 1 - \frac{f_c}{f'_c}$$

The relationship between the elastic modulus and the compressive damage factor is:

$$E = (1 - d)E_o$$

To capture the tension stiffening in the concrete, the Nayal and Rasheed (2006) model, modified by Wahalathantri et al. (2011), was used. Similar to the concrete compressive parameters, both the nonlinear stress-strain behavior and tensile damage was defined. Figure 2-48 below shows the tensile behavior of the concrete. The concrete behavior is linear until reaching the maximum tensile stress, f_{to}, corresponding to the cracking strain, ε_{cr}. Then, the stress decreases until $0.77f_{to}$, corresponding to $1.25\varepsilon_{cr}$. The stress decreases additionally to $0.45f_{to}$, corresponding to $4\varepsilon_{cr}$, until reaching $0.1f_{to}$, corresponding to $8.7\varepsilon_{cr}$. The maximum tensile stress was calculated using $7.5\sqrt{f'c}$, and the maximum tensile stress was calculated using Hooke's Law. Tension damage parameters were calculated in a similar fashion to compression parameters. Figure 2-49 describes the relationship between the compressive and tensile stress, and the compressive and tensile damage, respectively.

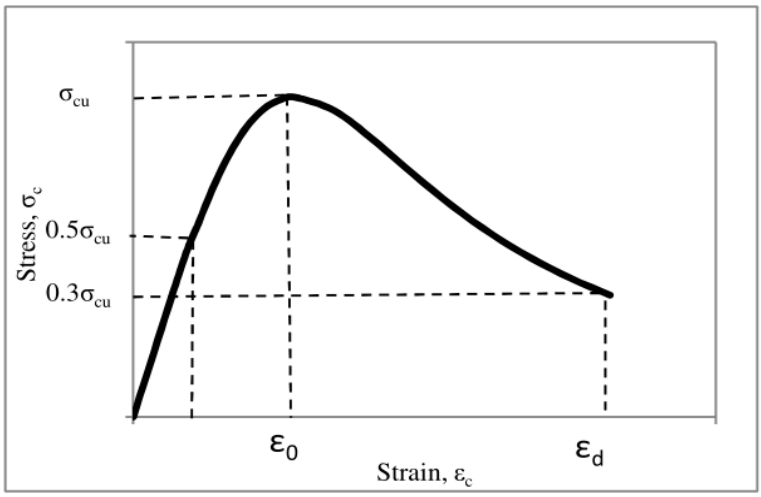

Figure 2-47. *Compression stress-strain surve. Source: Hsu and Hsu (1994).*

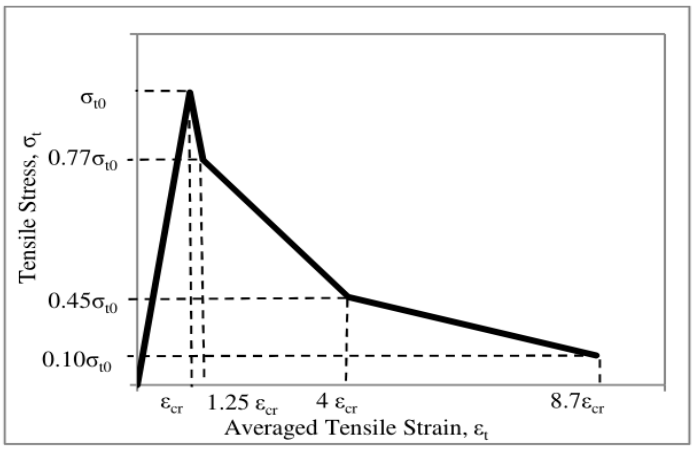

FIGURE 04: Modified Tension Stiffening Model for ABAQUS

Figure 2-48. *Tension stress-strain curve. Source: Wahalathantri et al. (2011).*

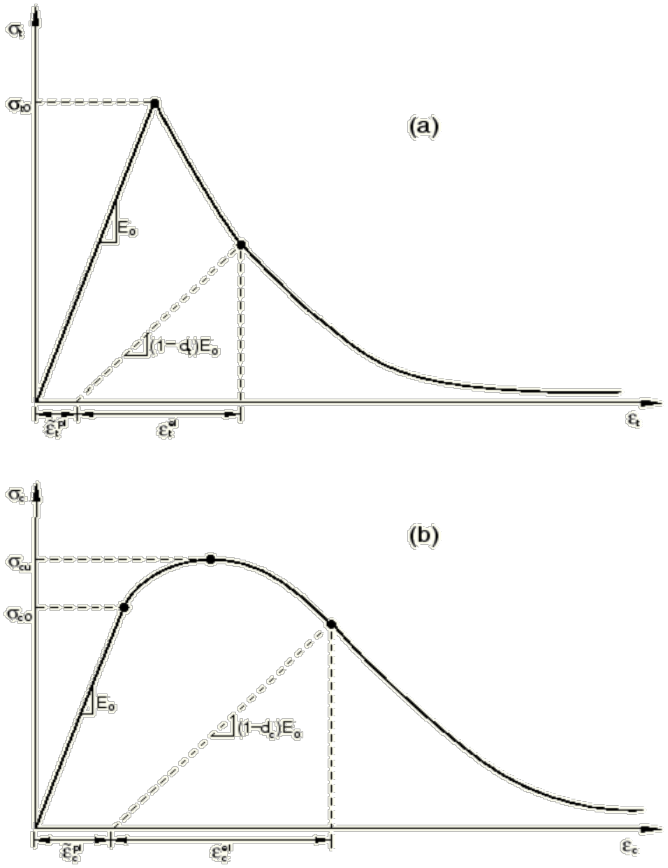

Figure 2-49. *Tension and compression stress-strain reponse with damage relationship. Source: ABAQUS (2013).*

In addition to the stress-strain tension and compression models, the following properties were utilized in the FE model:

- Dilation angle: 31°
- Eccentricity: 0.1
- Ratio of biaxial strength to uniaxial strength, f_{bo}/f_{co}: 1.16
- Ratio of the second stress invariant on tensile meridian, K: 0.667
- Viscosity parameter: 0.0005

2.6.2.2.2 Steel

Only elastic properties were defined for the reinforcing steel and the steel girders, as both of these components were expected to stay in their elastic range during testing. A modulus of elasticity of 29,000 ksi and a poisson's ratio of 0.19 was utilized for both.

2.6.2.3 Boundary Conditions and Constraints

In both FE models, the boundary conditions were the same. As shown in Figure 2-50, the bottom of the steel girders were fixed. Six inches in from the edge of the approach slab, a boundary condition restrained movement in the y direction, simulating a roller support.

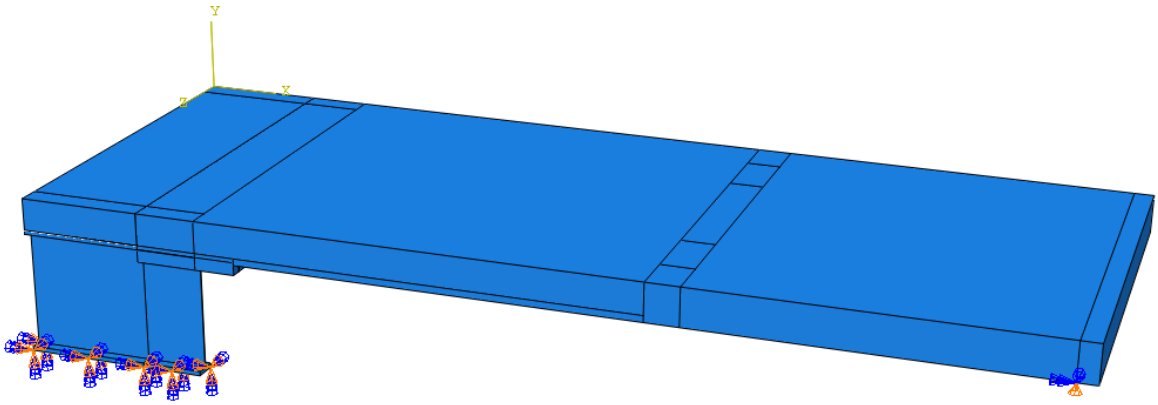

Figure 2-50. *Boundary conditions in both Test 1 and Test 2 FE models.*

Constraints were added to both models, tying the top of the steel girder to the bottom of the concrete resting against. This is shown in Figure 2-51. Additionally, the reinforcing was embedded into the concrete element.

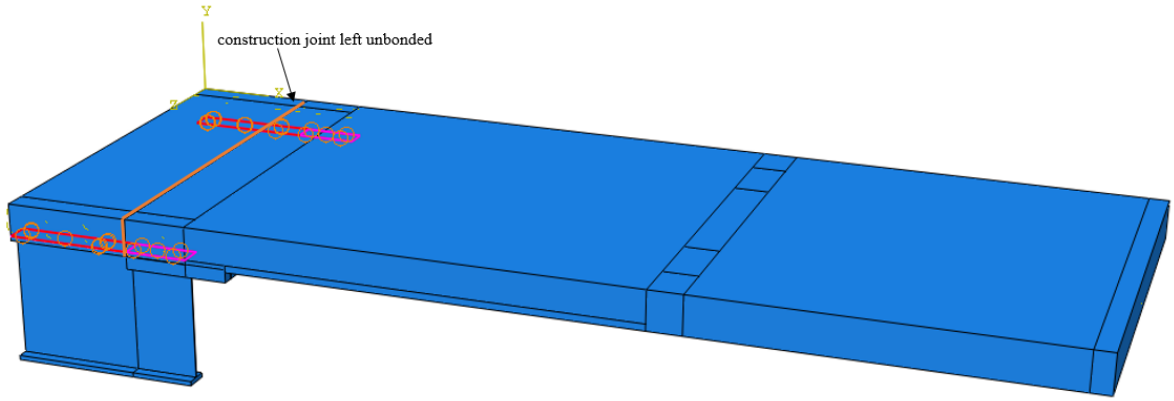

Figure 2-51. *Constraints in FE model and unbonded construction joint.*

For Test 2, a hard support was inserted under the approach slab, and the top concrete cover and reinforcing steel was cut centered above the support. The edge of the hard support was constrained to the bottom of the approach slab as shown in Figure 2-52. The bottom of the hard support was fixed, preventing it from moving translationally or rotationally. Besides these changes, all other constraints and boundary conditions were kept the same.

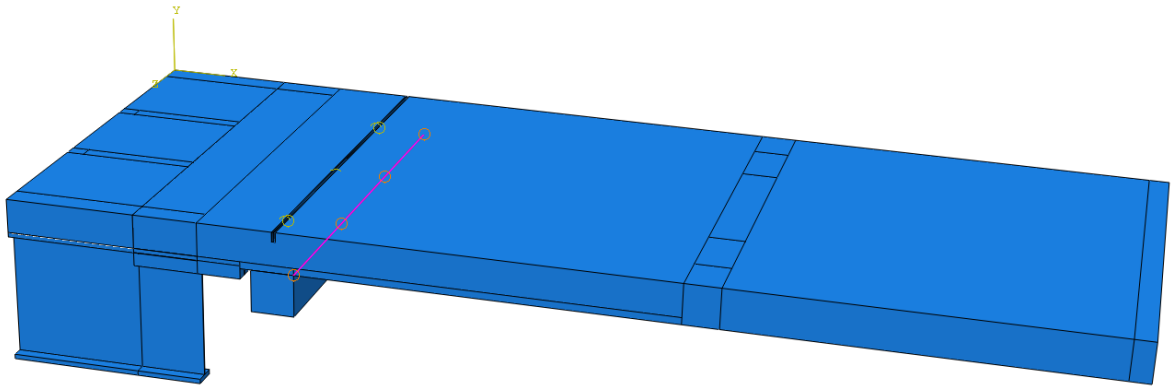

Figure 2-52. *Test 2 FE model and added elements.*

2.6.2.4 FE Model vs. Experimental Results

Figure 2-53 shows a comparison of the deflection along the length of the span for the FE model compared to Test 1 results. As shown, results are fairly consistent throughout. With these consistent results, more accurate results from Test 2 can be confidently found, not having to worry about a previously cracked specimen impacting the results.

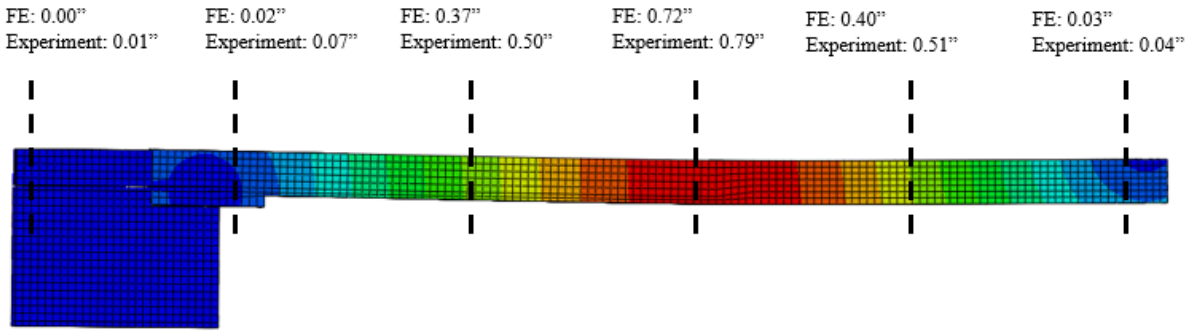

Figure 2-53. *Comparison between FE model and experimental results for deflection along length of specimen, Test 1.*

Cracking patterns in the finite element model are shown through tensile damage parameters. Cracking patterns for the specimen are presented in Figure 2-54 through Figure 2-57. One can see that the cracking patterns for Test 1 closely resemble those experienced by the specimen during the experiment. Fortunately, through FE modeling, the cracking that

would occur in Test 2 can be more accurately predicted. As shown, no cracking is experienced by the top of the specimen in Test 2, specifically in the existing bridge section due to the release of stress at the saw cut. Overall, tensile damage is similar on the bottom of the specimen between Test 1 and Test 2 FE models. However, cracks in the Test 1 model do extend slightly further along the length of the specimen, and cracks in the Test 2 model are spaced closer together. Both of these observations are due to the presence of the hard support.

This same pattern can be seen in Figure 2-58. Figure 2-58 presents the distribution of E11 strain along the length of the specimen during Test 1 and Test 2. Similar to those results mentioned above, one can see that the stress is spread more on the bottom of Test 1, as compared to Test 2. Additionally, one can see that the stress concentration in the diaphragm and bridge deck sections in Test 2 is concentrated to the saw cut area, whereas in Test 1 it is not. Figure 2-59 shows the same strain along the length of the specimen for Test 1 and Test 2, respectively, however, for the reinforcing. One can see that the Test 1 model has a larger stress concentration at midspan of the approach slab as compared to Test 2. However, a new stress concentration was formed above the hard support in Test 2, due to the high strain experienced by the bottom reinforcing. Finally, one can see the reinforcing carrying stress into the bridge deck in Test 1, whereas in Test 2 the stress is released before this point.

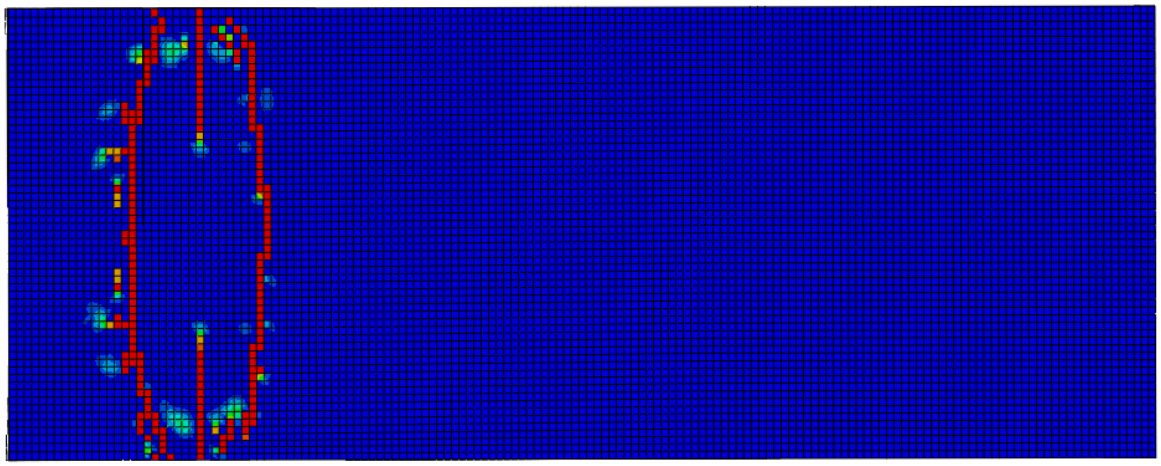

Figure 2-54. *Tensile damage on top of specimen, Test 1.*

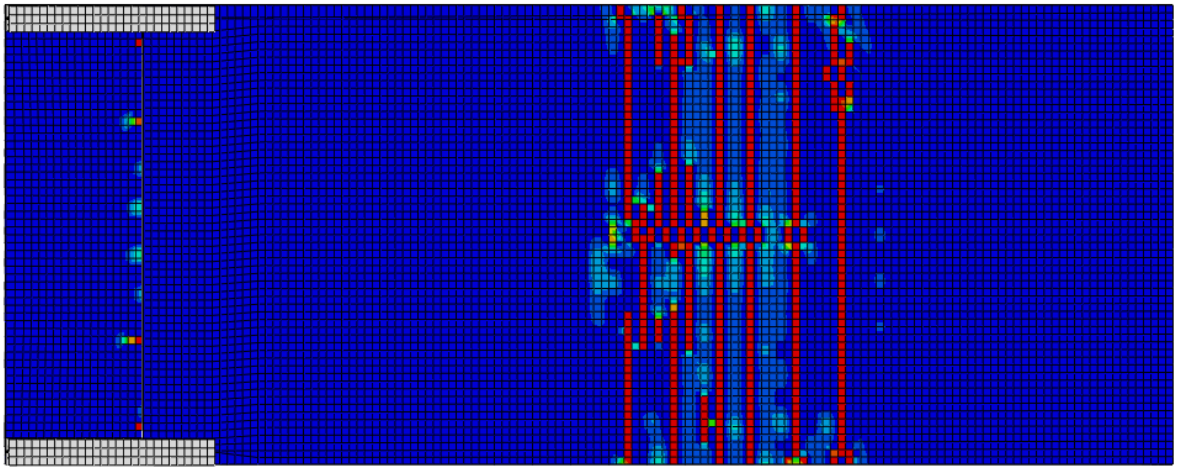

Figure 2-55. *Tensile damage on bottom of specimen, Test 1.*

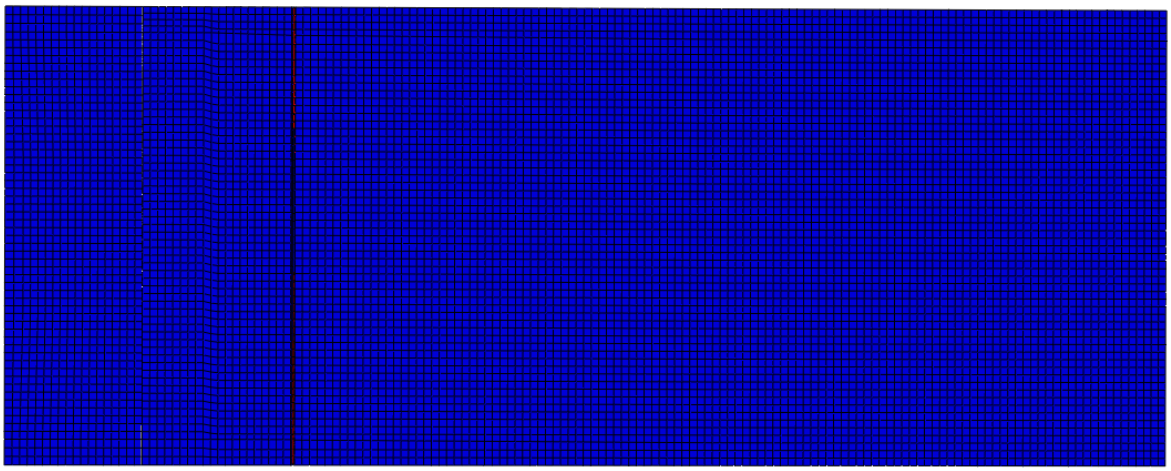

Figure 2-56. *Tensile damage on top of specimen, Test 2.*

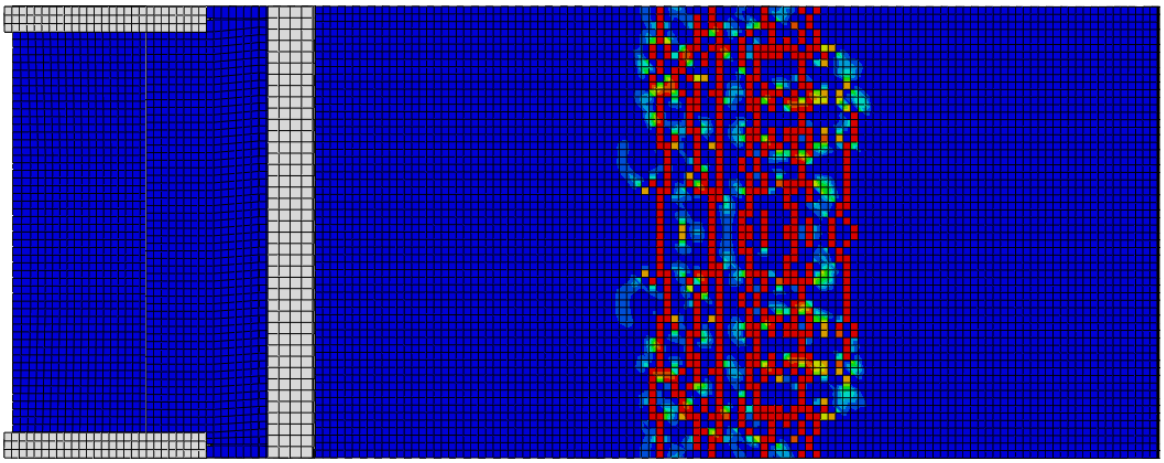

Figure 2-57. *Tensile damage on bottom of specimen, Test 2.*

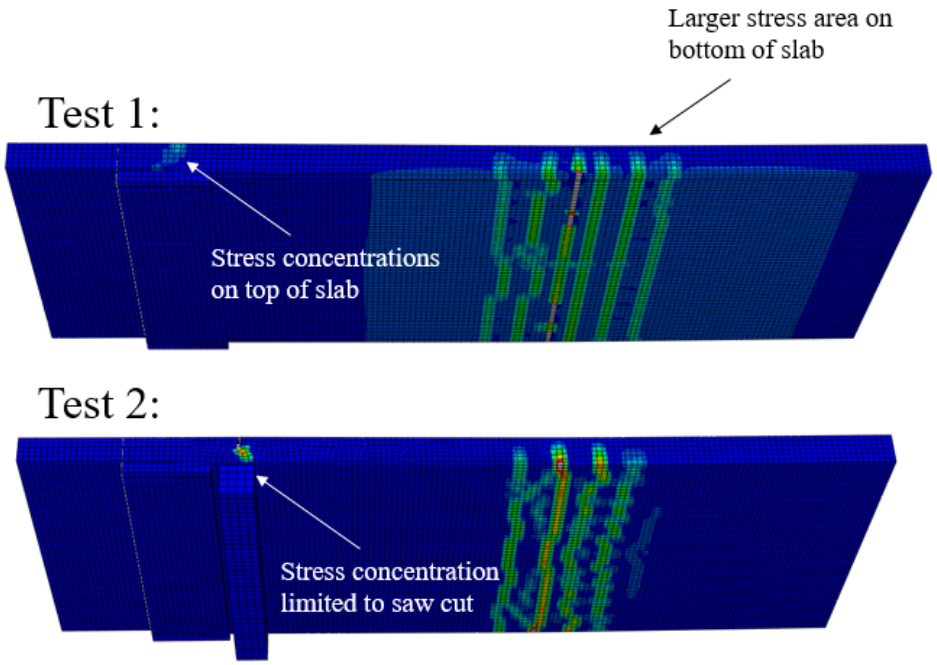

Figure 2-58. *Strain (E11) in concrete along length of specimen, Test 1 compared to Test 2.*

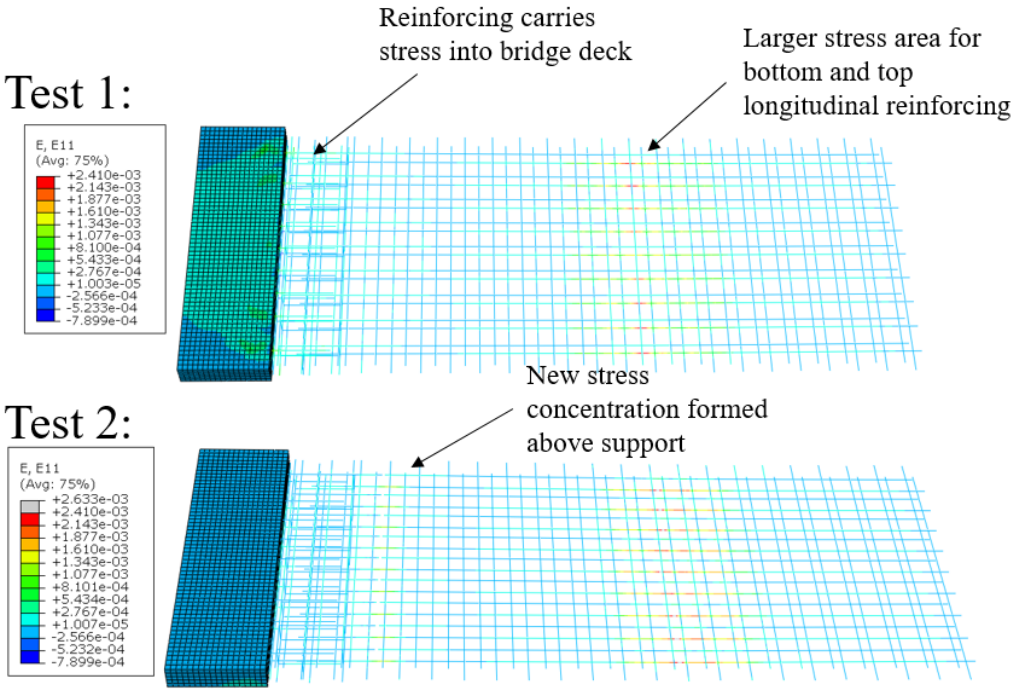

Figure 2-59. *Strain (E11) in reinforcing along length of specimen, Test 1 compared to Test 2.*

Similar to cracking experienced in testing, the Test 2 FE model shows a very large stress concentration near the saw cut and hard support. During testing, cracks propagated from the bottom of the saw cut to the bottom of the approach slab. Figure 2-60a shows similar cracking happening. Figure 2-60b shows the stress occurring in this area. One can see that a large stress concentration occurred where the approach slab was resting on the corner of the hard support. Because the slab had rotated, only a small part of the specimen was resting on this corner, causing a large stress concentration. The weakness of the saw cut, coupled with an increase in stress directly below, naturally caused cracking to occur at this location.

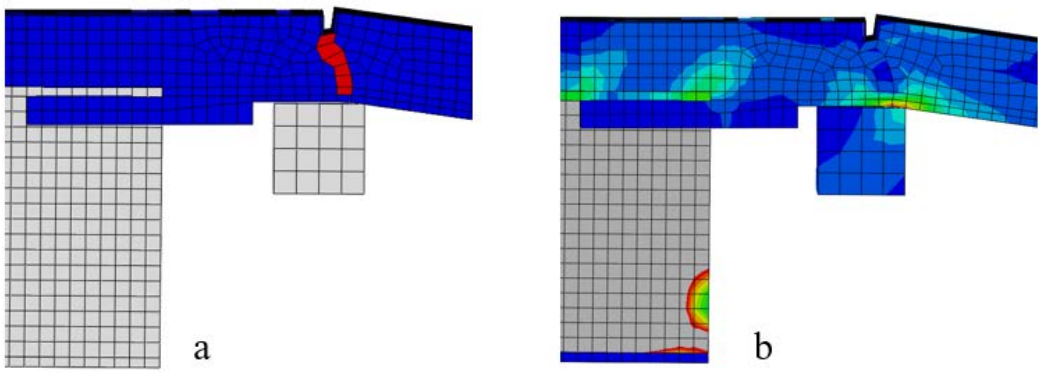

Figure 2-60. *Cracking and stress concentration at saw cut and hard support, Test 2.*

2.7 Conclusions and Future Work

Assessing the results from the laboratory specimen in both Tests 1 and 2, as well as the supporting results from the FE models, the following conclusions can be drawn relating to the performance of the detail, if utilized in a real bridge structure:

1. Cutting the top longitudinal reinforcing minimizes the stress that the bridge deck experiences from the negative moment caused by loading. If not cut,

cracks will form on the surface of the bridge deck, possibly leading to the leaking of harmful chemicals to the substructure.

2. If the decision is made to cut the top longitudinal reinforcing, special care must be made towards the filler material in the saw cut. The material should be able to withstand significant stretching and deformation. Additionally, the material should serve as a protective layer against cracking that could occur underneath the saw cut. This being said, creating a saw cut could lead to increased stresses underneath, and promote the formation of cracks. Due to cracking and deformation, this saw cut could create a bump in driving conditions.
3. Cracking could be mitigated underneath the saw cut by moving the cut to the edge of the backwall. When the saw cut is in the middle of the backwall, the rotation of the approach slab causes stress to transverse from the contact point to the bottom of the saw cut, creating cracking.
4. The end of the approach slab, independent of cutting the top longitudinal reinforcing, will experience rotation. When designing the connection between the roadway and approach slab, the engineer should take this upward rotation into account.
5. The presence of a backwall increases the moment capacity of the approach slab section, due to a decrease in the effective length. This, in turn, reduces the stresses felt by the section midspan.

6. If soil is present underneath the approach slab, the stresses experience by the lab specimen (as described by either Test 1 or Test 2) will be minimized, dependent on soil properties.

Considering the wide scope of this project, as well as the wide range of related topics, future work in the area could be a more in depth investigation of several different areas. A sampling of these possibilities are listed below.

1. Investigation of the best material to use to fill the saw cut, if made. This material would have to withstand extensive deformation, both horizontally and rotationally. Additionally, this material would have to withstand de-icing chemicals.
2. Research exploration of the interaction of the two surfaces at the construction joint. Research should seek to quantify the bond between the two surfaces, as well as find a way to improve the bond. Testing showed that if the top longitudinal reinforcing was continuous, the construction joint was one of the weakest parts of the specimen.
3. A study utilizing FE modeling on additional possible options for the end of the approach, in transition to the roadway. This could include investigation of using a sleeper slab or micropiles.

2.8 References

Aktan, H., Attanayake, U., and Ulku, E. (2008). “Combining Link Slab, Deck Sliding over Backwall, and Revising Bearings.” Kalamazoo, MI: Western Michigan University.

Alampalli, S., and Yannotti, A. P. 1(998). “In-Service Performance of Integral Bridges and Jointless Decks.” *Transportation Research Record*, 1(1624), 1-7.

Faris, A. 2009. “An integral precast approach slab to bridge connection.” Ames, Iowa: Iowa State University.

Federal Highway Administration. (2005). "Integral Abutment and Jointless Bridges." *2005 – FHWA Conference*, Baltimore, Maryland, 343.

Hoppe, E., Weakley, K., and Thompson, P. (2016). "Jointless Bridge Design at the Virginia Department of Transportation." Transportation Research Procedia, (14), 3943-3952.

Iowa DOT Office of Bridges and Structures. (2018a). *LRFD Bridge Design Manual.* Ames, IA.

Iowa DOT Office of Design. (2018). "Standard Road Plans – BR Series." Double Reinforcing 12" Approach (Slab Bridge), https://iowadot.gov/design/stdplne-br (Sep. 28, 2016).

Miller, A. M., and Jahren, C. T. (2014). *Rapid Replacement of Bridge Deck Expansion Joints Study – Phase I.* Ames, IA: Institute for Transportation Construction Management and Technology Program and Iowa State University.

Miller, A. M., and Jahren, C. T. (2015). *Rapid Replacement of Bridge Deck Expansion Joints Study – Phase II.* Ames, IA: Institute for Transportation Construction Management and Technology Program and Iowa State University.

Miller, A. M., Nelson, J. S., and Jahren, C. T. (2015). "Rapid Bridge Deck Joint Repair and Rehabilitation." Ames, IA, 17.

Ministry of Transportation, Ontario. (1999). "Semi-Integral Abutment Bridges." Toronto, Ontario, Canada: Ministry of Transportation Ontario.

Morandeira, David. (2018). "Rapid bridge deck joint repair investigation – Phase III," thesis, presented to Iowa State University at Ames, IA, in partial fulfillment of the requirements for the degree of Masters of Science in structural engineering.

White II, H. (2007). "Integral Abutment Bridges: Comparison of Current Practice between European Countries and the United States of America." Albany, New York: New York State Department of Transportation.

Wright, J. R., Rajabipour, F., Laman, J. A., and Radlińska, A. (2014). "Causes of Early Age Cracking on Concrete Bridge Deck Expansion Joint Repair Sections." *Advances in Civil Engineering*, 2014, 10.

Yannotti, A.., Alampalli, S., and White, H. (2005). "New York State Department of Transportation's Experience with Integral Abutment Bridges." IAJB 2005, Baltimore, MD, 12-19.

CHAPTER 3. BEHAVIOR OF REINFORCING CONCRETE WALLS WITH CIRCULAR OPENINGS

A paper to be submitted to Engineering Structures

Elizabeth Miller, Yinglong Zhang[2], Zhe Wang[3], Dr. An Chen

Abstract

A Tuned Liquid Wall Damper (TLWD) system created by Wu et al. (2017) allows typical gravity-load carrying walls to act as both gravity and lateral load resisting elements. The TLWD system not only increases the damping of a structure, thereby reducing stress and displacement, but also mitigates heat loss due to the filler liquid's large specific heat capacity.

Reinforced concrete is a commonly used building material that has a construction practice that would allow for the TLWDs to be built inside of walls. While the reinforced concrete TLWD system would increase the structure's damping, with the placement of the system would come an associated strength reduction due to the minimization of concrete material. This paper focuses on the strength reduction associated with the capillaries, or holes, caused by a scaled TLWD system in reinforced concrete walls. Using an optimized geometry, experimental testing was performed on six walls. Two walls were tested in axial compression, two walls were tested via a pushover test, and two walls were tested with a four-point bending test to yield the axial strength, strong-axis moment capacity, and weak-axis bending capacity, respectively. Cracking, failure load, and failure mode were monitored during testing. At the end of testing, finite element models were developed and correlated

[2] Designed geometry and reinforcing for reinforced concrete wall and footing. Completed multi-objective optimization to find wall with optimal hole solution. Completed laboratory work for four-point bending test, designed laboratory setup for pushover and axial load tests. Created preliminary finite element models.
[3] Assisted in development of finite element models.

with results. Then, models of solid reinforced concrete walls were created in order to compare the failure mode and load with the walls with holes. Results showed that the strength reduction from the solid wall case to the wall with holes case is highly dependent on the loading condition. The strength reduction associated with the walls with holes was not necessarily too large of a reduction to prevent from using the TLWD system. In considering pure axial compression, the failure load was directly related to the cross sectional area of the holes and the compressive strength of the concrete. In terms of flexural bending, the reduction of strength associated with the walls with holes could be mitigated by providing additional flexural reinforcing to the section.

This material is based in part upon work supported by the National Science Foundation under Grant No. CMMI-1562992. Any opinions, findings, and conclusions or recommendations expressed in this material are those of the authors and do not necessarily reflect the views of the National Science Foundation.

3.1 Introduction

Structural walls are typically designed to act either only as gravity load resisting components, or as both gravity and lateral load resisting components. Those walls designed to only carry gravity loads are inactive in resisting lateral loads. A Tuned Liquid Wall Damper (TLWD) design for walls, proposed by Wu et al. (2017), can allow typically gravity-load only carrying walls to act as both gravity and lateral load resisting elements.

Tuned Liquid Column Dampers (TLCDs) are a type of passive damping system. TLCDs consist of tubes, also called capillaries, connected at the bottom by a U-shape, allowing the liquid in the tubes to oscillate freely inside. The frequency of the TLCD system depends on the height of water filling the pipes, as well as the factor of loss, controlled by the size of the orifice located at the horizontal portion of the tubing (Chakroborty, Debbarma,

and Marano, 2012). When a building vibrates, due to either wind or seismic forces, the motion of the liquid inside of the columns counteracts the lateral forces on the structure. A TLWD is similar in notion to that of a TLCD, in that the damping of the system is a function of the head loss between each pipe. This is shown in Figure 3-1. Unlike TLCDs, however, TLWDs can be built inside of structural walls. Additionally, TLWDs can be installed over multiple floors, dependent on the damping needed in a building. This differs from traditional TLCDs, which are usually installed on the top floor of structures (Wu et al., 2017). Finally, TLWDs can be used to mitigate heat loss in a structure, due to a liquid's large specific heat capacity (Wu et al., 2017).

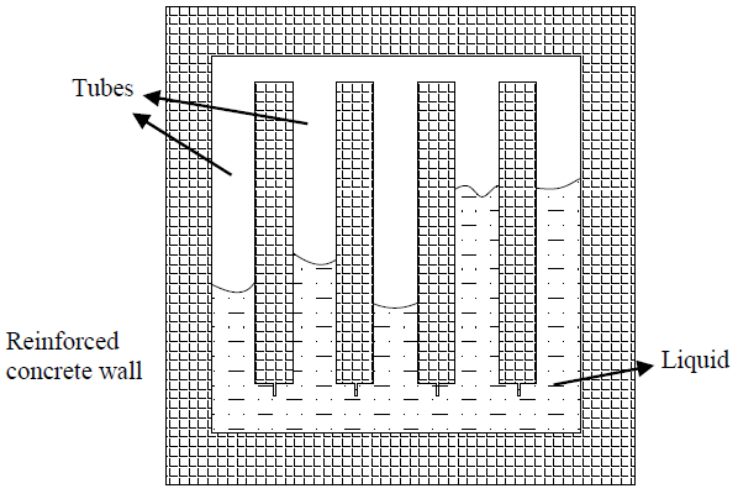

Figure 3-1. *Tuned liquid wall damper. Source: Wu et al. (2017).*

High-rise buildings of today, while sleek in design and effective in land use, come with an assortment of structural issues. High-strength steel components, lighter cladding and materials, and modern construction techniques have allowed buildings to have lower frequencies and damping values (Steffen, 2016). When subjected to lateral dynamic loads, through wind or seismic events, buildings with low damping are susceptible to increased amplitudes of motion and acceleration (Kwok et al., 2009; Chopra, 2014). Due to increased

lateral displacement, buildings will experience larger internal stresses and strains, possibly compromising structural stability. In order to increase the damping of high-rise buildings, tuned dampers can be placed inside of the structure. By utilizing a damper such as the TLWD as proposed by Wu et al. (2017), damping of the building can be increased, mitigating the structural response.

Reinforced concrete is commonly used for structural walls in building systems, and would have the geometry and construction practice that would allow for TLWDs to be built inside. Reinforced concrete walls are primarily used as bearing walls and shear walls. By placing TWLDs inside of reinforced concrete, bearing walls could serve dual purpose inside of a building's structural system. However, with the placement of the TLWD inside of the reinforced concrete wall, there will be an associated strength reduction due to minimization of concrete material. This research explores the strength reduction associated with a TLWD inside of a reinforced concrete wall.

3.2 Methodology

To explore the relationship between the efficiency of the TLWD versus the strength reduction in a reinforced concrete wall, both lab testing and numerical analyses were completed. First, an optimization of the geometry of the TLWD capillaries was completed using hand calculations. The optimization helped in selecting the size and number of pipes that would minimize the strength reduction of the wall, while still maximizing the damping effect of the TLWD. Optimization was completed by Yinglong Zhang, and details of calculations may be found in, "Behavior of reinforced concrete walls with circular openings" (Zhang, 2018). Next, lab testing was completed using the geometry that was decided upon from optimization. Three tests were completed on reinforced concrete wall samples. Axial load tests were completed to determine the bearing capacity of the wall. Four-point bending

tests were completed to determine the bending capacity in the weak axis configuration. Pushover tests were completed to determine the bending strength in the strong axis configuration, as well as the shear strength of the wall. Two walls were used for each test. After laboratory testing was complete, results were compared with finite element models. The strength of the walls with openings was compared to the strength of plain reinforced concrete walls without openings. Additionally, correlation and calibration of results allows the models to be used for further depictions of concrete wall behavior if geometry or loading conditions were changed.

3.3 Multi-Degree Optimization

The TLWD was optimized inside of a five foot tall, two foot wide, and four inch thick reinforced concrete wall, with #2 reinforcing. These dimensions are proportional to that of a typical structure wall, however, were shrunken due to laboratory space and loading limitations. Reinforcement design was completed using ACI 318-14 Building Code. It should be noted that the cover of concrete along the transverse direction of the wall was reduced from ¾ minimum (as specified by ACI 318-14) to 0.425”; this resulted from the limited space due to the proportionally small size of the wall. Capillaries in the walls were created using PVC tubes, for ease of construction. Optimization was completed by considering the damping associated each tube configuration, along with hand calculations assuming strength reduction. The minimum solution corresponded to a configuration with seven tubes that each have a diameter of 1.315 inches. This geometry was utilized for both lab testing, as well as correlation with finite element models. As noted earlier, a detailed description and presentation of equations used in this optimization may be seen in “Behavior of reinforced concrete walls with circular openings” (Zhang, 2018).

3.4 Experimental Investigation

Using the results from the multi-level optimization, six wall specimens were constructed to test the strength reduction associated with the openings in the walls. Two specimens were testing in flexural bending utilizing a four-point bending test, two specimens were tested in axial compression, and two specimens were tested utilizing a pushover test. Results from the laboratory testing were utilized to compare with finite element models.

3.4.1 Testing Objectives

The objectives of the experimental investigation were simple in nature:

1. Observe the performance of the wall when subjected to a four-point bending test, including failure load and cracking patterns.
2. Observe the performance of the wall when subjected to an axial compression test, including failure load and failure mode.
3. Observe the performance of the wall when subjected to a pushover test, including failure load and cracking patterns.

3.4.2 Testing Plan

Three distinct tests were carried out on the walls. The testing setup associated with each wall is shown in Figure 3-2. In the axial load test, three actuators applied load to a rigid steel beam filled with concrete mounted firmly to the top of the wall. In the pushover test, an actuator mounted to the loading frame via another steel member applied a horizontal load to the rigid beam on the top of the wall. The horizontal load was applied in the strong axis direction of the wall. Again, the rigid beam was mounted firmly to the top of the concrete wall, allowing the two to act as one structure. In both of these tests, the wall-footing assembly was tied to the strong floor of the laboratory. In the four-point bending test, the walls were laid flat, supported by steel tubes at either end. The left steel tube was fixed to a

bottom plate underneath, acting like a pinned connection. The right steel tube was left to move freely in the horizontal direction, acting like a roller support. Each tube was inset from the edge of the wall by two inches. Two beams were placed at third points on top of the wall, on top of which another beam was placed. An actuator applied load to the top beam, and the load was transferred to the two beams at the third points, testing the beam in flexure. All tests were run until failure. Force control was used at the beginning of testing, however, at the end of both the four-point bending tests and pushover tests, displacement control was used.

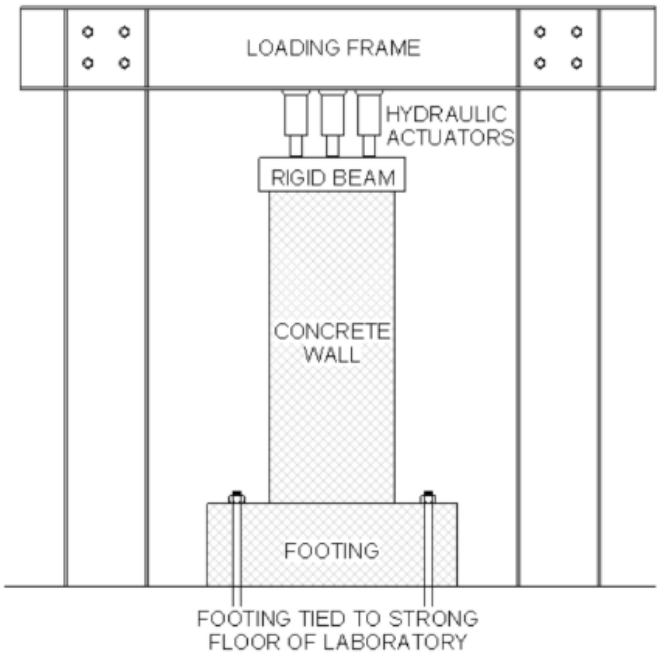

(a)

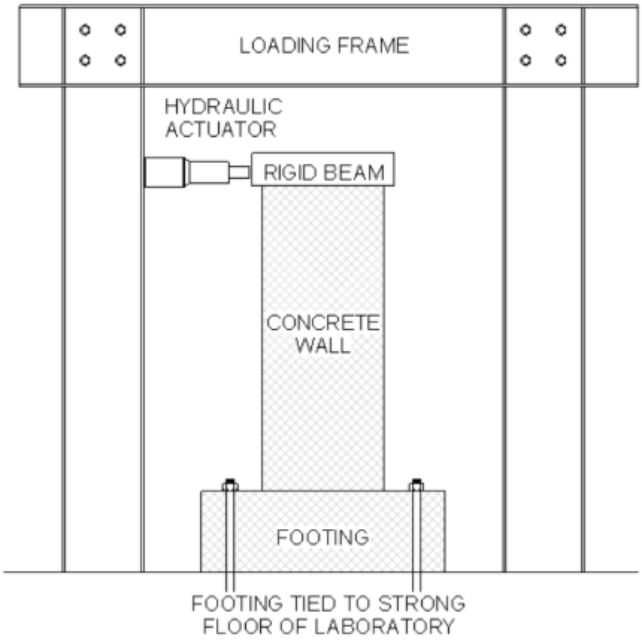

(b)

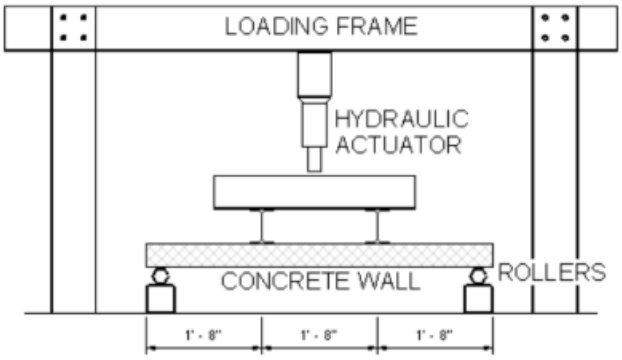

(c)

Figure 3-2. *Testing setup for (a) axial load test, (b) pushover test, (c) four-point bending test.*

3.4.2.1 Geometry

The geometry for each wall was identical, and is shown in Figure 3-3. As seen, from the optimization, seven 1.315 inch diameter tubes are used for the capillaries. For ease of construction, PVC tubes were utilized to create the holes. On either side of the PVC tubes, there were four vertical #2 reinforcing bars, and eight transverse #2 reinforcing bars tied

together. During construction, circular plywood blocks were utilized to hold the tubes in place in relationship with the steel reinforcing. This is shown in Figure 3-4.

As mentioned, for the axial loading and pushover tests, a reinforced concrete footing was provided at the base of the wall. The reason for this was solely to provide a means for the wall to tie to the strong floor of the laboratory floor, allowing the base of the structure to act in a fixed manner. Although the wall and footing were poured separately, reinforcing hooks were provided from the wall into the footing, encouraging the two pieces to act as one. Additionally, it is very rare for footings and walls to be poured continuously in construction practice.

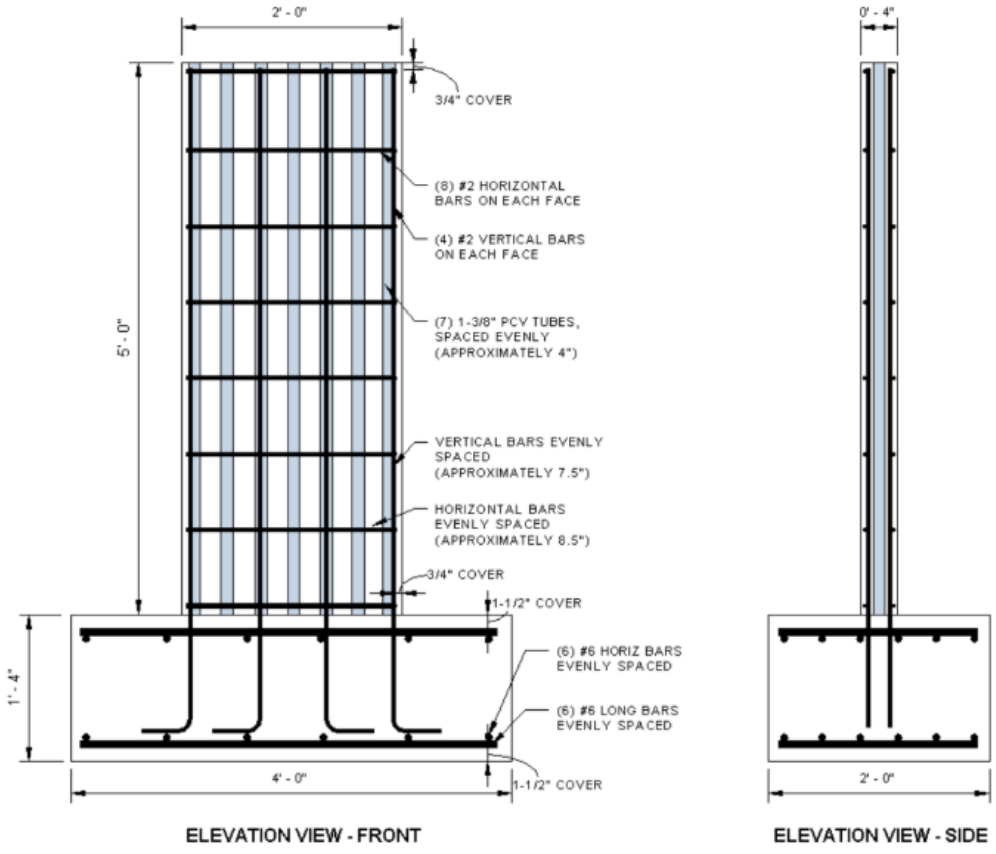

Figure 3-3. *Geometry of wall with PVC tubes.*

Figure 3-4. *Construction of wall with embedded PVC tubes.*

3.4.2.2 Materials

Because the cover provided for the concrete was so small, a C4 mix with maximum ¾" aggregate size was utilized for the walls. The compressive strength of the concrete was tested every time that a wall was tested in the laboratory. The average of all of these tests was approximately 7.5 ksi.

Number 2 steel bars were used for all reinforcing. Properties from uniaxial tests completed by Zhang (2018) were utilized to obtain the stress-strain relationship. A strain gage was attached to the center of a two-foot long piece of reinforcing, supported by two hydraulic wedge grips, as shown in Figure 3-5. The reinforcing was tested until failure.

Figure 3-6 shows the resulting stress-strain relationship. As indicated, the reinforcing showed nonlinear behavior at approximately 3,000 microstrain, yielded at approximately 5,000 microstrain, and fractured at approximately 35,000 microstrain, on average (Zhang, 2018).

Figure 3-5. *Uniaxial testing of NO. 2 reinforcing bar.*

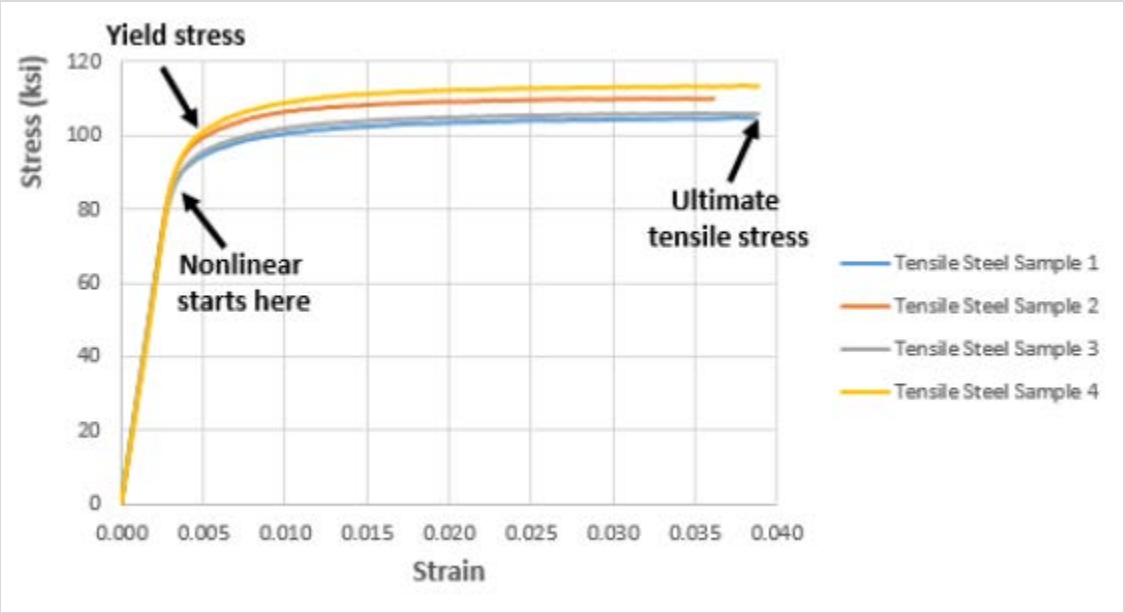

Figure 3-6. *Stress vs. strain curve for reinforcing. (Zhang, 2018)*

The PVC pipe utilized in the walls had a low strength and stiffness, and only acted to serve as molds for the holes.

3.4.2.3 Instrumentation

Each wall was instrumented with reinforcing strain gages, concrete strain gages, and LVDTs (linear velocity displacement transducers). Placement and nomenclature for strain gages corresponding to each test can be seen below in Figure 3-7. Gages were placed in areas of maximum expected stress and strain. Likewise, LVDTs were placed in areas of maximum expected displacement. For the axial load and pushover test, LVDTs were also placed in out-of-plane locations, to ensure that any out-of-plane behavior could be detected earlier in loading and rectified.

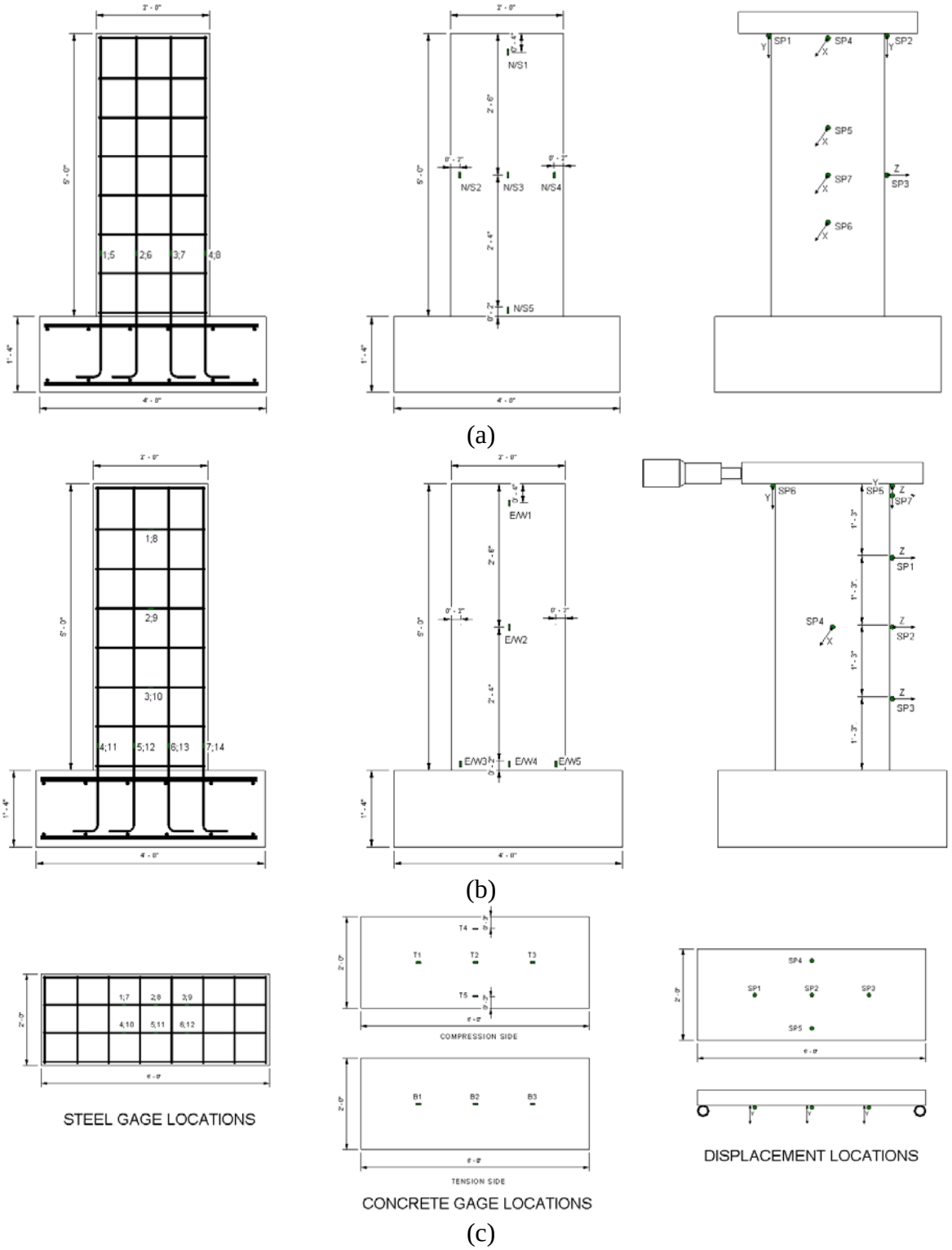

(a)

(b)

(c)

Figure 3-7. *Instrument locations for (a) axial load test, (b) pushover test, (c) four-point bending test.*

3.4.3 Experimental Results

3.4.3.1 Axial Compression Test

During axial tests, walls were loaded until failure. Force control was utilized during the duration of testing. Two walls were tested in axial compression, both following the test setup as defined in Figure 3-2. Actuators applied load to a top block that was firmly attached to the wall, in order to create a larger area for the actuators to rest on. During the first axial test, the top reinforced concrete block failed due to bursting. This bursting failure caused a crack to propagate into the wall, shown in Figure 3-8 and Figure 3-9. This crack and the failure of the top block caused the strength of the wall to be compromised, and the testing had to be halted prematurely.

Figure 3-8. *Bursting of top reinforced concrete block.*

Figure 3-9. *Crack developed within wall from bursting of top reinforcing concrete block.*

After testing the first wall, the top reinforced concrete block was replaced with a concrete-encased steel tube with rods tied through to prevent bursting. With this new top block, the second wall was successfully loaded until failure. At failure, the top of the wall burst in a violent fashion. As shown in Figure 3-10, the failure plane of the wall had a high angle, when looking at the thickness of the wall. During failure, both the PVC and the reinforcing exploded at the failure plane, indicating at as expected, the damping system would be ruined upon experiencing an axial failure. Failure of the wall either happened due to crushing of the concrete, or due to buckling. The failure mode of the wall will be discussed further in later sections.

Figure 3-10. *Failure of second axial load test wall.*

During the first axial test, the maximum load applied reached 346 kips. During the second axial test, the maximum load applied reached 485 kips before failure. Figure 3-11 shows the load versus displacement curve for displacement occurring in the vertical direction. Two LVDTs, SP1 and SP2, were placed under the top block of the wall. The average of these data sets is presented for each test. As seen, at failure during test two, the vertical displacement of the wall reached approximately 0.1". Additionally, one can see that the displacement curve is approximately linear for the majority of the load application. This could indicate that the failure of the wall was either due to compression or linear buckling.

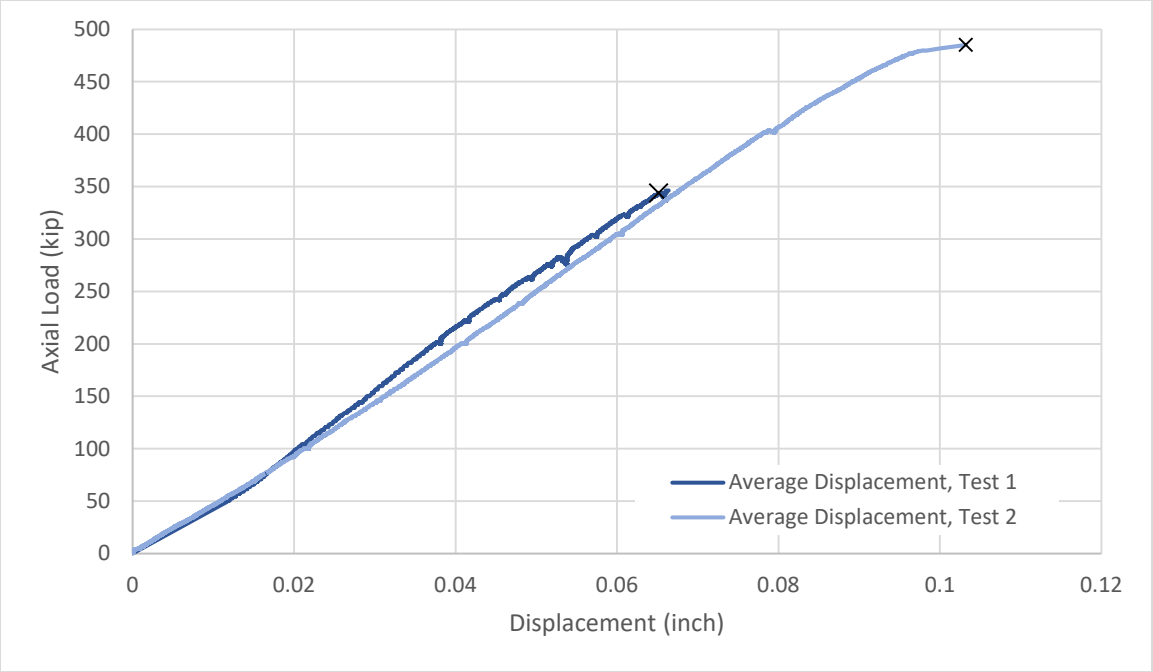

Figure 3-11. *Load vs. displacement in vertical direction, axial load test.*

Out-of-plane displacement during testing was also monitored utilizing the remaining LVDTs placed on the front and side faces of the specimens. While the top of the wall was not braced, the out-of-plane displacement during testing was minimized in order to prevent secondary moments through the p-delta effect from being introduced to the test. During the second test, the maximum out-of-plane displacement that occurred was 0.02 inches and 0.035 inches in the x-direction and z-direction, respectively. Out-of-plane displacements were controlled by leveling the base of the specimen with hydrostone before testing.

In looking at the strain experienced by the reinforcing during both tests, one can see that the increase in strain throughout the test was also linear. Figure 3-12 shows the strain experienced by the two outside lines of reinforcing, and Figure 3-13 shows the strain experienced by the two lines of inside reinforcing. Theoretically, if the wall was constructed perfectly symmetrically, and loaded in a perfectly symmetrical manner, those strain gages on

the two opposing sides of the wall should experience the same strain. For visual ease, the black lines present the average of the strains, allowing comparison between tests. One can see that the strain in the outside and inside reinforcing is very comparable from test one to test two. Again, the linear performance of the strain on both the inside and outside reinforcing bars coincides with the linear behavior seen in the displacement, as well as with the sudden failure of the second specimen. On average, the inside reinforcing bars experienced a slightly higher strain than the outside bars at failure. All strains presented are compressive strains.

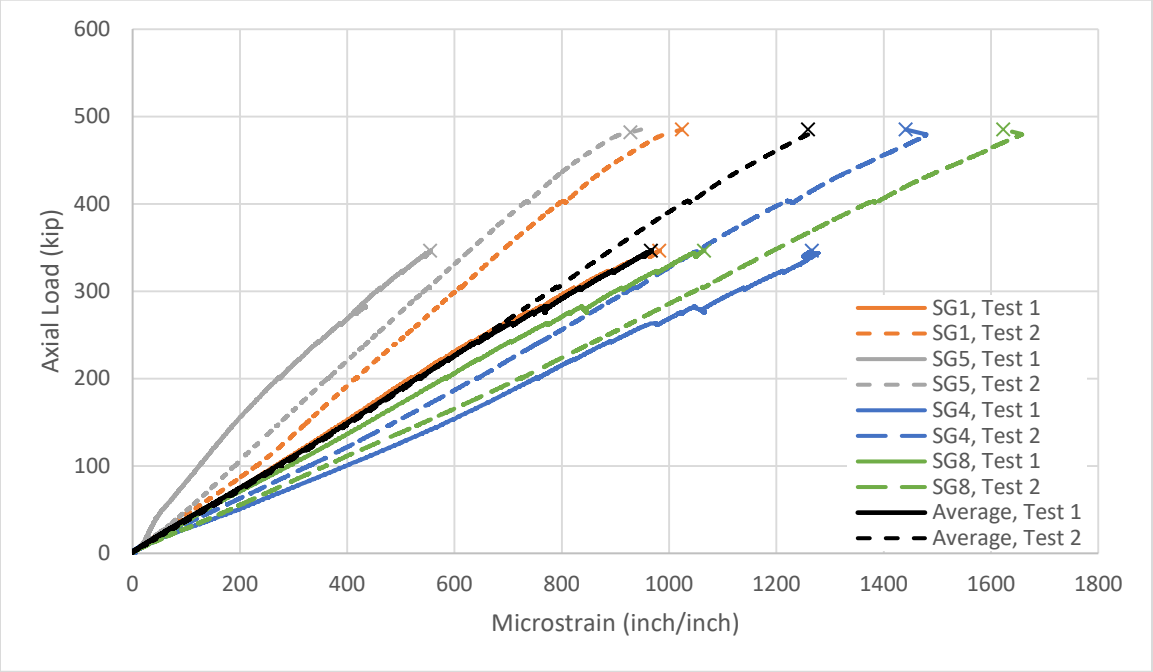

Figure 3-12. *Load vs. strain for outer reinforcing bars, axial load test.*

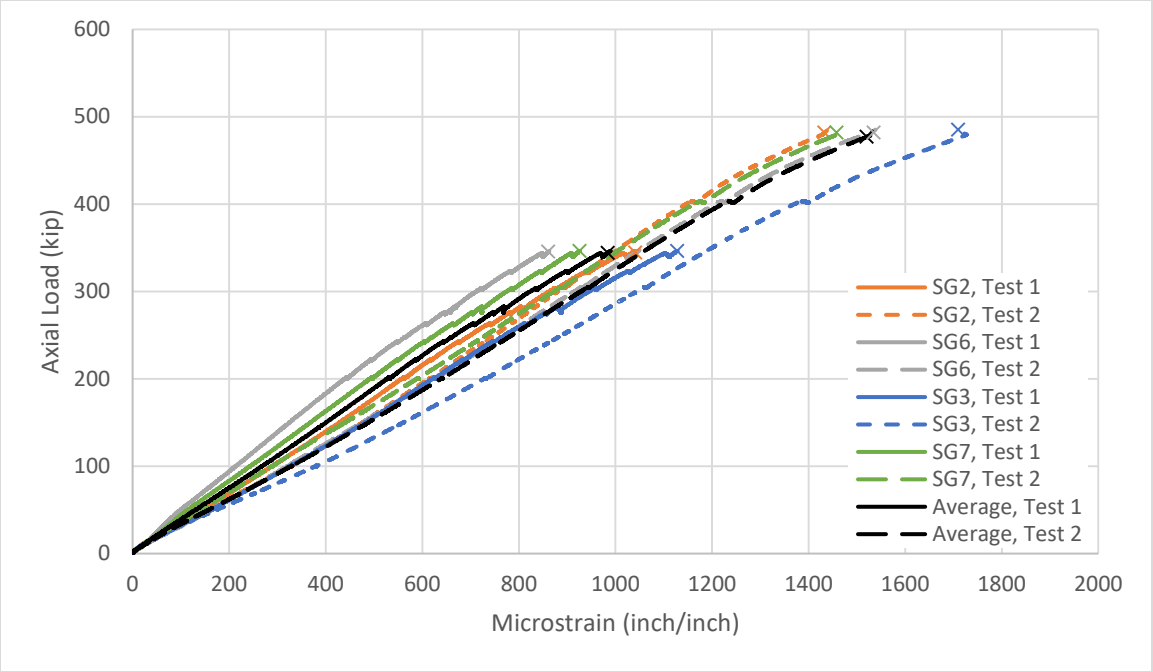

Figure 3-13. *Load vs. strain for inside reinforcing bars, axial load test.*

As expected, the strain experienced by the concrete during testing was very similar in nature to the strain experienced by the reinforcing. Overall, the concrete displayed a linear relationship between the stress and the strain. The largest stress experienced by the concrete occurred at the top of the wall, near where the failure plane occurred, and had a value of approximately 1600 microstrain. It is interesting to note that this is much less than the 3000 microstrain that is expected by concrete in a compression failure. However, before failure, the gages at this location (shown by N1 and S1), do begin to exhibit nonlinear behavior. The compression strain experienced by the concrete can be seen in Figure 3-14 and Figure 3-15.

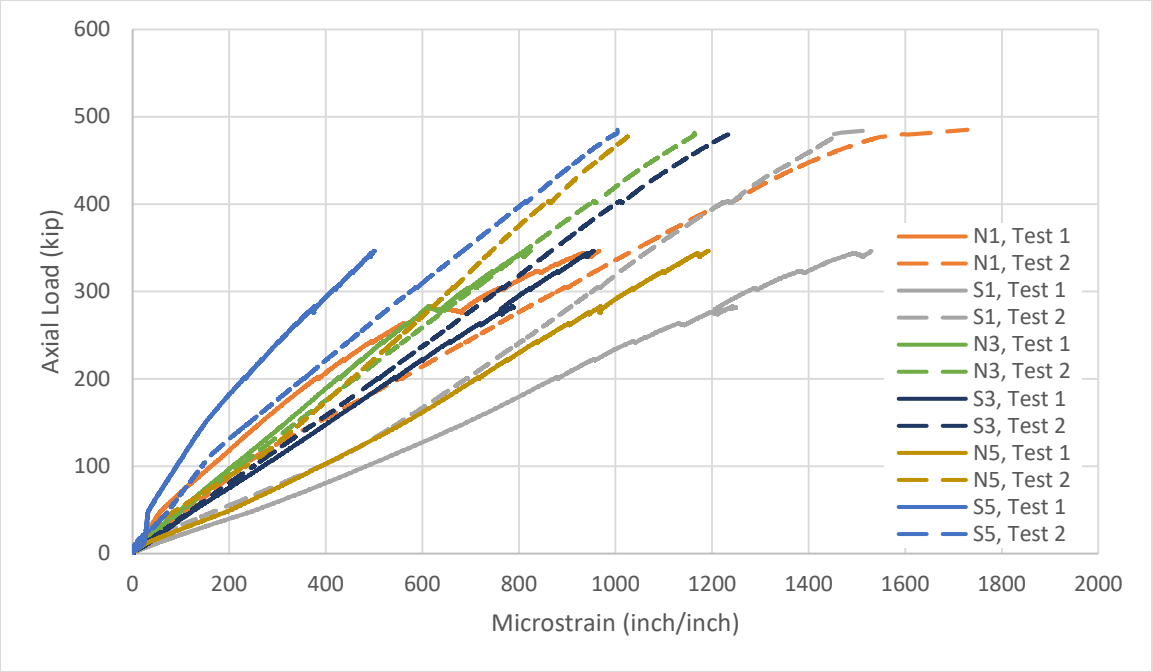

Figure 3-14. *Load vs. strain for concrete gages mid-width of wall, axial load test.*

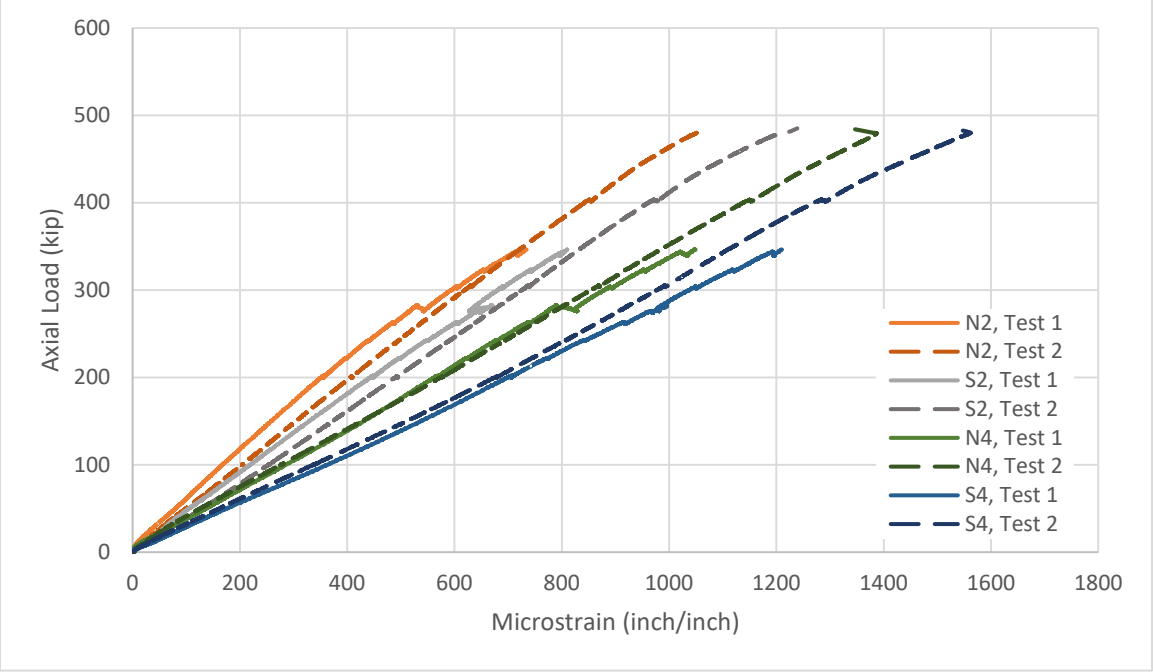

Figure 3-15. *Load vs. strain for concrete gages mid-height of wall, axial load test.*

The failure of the wall is presumed to be either a function of buckling, or due to compression. While buckling loading governs between the two cases in considering only linear properties, the sudden failure most often associated with crushing was observed during lab testing. The failure mode presumed to control will be discussed in the next section. It should be noted, however, that the small thickness of the wall, coupled with the placement of the PVC tubes, may have led to imperfections in the performance of the wall. If PVC tubes were off-center, or moved during concrete placement, the wall would have had a larger mass concentration on one side, adding strength to that side of the wall, and taking axial strength away from the other side of the wall. Because the axial strength is directly related to the amount of concrete the load is bearing on, this mass concentration, although conceptually small, could have had a real effect. Additionally, because the wall failed near the top, there might have been interaction between the top block and the PVC pipe that was not able to be seen during testing. For example, as the axial load was applied, the PVC tubes might have expanded outwards due to poisson's effect, adding to the stress experienced by the concrete. This stress would not have been on the surface of the concrete, and therefore would not have been captured by the gages during testing. Finally, improper confinement of the concrete could have led to a bursting failure, as seen in test two. As the concrete was compressed down, the sides would experience tension, eventually leading to bursting.

3.4.3.2 Four-point Bending Test

Two walls were tested on their sides to complete the four-point bending test. Both a front and side view of the testing setup can be seen in Figure 3-16. The wall was supported on one side by a pinned tube, and on the other by a tube that was free to move in the horizontal direction. Load was applied to a beam placed on two additional beams, spreading the load to the third points of the wall. The beams placed at the third points can be referred to

as “loading strips”. Load was applied first using force control in 500 lbs increments, however was continued with displacement control after the flexural reinforcement yielded.

Figure 3-16. *Testing setup for four-point bending test.*

For both wall panels tested, cracks started to appear on the bottom (tension) side near the loading strips at a load of 1.5 kips on each strip. As the load increased, cracks propagated into the center of the wall, between the two loading strips. When the displacement reached 0.4 inches at midspan, the speed of loading significantly dropped, indicating that the panel was losing strength, and the reinforcing was beginning to yield. Figure 3-17 shows the load-displacement curve at midspan for the two walls. At a displacement of 0.4 inches, one can see that displacement increases, even though the loading stays constant. Final failure occurred when the flexural reinforcement fully yielded. This pattern remains consistent when looking at the load-deflection curve for the left strip, shown in Figure 3-18, and the right strip, shown in Figure 3-19.

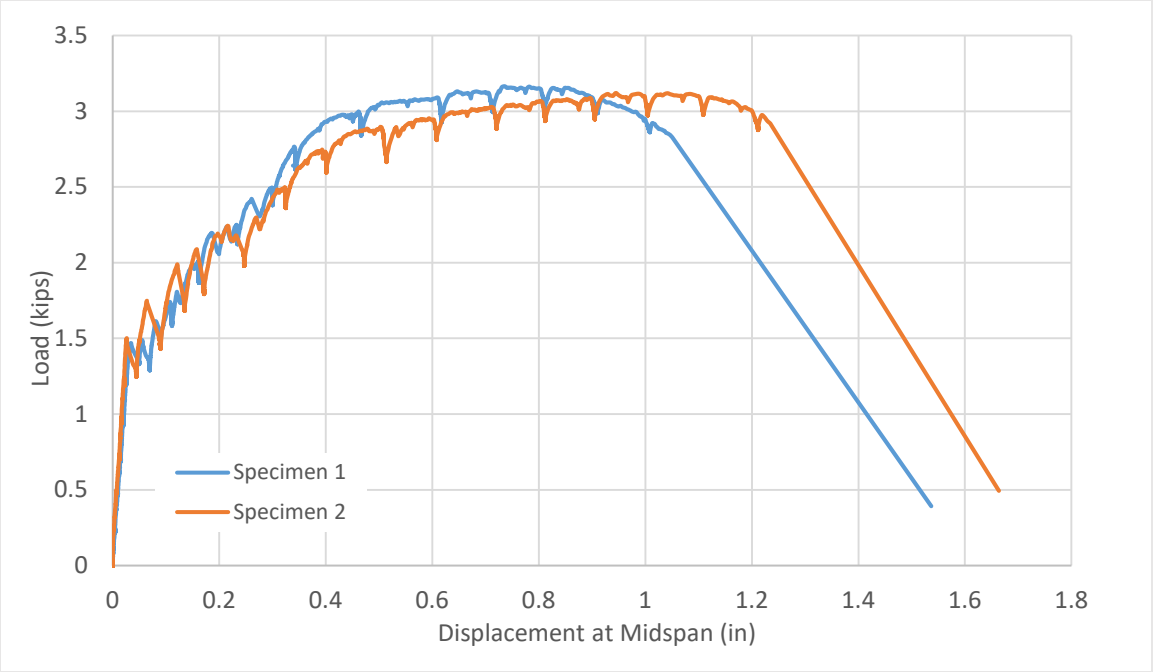

Figure 3-17. *Load vs. deflection at midspan of wall, four-point bending test.*

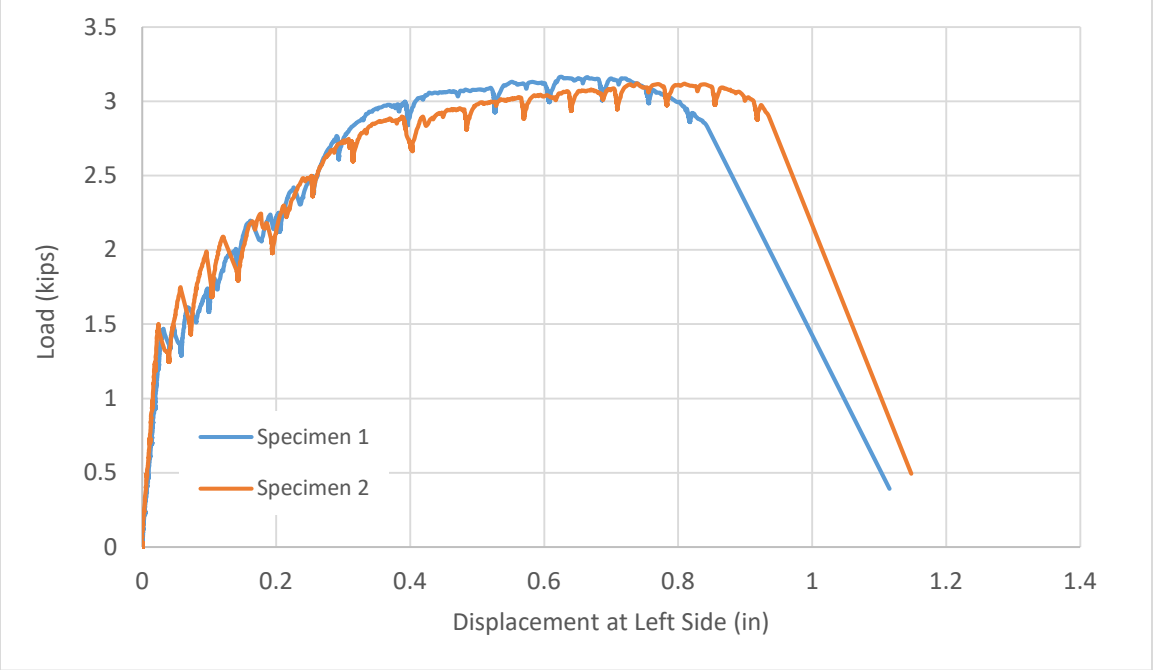

Figure 3-18. *Load vs. deflection under left loading strip, four-point bending test.*

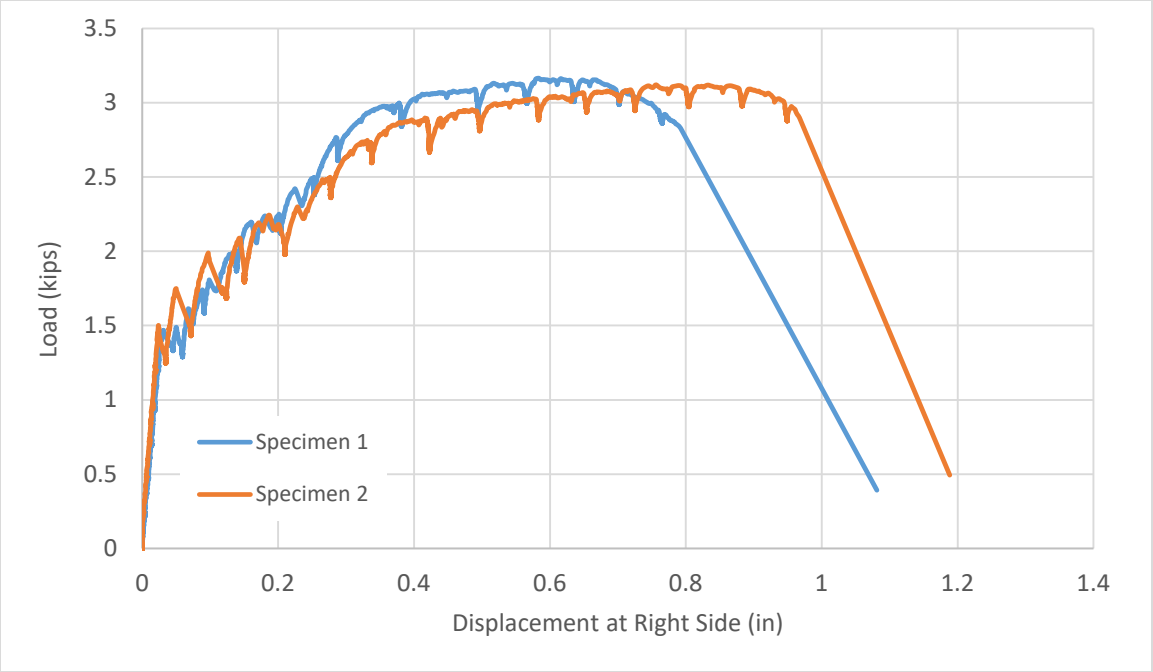

Figure 3-19. *Load vs. deflection under right loading strip, four-point bending test.*

Figure 3-20 shows the engagement of the bottom flexural reinforcement at midspan for both test one and test one. As shown, the bottom flexural reinforcement yielded when the displacement at the middle of the wall was approximately 0.6 to 0.7 inches. In both tests, this occurred near the expected yielded value for reinforcement.

Figure 3-21 shows the cracking experienced by both walls. Cracking extended from the bottom of the wall towards the top, cracks propagating as the load increased. Cracking resembled typical flexural cracking, and extended across the bottom width of the wall, as shown in Figure 3-22 and Figure 3-23. Cracks were relatively evenly spaced, approximately six to eight inches apart. Crushing did not occur on the top surface of the walls.

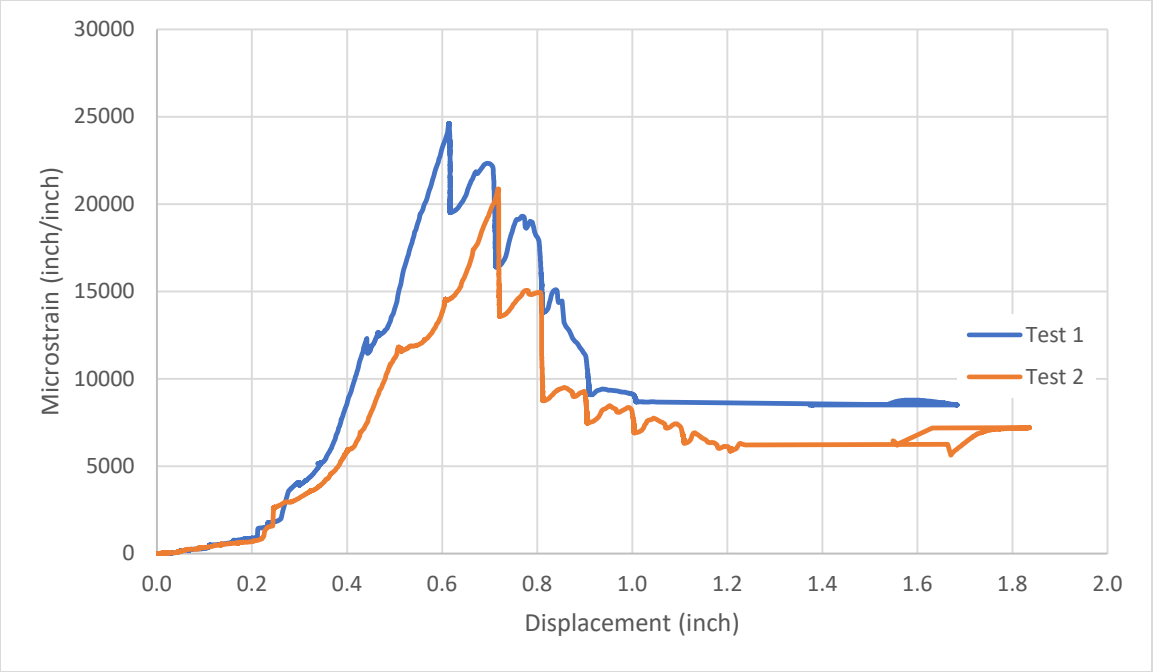

Figure 3-20. *Strain vs. displacement for bottom middle reinforcing, four-point bending test.*

Figure 3-21. *Cracking on sides of walls, four-point bending test.*

Figure 3-22. *Cracking on bottom of walls, four-point bending test.*

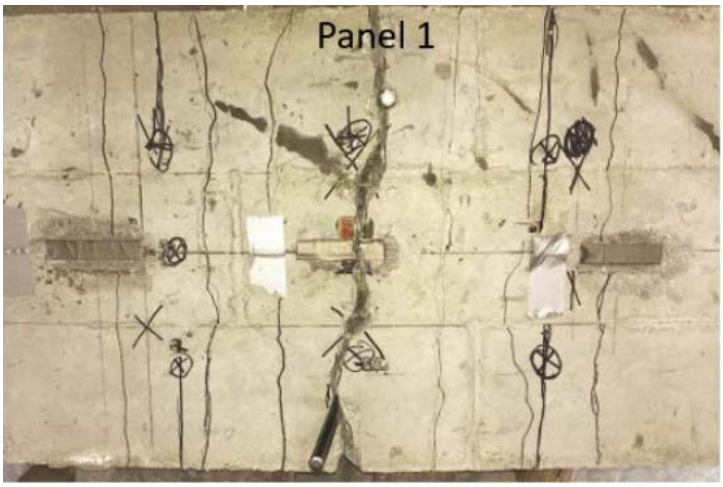

(a)

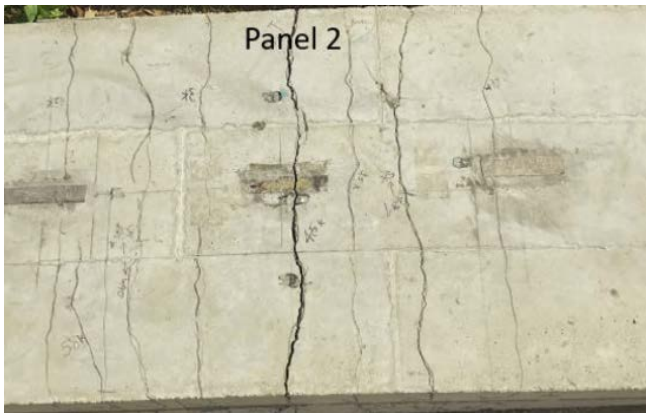

(b)

Figure 3-23. *Cracking on bottom of wall for (a) wall one and (b) wall two.*

3.4.3.3 Pushover Test

During the pushover test, the footing of the wall was pretensioned to the strong floor of the laboratory, in order to prevent any movement of the wall during loading. An actuator applied a horizontal force to steel tube mounted to the top of the wall. While force control was used sparingly at the beginning of testing, displacement control was used towards the end of testing. The testing setup can be seen in Figure 3-24.

Figure 3-24. *Pushover test setup.*

The north side of the wall was in compression during testing, while the south side of the wall was in tension. A very minimal amount of crushing was experienced by the wall on the north side during testing. Additionally, this crushing occurred at the end of testing, and is not the reason for the failure of the wall. Cracking between the interface of the wall and the footing occurred early in loading, starting on the south side of the wall, and extending towards the north side as testing continued. Cracking at this interface started when the load on the wall was approximately 4.5 kips (test one) to 5 kips (test two), extending from the south corner to the middle of the wall. Additionally, a parallel crack formed about one foot above the interface, extending slightly further along the wall. When 6.5 kips was applied, both the bottom and top crack extended to approximately three fourths the length of the wall.

Additionally, a crack formed along the vertical face of the wall, transferring the horizontal cracks. This vertical cracking occurred directly in front of the placement of a PVC tube. The cracking pattern can be seen in Figure 3-25. The cracking pattern for both walls tested was very similar. The first wall tested failed at approximately 6.7 kips, and the second wall failed at approximately 6.6 kips.

Figure 3-25. *Cracking at bottom of wall, pushover test.*

In looking at Figure 3-25, one can see that the failure of the wall did not occur from compression, but rather from tension on the south side of the wall. After early cracking of the wall, the response of the wall was highly dependent on the performance of the reinforcement. Figure 3-26 shows the load versus displacement curve for those LVDTs located on the south side of the wall. The order of string pots from top of the wall to the bottom of the wall is SP7,

SP1, SP2, and SP3. As expected, those meters that were placed higher on the wall experienced greater displacement. The displacement along the height of the wall was fairly linear.

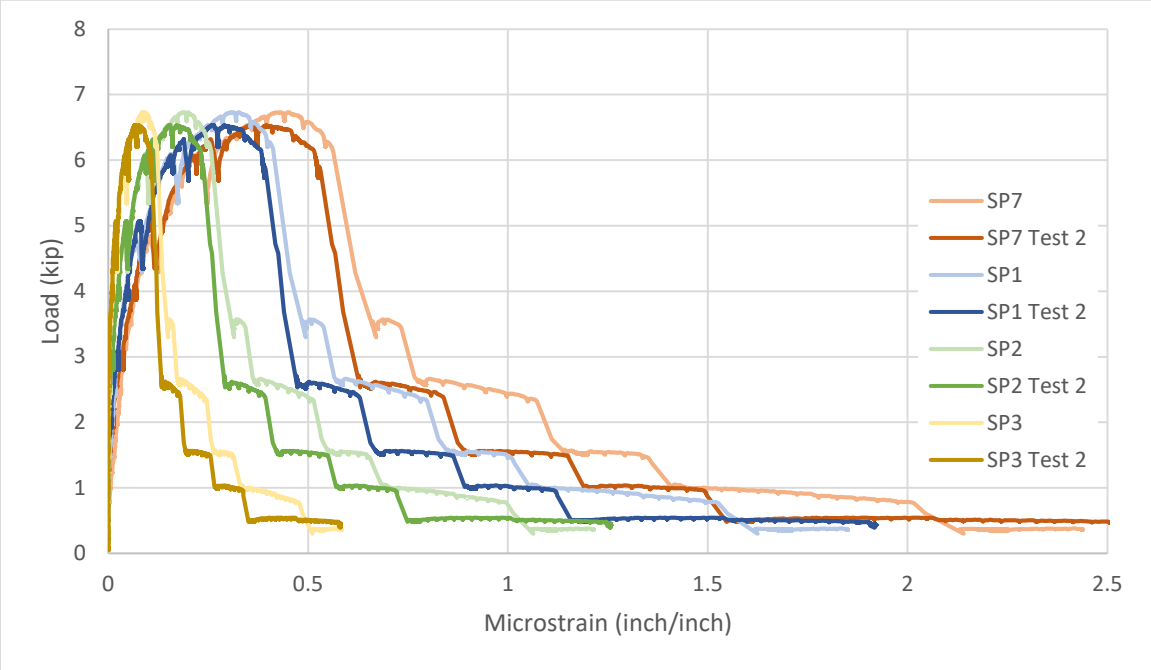

Figure 3-26. *Load vs. deflection curve for horizontal string pots, pushover test.*

In the first part of the load-displacement curve, one can see that the deflection increased linearly, until hitting the first cracking point, occurring at 4.5 kips and coinciding with results shown in Figure 3-25. As cracks continued to develop, the curve becomes less linear, until hitting the maximum load capacity at approximately 6.6-6.7 kips. At the peak loading, the majority of the base of the wall separated from the footing. After this point, the strength of the wall decreased rapidly, exhibiting a high horizontal displacement for a very low applied load. From the maximum load until full failure, one can see plateaus in the load-displacement curve. Each plateau corresponds to the fracturing of a piece of longitudinal

rebar. The test was stopped when the wall became unstable, almost entirely detached from the footing.

Figure 3-27 displays the strain-deflection curve for SG3 and SG10, located on the transverse reinforcing, approximately a foot and a half from the base of the wall. Theoretically, SG3 and SG10 should display the same strain if the wall was constructed and loaded perfectly symmetrically. However, although there is a difference of 200 microstrain at the peak strain (in both test one and test two), the pattern displayed by the two is similar. As shown, the peak strain in the transverse reinforcing at this location occurred when the horizontal deflection was approximately 0.5 inches, which corresponds to the maximum load applied. After this point, the strain in the reinforcing dropped drastically until maintaining a constant strain of 150 microstrain on average. Because the bottom of the wall had come apart from the footing, the reinforcing was not engaged, producing small linear strain values.

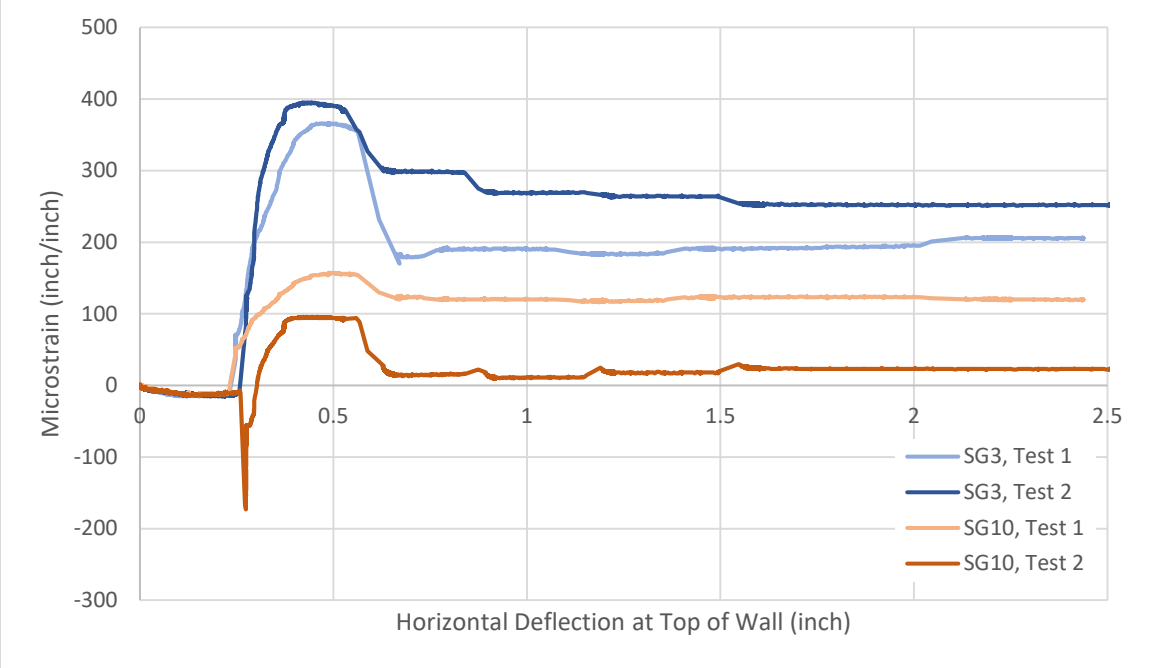

Figure 3-27. *Strain vs. deflection for transverse reinforcing, pushover test.*

Figure 3-28 and Figure 3-29 display the strain-deflection curve for those strain gages on the longitudinal reinforcing along the base of the wall for Test 1 and Test 2, respectively. The strain increases at different rates dependent on the distance from the south wall, as expected. Those strain gages on the reinforcing closest to the north wall (shown by the notation of "1st Line") experienced the highest tensile strain, while those strain gages on the reinforcing closest to the south wall (shown by the notation of "4th Line") experience compressive strain before experiencing small tensile strain. During testing, five longitudinal reinforcing bars fractured near the interface of the wall and the footing. The rows with damaged bars are indicated on the graph with an "x". An example of fracturing in one of the bars can be seen in Figure 3-30. Fracturing of bars occurred after the maximum loading point, and correspond to the plateaus earlier described in the load-displacement curve. After the reinforcing was fractured, the wall acted like a plain concrete wall, with a hinge on the base of the north side. Interestingly, the majority of bars fractured near their yielding strain, rather than their ultimate strain. This could be due to the rate of loading utilized.

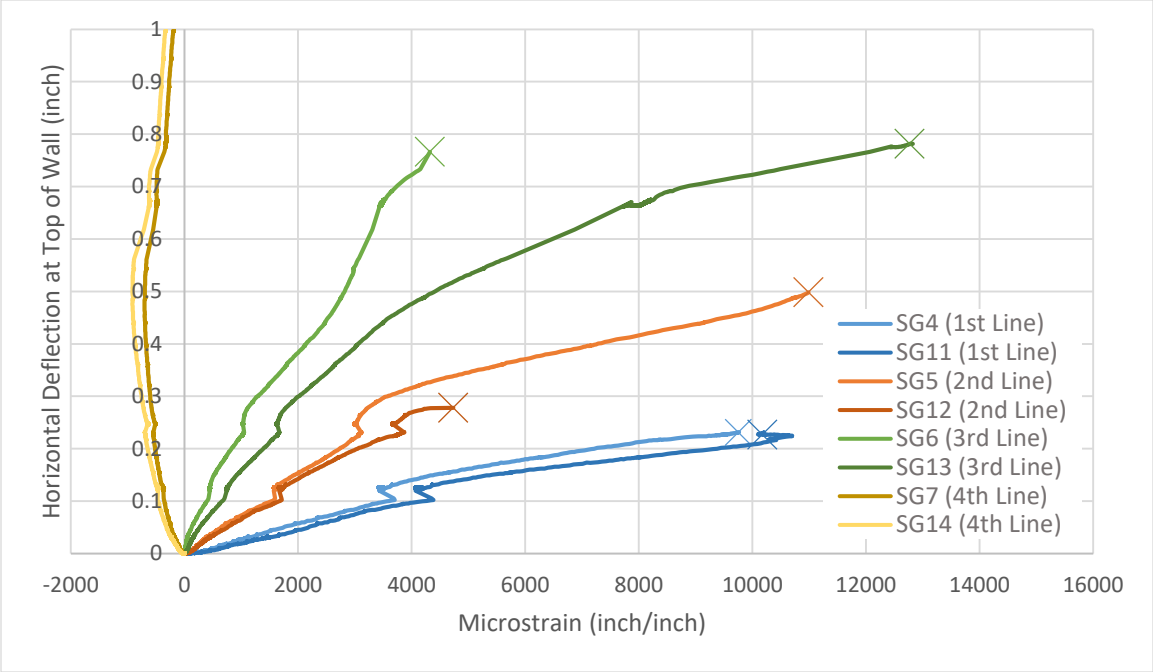

Figure 3-28. *Strain vs. deflection for longitudinal reinforcing, pushover test one.*

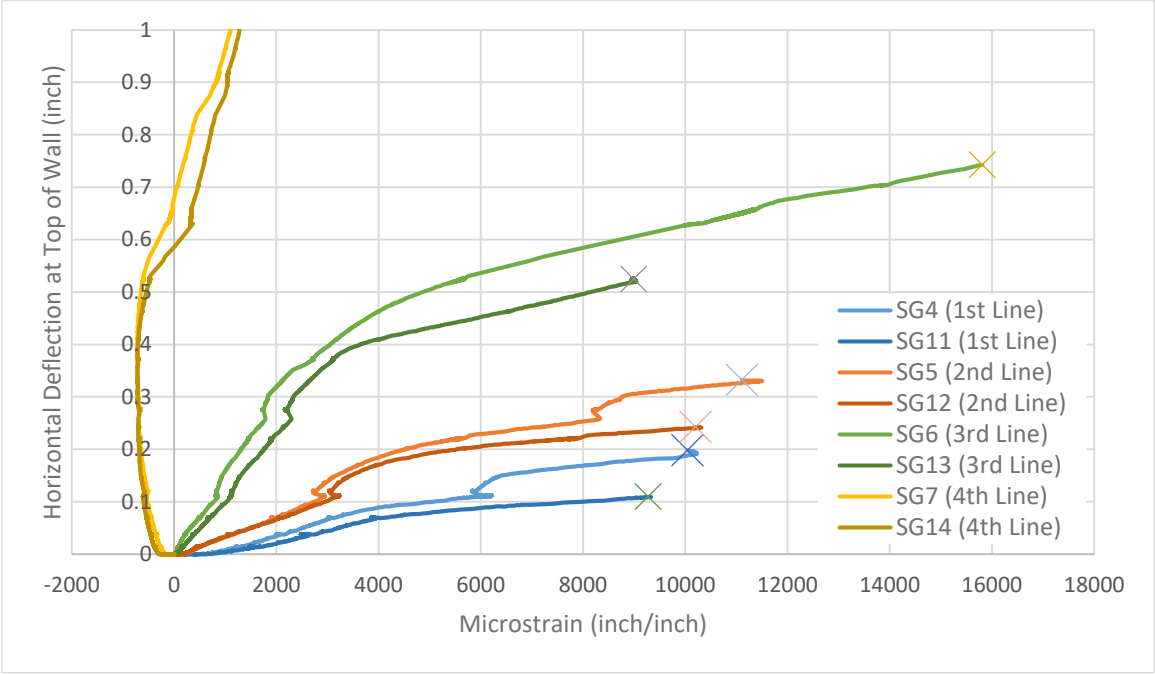

Figure 3-29. *Strain vs. deflection for longitudinal reinforcing, pushover test two.*

Figure 3-30. *Fracturing of longitudinal reinforcing, pushover test.*

There was very little strain captured by the concrete strain gages, which, in looking at the test results makes sense. The largest strain was compression strain, captured by those strain gages at the bottom north side of the wall (E5 and W5), shown in Figure 3-31. The rest of the concrete did not experience tension because any stress developed was quickly released by cracking at the bottom of the wall. It is very apparent when looking Figure 3-31 that the weakest part of the specimen was the connection between the wall and the footing, despite the continuous reinforcing. Perhaps if the two had been poured continuously, the failure of the wall would have performed differently.

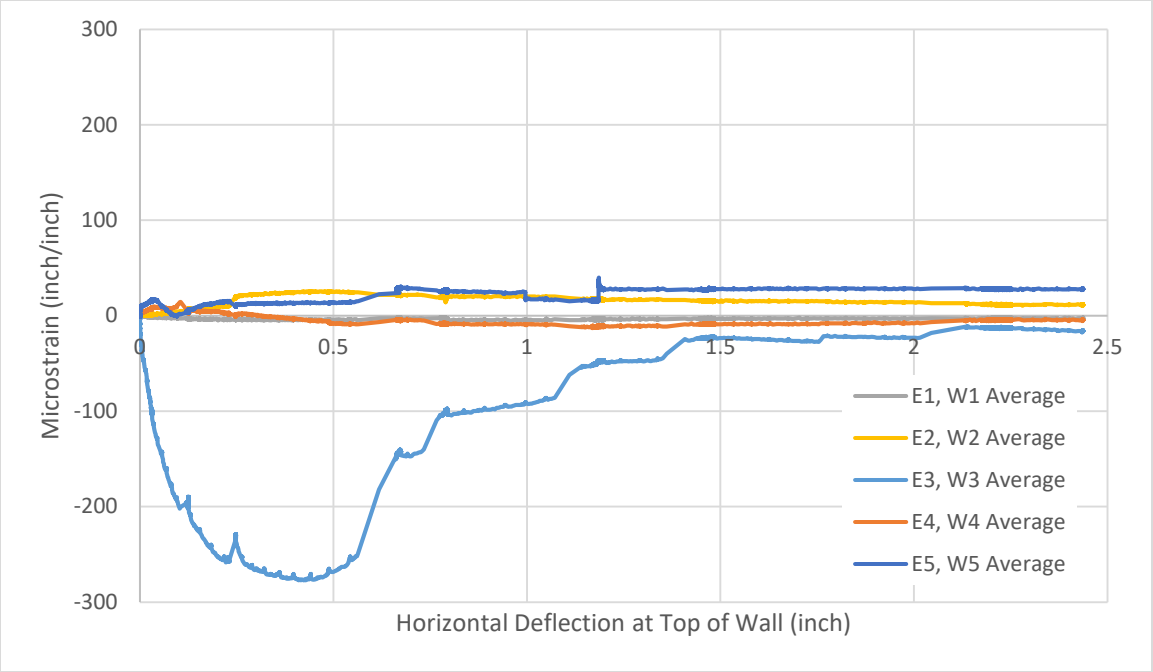

Figure 3-31. *Concrete strain vs. deflection, pushover test.*

3.5 Finite Element Modeling

A finite element model was made corresponding to each test performed in the laboratory. Laboratory results from testing were then correlated with the models to calibrate the model results. With the calibrated models, additional information in the future can be extracted from the models. With calibrated models, additional models of reinforced concrete walls without holes were created using the same material properties. This allowed for direct comparison of failure loads.

Additionally, the models can be used to accurately predict the behavior of walls with different damper configurations, including a change in the number of holes or size of holes. Although not completed in this study, the models could be used to show the performance of more complicated loading conditions that may be harder to simulate in the lab, such as performance of the TLWD under biaxial bending, seismic loading, etc.

3.5.1 Model Parameters

3.5.1.1 Geometry and Element Type

The finite element model was constructed to match the geometry of the wall specimens tested in the lab. The models used for the axial capacity and pushover analysis had a footing, while the model used for the bending analysis did not have a footing.

To model the geometry, three-dimensional solid shapes were used for the concrete slab and steel girders. The steel reinforcing was modeled using wire shapes, with an associated cross sectional area that matched that of #2 reinforcing steel bars. Hex elements were utilized for the three-dimensional shapes, in order to yield accurate results and reduce computational time. A linear 3D truss element was utilized to model the wire shapes.

3.5.1.2 Material Properties

3.5.1.2.1 Concrete

Elastic material properties for concrete included the mass density, poisson's ratio, and modulus of elasticity. The mass density was based on a typical density of 150 lb/ft^3. The modulus of elasticity was based on an average compressive strength of 7.5 ksi, gained from cylinder tests completed at the time of testing. Hsu and Hsu (1994) state that ACI 318-14 Building Code overestimates the modulus of elasticity with the typical equation $57{,}000\sqrt{f'_c}$. Therefore, an adjusted modulus of elasticity, calculated using was used.

$$E_0 = 1.2431 * 10^2 f'_c + 3.28312 * 10^3$$

Equation 3-1

Using this equation, the modulus of elasticity utilized in the model was 4252738 psi. The poisson's ratio was taken as 0.19.

Hsu and Hsu's model (1994) was used to generate the nonlinear stress-strain behavior for concrete. Unlike other models developed, Hsu and Hsu's model only relies on the

compressive strength of the concrete. As shown in Figure 3-32, the concrete follows a linear stress-strain relationship corresponding to the maximum compressive strength, f'_c. Hsu and Hsu's model begins at $0.5f'_c$, and ends when the stress descends to $0.3f'_c$. Between these points, the equation below describes the compressive stress values:

$$f_c = \left(\frac{\beta\left(\varepsilon_c/\varepsilon_o\right)}{\beta - 1 + \left(\varepsilon_c/\varepsilon_o\right)}\right)f'_c$$

Equation 3-2

where

$$\beta = \frac{1}{1-\left[f'_c/\varepsilon_o E_o\right]} \text{ and } \varepsilon_o = 8.9 * 10^{-5} f'_c + 2.114 * 10^{-3}$$

The inelastic strain of the concrete, ε_c^{in}, is equivalent to the total strain, ε_c, minus the elastic strain, dictated as:

$$\varepsilon_c^{in} = \varepsilon_c - \frac{f'_c}{E_o}$$

Equation 3-3

A damage factor was used to represent the degradation of the elastic stiffness of the system, and can be calculated using the following equation:

$$d = 1 - \frac{f_c}{f'_c}$$

Equation 3-4

The relationship between the elastic modulus and the compressive damage factor is:

$$E = (1 - d)E_o$$

Equation 3-5

To capture the tension stiffening in the concrete, the Nayal and Rasheed (2006) model, modified by Wahalathantri et al. (2011), was used. Similar to the concrete

compressive parameters, both the nonlinear stress-strain behavior was defined, and the tensile damage. Figure 3-33 below shows the tensile behavior of the concrete. The concrete behavior is linear until reaching the maximum tensile stress, f_{to}, corresponding to the cracking strain, ε_{cr}. Then, the stress decreases until $0.77f_{to}$, corresponding to $1.25\varepsilon_{cr}$. The stress decreases additionally to $0.45f_{to}$, corresponding to $4\varepsilon_{cr}$, until reaching $0.1f_{to}$, corresponding to $8.7\varepsilon_{cr}$. The maximum tensile stress was calculated using Hooke's Law. Tension damage parameters were calculated in a similar fashion to compression damage parameters. Figure 3-34 describes the relationship between the compressive and tensile stress, and the compressive and tensile damage, respectively.

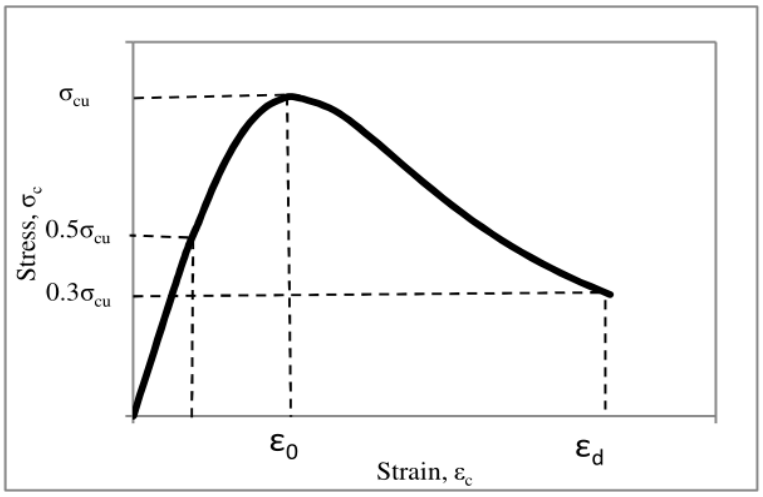

Figure 3-32. *Compression stress-strain curve. Source: Hsu and Hsu (1994).*

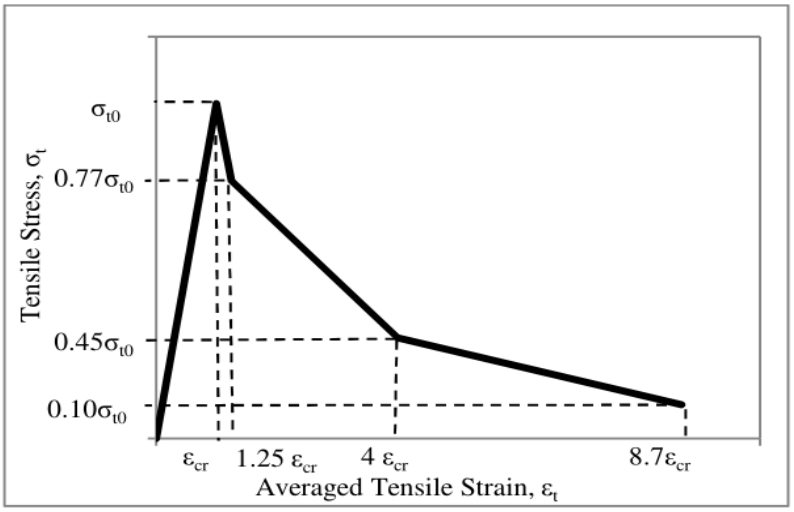

FIGURE 04: Modified Tension Stiffening Model for ABAQUS

Figure 3-33. *Tension stress-strain curve. Source: Wahalathantri et al. (2011).*

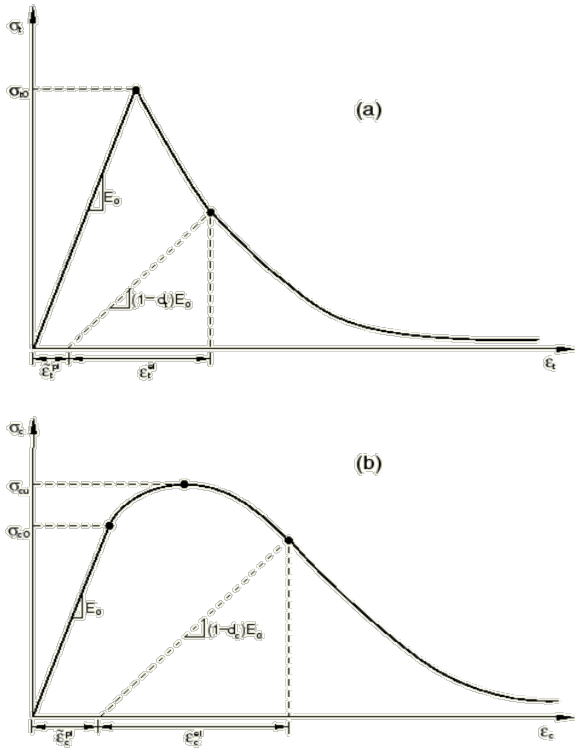

Figure 3-34. *Tension and compression stress-strain response with damage relationship. Source: ABAQUS (2013).*

In addition to the stress-strain tension and compression models, the following properties were utilized in the FE model:

- Dilation angle: 31°
- Eccentricity: 0.1
- Ratio of biaxial strength to uniaxial strength, f_{bo}/f_{co}: 1.16
- Ratio of the second stress invariant on tensile meridian, K: 0.667
- Viscosity parameter: 0.0005

3.5.1.2.2 Steel

Both elastic and plastic properties were defined for the steel reinforcing. Plastic properties from steel were developed from results of uniaxial testing, presented earlier in this paper. Similar to the concrete model, the plastic strain of the steel was calculated using the total strain minus the elastic strain.

Ductile damage properties were additionally assigned to steel elements in the finite element models. To define ductile damage, a fracture strain and a displacement at failure were assigned. A fracture strain of 0.03 and a displacement of 0.8 inches at failure were selected for damage criteria.

3.5.2 Mesh Convergence Study

A mesh convergence study was completed on all three finite element models, each model corresponding to a different load test. By performing the convergence study on all three models, a singular common mesh size could be chosen that gave acceptable results throughout. To complete the mesh convergence study, the load or displacement applied in each model was kept constant, while the mesh size was minimized. Both the number of elements along the edge of the holes, as well as the global mesh size, were altered. The

increased number of divisions along the perimeter of the hole, the more accurate the shape would become. Similarly, the smaller the global mesh size, the more accurate the results could be. However, the smaller the mesh size also resulted in an increase in computational time and capacity. For each model, the starting global mesh size was two inches. This convergence study was completed by Zhang (2018), however a summary of the results are presented.

3.5.2.1 Axial Model Convergence Study

The axial loading model had a 1000-psi pressure applied to the top surface of the wall, as shown in Figure 3-35. The base of the footing was fixed. Throughout the convergence study, the maximum vertical displacement was recorded.

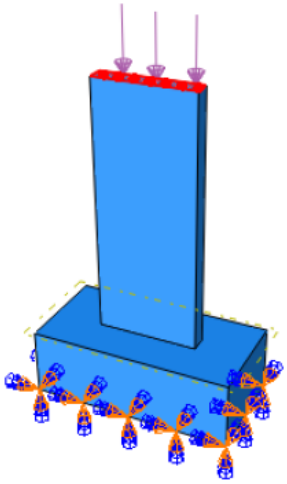

Figure 3-35. *Boundary conditions and loading for convergence study, axial test model.*

The results of the convergence study for the axial loading case can be seen in Figure 3-36. The maximum vertical displacement recorded converged at 0.0166 inches, corresponding to a global mesh size of 0.667 inches, and 12 elements along the edge of the holes.

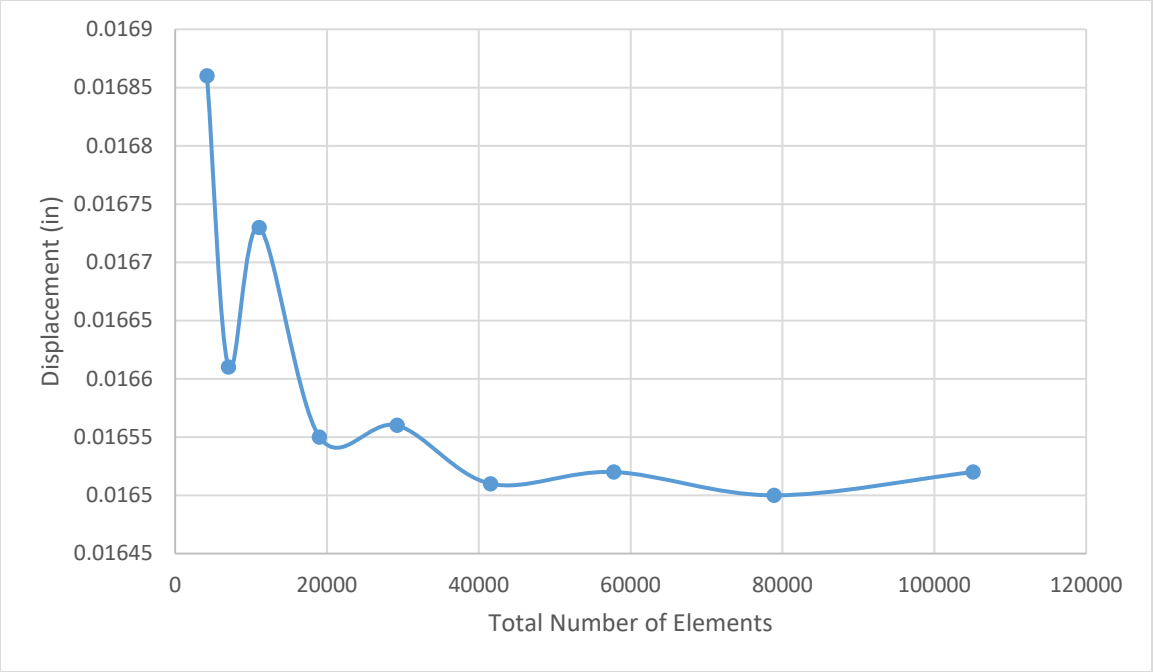

Figure 3-36. *Convergence study results for axial test model. Source: Zhang (2018).*

3.5.2.2 Four-point Bending Model Convergence Study

The four-point bending model was assigned a pin support on the right hand side, and a roller support on the left hand side, as shown in Figure 3-37. This matched the boundary conditions in the lab testing. Loading conditions for the convergence study consisted of a 10-psi pressure applied to each loading strip, spacing the same as demonstrated in the laboratory test.

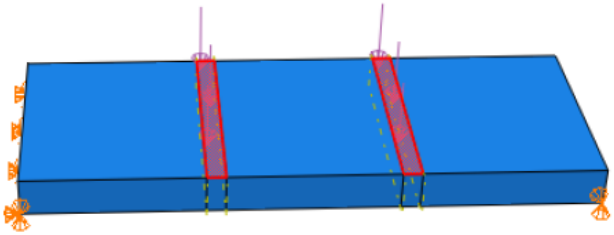

Figure 3-37. *Boundary conditions and loading for convergence study, four-point bending test model.*

The results of the convergence study can be seen below in Figure 3-38. The maximum vertical displacement recorded converged at 0.007651 inches, corresponding to a global mesh size of 0.667 inches, and 12 elements along the edge of the hole.

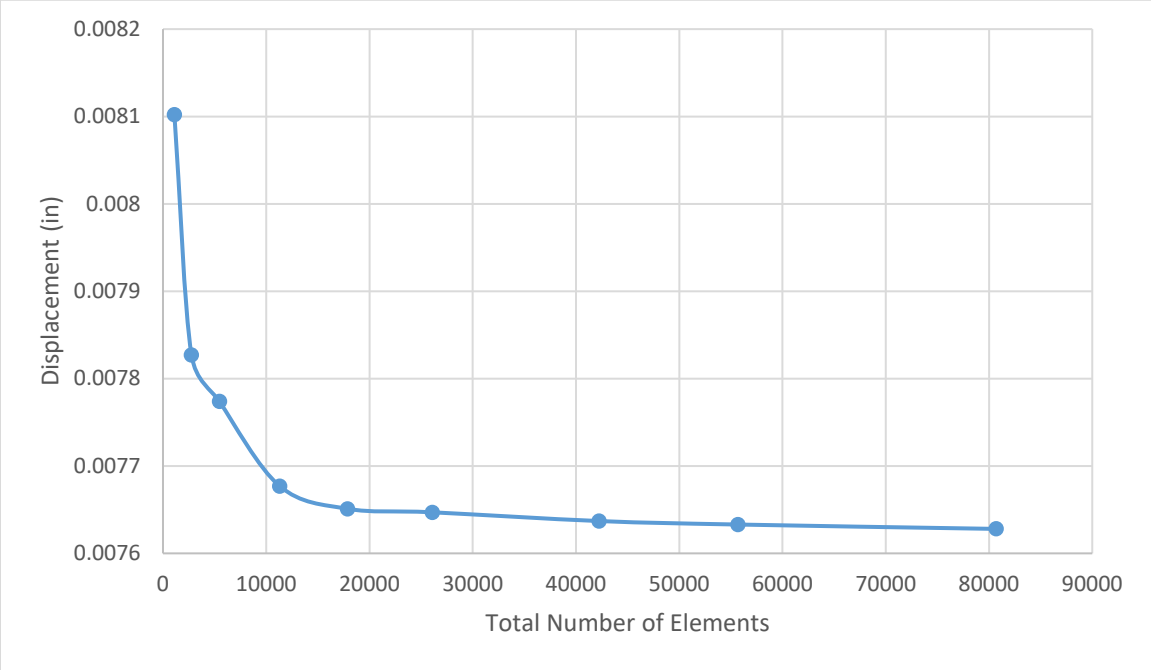

Figure 3-38. *Convergence study results for four-point bending model. Source: Zhang (2018).*

3.5.2.3 Pushover Model Convergence Study

The pushover model had a 50-psi pressure applied to a 4” by 5” area on the top side of the surface. The maximum horizontal displacement of the wall was recorded for the convergence study. Similar to the axial loading model, the base of the footing was fixed.

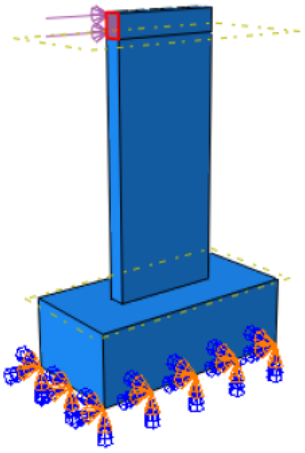

Figure 3-39. *Boundary conditions and loading for convergence study, pushover test model.*

The results of the convergence study for the pushover model can be seen in Figure 3-40 below. The maximum horizontal displacement recorded converged at 0.00568 inches, corresponding to a global mesh size of 0.571 inches, and 14 elements along the edge of the hole.

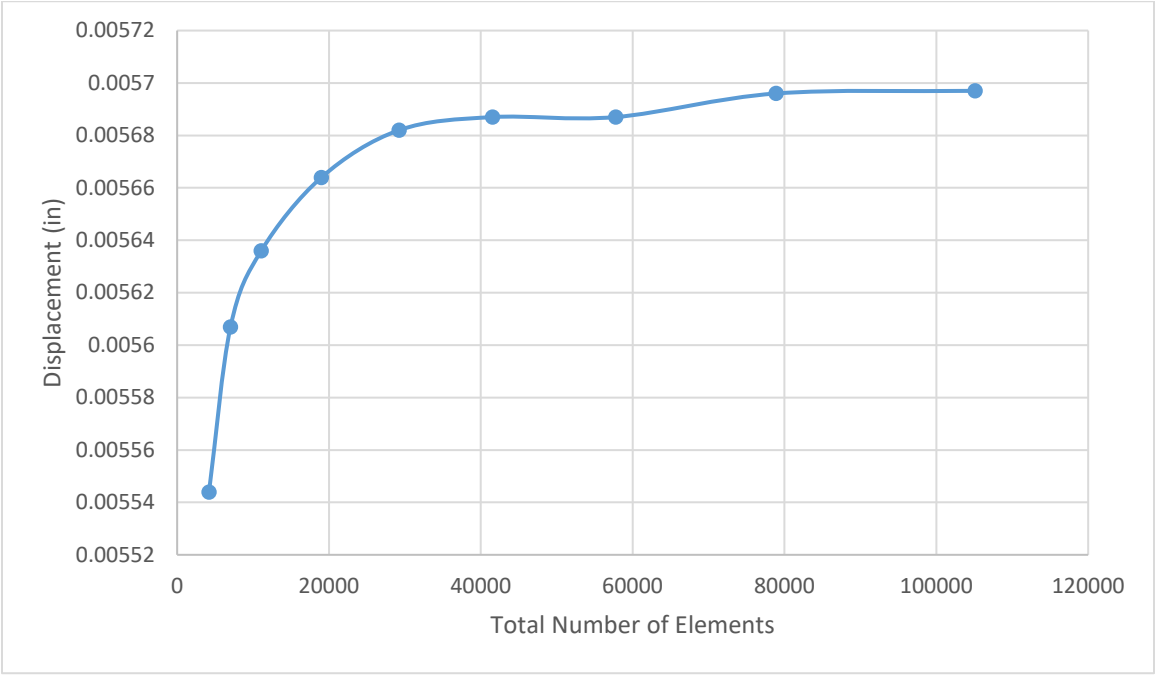

Figure 3-40. *Convergence study results for four-point bending test model. Source: Zhang (2018).*

From the three convergence studies, the smallest mesh size was taken as the mesh size used for the models. Therefore, a global mesh size with a width of 0.571 inches was utilized for the wall. The edges of the holes were split into 14 increments. The footing was left with a global mesh size of two inches, as the footing was not of interest in the study. Figure 3-41 shows the mesh size used for all three models.

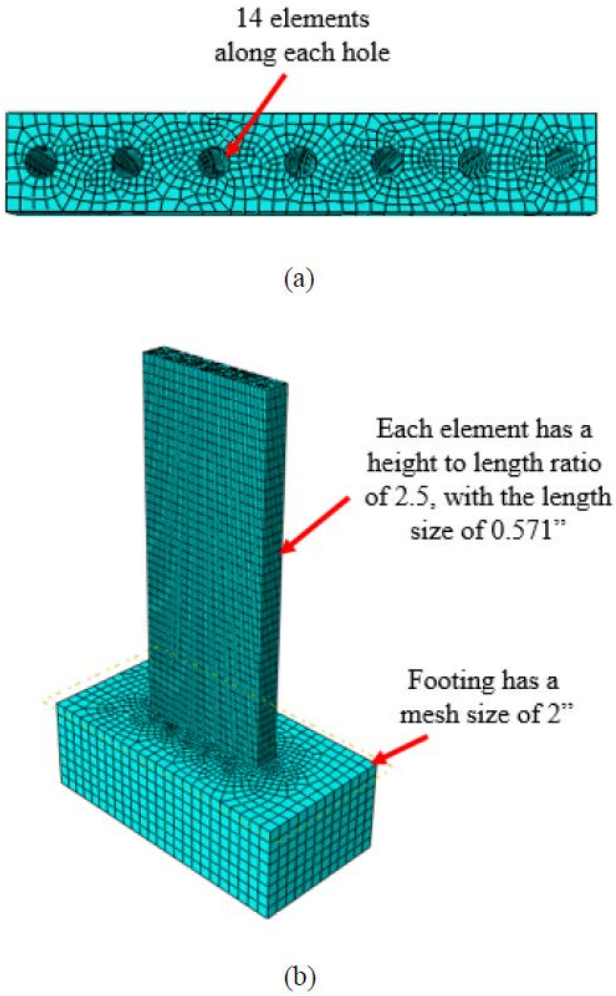

Figure 3-41. *Resulting chosen mesh size from convergence study including (a) divisions around perimeter of holes and (b) global mesh size.*

3.5.3 Comparison of Testing Results with Finite Element Model

3.5.3.1 Axial Loading Test

Hand calculations showed that if the top of the wall was considered as "free", then linear buckling of the wall could control over a pure compression failure, using Euler's equation for buckling as shown below:

$$P_{cr} = \frac{\pi^2 EI}{(KL)^2}$$

In this equation, (KL) represents the effective length of the wall. The constant K determines the condition of the wall. For the fixed-free condition, K is 2.0. Using this equation, the critical load for the wall is 429 kips.

An eigenvalue analysis was completed in ABAQUS in order to verify the buckling load for the wall. With the eigenvalue analysis, ABAQUS is able to compute the buckling load and corresponding eigenvectors for a given number of modes. The smaller the mode shape (i.e., 1) corresponds to a greater likelihood that bucking will happen in this manner, and therefore has a corresponding lower buckling load as compared to other modes.

When completing the buckling analysis in ABAQUS, the bottom of the footing was fixed, and the bottom of the wall was constrained to the top of the footing. The top of the wall was left free, however, a multi-point constraint (MPC) was added to the top surface of the wall. Using a beam type MPC, the rotation and displacement of the entire top surface of the wall was constrained to match that of a "master" node, chosen in the center of the surface. This constraint ensured that the FE model acted similarly to that of the test, with the top surface deforming evenly. A top pressure was evenly applied to the top surface of the wall.

Figure 3-42 shows the buckling shape associated with the first mode when completing the linear eigenvalue analysis. The eigenvalue associated with this modal shape was 427 kips. As mentioned, hand calculations performed using Euler's buckling formula yield a buckling load of 429 kip, very close to ABAQUS results.

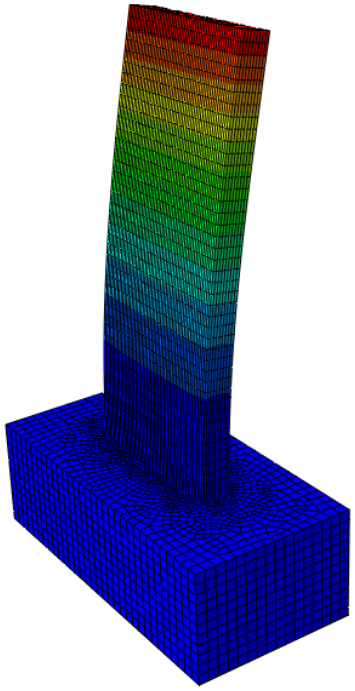

Figure 3-42. *Buckling shape of first mode.*

In order to ensure that linear buckling was the failure mode of the wall, a pure axial compression case for loading was also completed. In this model, the wall was fixed to the footing via a tie constraint, and the bottom of the footing was given a fixed boundary condition as shown in Figure 3-43. This mimicked the tie-downs used on the footing in the laboratory setting. A two inch downward displacement was applied to the top surface of the wall to provide the axial load.

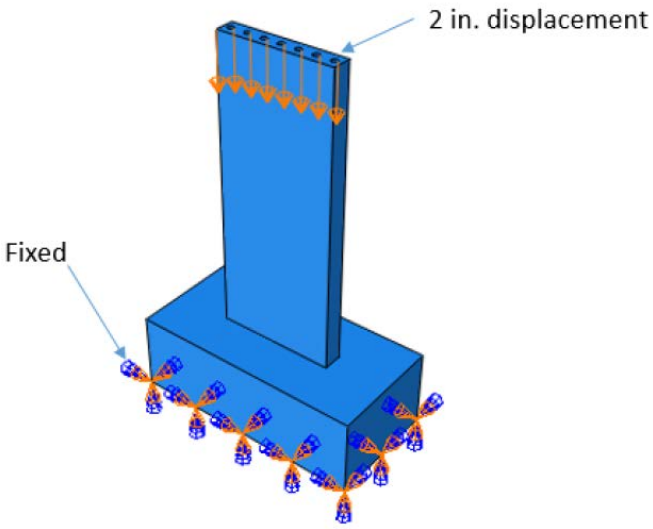

Figure 3-43. *Boundary conditions and loading for axial load model.*

The general load-displacement curve for the top of the wall in pure axial compression is shown in Figure 3-44. The failure load for the wall with the optimized TLWD is approximately 610 kips in the FE model. This is approximately 33% higher than the critical buckling load, and 22% higher than the largest axial load seen in laboratory testing. Throughout the remainder of this section, the results of pure axial compression will be presented, with an indication of when elastic buckling occurred.

In comparing the strain experienced by the concrete from laboratory testing to the compression FE model, one can see in Figure 3-45 that the strain experienced by the concrete at the top of the wall was less in the finite element model than experienced in lab testing at the lab testing failure point of 485 kips. However, the concrete strain in the remainder of the wall was comparable between the FE model and lab data for the remaining areas, as shown in Figure 3-46 and Figure 3-47.

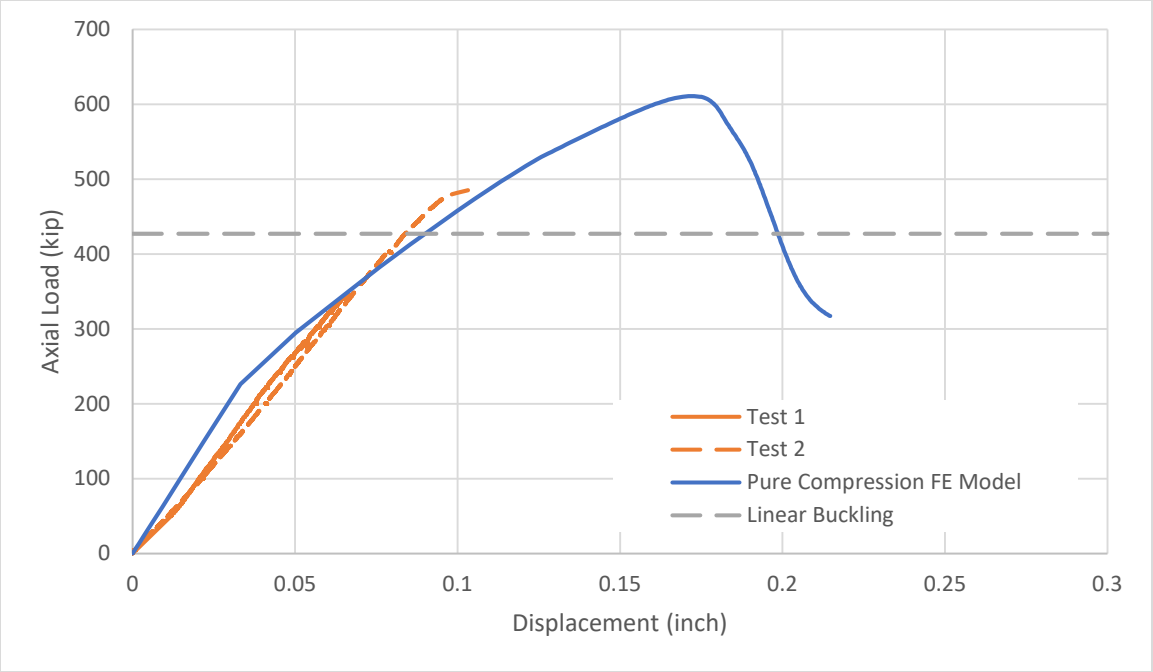

Figure 3-44. *Load-deflection behavior for laboratory results, pure compression FE model, and post-buckling FE model.*

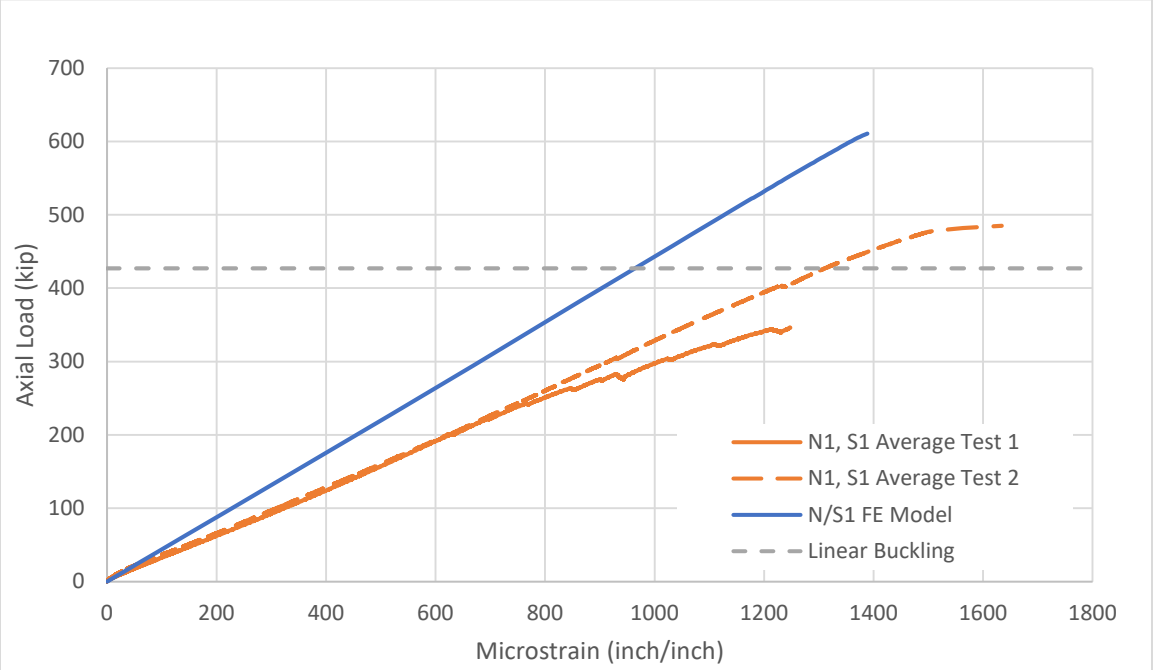

Figure 3-45. *Comparison of load-strain behavior of concrete at top of wall.*

.

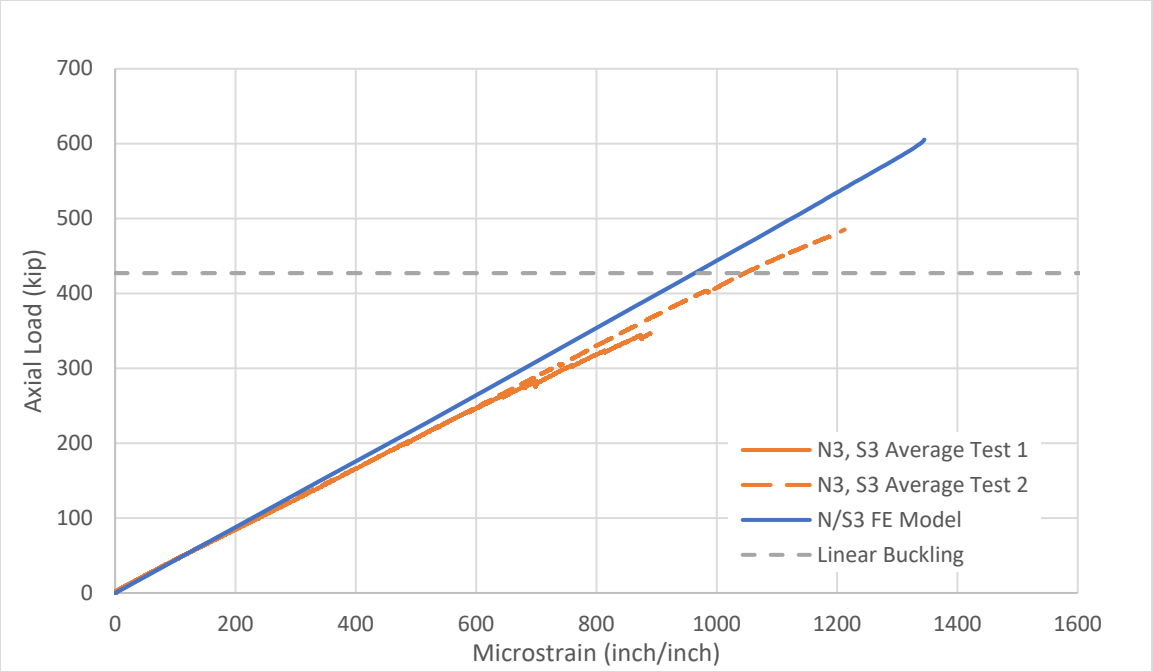

Figure 3-46. *Comparison of load-strain behavior of concrete at middle of wall.*

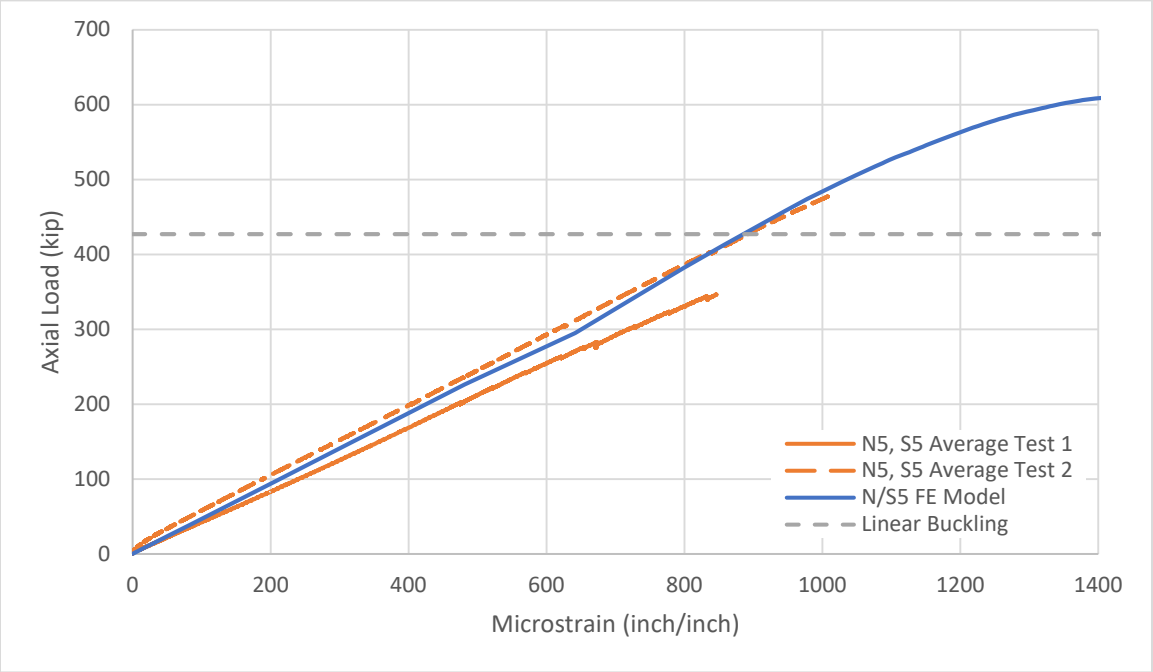

Figure 3-47. *Comparison of load-strain behavior of concrete at bottom of wall.*

3.5.3.1.1 Comparison with Hand Calculations

As mentioned previously, hand calculations considering linear buckling yield a critical buckling load of 429 kips. This is approximately 12% lower than the critical load in the laboratory, however, very close to FE results. If one were to considering pure axial compression, hand calculations of the axial capacity of the wall show that the failure load is 648 kips. This is 28% higher than the performance of the second wall in the laboratory test, and approximately 6% higher than the performance of the finite element model.

3.5.3.1.2 Comparison to Wall with No Openings

Both a buckling analysis and pure axial compression test were performed on a FE model containing a wall without openings to compare to the wall with optimal openings. The wall without openings had an eigenvalue of 432 kips, less than 1% higher than the wall with openings. The change was small due to the small change in moment of inertia. Additionally, the wall without openings had an axial strength of more than 700 kips, approximately 15% higher than the wall with optimal openings, due to the increase in cross-sectional area. A comparison of the axial strength can be found in Figure 3-48.

It is additionally interesting to note the difference in failure mode when comparing the two cases in pure axial compression. Figure 3-49 shows the damage occurring in a wall with no openings, while Figure 3-50 shows the damage occurring in a wall with the optimal opening configuration. One can see that while the wall without openings fails primarily due to shear, the wall with openings fails primarily due to crushing at the base.

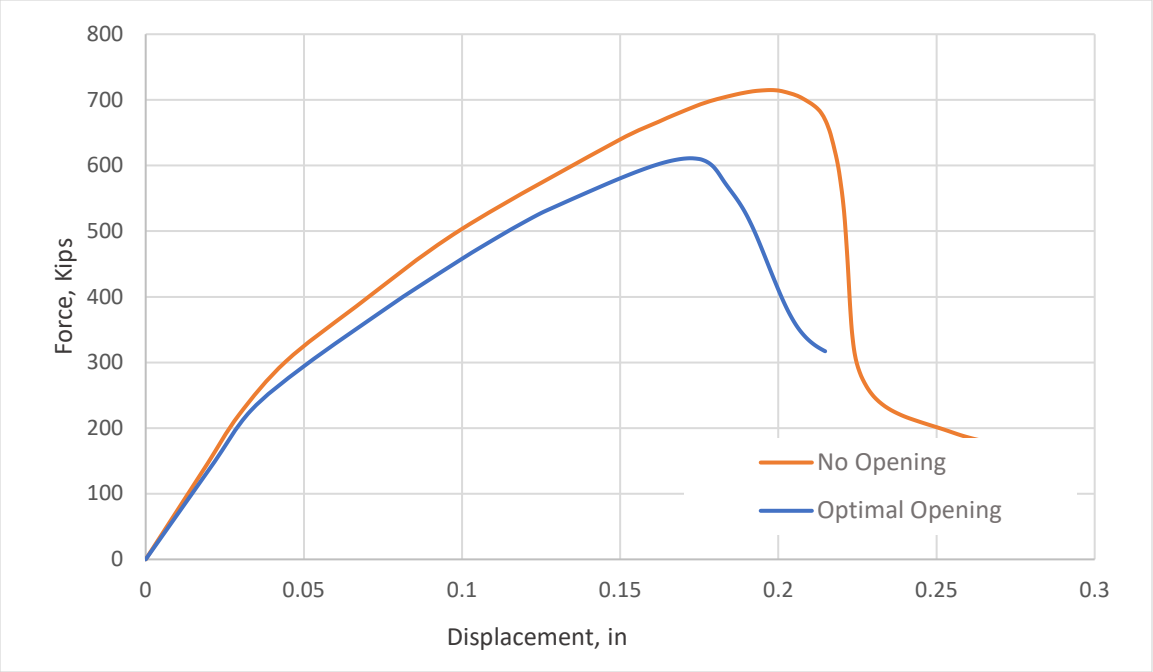

Figure 3-48. *Comparison of axial strength, wall with no openings vs. wall with openings.*

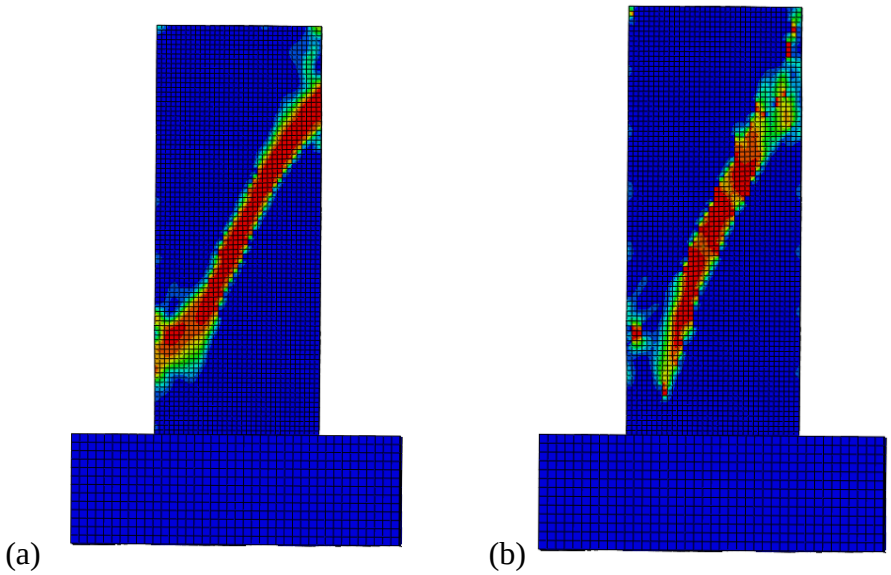

Figure 3-49. *(a) Compression damage and (b) tension damage in wall with no openings in pure axial compression.*

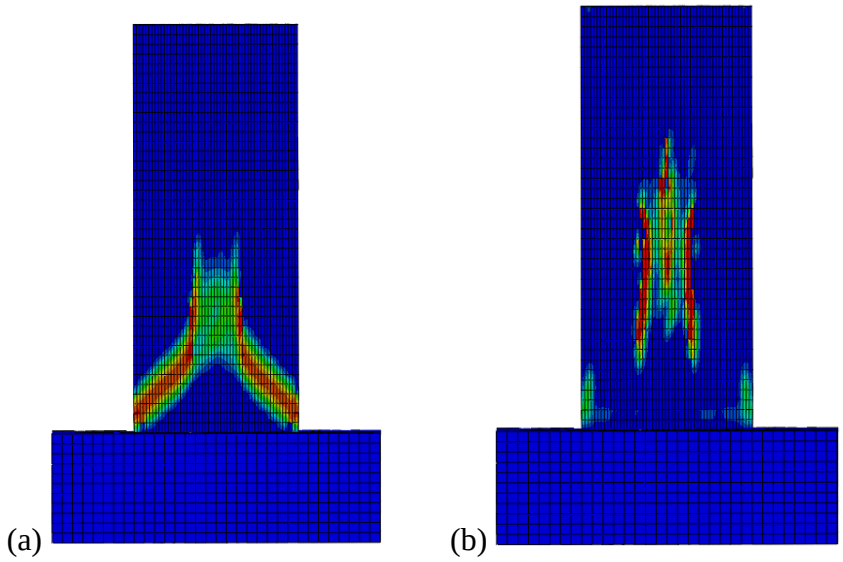

Figure 3-50. *(a) Compression damage and (b) tension damage in wall optimal opening configuration in pure axial compression.*

3.5.3.2 Four-point Bending Model

In the four-point bending model, the wall was laid flatwise. One end of the wall was supported with a pin connection, and the other side was supported with a roller. Two three-inch displacements were applied along the third points, coinciding with the two loading strips from laboratory testing. This is shown in Figure 3-51.

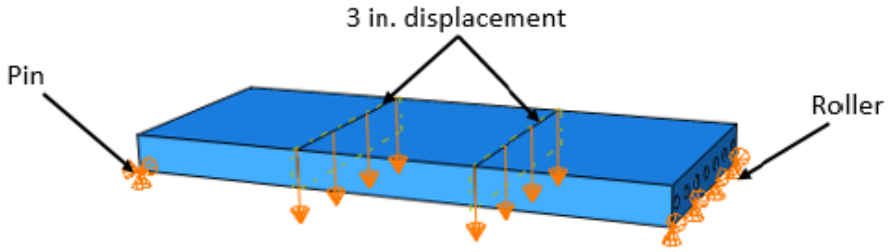

Figure 3-51. *Boundary conditions and loading for four-point bending model.*

Figure 3-52 shows the load-displacement curve for the midspan of the specimen from the finite element model.

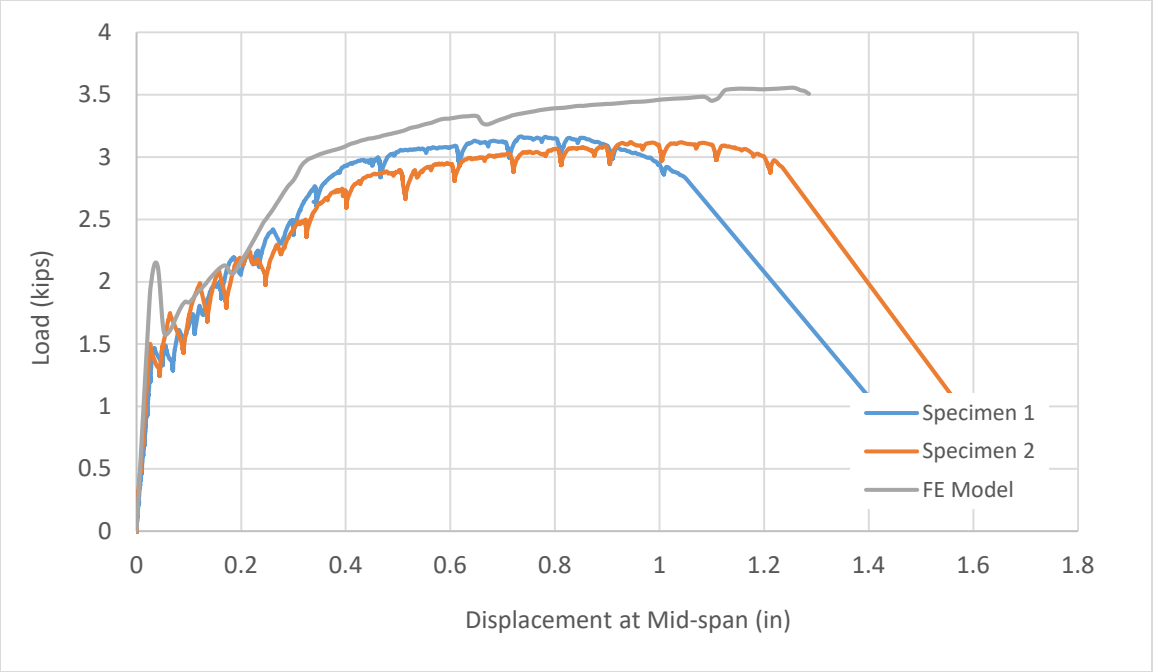

Figure 3-52. *Load vs. displacement for mid-span of FE Model vs. laboratory results, four-point bending test.*

Figure 3-53 shows the tensile damage occurring on the bottom of the wall in the FE model. Cracking is similar to that as experienced during laboratory testing. Similar to seen in testing, the first cracks to appear in the FE model occur at the third points under the loading strips. No compression damage occurs on the top of the wall in the FE model, again corresponding to those results observed in laboratory testing.

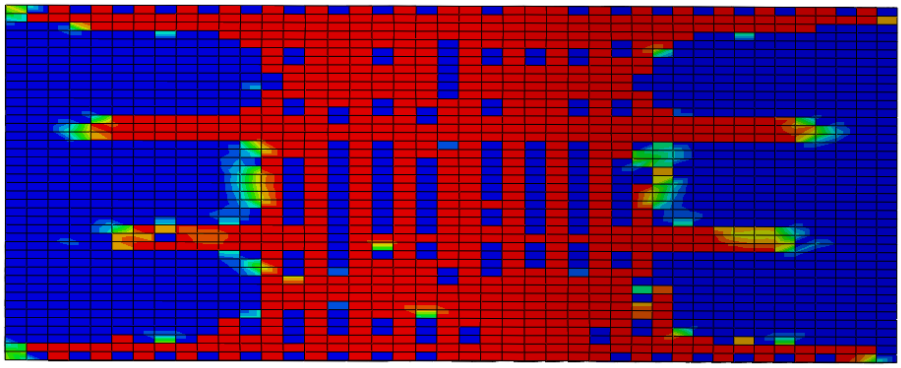

Figure 3-53. *Tensile damage of bottom of wall in FE model, four-point bending test.*

3.5.3.2.1 Comparison with Hand Calculations

Hand calculations show that the weak-axis moment capacity of the wall is 5.637 kip-ft. This is approximately 3% lower than the weak-axis moment capacity of the wall as calculated by the finite element model, and 5% higher that the weak-axis moment capacity of wall, as shown by the average of the two laboratory tests.

3.5.3.2.2 Comparison to Wall with No Openings

Figure 3-54 displays the load-deflection curve for the wall with optimal openings, as shown above, as well as for a wall with no openings. As seen, the behavior for both walls is very similar, although the wall with no holes is not surprisingly stronger. The first bump in both curves occurs when damaged mesh appears first in the test.

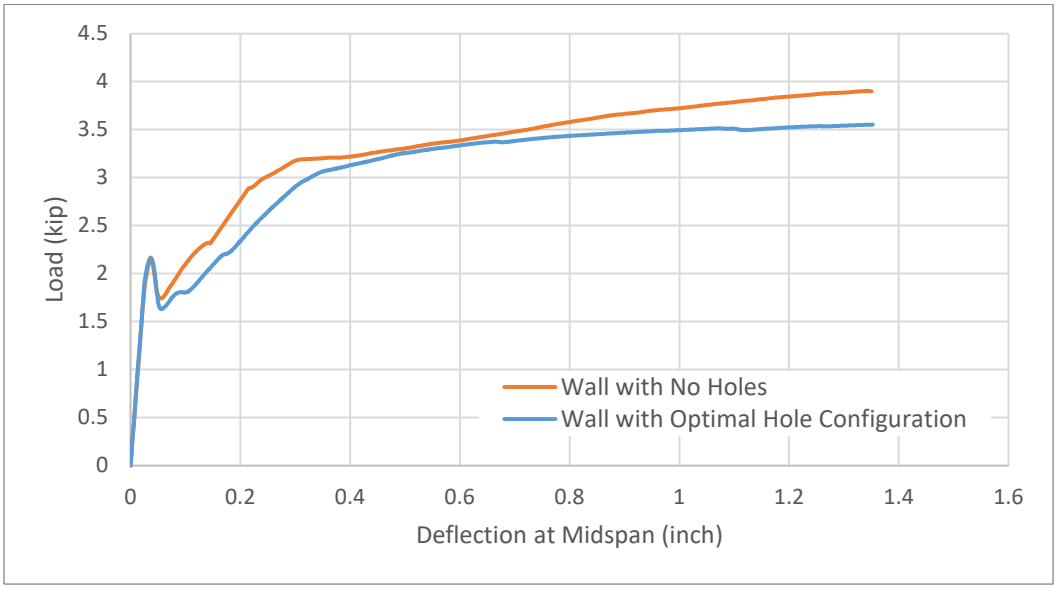

Figure 3-54. *Comparison of wall with no openings to wall with optimal opening configuration, four-point bending test.*

Figure 3-55 and Figure 3-56 below provide the compression and tensile damage occurring in the specimen at failure, respectively. As shown, unlike the wall with holes, crushing does occur on the top surface of the wall without holes near the loading areas,

although very concentrated to these locations and minimal. Additionally, the tensile damage occurring on the wall without holes is less than the wall with the holes.

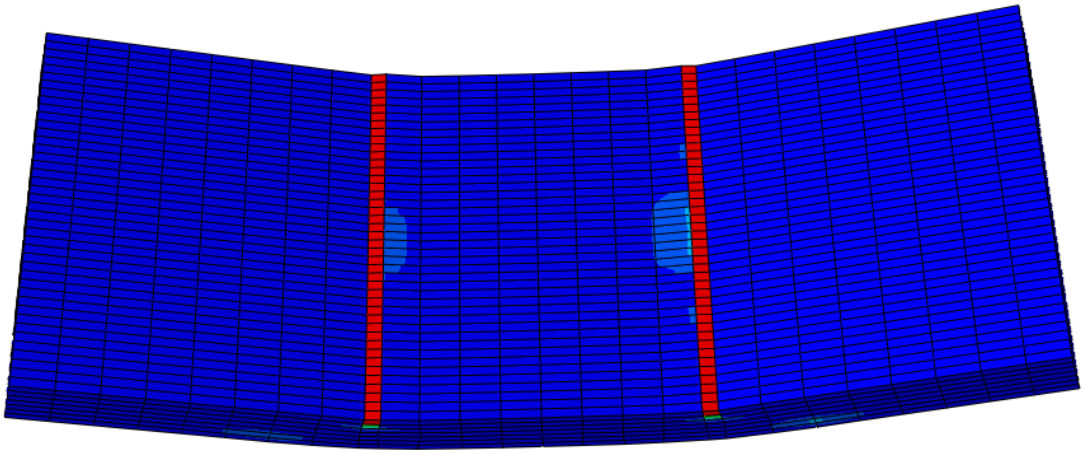

Figure 3-55. *Compression damage occurred on top surface of wall with no openings, four-point bending test.*

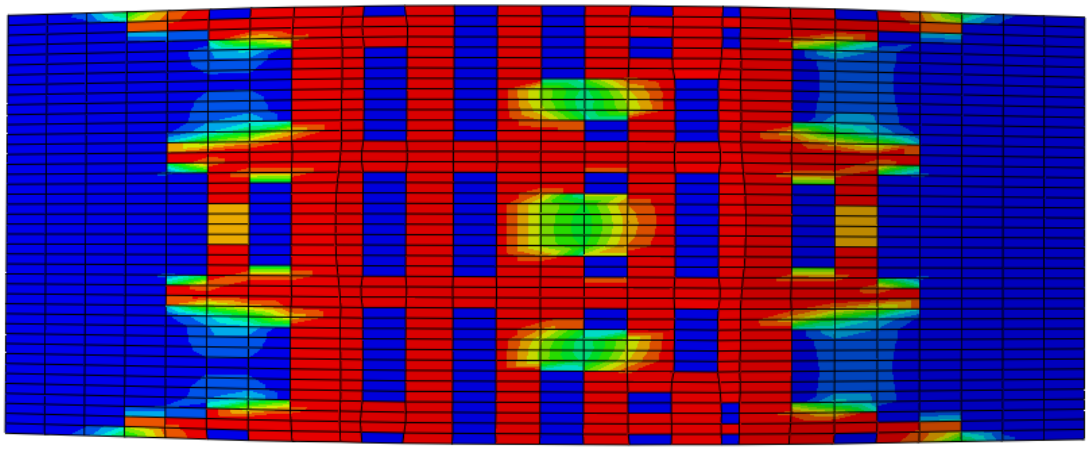

Figure 3-56. *Tension damage occurring on bottom surface of wall with no openings, four-point bending test.*

3.5.3.3 Pushover Model

During testing it was observed that the load-displacement behavior of the specimen was solely dependent on the performance of the reinforcing after cracking occurred between

the wall and the footing. In the developed finite element model, this behavior was taken into consideration. In order to model the behavior of the joint between the wall and footing properly, extensive material tests would have to be performed in order to quantify the bond of the joint. Instead of performing these tests, a lower bound and upper bound were developed to compare to testing results. The lower bound model did not fully bond the bottom of the wall to the top of the footing; rather, the corner edge of the wall was constrained to the footing below it. This constraint allowed the corner of the wall to act like a hinge, with the reinforcing acting as the only element tying the remainder of the wall to the footing. Therefore, the failure of this model is dependent on the failure of the reinforcing. The boundary conditions of the lower bound model and the corresponding deformed shape can be seen in Figure 3-57. The upper bound model fully constrained the bottom of the wall to the top of the footing. This model resembles a situation where the wall does not come apart from the top of the footing. The boundary conditions of the upper bound model can be seen in Figure 3-58. The failure of this model is dependent on the failure of the concrete.

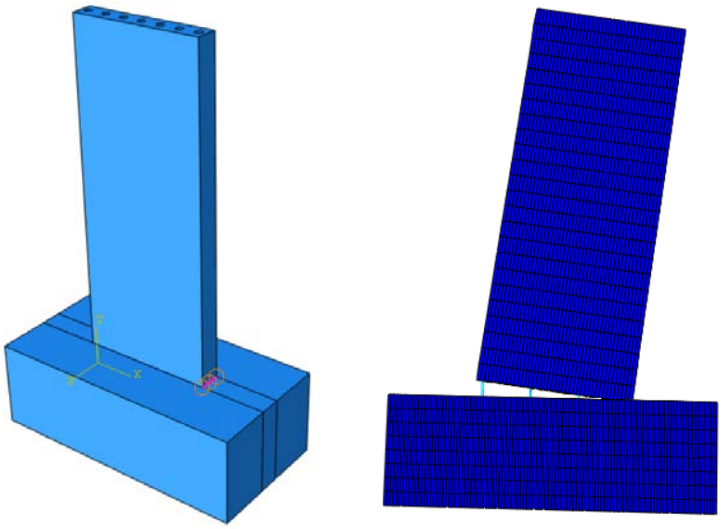

Figure 3-57. *Lower bound FE model, pushover test.*

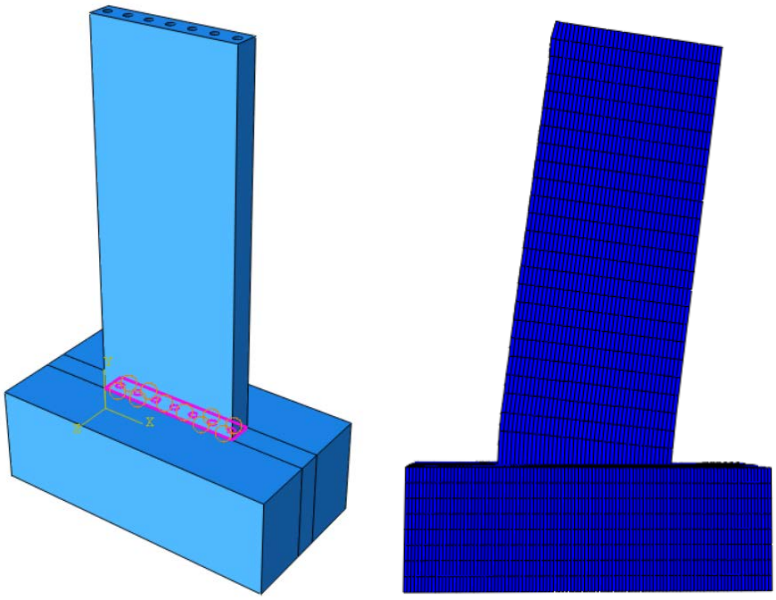

Figure 3-58. *Upper bound FE model, pushover test.*

In each model, a displacement of three inches is applied to the top of the wall. Figure 3-59 presents a comparison of the upper and lower bound FE models with the results from laboratory testing. The displacement of each set of results is taken from the point of highest horizontal displacement at the top of the wall. The laboratory results fall in the middle of the upper and lower bounds, as expected. The wall tested in the laboratory failed at approximately 6.7 kips, while the lower and upper bounds fail at approximately 6.1 and 8.5 kips, respectively. The overall behavior of the tested wall, however, acts closely to that of the lower bound. In each of these instances, the wall acts like a hinged member, with the load-displacement relationship fully reliant on the performance of the steel after cracking at the wall-footing interaction.

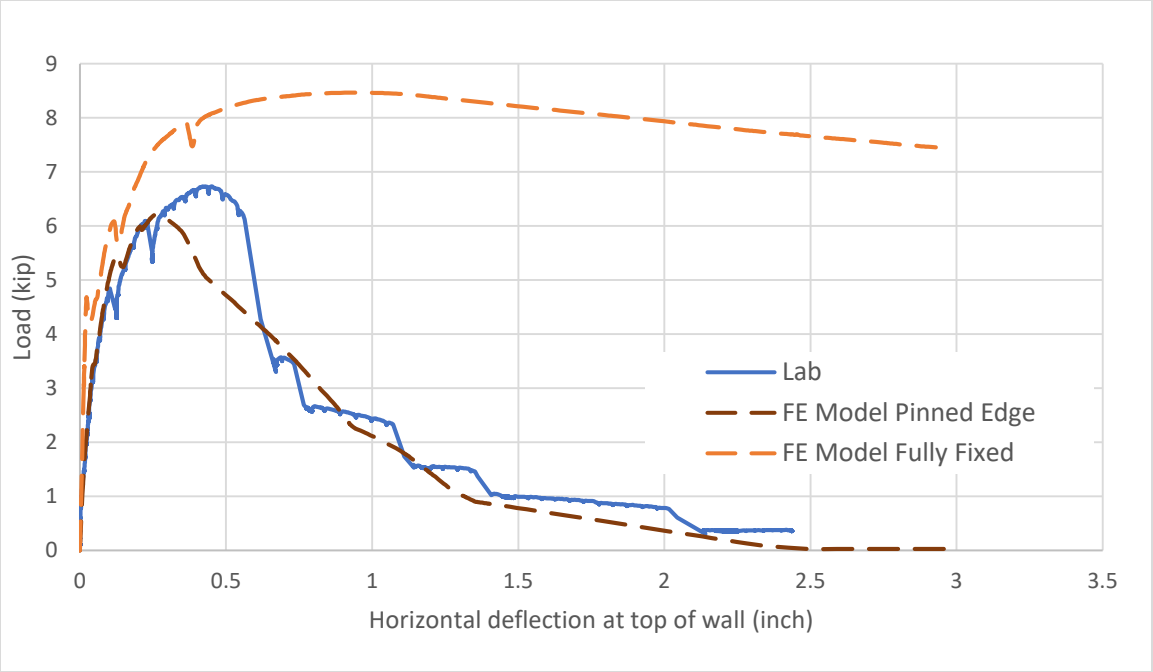

Figure 3-59. *Load vs. deflection for upper and lower bound FE models vs. laboratory results, pushover test.*

Dependent on the model and type of interaction specified between the bottom of the wall and the top of the footing, depended on the magnitude of strain that the longitudinal reinforcing experienced at the base of the wall. Figure 3-60 through Figure 3-62 present the strain experienced by the first three main lines of longitudinal reinforcing along the wall, comparing the upper and lower bounds of FE model results with that of the laboratory testing. In general, the reinforcing in the lower bound model reaches fracture much quicker than the reinforcing in both the upper bound model and laboratory testing. This is understandable, as the reinforcing is taking all load in the lower bound model. As expected, the reinforcing from the laboratory tests falls in between the lower and upper bounds. Similar to laboratory testing, in both the upper and lower bound models, rebar in the first three lines of longitudinal reinforcing fracture.

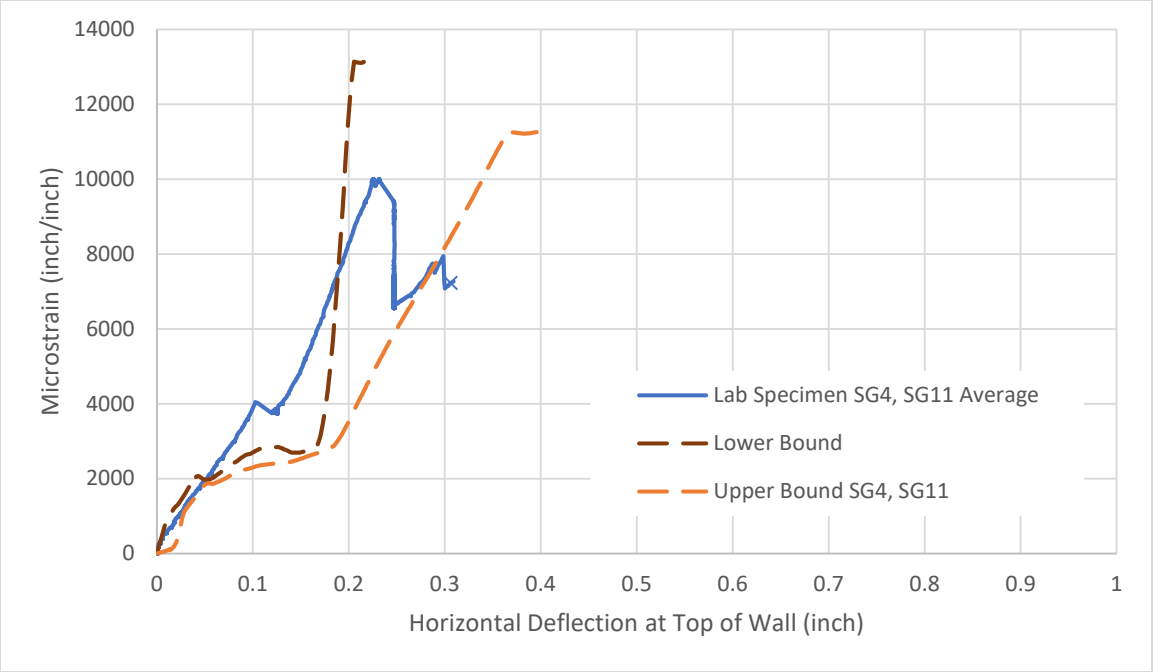

Figure 3-60. *Strain vs. deflection for first line of longitudinal reinforcing; upper and lower bound FE models vs. laboratory results, pushover test.*

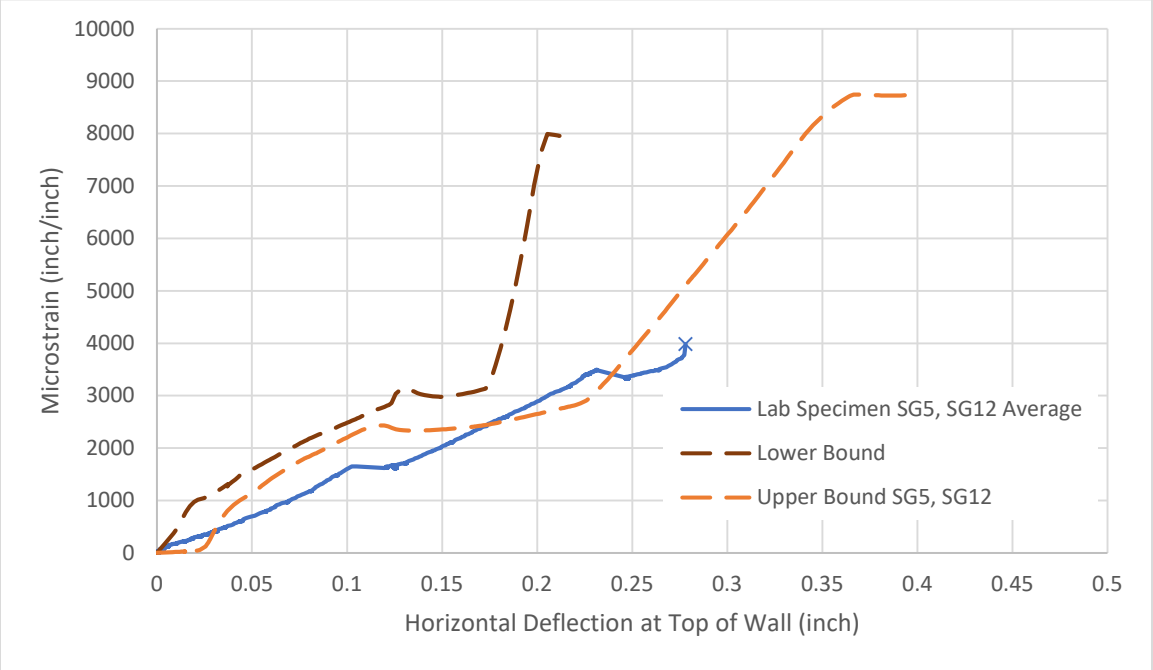

Figure 3-61 *Strain vs. deflection for second line of longitudinal reinforcing; upper and lower bound FE models vs. laboratory results, pushover test.*

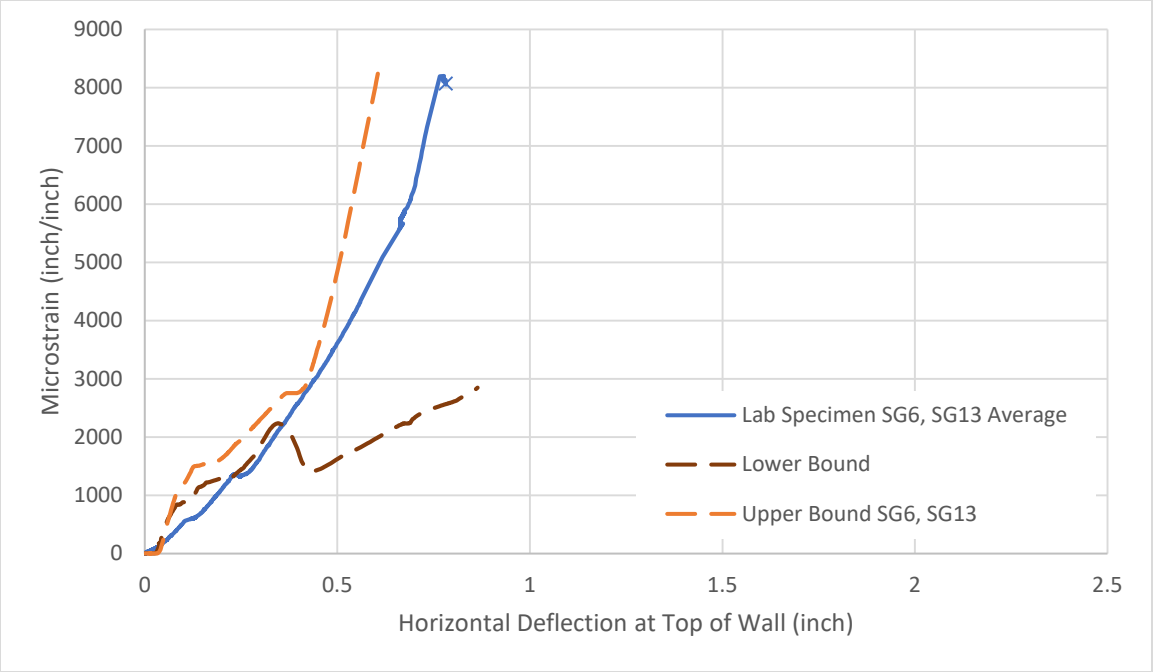

Figure 3-62 *Strain vs. deflection for third line of longitudinal reinforcing; upper and lower bound FE models vs. laboratory results, pushover test.*

The cracking patterns shown in both the upper and lower bound FE models are similar in nature to that of the laboratory specimen, shown in Figure 3-63. As shown, the cracking started at the bottom interface of the wall, and continued to grow horizontally. As this crack grew and more load was applied, additional horizontal cracks formed. Vertical cracks also formed, joining the horizontal cracks together. The cracking experienced by the laboratory specimen most closely resembles that of the lower bound model. Additional cracking was seen in the upper bound model, as the stress experienced by the bottom face of the wall could not be released by a crack at this interface due to the constraints specified.

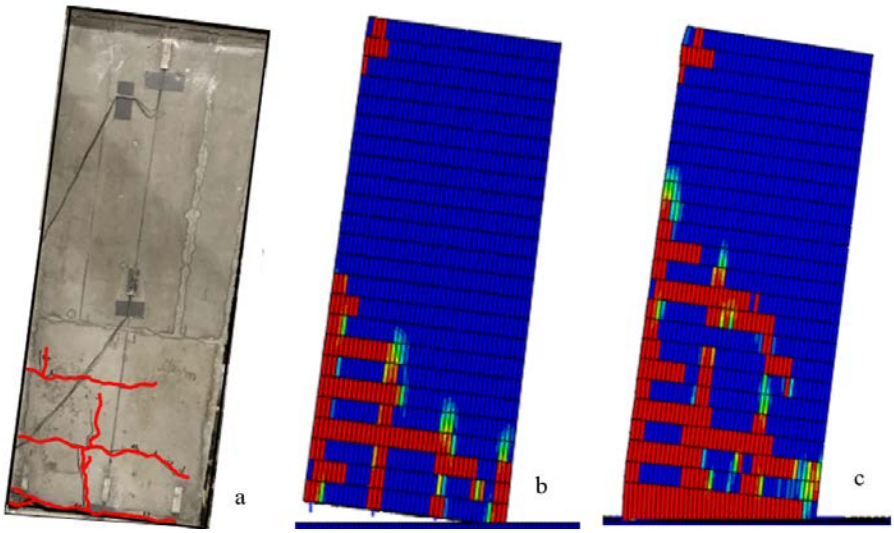

Figure 3-63. *Comparison of cracking (tension damage) between (a) laboratory specimen, (b) lower bound FE model, (b) upper bound FE model, pushover test.*

Both the upper and lower bound models showed minimal crushing occurring on the north side of the wall. This is shown in Figure 3-64. There was hardly any crushing experienced by the concrete in the laboratory test. The back base of the wall is shown in Figure 3-65, and the small crushing that did occur is highlighted in blue. In both laboratory testing and the FE models, cracking of the concrete occurred well before crushing of the concrete.

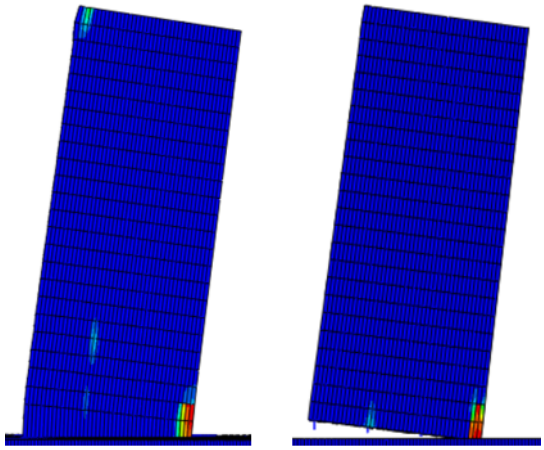

a b

Figure 3-64. *Compressive damage in (a) upper bound and (b) lower bound FE models, pushover test.*

Figure 3-65. *Area of minimal crushing in laboratory specimen, pushover test.*

During laboratory testing, only the concrete on the northern base of the wall experienced strain, as the rest of the concrete was released from feeling stress by the crack on the bottom of the wall. Comparing the concrete strain in this area from testing to the FE models is very interesting. Presented in Figure 3-66, one can see that the concrete strain data from laboratory testing most closely resembles that of the lower bound. In both of these cases, the concrete first experiences compression, and then transitions back to experiencing very little strain as cracks propagate and the hinge on the outer concrete edge is formed. Once the hinge is formed, the concrete in this area is released from stress. The concrete strain in this area experienced by the upper bound, however, experiences a slightly different pattern of stresses. First, the strain follows similarly to the lower bound, experiencing compression as the wall is first pushed. Next, the strain goes into tension as the reinforcing yields, and the strength of the wall becomes reliant on the concrete. Finally, the concrete experiences significant compressive strain, eventually experiencing crushing. This pattern is also shown

visually in Figure 3-67, where the transition of strain in the y-direction is presented for the bottom of the wall.

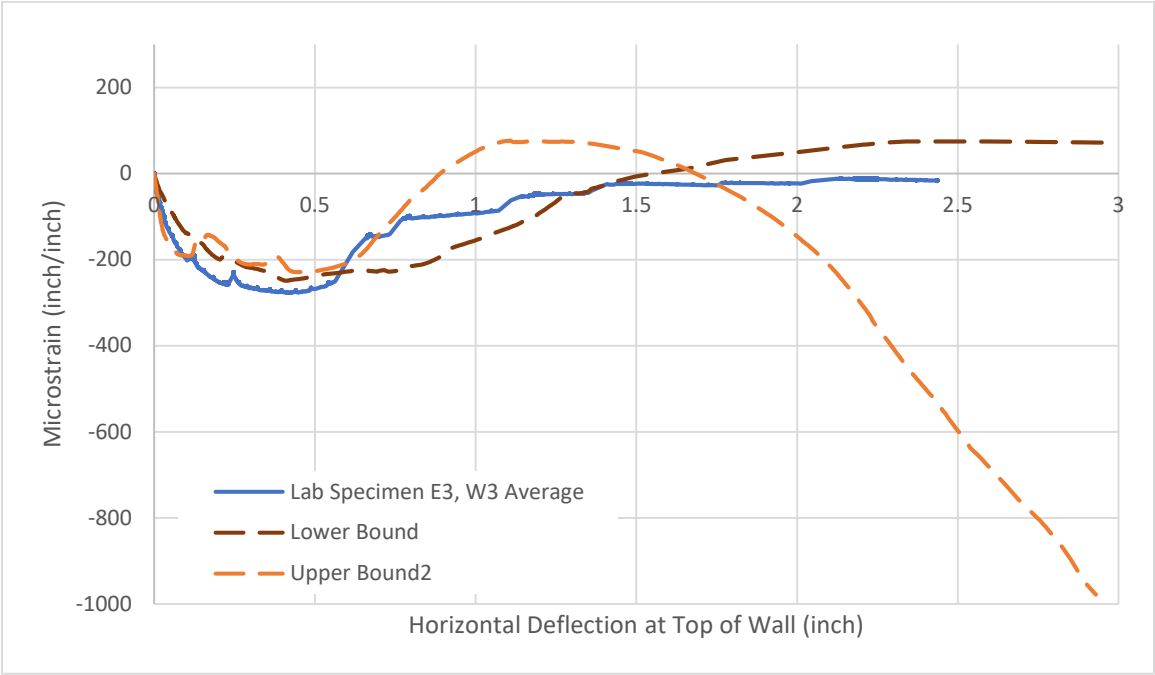

Figure 3-66. *Strain vs. deflection in concrete at northern corner of the wall; upper and lower bound FE model vs. laboratory results, pushover test.*

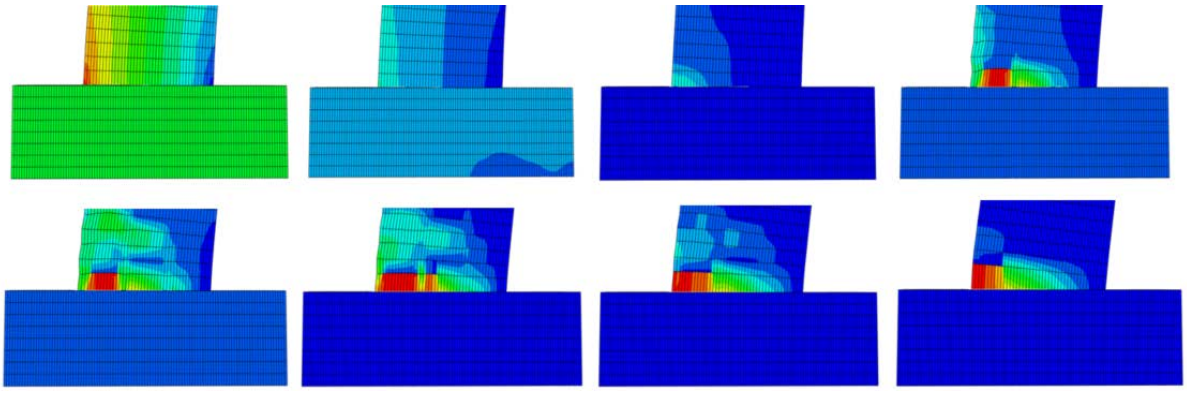

Figure 3-67. *Strain at bottom of wall during life cycle in upper bound FE model, pushover test.*

3.5.3.3.1 Comparison with Hand Calculations

The failure of the wall was dependent on both the shear strength and the strong-axis moment capacity of the reinforced concrete wall. The shear capacity of the wall was calculated as 9.78 kip, and the moment capacity of the wall was calculated as 22.57 kip-ft. Dividing the moment capacity of the wall by the height gives a force of 4.51 kip. Therefore, the moment capacity of the wall will govern the behavior, resulting in a maximum hand calculated force of 4.51 kip. This is 39% lower than the failure load of the laboratory test, 31% lower than the lower bound FE model, and 60% lower than the upper bound FE model.

3.5.3.3.2 Comparison to Wall with No Openings

Both the upper and lower bound cases were considered when comparing the wall with optimal openings to a wall with no openings. Figure 3-68 shows a comparison of these cases. As shown, the two walls act very similar. This is expected, as the strong axis bending moment capacity is negligibly affected by the presence of holes. Rather, the performance of the wall is dependent on the size and spacing of the longitudinal rebar. Because the placement of the reinforcing was the same for both walls in consideration, the results are similar. One can see that the maximum load that the upper bound, fully fixed, models can take for the two cases are identical in nature. However in looking at the lower bound, the wall with no holes has a slightly smaller maximum load than the wall with optimal holes, when considering the wall with the optimal hole configuration. Additionally, the lower bound model of the wall without holes had less cracking associated with it, as shown in Figure 3-69. Similar to the wall with optimal holes, there was minimal crushing in the plain wall.

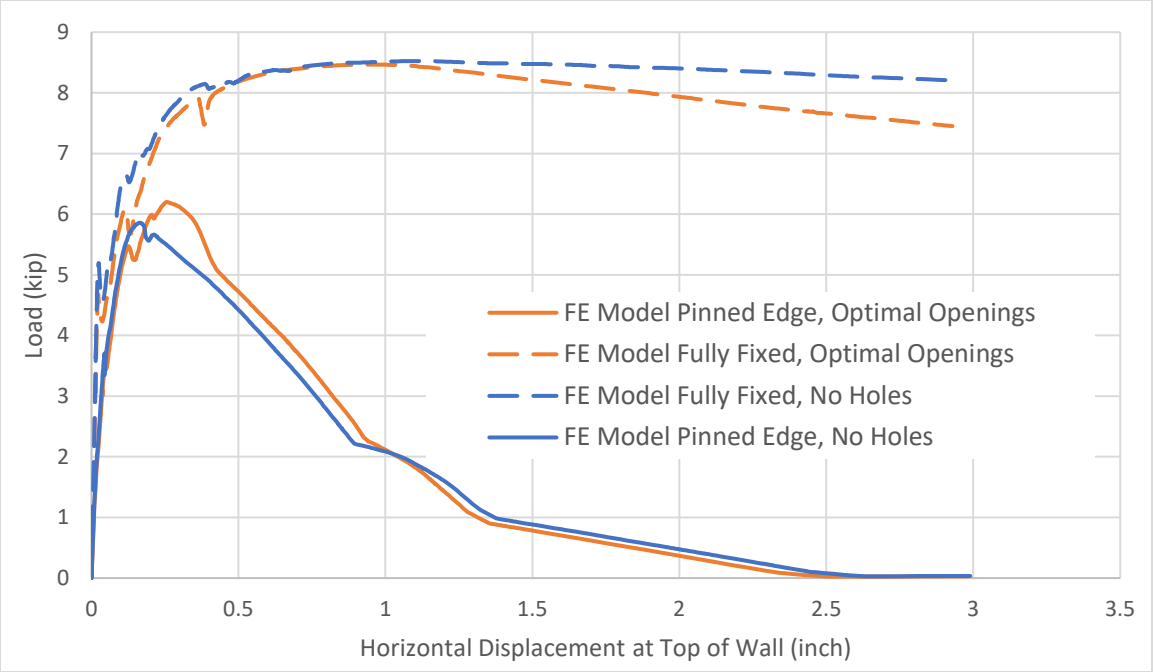

Figure 3-68. *Comparison of wall with no openings to wall with optimal opening configuration, lower and upper bounds for pushover test.*

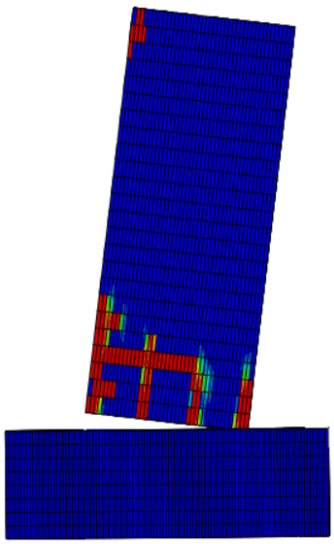

Figure 3-69. *Tension damage for lower bound FE model wall without holes, pushover test.*

3.6 Conclusions and Future Work

As expected, those reinforced concrete walls with openings are associated with a strength reduction, due to a reduction in material able to contribute to resisting load.

However, fortunately, the maximum load expected by the wall with holes was one that was close to expected values found via hand calculations. The following conclusions can be made from this study, and taken into consideration when designing TLWD systems:

1. In general, the strength reduction associated with the wall in different loading conditions may be accounted for by adding additional reinforcing. This will cause the width of the wall to increase, however, this is a necessary step to take in order to prevent failure.
2. The axial load strength of the wall is directly related to the maximum compressive strength and reduction of area due to holes in the wall. If a wall with openings is being used for a large bearing load, a high compressive strength of concrete should be used. If the top of the wall is braced, buckling should not govern when designing. However, this is also dependent on the reduction in moment of inertia associated with the holes, and should be checked via hand calculations or finite element analysis.
3. The weak-axis moment capacity of a wall with openings can be adequately calculated via hand calculations. If an adequate amount of flexural reinforcing is present, the wall should experience a flexural failure. No stress concentrations were noticed around the holes during flexure.
4. Results from the pushover test showed that the strength of the wall was highly dependent on the connection between the wall and the footing, as well as the strength of the reinforcing. It was seen that the strong-axis moment capacity governed over the shear capacity of the wall. However, this could change if

additional and adequate flexural reinforcing is provided, along with reinforcing hooks to the footing.

5. Failure modes must be taken into consideration if using reinforced concrete walls with openings for a TLWD system. A failure mode that may be typically expected for a wall without openings may not be the same as for a wall with openings. If failure occurs in a TLWD system, the system could be permanently damaged. This could lead to additional structural damage if occurring during a seismic or large wind event.

There are several additional topics of interest related to this study that need to be further explored before utilizing reinforced concrete walls with openings. Future research topics could include the following:

1. Exploration of material used to create capillaries. While PVC tubes were used for ease of construction in this laboratory experiment, capillaries constructed of steel or FRP could be utilized, possibly adding an additional strength element to the wall. This “additional reinforcement” could possibly make up for the strength reduction in the wall associated with the openings.
2. Multi-loading scenarios utilizing finite element models. It is rare that structural walls are subjected to just one loading condition, as performed in this study. However, now that the finite element models are calibrated, continued testing with models can be performed with multi-loading scenarios. This could include walls subjected to both horizontal and vertical loads, walls subjected to dynamic loading while under axial compression, and walls subjected to bi-axial bending.

3. Cyclic loading of reinforced concrete walls. If walls are to be utilized for mitigation in dynamic events, cyclic loading should be performed on the walls to ensure that the holes do not form stress concentrations, or cause premature failure.
4. Behavior of walls with openings in large-scale setting. Finite element models could be developed using reinforced concrete walls with openings at a building system level. Overall performance with the diaphragm and other structural elements could be assessed.

3.7 References

Abaqus/CAE User's Manual (6.12) – Abaqus Version 6.12. (2012).

American Concrete Institute. *Building Code Requirements for Structural Concrete (ACI 318-14).* Farmington Hills, MI, USA, 2014.

Chai, W., & Feng, M. Q. (1997). Vibration Control of Super Tall Buildings Subjected To Wind Loads. *Int J. Non-Lmear Mechanics*, *32*(4), 657–668.

Gebreyohaness, a S., Clifton, G. C., & Butterworth, J. W. (2012). Finite element modeling of non-ductile RC walls. *15th World Conference on Earthquake Engineering (15WCEE), Lisbon, Portugal*, *11*.

Hsu, L. S., & Hsu, C.-T. T. (1994). Complete stress — strain behaviour of high-strength concrete under compression. *Magazine of Concrete Research*, *46*(169), 301–312.

Lefas, I., Kotsovos, M., & Ambraseys, N. (1990). Behavior of reinforced concrete structural walls: strength, deformation characteristics, and failure mechanism. *ACI Structural Journal*, (87), 23–31.

Novoselac, S., Ergic, T., Balicevic, P. "Linear and nonlinear buckling and post buckling analysis of a bar with the influence of imperfections." Technical Gazette 19, 3(2012), 695-701.

Sung, Yu-Chi et al. "A study on pushover analyses of reinforced concrete columns." Journal of Structural Engineering and Mechanics, Vol. 21, No. 1 (2005) 35-52.

Thi Thu Ho, Chung. (2010). "Analysis of thermally induced forces in steel columns

subjected to fire," thesis, presented to The University of Texas at Austin at Austin, TX, in partial fulfillment of the requirements for the degree of Masters of Science.

Vasios, Nikolaos. (2015). "Nonlinear analysis of structures. The arc length method: formulation, implementation, and applications." thesis, presented to Harvard University at Cambridge, MA, in partial fulfillment of the requirements for the degree of Doctor of Materials Science and Mechanical Engineering.

Wahalathantri, B. L., Chan, T. H. T., & Fawzia, &. (2011). A Material Model for Flexural Crack Simulation in Reinforced Concrete Elements Using Abaqus. *In Proceedings of the First International Conference on Engineering, Designing and Developing the Built Environment for Sustainable Wellbeing*, 260–264.

Wight, J. K. (2016). *Reinforced Concrete*.

Wu, H., Cao, L., Chen, A., & Laflamme, S. (2017). A novel tuned liquid wall damper for multi-hazard mitigation. *Proceedings of SPIE - The International Society for Optical Engineering*, *10164*(April 2017).

Wu, J. S., & Hsieh, M. (2002). Study on the dynamic characteristic of a U-type tuned liquid damper. *Ocean Engineering*, *29*(6), 689–709.

Zhang, Yinglong. (2018). "Behavior of reinforced concrete walls with circular openings," thesis, presented to Iowa State University at Ames, IA, in partial fulfillment of the requirements for the degree of Masters of Science in structural engineering.

CHAPTER 4. USABILITY OF A MOBILE AUGMENTED REALITY APPLICATION TO TEACH STRUCTURAL ANALYSIS

A paper to be submitted to Educational Technology Research and Development

Elizabeth Miller, Dr. Aliye Karabulut Ilgu, Suhan Yao[4], David Wehr[5], Dr. An Chen

Abstract

This research assesses the functionality of a mobile augmented reality application designed to transform the educational experience of undergraduate students in a structural analysis class. Functionality was assessed through usability testing, in which users completed a protocol forcing them to interact with all aspects of the user interface. During testing, data was collected both qualitatively and quantitatively through a think-aloud protocol, tracking of participant clicks, video and audio recording, and survey results. All components of the user interface were assessed, and results from usability testing allowed researchers to make improvements to the application before implementation into a classroom setting. This paper comments on the usability testing protocol design, results, and analysis of data leading to improvements.

This material is based in part upon work supported by the National Science Foundation under Grant No. DUE-1712049. Any opinions, findings, and conclusions or recommendations expressed in this material are those of the authors and do not necessarily reflect the views of the National Science Foundation.

4.1 Introduction

Structural analysis is an introductory course taught in every undergraduate civil engineering program at approximately 300 institutions in the United States, as well as in

[4] Helped in writing usability testing protocol, conducting usability testing, and collating data.
[5] Developed AR application and tracking framework.

most architectural and construction programs. Despite its critical role in the curriculum, most novice learners in this course do not appear to have a sound understanding of the fundamental concepts. This includes concepts such as load types, load effects, and visualization of the deformed shape of simple structures, a necessary skill to conceptualize structural behavior beyond theoretical formulas and methods (Davalos et al., 2003; Teng, Song, & Yuan, 2004). In particular, students have difficulty in relating basic structural members, including trusses, beams, frames, and others, to more complex structural systems, such as buildings and bridges. Such learning deficiencies can be largely attributed to the ineffectiveness of the traditional lecturing mode of teaching. Within lecturing, much effort is spent on the analysis of individual members, with a small emphasis devoted to understanding the behavior of the entire structure in a three-dimensional context.

In this study, an augmented reality (AR) application was developed to facilitate the teaching of structural analysis concepts. AR combines the real world with the virtual content so that it conserves users' awareness of the real world environment in a 3D space (Azuma et al., 2000). AR has been implemented in the Architecture, Engineering, and Construction (AEC) domains. However, the integration of such technology into undergraduate teaching practices has been somewhat limited, despite the evidence that it facilitates learning of abstract and difficult-to-understand topics (Shirazi & Behzadan, 2015).

This paper presents the results of usability testing conducted on the developed application. Usability testing is a systematic process that evaluates user's ease of use of a tool to achieve a certain goal. Testing, therefore, focuses on the end user of a particular product, the results of which inform the systematic refinement of the product by identifying usability issues at an early stage and quickly rectifying them before full implementation (Sandars and

Lafferty, 2010). For the purpose of this particular study, the goal was to discover if the provided AR application interface was user-friendly, with functions meaningful, easy to use, and easy to locate.

4.2 Description of iStructAR Interface

The AR application, iStructAR, aims to supplement teaching traditional structural analysis concepts by helping students better visualize how structures behave under certain loading conditions. A pedestrian skywalk connecting two campus buildings was selected as the structure to teach the concepts of loads (specifically, live and dead load) and the resulting reaction forces and deflections for typical beam-type structures. This scene, referred to as the skywalk module, was solely used for usability testing. Those changes that were made to the skywalk module through usability testing were made to later developed modules, in order to make the student experience with all aspects of the application consistent.

iStructAR utilizes vision-based AR as defined by Dunleavey (2014), with both indoor and outdoor targets to provide flexibility for the users and instructors. Using an iPad, students are able to project structural information onto either an inherent picture of the skywalk, a printed or digital photo of the skywalk, or the real structure itself. They can then modify the structural load, changing both its magnitude and distribution, to observe the effects on the structure. This is shown below in Figure 4-1.

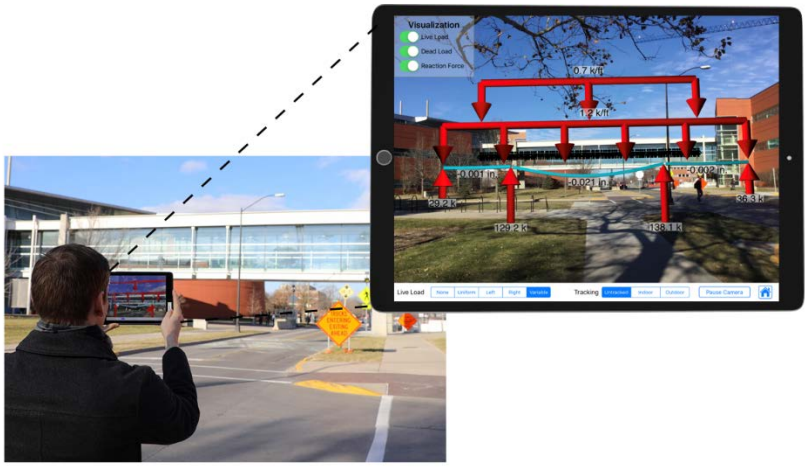

Figure 4-1.*Student holding an iPad in front of the on-campus skywalk structure, projecting various loading conditions through AR while observing effects real-time.*

Figure 4-2 describes the main functionalities of iStructAR, through the lens of the skywalk module. These functionalities are referenced throughout this paper. Figure 4-2 is of a preliminary version of iStructAR, before usability test was completed. The final user interface will be presented at the end of this chapter.

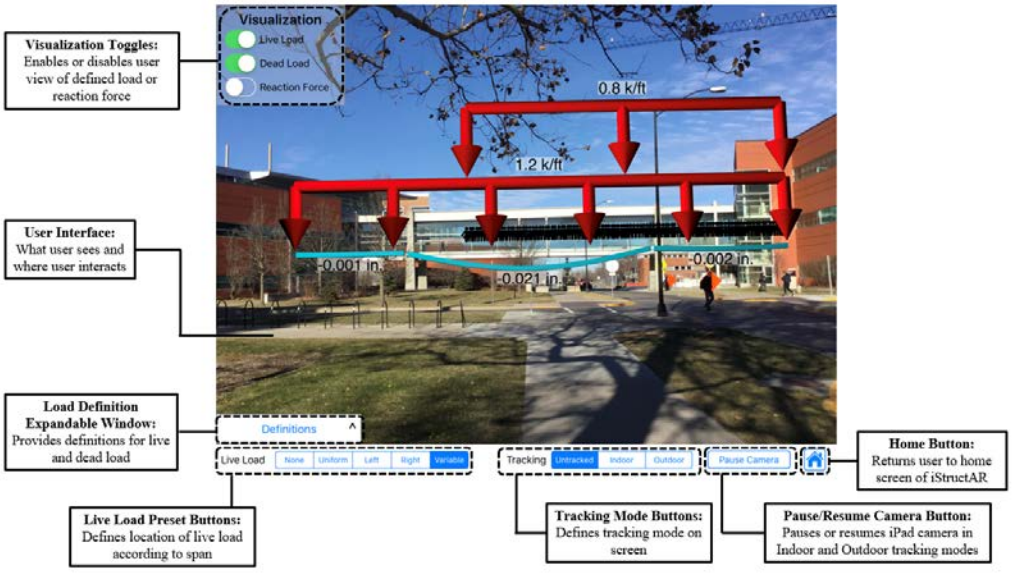

Figure 4-2. *Functionality nomenclature and definitions within skywalk scenario.*

4.3 Methodology

The purpose of this particular study was to discover if the provided AR interface was user-friendly, with functions meaningful and easy to locate and use. For the above described skywalk model, two versions - “guided” and “unguided” - were created. One objective of the usability tests was to decipher which version was preferred by users. The guided version of the app module included step by step text guidance, describing the visualization of loads, reaction forces, and deflection. Within this version, certain functions were disabled during preliminary steps, encouraging students to understand concepts before using the full functionality of the application, as seen in Figure 4-3. This screenshot from the guided version shows Step 3 of a six step procedure, describing the application of dead load and resulting deflection values. Note that the different live load preset buttons in the bottom left of the screen are disabled, as the procedure has not yet described the application of live load.

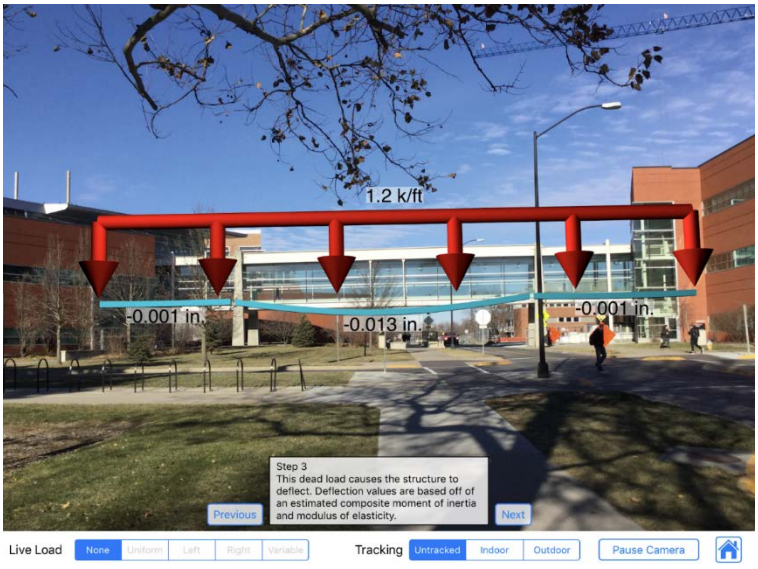

Figure 4-3. *Guided version of skywalk application, with an example procedural step explaining deflection values.*

The “unguided” version, shown in Figure 4-2, differs from the guided version simply in that procedural directions are not provided within the application at any time. While

different visualizations of loading and options appear at different steps in the guided version, all visualization options are enabled at all times throughout the unguided version.

The overall methodology utilized in the usability testing can be seen below in Figure 4-4. First, students were observed interacting with the application through a given usability protocol. Next, students completed an end-of-test survey indicating aspects of the application that they liked and/or disliked. Students also notated areas that could use improvement. This testing cycle was repeated with ten students. At the end of usability testing, common issues that students had during testing were identified, and improvements needed in the application were made.

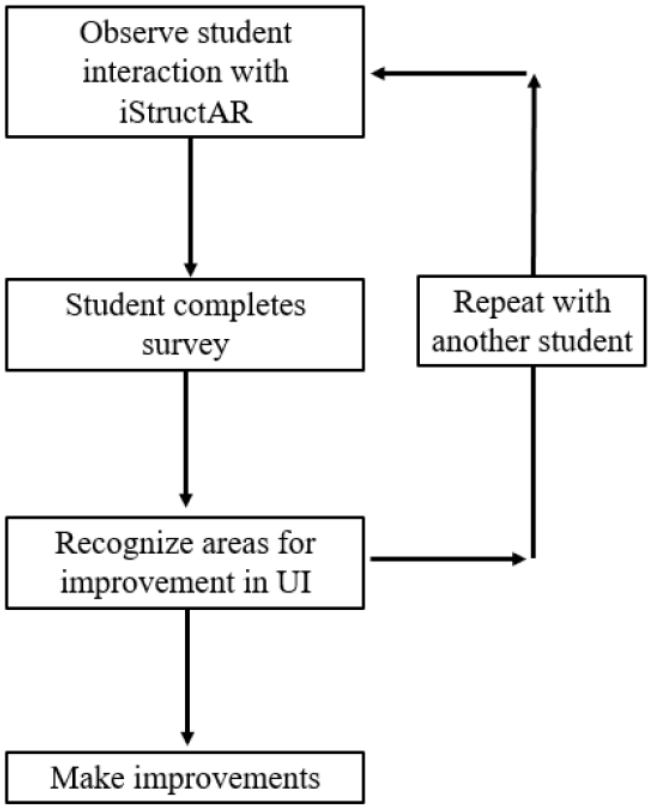

Figure 4-4. *Usability testing methodology.*

4.3.1 Participants

As previously stated, the purpose of the usability tests was to evaluate the usability of the application, rather than the teaching impact, which is investigated in another study. Therefore, it is acceptable to have a small set of participates to provide feedback on various usability issues (Sandars & Lafferty, 2010). One student (Student 1) participated in an initial usability test. After this particular test, small modifications were made to the overall testing protocol. The test results from this student are included with data throughout this paper, however, are not included in final survey results, as questions were altered too much. After the initial testing period with Student 1, nine additional students participated in the study. Total, five of these students experienced the guided version of the app, and five students experienced the unguided version.

Table 4-1 below shows preliminary information gathered on the students. The last column of the table indicates which version of the app the students used for testing. Of the ten students, four students owned an iPad. Of these students, most communicated that they used their device for browsing websites (such as social media), playing games through applications, or completing schoolwork (either completing homework assignments or taking notes in class). Of the ten students, only two students had ever experienced augmented reality before. Both of these students experienced AR through video games, such as the popular Pokemon Go! application. All students had previously taken a structural analysis class.

Table 4-1. *Background information on student participants.*

Student #	Gender	Major	Year of Study	iPad Possession	Experience with AR	Test
S1	Male	Civil Eng.	Senior	Yes, uses once per week	No	Guided
S2	Male	Civil Eng.	Graduate Student	No	No	Guided
S3	Male	Civil Eng.	Senior	No	No	Unguided
S4	Male	Civil Eng.	Graduate Student	No	No	Unguided
S5	Male	Civil Eng.	Senior	No	No	Guided
S6	Female	Civil Eng.	Graduate Student	No	Yes, videogames	Guided
S7	Male	Civil Eng.	Graduate Student	Yes, weekly	Yes, videogames	Unguided
S8	Female	Civil Eng.	Graduate Student	Yes, weekly	No	Unguided
S9	Female	Civil Eng.	Senior	No	No	Guided
S10	Male	Civil Eng.	Graduate Student	Yes, sometimes	No	Unguided

4.3.2 Data Collection Materials, Procedures, and Analysis

A mixed-method approach was adopted where multiple data sources were included in order to identify issues from varying perspectives. Main data sources for each test included a background survey, a think aloud protocol, a functionality timeline, structural analysis example problems, and a survey at the conclusion of the testing. The background survey asked students to identify their year in school, major, and experience with tablets and augmented reality. The think-aloud protocol asked students to verbalize their thought processes while completing predefined tasks within iStructAR. Any verbally expressed areas of concern and/or enjoyment by students were notated. Participant audio and interaction with the app interface was recorded using a GoPro action camera (example video shot seen in Figure 4-5 below), as well as an elevated camera. A functionality timeline was utilized to track participant interactions with the app on a timescale. Time-related tasks such as the

duration for students to answer structural analysis questions, find a particular function on the screen, or manipulate loads to certain locations were all measured. Structural analysis example problems were given at the end of the main body of the usability test. These questions tested whether students understood the connection between classroom structural analysis concepts and the application, and whether students relied on, referenced, or ignored the app during problem solving. All questions given to students could be solved without the use of the app or a calculator, so use of the app for solving was a user-defined choice. Finally, at the end of all interaction and tasks with iStructAR, students were asked to complete a survey, containing specific questions pertaining to each functionality that the app contained.

Figure 4-5. *GoPro filming student interact with iStructAR during usability test.*

Qualitative data analysis approaches were used to analyze the data. Report results were utilized to refine the application before full implementation.

4.4 Results and Discussion

4.4.1 Guided vs. Unguided

As described above, a guided version of the app provided step by step text descriptions of structural analysis concepts, while an unguided version provided no guidance and allowed users to explore all functionality of the app at any time. Table 4-2 below collates the main distinctions between the guided and unguided versions of the application. These distinctions provided points of focus during usability tests, in order to note if student performance was aided, deterred, or maintained consistent through the two different app versions.

Table 4-2. *Distinctions of functions between guided and unguided versions of application, and points of focus during usability tests.*

Function	Guided	Unguided	Point of Focus
Description of structural analysis concepts	Provided through procedural steps	Provided through expandable window defining dead and live load	Necessary instructional guidance needed
Live load preset button enabling	Unlocked at end of procedural steps, encouraging students to read all text before interaction	Always unlocked, allowing students to interact from start to end of app interaction	Controlled interaction with location of live load
Load and reaction force visualization	Going forwards and backwards through steps enables and disables visualization of loads and reaction forces	Utilization of visualization buttons enables or disables load and reaction force symbols	Ease of visualization of load and reaction forces

Five students utilized the guided version of the application, while five students utilized the unguided version of the app. Points of focus could be observed through the think-aloud protocol, the functionality timeline, and responses to the structural analysis example problems. The following sections describe results of usability testing in regards to the function provided in Table 4-2.

4.4.1.1 Function: Description of structural analysis concepts

Three problems were given to students as a physical handout at the conclusion of the think aloud portion of the usability test. The responses given by students to these three questions helped to assess the functionality of the app, as well as the difference in the two versions, in regards to description of structural analysis concepts. Accuracy of responses to structural analysis example problems given can be seen in Table 4-3. Problems 1 and 2 focused on deflection concepts, while Problem 3 focused on reaction force concepts and values. Overall, an increased dependence was seen on those students answering questions with the guided version of the application – rather than utilizing the app to check a solution that the student had written or verbalized, Students 1 and 2 directly manipulated loads on the app to find the answer, then answered the question.

Table 4-3. *Results of structural analysis problems for students using the guided and unguided versions of iStructAR.*

Student	**Problem 1**		**Problem 2**		**Problem 3**	
	Correct?	App?	Correct?	App?	Correct?	App?
S1 – G	Yes	Uses	Yes	Uses	Yes	Uses
S2 – G	Yes	Uses	Yes	Uses	Yes	Uses
S3 – U	Yes	References	Yes	References	Yes	Uses
S4 – U	No	References	No	References	No	Uses
S5 – G	Yes	References	Yes	Uses	Yes	Uses
S6 – G	Yes	No	Yes	No	Yes	Uses
S7 – U	Yes	References	Yes	Uses	Yes	Uses
S8 – U	Yes	References	Yes	Uses	Yes	Uses
S9 – G	Yes	Uses	Yes	Uses	No	Uses
S10 – U	Yes	References	No	No	Yes	No

The amount of time that students took to respond to structural analysis problems was fairly consistent between all students, and there were no distinct timing differences between those students using “guided” versus “unguided” versions.

During usability testing, three students submitted incorrect answers to one or more of

the three questions given. The incorrect answers could not be attributed to either the use of the guided or unguided versions, and were due to either incorrect manipulation of load, or incorrect calculation without reference to the app at all.

Three questions were given to students on the survey regarding the specific functions in the unguided and guided versions of the app. These include questions 5, 6, and 8, and can be seen in Table 4-7. As shown, there was no distinct difference between ratings of students in these questions.

4.4.1.2 Function: Live Load Preset Button Enabling

Live load preset buttons were disabled until Step 4 of 6 on the guided version, as seen in Figure 4-3. The unguided version had live load preset buttons enabled at all times. Some students using the guided version experienced confusion during steps 1 through 3 as to why live load preset buttons were disabled. Although procedural steps had not yet described live load, students still tried to push disabled buttons, showing that the procedural steps did not provide a controlled and focused flow as intended.

4.4.1.3 Function: Load and Reaction Force Visualization

The unguided version contained visualization buttons that created the appearance or disappearance of loads and reaction forces on the screen. To produce the same effect, the guided version required students to go forwards or backwards through steps.

To test the difference in the functionality of visualizing the load and reaction forces in the unguided vs. guided versions, the number of clicks and “drags” that students completed while answering questions one through three were recorded. Any interaction that students had with the app, resulting in any change of the conditions before the interaction, was considered a click or drag. It should be noted that if a student “mis-clicked”, and had to re-tap the iPad screen, this was not counted in the click/drag count, as the condition changed

was not meaningful.

Table 4-4 below shows the results of clicks/drags carried out by students per question. The table is separated into students who completed the guided version, versus the unguided version. On average, students who took the guided usability test were 1.3 times more likely to have to click/drag when answering than those who completed the unguided usability test. Notably, students were more than four times likelier to click/drag on question one when completing the guided usability test, than the unguided test. While the results presented in Table 4-4 suggest that it may be clumsier for students to complete questions when using the guided version of the app, results are highly dependent on the student type that completed each test. Some students may have tendencies to interact more or less with the app, independent of their performance on the questions given.

Table 4-4. *Number of clicks/drags used by students when solving structural analyis problems.*

Clicks/Drags Per Problem							
Guided							
Question #	**S1**	**S2**	**S5**	**S6**	**S9**	**Average**	**SD**
1	3	3	0	0	1	1.4	1.52
2	4	10	5	0	5	4.8	3.56
3	1	2	1	7	1	2.4	2.61
Total	8	15	6	7	7	8.6	3.65
Unguided							
Question #	**S3**	**S4**	**S7**	**S8**	**S10**	**Average**	**SD**
1	0	1	0	1	0	0.4	0.55
2	0	2	2	14	2	4	5.66
3	2	3	1	3	1	2	1.00
Total	2	6	3	18	3	6.4	6.66

Question number 7 on the survey asked students to rate the ease of enabling the visualization of the load, as seen in Table 4-7. All students responded positively, recording either responses of “agree” or “strongly agree”. On average, students who took the unguided version of the usability test felt as though it was easier to enable the visualization of the load, as presented in Figure 4-6 below.

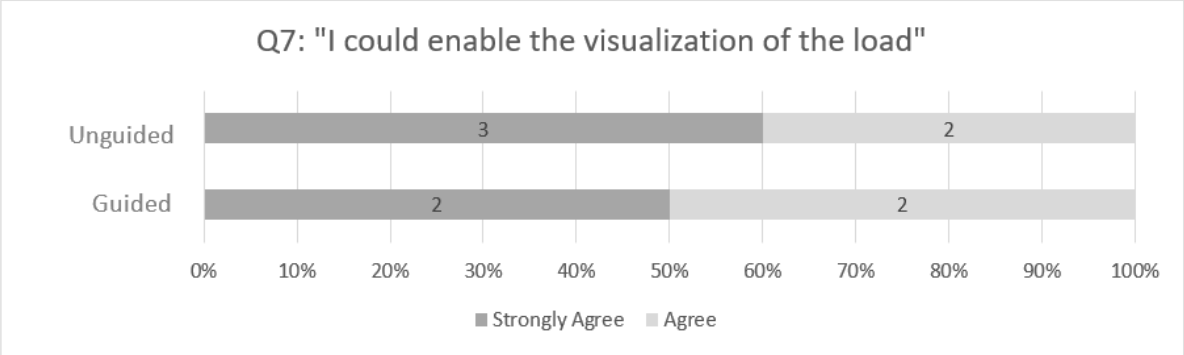

Figure 4-6. *Results of question 7 on usability test survey.*

4.4.2 Preset Buttons vs. Dragging

In order to manipulate the location of the live load, students had two main functionality type choices: one, use of predefined live load preset buttons, or two, use of dragging the load directly (direct manipulation). Both of these functions can be seen in Figure 4-2. Students were forced to make a decision between these two choices whenever directions given by the test facilitator indicated to move the live load to either just the right span, the left span, or all spans of the structure. This option arose four times within the usability test procedure. As seen in Table 4-5 below, the average student chose to utilize a preset button, allowing the application to self-direct the live load to either the left span, right span, or all spans. As mentioned previously, testing protocol experienced minor changes after usability testing with student 1; choice numbers 2 and 3 from the table were not included in this preliminary procedure.

Table 4-5. *Student preference of live load location preset buttons vs. dragging (direct manipulation).*

Choice #	S1	S2	S3	S4	S5	S6	S7	S8	S9	S10
1	Drag	Preset	Preset	Preset	Preset	Preset	Preset	Preset	Drag	Preset
2	-	Preset	Preset	Preset	Preset	Preset	Preset	Preset	Preset	Preset
3	-	Preset	Preset	Preset	Preset	Preset	Preset	Preset	Drag	Preset
4	Drag	Preset	Preset	Drag	Preset	Drag/Preset	Preset	Preset	Drag	Preset

While students chose preset buttons on average over dragging when redirecting loads to particular spans, all students were forced to drag load locations directly at one point within the usability test. This choice is not included in Figure 4-5 above. Students did not experience any issues or concerns moving the load directly from a usability standpoint. Many students expressed concern over inaccuracy of load location. Users were not given any datum or span lengths, so students could not be positive of the accuracy of where they dragged the load.

Questions 14 and 15 in the given survey pertained to the use of preset buttons vs. dragging when manipulating the live load, as seen in Table 4-7. Overall, students responded that they could easily change the load location, but had no preference in how this was achieved. These results are shown in Figure 4-7 and Figure 4-8 below.

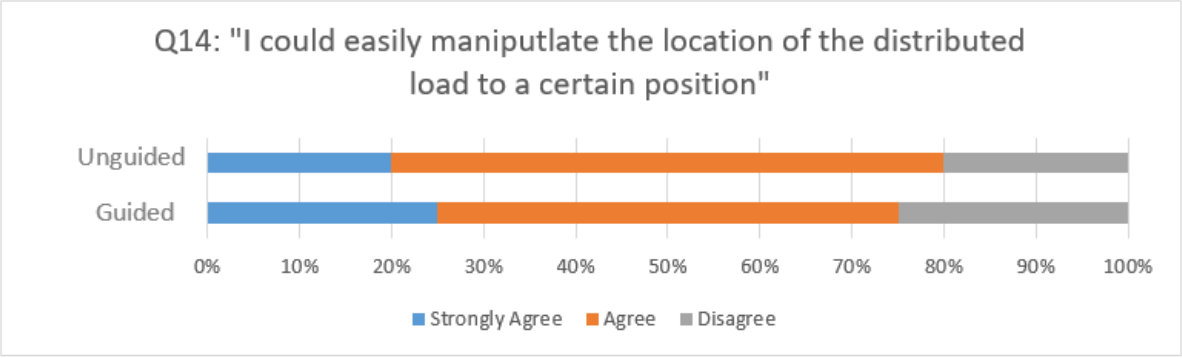

Figure 4-7. *Results of question 14 on usability test survey.*

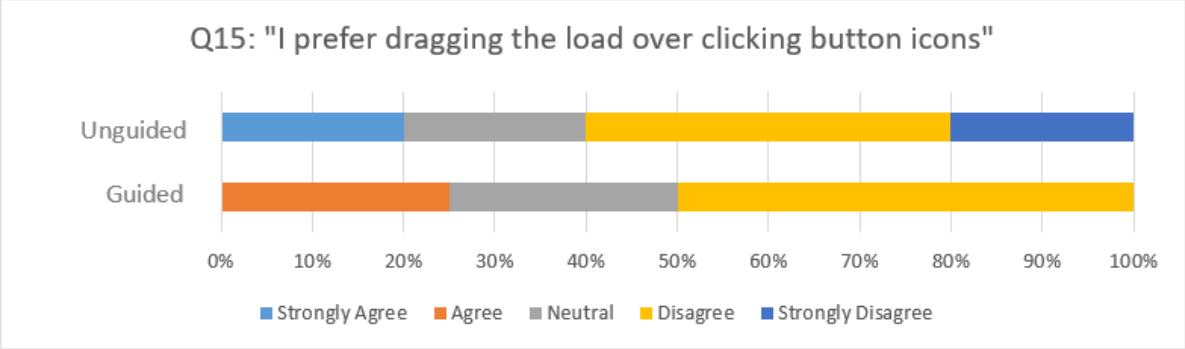

Figure 4-8. *Results of question 15 on usability test survey.*

4.4.3 Augmentation

Within the usability procedure, students were forced to change tracking modes from an “untracked” to an “indoor” tracking. Outdoor tracking was not utilized in the study in order to minimize testing time for relocation, as well as to control the testing environment. Within the indoor tracking mode, students were asked to complete tasks similar to those asked in the previously used untracked mode, while holding up the iPad to a printed picture of the skywalk as shown in Figure 4-9. Loads could be manipulated in the same way as the untracked mode. Testers looked for any problems related to misunderstanding of loads projected onto the skywalk image, handling of the iPad, and technical malfunctions. The “Pause Camera” and “Resume Camera” functions were also tested during this time.

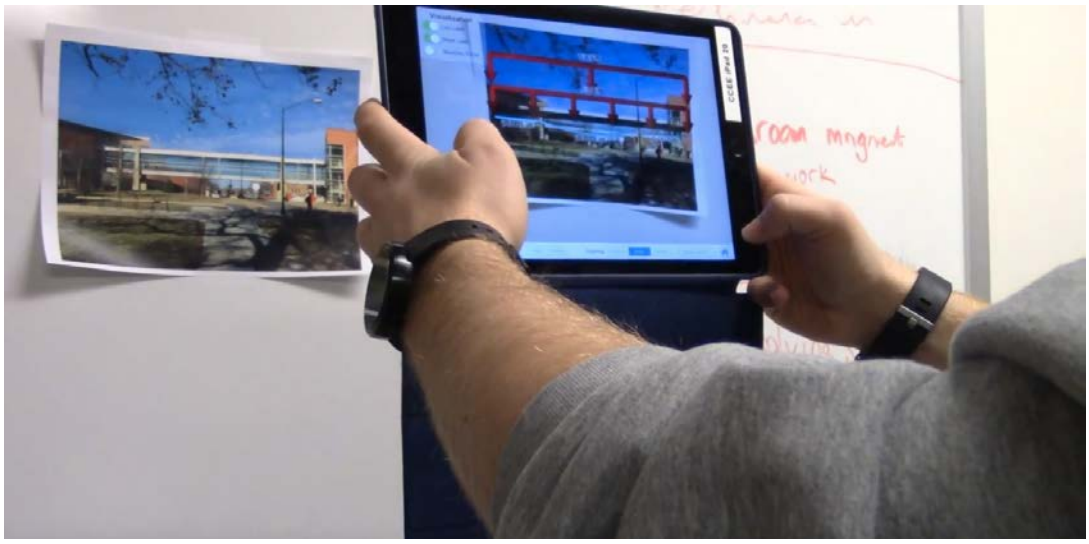

Figure 4-9. *Student changes the magnitude and location of the live load on a printed photo of the skywalk through augmentation.*

All students encountered difficulty when taking a screenshot of the app during the augmentation, due to awkwardness of hand placement. This correlates with the result of question 12 on the survey, as well as with verbal confirmation of students. As seen in Table 4-7, question 12 received a lower rating by students.

Overall, testers noticed an increased level of interest when students used the augmented reality functionality of the application. Perceived enjoyment of the users increased, many students commenting that this feature was their favorite functionality of the application. No problems were encountered with the Pause Camera or Resume Camera functionalities.

4.4.4 Other Functionalities

All students were asked to take screenshots of the user interface, in both “Untracked” and “Indoor” tracking modes (both in and apart from augmentation). In future classroom use, professors may ask students to take a screenshot of a current loading situation to reference in following lectures. While the normal screenshot key combination is inherent to the tablet

rather than iStructAR, testers wanted to confirm that users could easily complete the task. However, all students, regardless of previous iPad or tablet experience, encountered trouble taking a screenshot. Approximately 60% of student had to be instructed of the correct key combinations to use when taking their first screenshot during the test.

4.5 Survey Results

Table 4-7 and Table 4-6 below compiles results from the survey given to students at the end of testing. Table 4-6 describes the questions given on this survey, and Table 4-7 presents the results given my individual students. Ratings were based on a 5 point score, with 5 correlating to “strongly agree”, and 1 correlating to “strongly disagree”. Again, student one is not included in survey results, as both the usability test protocol and survey changed after this student completed the trial usability test.

When comparing guided and unguided versions, significant differences in averages are seen in questions two, four, nine, eleven, and twelve (greater than 0.5 difference). Questions nine, eleven, and twelve were independent of the version of usability test that students were taking, and were solely reliant on the functionalities and appearance of the application. However, questions two and four could have had results affected by the type of test that students were taking. Question two refers to selecting desired functionalities at given times, and question four refers to initiating action within the application from directions given by the test facilitator. For both of these survey questions, students who completed the guided version responded with an average score of four (pertaining to “Agree”), while students who completed the unguided version responded with an average score of 4.75 (closer to “Strongly Agree).

Table 4-6. *Description of questions given in usability test survey.*

Question #	Question Description
1	I could identify the functionality of the available options through icons
2	I could select the desired function on the app all the time
3	I could easily undo/redo any action if I felt to do it
4	I could easily figure out what to do next given the instructions
5	I could understand the messages that appeared in the app
6	I was not confused or lost while performing the tasks
7	I could enable the visualization of the load
8	I could easily distinguish the different types of load on the screen
9	I believe the arrows are appropriate representations of loads on the structure
10	I believe the curved line is a good representation of the structure's deflection
11	I could easily read the load values, reaction force values, deflection values
12	I could easily take a screenshot of the app screen
13	I could easily change the load to a certain magnitude given by the test facilitator
14	I could easily manipulate the location of the distributed load to a certain position
15	I prefer dragging the load over clicking button icons
16	The definitions (...) helped me to understand the different types of load

Table 4-7. *Compiled results of usability test survey.*

Question/ Student	Guided						Unguided							Combined	
	S2	S5	S6	S9	Average	SD	S3	S4	S7	S8	S10	Average	SD	Average	SD
1	3	5	4	4	4.00	0.82	5	4	4	4	4	4.25	0.50	4.11	0.60
2	4	4	4	4	4.00	0.00	5	5	4	5	5	4.75	0.50	4.44	0.53
3	5	5	4	5	4.75	0.50	5	5	5	5	4	5.00	0.00	4.78	0.44
4	4	5	3	4	4.00	0.82	5	5	5	4	5	4.75	0.50	4.44	0.73
5	5	5	4	5	4.75	0.50	5	5	5	4	5	4.75	0.50	4.78	0.44
6	4	3	4	4	3.75	0.50	4	4	3	4	4	3.75	0.50	3.78	0.44
7	4	5	4	5	4.50	0.58	5	5	5	4	4	4.75	0.50	4.56	0.53
8	5	5	4	5	4.75	0.50	5	5	4	4	5	4.50	0.58	4.67	0.50
9	5	5	4	4	4.50	0.58	5	5	5	5	5	5.00	0.00	4.78	0.44
10	4	5	4	4	4.25	0.50	5	5	4	5	5	4.75	0.50	4.56	0.53
11	5	5	4	4	4.50	0.58	5	5	5	5	5	5.00	0.00	4.78	0.44
12	3	3	4	3	3.25	0.50	4	3	5	4	5	4.00	0.82	3.78	0.83
13	4	3	2	5	3.50	1.29	4	5	1	4	4	3.50	1.73	3.56	1.33
14	5	4	4	2	3.75	1.26	5	4	2	4	4	3.75	1.26	3.78	1.09
15	3	2	2	4	2.75	0.96	3	5	1	2	2	2.75	1.71	2.67	1.22
16	5	5	4	5	4.75	0.50	3	5	5	5	3	4.50	1.00	4.44	0.88

**Student Ratings are on a 5 point scale: 1: Strongly Disagree; 2: Disagree; 3: Neutral; 4: Agree; 5: Strongly Agree*

4.6 Conclusion and Decided Improvements

Overall, no problems were encountered through usability testing that disabled students from completing assigned tasks or caused extreme frustration. Main focuses centered on differences of student performance when using “guided” versus “unguided” versions, utilization of preset buttons over direct manipulation (dragging) of live load locations, and student interaction with augmentation.

Instructional guidance provided by the guided version did not increase accuracy when solving structural analysis problems, or giving verbal answers related to structural analysis

concepts in the think-aloud protocol. However, the guided version proved to add clumsiness when interacting with live load preset buttons and visualization of loads and reaction forces. Based on listed results, researchers decided to proceed with making modifications to the "unguided" version only.

Students utilized both preset buttons and direct manipulation (dragging) when moving the location of the live load. Testing showed the necessity for both options. However, the presence of a datum or numbered axis was added aid in load location when dragging the live load.

Student interaction with augmentation was positive, met with increased user interest and enjoyment. No problems were encountered with the current user interface. However, students did struggle to take a screenshot of the interface while in Indoor tracking mode. To increase ease of taking screenshots, a single button was added to the user interface that will make the application take a picture of the current screen.

Table 4-8 collates all functions of the application, any problems seen during usability testing, and if necessary, suggested modifications. Those modifications highlighted were implemented into the final version of the application.

Table 4-8. *Summarized functionality problems and suggested modifications from usability testing.*

Function	Problem Severity*	Problem Description	Suggested Modification
Visualization Toggles	None	-	-
Load Definition Expandable Window	None	-	-
Live Load Location Preset Buttons	Minor	Misunderstanding of "Variable" preset button; when pushed, live load shows no change	Remove "Variable" live load preset button; no functionality of application will be lost
Tracking Mode	Minor	When camera is blocked by item, students do not understand Indoor and Outdoor tracking modes	None
Pause/Resume Camera Button	None	-	-
Home Button	None	-	-
Direct Manipulation of Live Load Location (Dragging)	Minor	Unknown exact location of live load; imprecision when relating to hand calculations	Add datum showing dimensions of loads and spans
Direct Manipulation of Live Load Magnitude (Dragging)	None	-	-
Take Screenshot of iPad	Minor	Student unawareness of proper controls on iPad to take screenshot; awkward when in Indoor tracking mode	Add single button in interface that will take screenshot

**Problem Severity Types: Severe: problem type prevented students from completing a task or interacting with the application; Moderate: problem caused interaction with the application to be difficult or undesirable; Minor: problem type did not create barrier from completed tasks, but caused annoyance in users*

Figure 4-10. *User interface after usability testing improvements.*

Figure 4-10 above shows the interface of the application after making the above notated changes. As shown, the screenshot button was added next to the "resume camera" button, to put similar functionalities in proximately. Additionally, a ruler visualization toggle button was added, allowing students to see span lengths of the Skywalk structure.

4.7 References

Azuma, R., Baillot, Y., Behringer, R., Feiner, S., Julier, S., & MacIntyre, B. (2001). Recent advances in augmented reality. *IEEE computer graphics and applications, 21*(6), 34-47.

Behzadan, A. H., Dong S., & Kamat V.R. (2015). Augmented reality visualization: A review of civil infrastructure system applications. *Advanced Engineering Informatics, 29*(2), 252-267.

Behzadan, A. H., & Kamat, V. R. (2005). Visualization of construction graphics in outdoor augmented reality. In *Proceedings of the 37th conference on Winter simulation* (pp. 1914-1920). Winter Simulation Conference.

Behzadan, A. H., & Kamat, V. R. (2009). Interactive Augmented Reality Visualization for Improved Damage Protection and Maintenance of Underground Infrastructure. In *Construction Research Congress* (pp. 1214–1222).

Davalos, J. F., Moran, C. J., & Kodkani, S. S. (2003). Neoclassical active learning approach for structural analysis. In *Proceedings of the 2003 American Society for Engineering Education Annual Conference & Exposition*.

Dunleavey, M. (2014). Design principles for augmented reality learning. *TechTrends, 58*(1), 28-34.

Dunston, P., Wang, X., Billinghurst, M., & Hampson, B. (2003). Mixed reality benefits for design perception. *NIST SPECIAL PUBLICATION SP*, 191-196.

Dunston, P. S., & Shin, D. H. (2009). Key areas and issues for augmented reality applications on construction sites. Eds In *Mixed Reality In Architecture, Design And Construction*, 157–170.

Dunleavy, M. & Dede, C. (2014). Augmented Reality Teaching and Learning, pp. 735–745. Springer New York, New York, NY.

Henderson, S. J., & Feiner, S. (2009). Evaluating the benefits of augmented reality for task localization in maintenance of an armored personnel carrier turret. Science and Technology Proceedings - *IEEE 2009 International Symposium on Mixed and Augmented Reality*, ISMAR 2009, 135–144.

Park, C.-S., Lee, D.-Y., Kwon, O.-S., & Wang, X. (2013). A framework for proactive construction defect management using BIM, augmented reality and ontology-based data collection template. *Automation in Construction*, 33, 61–71.

Quarles, J., Lampotang, S., Fischler, I., Fishwick, P., & Lok, B. (2008). Collocated AAR: augmenting after action review with mixed reality. In *Proceedings of the 7th IEEE/ACM International Symposium on Mixed and Augmented Reality* (pp. 107-116). IEEE Computer Society.

Rublee, E., Rabaud, V., Konolige, K., & Bradski, G. (2011). ORB: An efficient alternative to SIFT or SURF. In *Computer Vision (ICCV), 2011 IEEE international conference on* (pp. 2564-2571). IEEE.

Sandars, J. & Laffery, N. (2010). Twelve tips on usability testing to develop effective e-learning in medical education, *Medical Teacher*, 32, 956-960.

Shirazi, A., & Behzadan, A. H. (2015). Content delivery using augmented reality to enhance students' performance in a building design and assembly project. *Advances in Engineering Education*, 4(3), 1–24.

Teng, J. G., Song, C. Y., & Yuan, X. F. (2004). Fostering creativity in students in the teaching of structural analysis. *International Journal of Engineering Education*, 20(1), 96-102.

Woodward, C., Hakkarainen, M., Korkalo, O., Kantonen, T., Aittala, M., Rainio, K., &

Kähkönen, K. (2010). Mixed reality for mobile construction site. In *10th International Conference on Construction Applications of Virtual Reality* (pp. 1–10).

Wursthorn, S., Coelho, A. H., & Staub, G. (2004). Applications for mixed reality. In *XXth ISPRS Congress, Istanbul, Turkey* (pp. 12-23).

Xue, H., Quan, H., Song, X., & Wu, M. (2013). Construction of simulation environment based on augmented reality technique. In Asiasim. Springer.

Yuan, X. F. and Teng, J. G. (2002). Interactive Web-based package for computer-aided learning of structural behavior. *Computer Applications in Engineering Education*, 10(3), 121–136.

CHAPTER 5. MOBILE AUGMENTED REALITY APPLICATION FOR TEACHING STRUCTURAL ANALYSIS

A paper to be submitted to Journal of Engineering Education

Elizabeth Miller, Dr. An Chen, Dr. Aliye Karabulut-Ilgu, Suhan Yao[6]

Abstract

Previous research completed shows that augmented reality is a useful and innovative tool that can be utilized in undergraduate education to enhance the student learning experience. This paper focuses on the implementation of an augmented reality application, iStructAR, into a structural analysis classroom. The application allows students to interactively change the load and observe the resulting reaction forces and deflection shape of a structure with instant feedback provided by the AR interface. Two classes of structural analysis were utilized for an in-class experiment. One class served as the control class, taught in a traditional lecture style, and the other served as an experimental class, taught utilizing iStructAR in a supplementary manner. Performance of students in both classes were compared over a semester utilizing pretest-posttest measures, in-class observations, results to problem sets, and surveys. Results indicated that the application has the potential to increase student engagement and interest in the subject of structural analysis. Additionally, the application was successful in aiding students in visualization of structural components. Survey results indicated that students found value in the use of the application.

This material is based in part upon work supported by the National Science Foundation under Grant No. DUE-1712049. Any opinions, findings, and conclusions or

[6] Assisted in conducting literature review.

recommendations expressed in this material are those of the authors and do not necessarily reflect the views of the National Science Foundation.

5.1 Introduction

Structural analysis is an introductory course for structural engineering, taught in every undergraduate civil engineering program at approximately 300 institutions within the United States. Structural analysis is also taught in most architectural and construction science and engineering programs as a core course. Despite its crucial role in the curriculum for these programs, most students taught in this course do not appear to have a sound understanding of the fundamentals concepts taught. In general, students lack the ability to visualize the deformed shape and predict the effects of loads on simple structures. This research focused on the implementation of a mobile augmented reality (AR) application within a structural analysis setting to transform the existing teaching pedagogy. In the application, virtual elements overlay related physical components in structures to help students transfer abstract concepts taught in class to real world situations.

5.2 Augmented Reality in Education

Azume et al. (1997) defined AR as combing real-world and virtual elements that are interactive and displayed in real time. Azume also specified that the element must be tied to 3D, real-world information. Many researchers today believe that AR has the potential to enhance learning environments within education. AR applications have been used in a variety of educational settings including medical training simulations, engineering, architecture, interior design, mathematics, and science (Yuen et al., 2011; Azuma, 1997).

5.2.1 Benefits of Augmented Reality in Education

Yuen et al. (2011) listed the potential learning benefits from AR, as compiled from other researchers. These benefits include, but are not limited to: engagement and motivation

of students to explore class material from a different perspective; teaching of material in a manner that is not normally feasible, allowing students to gain first-hand knowledge; enhancement of the teacher to student relationship; fostering of student creativity; empowering students to control their learning pace; and creating a learning environment that supports a variety of learning styles (Yuen et al. 2011).

Several researchers have reported on the benefits of utilizing augmented reality specifically in engineering education. One of the top benefits of implementing AR into engineering classrooms is an increased student engagement and motivation (Fonseca et al 2014; Shirazi & Behzadan 2014; Gutierrez and Fernandez 2014; Alvarez et al 2017; Fiorentino et all 2009).

AR could also help to increase students' spatial skills, the ability to mentally visualize 3D elements or shapes. Dominguez et al. (2012) noted the importance of spatial skills in engineering professionals, as the majority of 3D elements in the field are sketched in two-dimensional methods. The spatial skills that engineering students develop within their education can be seen as a direct link to future success in their careers (Adanez and Velasco, 2002; Miller, 1996; Sorby, 1999). Carrera and Asensio (2017) utilized an AR application on iPads in an engineering class focused on spatial reasoning in cartopgraphy. Using repeated performance-based measures, the researchers found that those students exposed to the AR application had significantly higher scores on a standardized test than those not exposed. A similar study found that students who used augmented reality to view models in the Vandenberg Mental Rotation Test had increased performance time and accuracy (Connolly et al, 2010).

Many researchers have reported the use of AR in increasing students' understanding of abstract concepts in engineering. Shanbari et al. (2016) observed specific elements of a construction industry related roof assembly that, when presented in a classroom setting, restricted students from fully understanding the process due to the limitations in a traditional lecturing style. After implementing an augmented reality video that helped to display these concepts, researchers found that there were significant difference in test results from those students who had seen the AR video. Similarly, studies have reported that the use of AR applications have improved students' practical performance in completing tasks. Shariza and Bahzadan (2014) designed an AR application that enhanced a classroom textbook using 3D and virtual information. When a handheld device, such as an iPhone, was moved over a textbook, 3D images, videos, and sounds would appear on top of the static textbook. Over 75% of students who utilized this technology in the classroom responded that they found it helpful in their learning.

AR learning in an education setting, lastly, has been found to support students' autonomous learning. Autonomous learning has been described as behaviors that indicate that students are intrinsically motivated and internally regulated (Black & Deci, 2000). When students are intrinsically motivated, they act out of their own personal interest, rather than acting out of offer of a reward. Gutiérrez completed a study in which students were given an introduction to an AR book that showed 3D objects. Students were then required to use the AR book independently, and draw orthogonal views of the 3D objects presented. Students worked with only the AR book, a computer, and a solution manual. Those students that used the AR toolkit autonomously showed a significant increase in test scores (Gutiérrez et al., 2010).

5.2.2 Challenges of Augmented Reality in Education

Although utilizing augmented reality in the engineering classroom can provide many benefits, researchers have also commented on challenges that the technology can bring to both students and instructors. First, the unfamiliarity of a device or AR technology to students can cause not only frustration to students, but may cause delays in the classroom as students familiarize themselves (Shirazi and Behzadan, 2015). Another challenge can be found in the manipulation of the technology. In a study completed by Turkan et al. (2017), students sometimes found difficulty in holding a tablet up, while still interacting with the screen. Monroy Reyes et al. (2016) notated a similar limitation, stating that if students hold a device, such as a smartphone, one hand is always occupied manipulating this device. From an instructor's perspective, researchers have commented that utilizing an AR technology in the classroom can be difficult due to the extended technologic knowledge that is required of professors (Yuen et al. 2011, Monror Reyes et al. 2016). Dede and Barab (2009) and Shirazi and Behzadan (2014) stated that AR presented "unique technological, managerial, and cognitive challenges to teaching and learning" amongst its provided benefits.

5.3 iStructAR: System Design

The AR structural analysis application, named iStructAR, was developed with the intention of being used on iPads. This way, students would use the familiar iOS user interface framework, minimizing learning of a new software or interface. The application was developed using both Vuforia, an off-the-shelf AR toolkit for indoor tracking modes, as well as a custom tracking approach for outdoor tracking. The custom tracking, explained briefly, extracts the planar surface of the structure to be tracked, and then executes a typical 2D image tracking pipeline using ORB feature descriptors (Rublee et al. 2011).

The user interface of the application was refined through usability testing, completed before implementation into any educational setting. Usability testing focused on making functions within the application meaningful and easy to use. Usability testing was performed with ten students who were familiar with structural analysis and who provided feedback after engaging with the application through a developed protocol.

Educationally, the application was developed with an increased focus on student experiential learning. Students can interactively change the load or parameters of the virtual elements and obtain instant feedback by observing the effect on the structural system through the virtual representation of the building. The design of the application was done in such a way that students could utilize iStructAR on their own, without additional instruction. It is important to note that the application was not designed to replace the instructor in the classroom; rather, it was designed as a teaching tool that could aid in student's learning.

5.3.1 Implementation in a Classroom Setting

The application was utilized in structural analysis classrooms in four distinct lessons throughout the semester. During integration, students were each given an iPad for use, allowing the iPad to student ratio to be 1:1. The application was utilized to introduce a new concept taught in the classroom. For example, iStructAR would be used the first day that trusses were introduced. Students were guided through using the application by completing a series of tasks given through in-class worksheets. While completing these worksheets, students were encouraged to work in groups, encouraging collaborative teamwork. After completing the worksheets, the professor led a discussion focusing on the main concepts taught through the activity. During this discussion, students were encouraged to project loading conditions that they selected on their user interface to the class through the use of the Apple TV. This procedure was completed four times throughout the first half of the semester,

each coinciding with the introduction of a new topic. The topics included load (dead load, live load, wind load, and seismic load), behavior of beams (simply supported and cantilevered), behavior of frames, and behavior of trusses.

5.4 Experimental Design

Students were divided into groups based on their enrollment in one of two sections of structural analysis. The same instructor taught both sections. Only one section of the class was taught utilizing the AR application in the classroom, notated as the experimental group. The other section was taught in a traditional manner, with no introduction to iStructAR, notated as the control group. Four different data collection methods were utilized: pretest-posttests, surveys, transfer problem sets, and in-class observations.

5.4.1 Pretests and Posttests

Throughout the semester, students were given three distinct pretest-posttest measures. Each pretest-posttest measure focused on a lesson taught within the course. The three pretests were given during the first week of class in the semester, prior to any knowledge gained by students in the class. Posttests were given throughout the first half of the semester, shortly after completing the lesson in which the posttest focused on. Both the control and experimental groups took the pretest and posttest measures at the same time during the semester. For the pretest-posttest measure, the topics of loads and beams were combined into one testing measure.

5.4.1.1 Pretest and Posttest Development

Pretest and posttest questions were developed to mirror those questions given in class, for homework, and referenced in the textbook. In order to test the reliability of the questions, one pretest-posttest was given to students in the fall of 2018, one semester before the implementation of iStructAR in the classroom. The pretest-posttest was given to one

structural analysis class, and one reinforced concrete design class. The test given to the structural analysis class served as a pretest measure, and the test given to the reinforced concrete design class served as a posttest measure. Because structural analysis was a prerequisite to reinforced concrete design, those students in this class should have acquired the knowledge to answer questions correctly on the posttest. While repeated measures from individual students was not gained, the average and standard deviations from both classes on each question could be compared and analyzed. The pretest-posttest consisted of a mixture of multiple choice questions and free response questions asking students to draw deflection shapes. Results from the pretest-posttest are shown in Table 5-1.

Table 5-1. *Trial pretest and posttest results during test development.*

	Structural Analysis (Pretest)	**Reinforced Concrete Design (Posttest)**
# Students	41	54
Average (%)	67.3	75.4
SD	2.60	1.96
Normally Distributed?	Yes	No

The distribution for the posttest data was not normally distributed, as an uneven percentage of students scored high on the test, as expected. Using data from the trial pretest-posttest, an item analysis was completed. An item analysis can be used to examine student responses to individual test questions in order to assess the quality of the questions given. The item analysis helped to point to questions that were well constructed, as well as those that may have been poorly constructed. Additionally, a difficulty index was completed for each question. This index looked at the proportion of students who answered each test item correctly. Those questions with a difficulty index of 75% or higher (indicating question were too easy), or 25% or lower (indicating questions were too difficult), were revised. Finally, a

discrimination index was completed on the gathered data. The discrimination index can tell how well the quiz differentiated between high and low scores, based on the performance of students. High-performance students were expected to select the correct answer for each question more than low performance students. Positive discrimination existed if the index was between zero and one, and negative discrimination indices indicated that the question should be revised. Using the results from the item analysis, questions were revised for the final pretest-posttest. The questions on the remaining pretests and posttests were written to mirror the setup and wording of those questions deemed "successful" from the item analysis. In addition to the item analysis, the pretest-posttest measures were reviewed by structural analysis faculty.

5.4.2 Surveys

Students in both classes also completed three surveys. Each survey was given after the completion of an AR activity. Surveys focused on attitudes related to using the AR app, as well as attitudes towards the class and structural engineering in general. Those surveys given to the experimental group had specific questions related to the use of a certain module within the application that was previously utilized in class. Those surveys given to the control group did not have any questions related to AR or iStructAR, and focused only on attitudes of students towards the class, and towards structural engineering in general.

5.4.3 Transfer Problem Sets

Students in both the control and experimental classes were asked to complete three sets of problems, referred to as "transfer problem sets". Each transfer problem set, similar to the pretest-posttests and surveys, focused on a particular lesson being taught within structural analysis. The problem sets consisted of fifteen questions, with the last problem being one that required a transfer of knowledge from analyzing a structure in the typical 2D stick model

format as taught in a traditional classroom style, to an actual structure in the real, three-dimensional world. If a student answered a question correct, they were automatically routed to this final question. If students answered a question incorrect, they were sent to the question after that which they had gotten correct last. Students were only complete with the problem set until they answered the transfer problem correct, or until they worked through all of the questions (and either answered them all correct or incorrect).

5.4.4 In-Class Observations

In addition to collecting quantitative data, in-class observations were recorded. Classroom observations were performed every class period during the first half of the semester, the duration of which the application was implemented and associated topics were taught. Additionally, the Research Institute for Studies in Education (RISE) at Iowa State University performed evaluation and assessments of both the control and experimental class periods when iStructAR was utilized.

5.4.5 Sample Size and Setting

Sample sizes of students depended entirely on the enrollment of students into structural analysis the semester the implementation was completed. Fifty-five students enrolled into the afternoon class, held at 1:10 pm, whereas 18 students were enrolled into the morning class, held at 8:00 am. The afternoon class was chosen as the experimental group, and the morning class was chosen as the control group. When doing analyses of data, those students that did not compete a pretest, a posttest, a survey, a transfer quiz, or did not attend an AR session, were taken out of the student sample size. Therefore, with these students subtracted, the sample size for data analysis was narrowed to 14 students in the control group, and 38 students in the experimental group. Differences in class size and time may have played a role in data results, and will be discussed in later sections.

Students in both classes were drawn from the same student population, and students chose their own class times, so no systemic bias took place. The experimental group consisted of 22% females, 78% males, and the control group consisted of 33% females, and 67% males. The experimental group consisted of 40% construction engineering students, 58% civil engineering students, and 2% of students with other majors, and the control group consisted of 22% construction engineering students, 72% civil engineering students, and 6% of students with other majors. Additionally, the experimental group consisted of 80% juniors, 16% seniors, and 4% of students in other grades, and the control group consisted of 83% juniors, 11% seniors, and 6% of students in other grades. The instructional setting for both groups consisted of larger lecture classrooms, with seating for approximately 60 students. Due to the larger class size, the experimental class was much tighter in space, and students had resistricted space to work in.

5.5 Data Results and Discussion

5.5.1 Pretest-Posttest Results

To compare results from the three given pretest-posttest, the p-value test was completed. Within this test, a p-value is calculated based on the presented data. This p-value represents the probability that the null hypothesis, H_o, is true. If the calculated p-value is lower than the significance level chosen, than the alternative hypothesis, H_1, is accepted, and the null hypothesis is rejected. In the case of this study, the null hypothesis is that the two classes will increase the same amount in knowledge from the pretest to the posttest, captured by an increase in scores. The alpha value chosen is 0.05, reasonable for studies of this type. The t-value is similar to the p-value, however, represents the difference between the sample mean and the population in units of the standard error (Colardarci, 2004).

Table 5-2 below shows the statistical measures of the comparison of change in scores from pretest to posttest between groups. Therefore, the mean presented shows the mean change for students from pretest to posttest (calculated through posttest score minus pretest score). The t-test was used to calculate the p-value, as the data for both sections was normally distributed.

Table 5-2. *Pretest to posttest comparison between groups, test one.*

Group	*n*	*M*	*SD*	*DF*	*t*	*p*
Control	14	3.71	2.30	51	-0.76	0.45
Exp.	38	3.13	2.79			

Results from pretest-posttest two are shown in Table 5-3 below. The Wilcoxon rank-sum test, a nonparametric version of the t-test, was utilized to calculate the p-value, as both of the sections did not have normally distributed data.

Table 5-3. *Pretest to posttest comparison between groups, test two.*

Group	*n*	*M*	*SD*	*Score Sum*	*Score Mean*	*t*	*p*
Control	14	2.79	2.39	423	30.21	0.28	0.28
Exp.	38	1.58	3.89	955	25.13		

Results from pretest-posttest three are shown in Table 5-4. Similar to test one, both sections displayed normally distributed data, and therefore, a t-test was utilized to analyze group differences.

Table 5-4. *Pretest to posttest comparison between groups, test three.*

Group	*n*	*M*	*SD*	*DF*	*t*	*p*
Control	14	0.86	2.48	51	0.62	0.54
Exp.	38	1.34	2.56			

One can see that in all tables, the p value presented is larger than 0.05, and the null hypothesis cannot be rejected. Therefore, there was not a significant difference in the growth of scores between the two sections. The mean in the difference between pretest and posttest for the control group was higher than for the experimental group in tests one and two. The opposite was true for test three. However, with the small student population overall, differences are minimal.

Figure 5-1 provides a visual representation of the scores from all tests for both the control and experimental groups, represented by “C” and “E” on the x-axis. As shown visually, the mean score for each test from pretest to posttest increased for both groups on each testing measure. Additionally, aside from experimental scores for posttest two, the standard deviation for all tests decreased. This is expected, as students should be attaining knowledge in the subject matter they are testing on, progressing more from a “guessing” mindset to a “knowing” mindset.

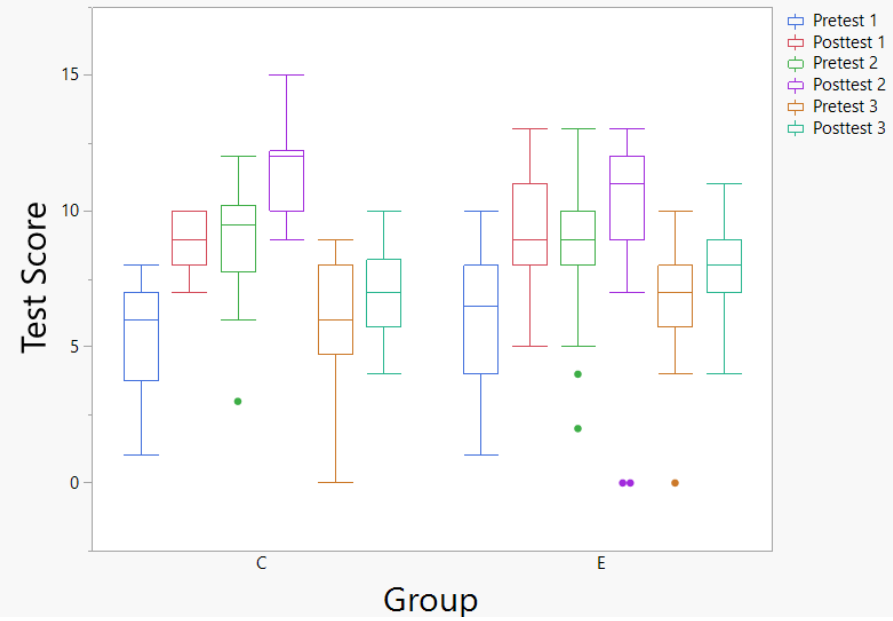

Figure 5-1. *Boxplot of all tests, separated by group.*

An analysis utilizing the results of all three pretest and posttest data was also completed. Figure 5-2 presents a comparison of the sum of all of the pretests versus the sum of the difference in test scores for all three tests. The larger the slope of the trend indicates a stronger growth in posttest score. One can see that the slopes of the two groups are comparable. However, the slope of the control group is slightly steeper. This indicates that, on average, the control group performed better the posttests that the experimental group, as compared with their respective pretest scores. It should be noted that correlation between data yields low R values, mainly due to the lack in numbers of students available for testing. With a larger number of students it is expected that stronger correlations in data would present themselves.

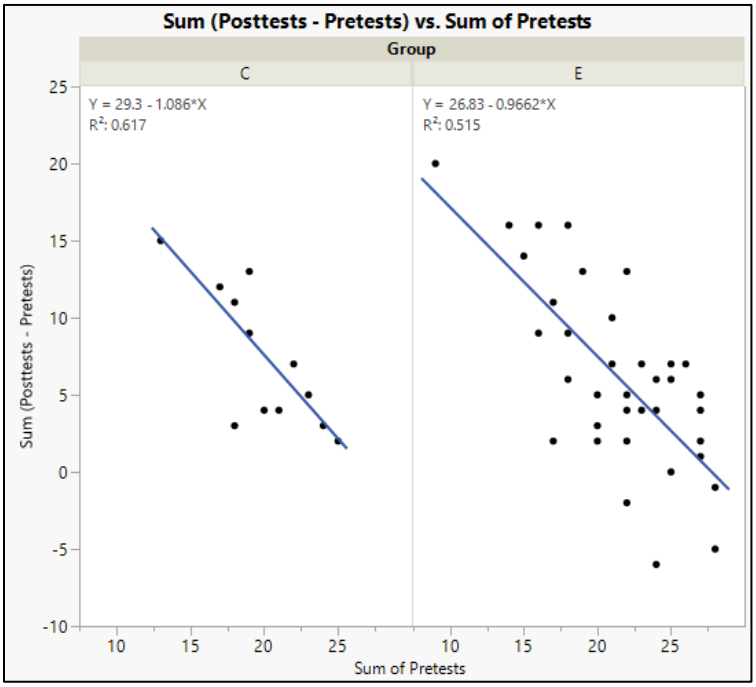

Figure 5-2. *Total change in score vs. pretest score for all tests, separated by group.*

Using data from the surveys, presented in the following section, test scores were also separated by different measures of student perception towards the structural analysis course

in general. It may be true that students who did not care about the course, or were not excited about the course, did not put as much effort forth, thereby reducing scores on tests. Three questions in general provided feedback on the general perception of students towards the class and subject matter. Figure 5-3 groups students based on their response to how engaged they felt in the class. Figure 5-4 groups students based on their response to how useful they felt the information in the class was. Finally, Figure 5-5 groups students based on how interesting they found the class. For each figure, a rating of "5" correlated to a response of "strongly agree" and a rating of "1" correlated to a response of "strongly disagree". In all three figures, those students in the experimental group who responded with a 5 to the statement presented performed better on posttests than those who responded the same in the control group. This is shown with a slightly larger slope. However, the differences are once again minimal.

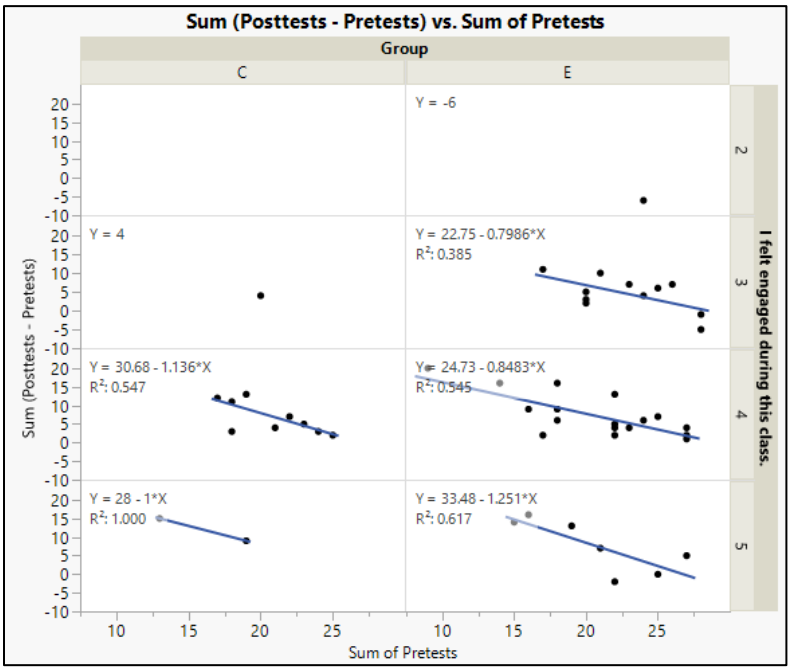

Figure 5-3. *Total change in score vs. pretest score for all tests, separated by survey response and group.*

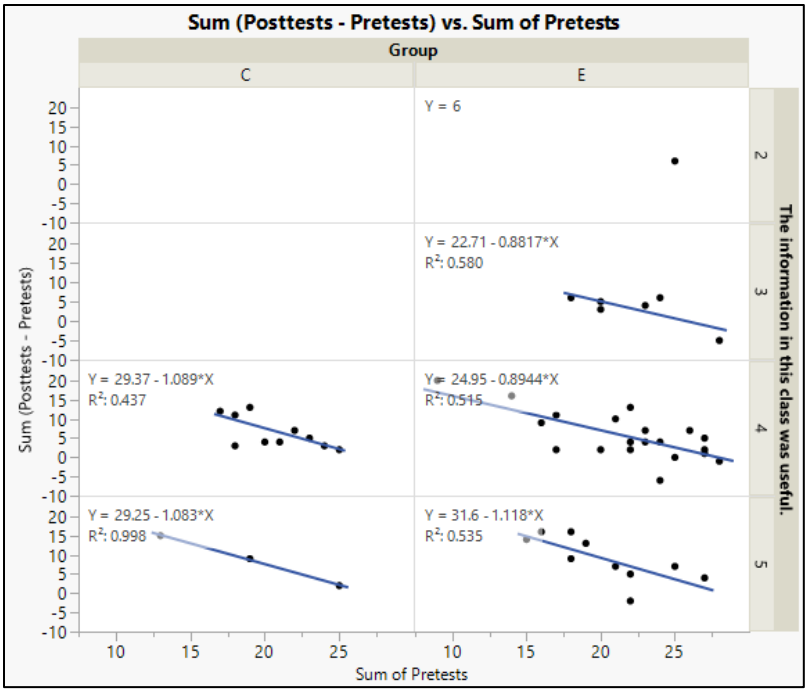

Figure 5-4. *Total change in score vs. pretest score for all tests, separated by survey response and group.*

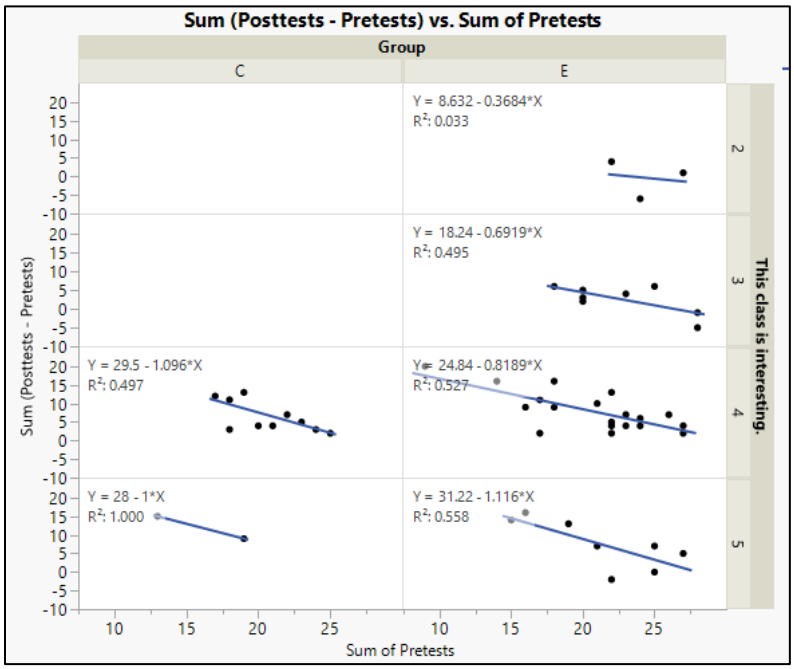

Figure 5-5. *Total change in score vs. pretest score for all tests, separated by survey response and group.*

Table 5-5, Table 5-6, and Table 5-7 present the statistical analysis for differences within groups from pretest to posttest. All groups showed a statistical increase of scores from pretest to posttest except for the control group in the third pretest-posttest measure. Overall, performance on the third posttest showed the least growth from pretest in both groups. It is clear when looking at other data sources that students struggled more on the concepts that were presented in this third lesson that in the previous two across both groups.

Table 5-5. *Pretest to posttest comparison within groups, test one.*

Group	*n*	*Pretest (M, SD)*	*Posttest (M, SD)*	*t*	*p*
Control	14	5.36, 2.17	9.07, 1.0	-5.82	0.0001
Exp.	38	6.21, 2.46	9.34, 1.92	-6.18	0.0001

Table 5-6. *Pretest to posttest comparison within groups, test two.*

Group	*n*	*Pretest (M, SD)*	*Posttest (M, SD)*	*t*	*p*
Control	14	8.79, 2.36	11.57, 1.74	-3.07	0.0021
Exp.	38	8.66, 2.39	10.24, 3.04	-3.53	0.0004

Table 5-7. *Pretest to posttest comparison within groups, test three.*

Group	*n*	*Pretest (M, SD)*	*Posttest (M, SD)*	*t*	*p*
Control	14	6.07 (2.37)	6.93 (1.82)	-1.07	0.9
Exp.	38	6.63 (1.96)	7.97 (1.53)	-3.32	0.001

5.5.2 In-Class Observations

Formal observations made by RISE were completed using the Teaching Dimensions Observation Protocol (TDOP). Four TDOP evaluations were completed in each the control and experimental classes, one observation pertaining to each time an iStructAR activity was completed in the experimental class. TDOP was designed to provide descriptions of teaching, rather than a judgement of the quality of teaching (citation). Observations focused specifically on students' potential cognitive engagement in the classroom. Every two minutes

of the class period, observers recorded a code relating to student cognitive engagement. Three codes were utilized to categorize cognitive engagement. They are as follows:

1. CNL: Making connections to own lives/specific cases: Students are given specific information that relates an abstract concept to something meaningful, or real, in students' lives. An example of this would be discussion of an on-campus structure in reference to the in-class discussion of beams.
2. PS: Problem solving: Students are asked to actively solve a problem, either through a written or verbal request. An example of this would be the professor asking students to solve the forces at a particular joint on their own, before showing the solution.
3. CR: Creating: Students are given tasks where there is not one specific solution, but rather, the outcome is open-ended. An example of this would be asking students what wind load is affected by, as there are numerous answers that could be given.

Figure 5-6 through Figure 5-9below shows a measure of the cognitive engagement experienced by students in both the control and experimental sections over the four formal observation periods. Each time the observer noted a cognitive behavior during a two minute time period was noted as "one" observed behavior in the figures. For example, in Figure 5-6, the observer notated that the control group displayed cognitive behavior relating to making connections to one's own lives four times within one fifty minute class period.

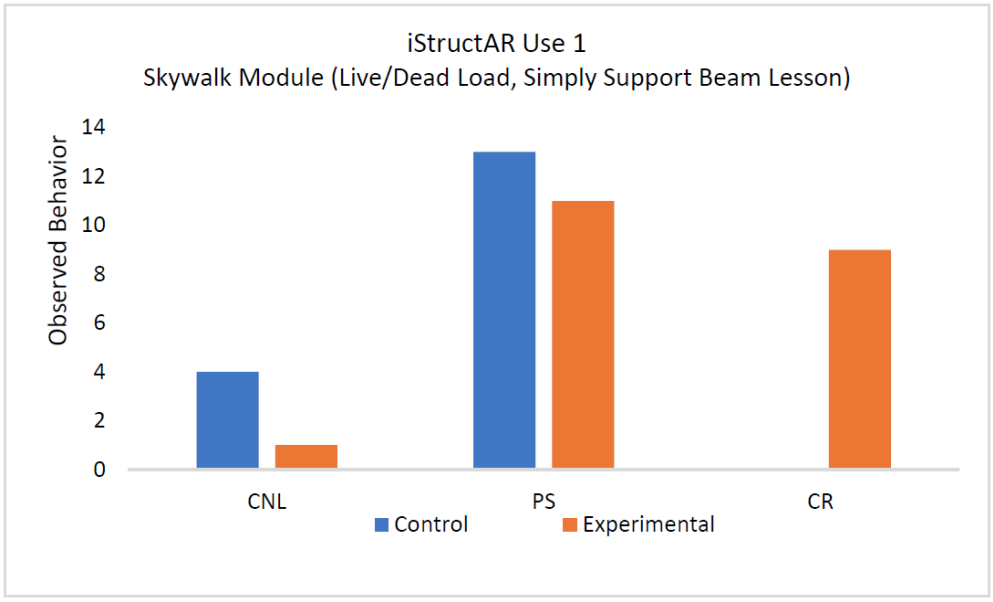

Figure 5-6. *Cognitive engagement, iStructAR use one: Skywalk module (live/dead load, simply supported beam lesson).*

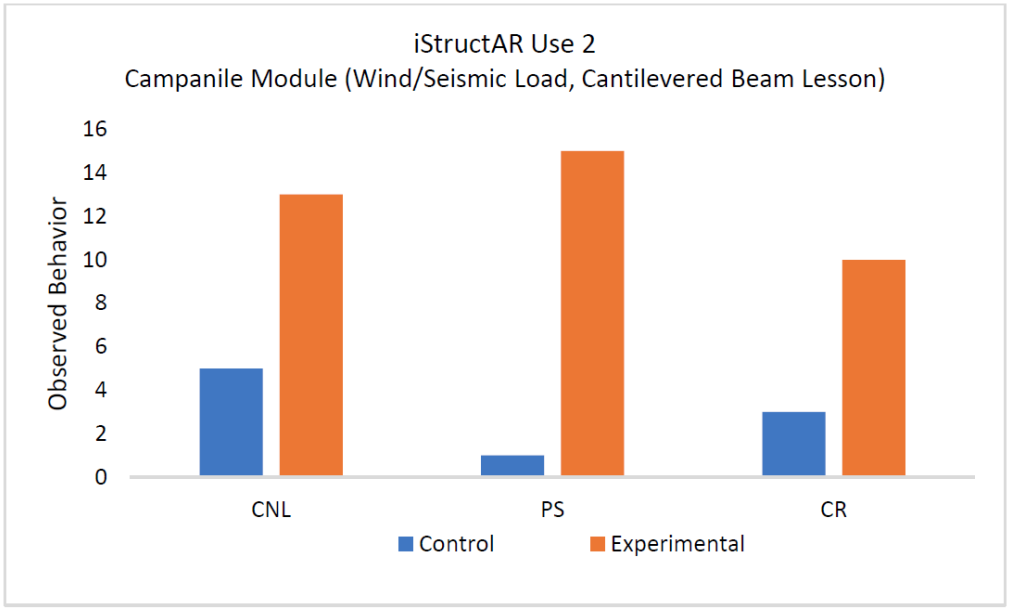

Figure 5-7. *Cognitive engagement, iStructAR use two: Campanile module (wind/seismic load, cantilevered beam lesson).*

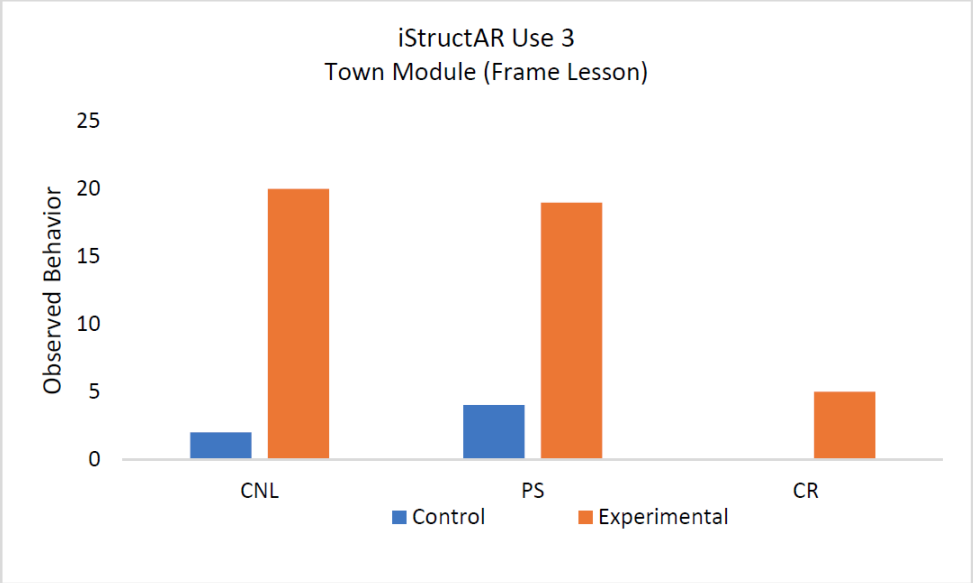

Figure 5-8. *Cognitive engagement, iStructAR use three: Town module (frame lesson).*

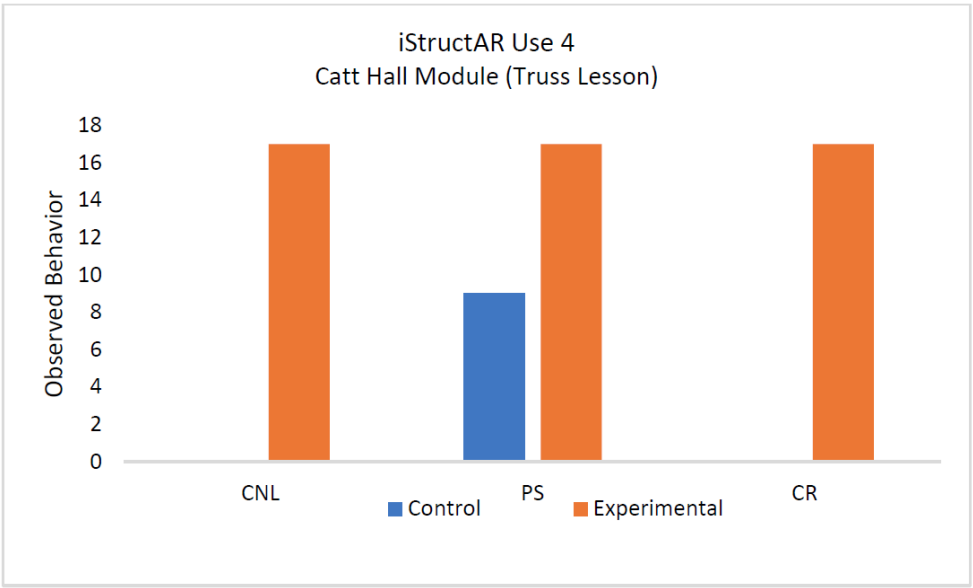

Figure 5-9. *Cognitive engagement, iStructAR use four: Catt Hall module (truss lesson)*

As seen, in observation periods two, three, and four, the students in the experimental class were more cognitively engaged. While students in the control class were more engaged in CNL and PS categories for class period one, experimental students were more creatively

cognitively engaged during this period. Overall, when looking at the four class periods as a whole, one can say that the students in the class period were more cognitively engaged.

In general, during iStructAR activities, students in the experimental class worked with peers to solve the in-class problems given. While the majority of students stayed on topic, it should be noted that at times, students became distracted by the iPads and peers, and went off topic. This was exacerbated by the large number of students in this class period.

Throughout the entire first half of the semester, the class size of the experimental group had an effect on the engagement and participation of students. Overall, those students in the morning class were more attentive and participatory, even though there were less than one half of the students. The distractions provided by a tight learning environment might have hindered the learning ability of students. While this could not be quantitatively captured, it was observed qualitatively several times, and should be kept in mind while observed data trends from other measures.

5.5.3 Transfer Problem Set Results

Transfer problem sets were designed to test the transfer of student's knowledge from the classroom to real world structures. The application was developed with the intention of increasing student's understanding of structural analysis by demonstrating intangible concepts on real structures. If the implementation of the application was successful in student understanding, theoretically, students in the experimental group should perform better on the transfer problem set results.

Table 5-8 through Table 5-10 present the results from the three transfer problem sets. The second and third row of each table presents what percentage of students in each class got the last question correct. If students got the last question correct, this means that they successfully completed the transfer problem set. If students did not get the last question

correct, this means that they either completed all questions or did not finish the problem set. The last row of the tables presents the average number of questions that students completed, divided into those students that answered the last question correct versus those that did not. For example, in looking at Table 5-8, one can see that in the 73% of students in the experimental group that got the last question correct, the average number of questions that students had to solve before completing the last question correctly was 2.41.

One can see that for problem sets one and two, students in the experimental group performed better on average that those students in the control group. First, there was a larger percentage of students in the experimental group that completed the last question correctly. Additionally, those students that did complete the last question correctly did it in fewer questions in the experimental group as compared to the control group. This indicates that use of iStructAR may have aided students in the experimental group in the transfer of structural analysis concepts to real structures.

Results from transfer problem set three are not as conclusive; one can see that on average, students in both classes struggled more with the concepts presented. Results from this data set are comparable in that almost the same percentage of students in each class completed the last question correctly. It should be noted that students also performed worse in pretest-posttest set three as compared to one and two. Pretest-posttest three covered the same subject matter as transfer problem set three. It is notable that students, regardless of class, struggled more with the concept of trusses than with those topics presented in tests one and two.

Table 5-8. *Transfer problem set one results.*

	Experimental		Control	
Last Question Correct?	Yes	No	Yes	No
% of Students	73%	27%	46%	54%
Avg. Questions Answered	2.41	13.79	2.86	12.43

Table 5-9. *Transfer problem set two results.*

	Experimental		Control	
Last Question Correct?	Yes	No	Yes	No
% of Students	85%	15%	72%	28%
Avg. Questions Answered	2.11	13.00	2.69	13.00

Table 5-10. *Transfer problem set three results.*

	Experimental		Control	
Last Question Correct?	Yes	No	Yes	No
% of Students	36%	64%	38%	62%
Avg. Questions Answered	2.38	9.71	1.60	14.00

5.5.4 Survey Results

Surveys given to the experimental group consisted of five sections. Section one asked questions relating to a specific AR activity that students completed in class. For example, section one asked students to rate how well iStructAR helped them to visualize how a frame deflected under certain loads. This question was specific to use of the Catt Hall module, which helped students visualize frames. Section two asked students about their opinions relating to the helpfulness of the AR app, and section three asked students about their opinions relating to AR in general. Section four asked students to rate their level of agreement with items relating to their level of engagement. Finally, the last section asked students to rate their level of agreement with items relating to their perception of structural engineering. Surveys given to the control group consisted of only the last two sections. Surveys were given to both groups three times. Therefore, students in the experimental group

answered sections two, three, four, and five three times, and students in the experimental group answered sections four and five three times. Questions in these sections remained the same, in order to see the change in attitudes of students throughout the first half of the semester.

Table 5-11 and Figure 5-10 present the results of section one for the experimental group in regards to the Skywalk and Campanile AR activities focusing on beams and loads. A higher average represents more students responding that the activity was helpful. The average is out of five, with five corresponding to “very helpful”. Students overall responded that the activity helped them in visualizing the deflection and reaction forces of a beams. Students did not think that the application helped in knowing how to calculate loads. This is expected, as the AR application was not intended and designed for this purpose.

Table 5-11. *Section one survey results for experimental group, beam and load AR activity.*

1. Please rate how helpful the Beam and Load (Skywalk and Campanile) AR activity was for you to:	**Avg.**	**Avg %**	**SD**
1. Visualize the structural components of a building	4.35	86.25	0.98
2. Understand the difference in dead, live, wind, seismic loads	4.22	84.38	0.99
3. Understand how to calculate loads	3.69	73.75	1.13
4. Analyze a simply supported beam	4.31	86.25	0.92
5. Analyze a cantilever beam	4.22	84.38	0.96
5. Visualize how a beam deflects under certain loads	4.41	88.13	1.00
6. Visualize the reactions of a beam caused by certain loads	4.41	88.13	1.00
7. Draw the deflection shape of a beam	4.00	80.00	1.15
8. Understand equilibrium in beams	4.00	80.00	1.00
5=Very helpful, 1=Somewhat helpful, 3=Neutral, 2=Somewhat unhelpful, 1=Very unhelpful			

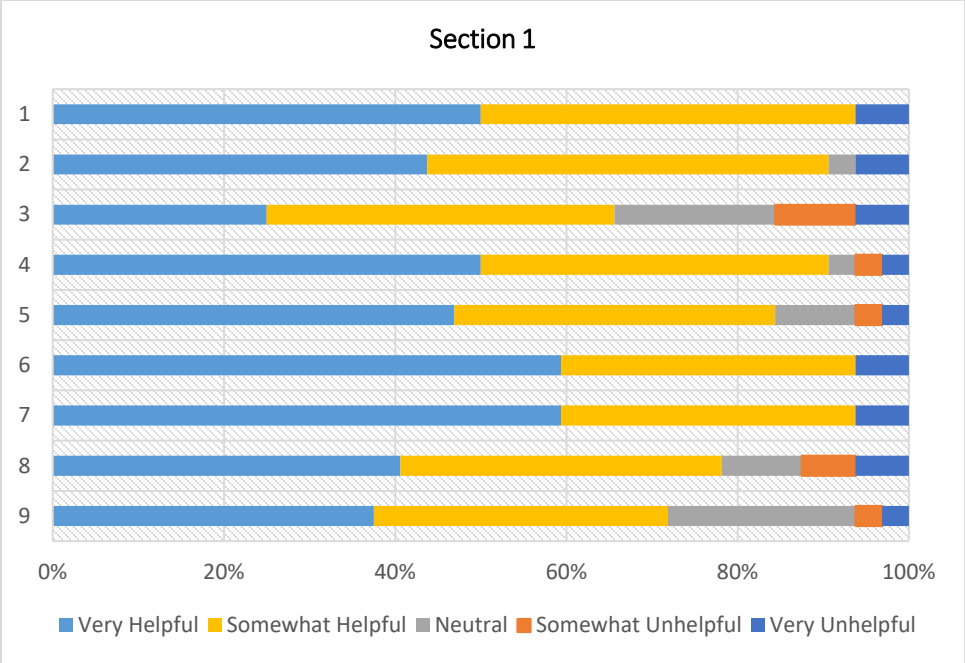

Figure 5-10. *Section one survey results for experimental group, beam and load AR activity.*

Table 5-12 presents the results of section one for the experimental group in regards to the Town AR activity focusing on trusses. A higher average represents more students responding that the activity was helpful, similar to the previous table. Students overall responded that the activity helped them in visualization of certain aspects related to frames. However, students responded again that the activity did not help students in understanding how to calculate loads. Figure 5-11 presents a visualization of the table. As seen, the majority of students responded positively, saying that the activity was somewhat to very helpful for all of the questions. Additionally, most students responded that the AR activity helped them to visualize the forces acting on joints in a frame, an important concept often found confusing by students in structural analysis.

Table 5-12. *Section one survey results for experimental group, frame AR activity.*

1. Please rate how helpful the Frame (Town) AR activity was for you to:	**Avg.**	**Avg %**	**SD**
1. Visualize the structural components of a building	4.35	87.03	0.94
2. Visualize the forces acting on joints in a frame	4.46	89.19	0.95
3. Understand how to calculate loads	3.62	72.43	1.26
4. Analyze a frame	4.25	85.00	0.98
5. Visualize how a frame deflects under certain loads	4.46	89.19	0.98
6. Visualize the reactions of a frame caused by certain loads	4.46	89.19	0.95
7. Draw the deflection shape of a frame	4.03	80.54	1.05
8. Understand equilibrium in joints, beams, and columns in a frame	4.14	82.70	1.07
5=Very helpful, 1=Somewhat helpful, 3=Neutral, 2=Somewhat unhelpful, 1=Very unhelpful			

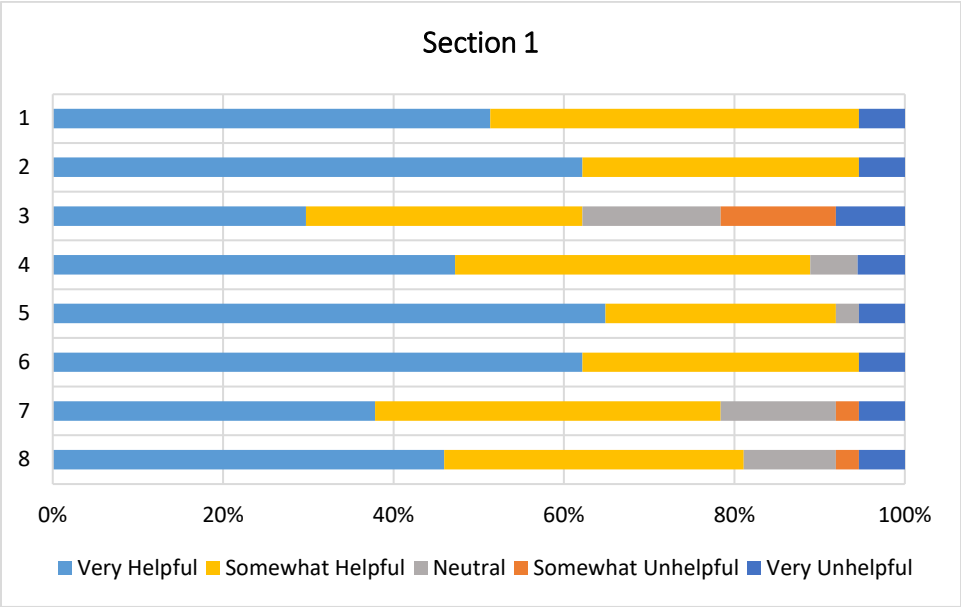

Figure 5-11. *Section one survey results for experimental group, frame AR activity.*

Table 5-13 presents the results for section one from the experimental group after using the Catt Hall module focusing on trusses. The average responses for the truss module survey were lower than the other two surveys. This coincides with lower scores on the pretest-posttest measures and the transfer problem sets for the same concept. Again, students responded with lower scores to question three of section one, saying that the truss module

was of average help in understanding how to calculate loads. Figure 5-12 presents a visualization of the results presented in Table 5-13.

Table 5-13. *Section one survey results for experimental group, truss AR activity.*

1. Please rate how helpful the Truss (Catt Hall) AR activity was for you to:	**Avg.**	**Avg %**	**SD**
1. Visualize the structural components of a building	4.15	83.00	0.91
2. Understand how to calculate loads	3.73	74.50	1.12
3. Analyze members of a truss	4.08	81.50	0.93
4. Analyze joints of a truss	4.05	81.00	1.07
5. Visualize compression and tension forces in a truss	4.23	84.50	0.91
6. Visualize the external reactions of a truss structure	4.30	86.00	0.95
7. Understand equilibrium in sections and joints	4.13	82.50	0.84
1=Very helpful, 2=Somewhat helpful, 3=Neutral, 4=Somewhat unhelpful, 5=Very unhelpful			

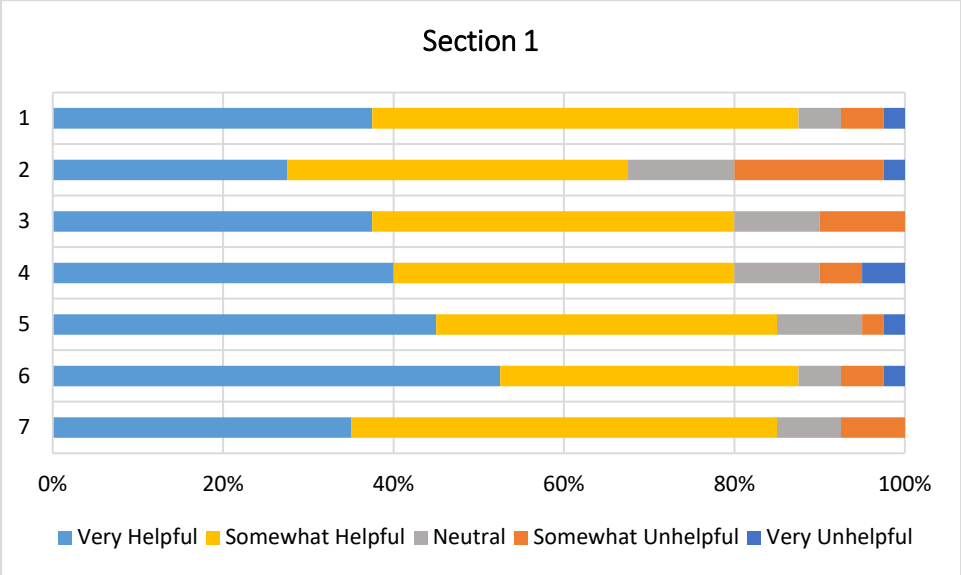

Figure 5-12. *Section one survey results for experimental group, truss AR activity.*

Table 5-14 presents the results from section two of the survey for the experimental group from surveys one, two, and three. Question eight in survey two was provided to see how well students were paying attention when completing the survey. Theoretically, students should have provided somewhat opposite of responses to seven and eight. No surveys

included in the final student population were considered as bad data due to opposing answers from these questions. Overall, students enjoying using the AR application, and would recommend using it to their peers. More importantly, students responded strongly to questions three and four. These questions focused on students seeing the real time response of the structures when loads were manipulated. Both of these questions, as well as question one, were most directly tied to the intent of the application, beyond the augmented reality portion. Question one focused on if students thought that the application helped in connecting a 2D stick model to real buildings.

Table 5-14. *Section two survey results compiled for experimental group.*

	Survey 1		**Survey 2**		**Survey 3**	
2. Please rate your level of agreement for each of the statements related to using the AR app.	**Avg.**	**SD**	**Avg.**	**SD**	**Avg.**	**SD**
1. Seeing the hidden structure of a building on campus through the AR app helped me visualize the connection between a model and the real building	4.31	0.73	4.11	0.65	4.28	0.67
2. Using the AR app allowed me to solve structural analysis problems on my own	4.06	0.83	3.62	1.00	3.70	1.03
3. Manipulating the magnitude of the load in the app helped me understand how the load influenced the structural behavior (i.e. deflection shape, reaction forces)	4.38	0.7	4.38	0.54	4.25	0.80
4. Being able to manipulate the location of the load in the app helped me understand the effect that the load location has on structural behavior (i.e. deflection shape, reaction forces)	4.41	0.55	4.35	0.62	4.18	0.80
5. It was fun to use the AR app to see the hidden structures of a building on campus	4.41	0.65	4.32	0.81	4.23	0.85
6. The AR system allows learning by playing	4.28	0.72	4.24	0.91	4.08	0.88
7. I enjoyed using the AR app	4.28	0.80	4.14	0.85	4.08	0.88
8. Learning through the AR app was boring	2.58	1.43	2.75	1.38	2.65	1.28
9. Using the AR app would facilitate better understanding of complex engineering concepts.	4.19	0.68	4.08	0.75	4.00	0.87
10. I would like to use the AR app in the future if I had the opportunity.	4.19	0.92	4.14	0.99	4.03	0.91
11. I would like to recommend this AR app to my fellow students.	4.16	0.87	4.14	0.83	3.98	0.99
1=Strongly disagree, 2=Disagree, 3=Neither, 4=Agree, 5=Strongly agree						

Table 5-15 describes the responses of the experimental class to section three of the survey, which focused on student opinion of augmented reality. Unfortunately, due to weather conditions, augmented reality was only able to be used in an indoor setting. Instead of students going to the real structure on campus, the application was utilized in conjunction with large printed photos of the structure. However, despite this fact, students still responded positively towards utilizing augmented reality. The majority of students found augmented reality to be positive in learning structural analysis, and would be interested in using augmented reality in other engineering subjects. This points to the promise of not only using augmented reality in engineering undergraduate classrooms, but integrating additional technology to the undergraduate curriculum in order to enhance the student learning experience.

Table 5-15. *Section three survey responses compiled for experimental group.*

	Survey 1		**Survey 2**		**Survey 3**	
3. Please rate your opinions about using AR in general.	**Avg.**	**SD**	**Avg.**	**SD**	**Avg.**	**SD**
1. The use of AR makes learning more interesting	4.34	0.59	4.27	0.72	4.10	0.77
2. I believe the use of AR improves learning in a classroom environment.	4.28	0.80	4.03	0.85	4.10	0.86
3. I believe using an AR app to learn structural analysis concepts is a good idea.	4.31	0.73	4.22	0.70	4.18	0.70
4. I would like to use an AR app to learn other related topics in Structural Analysis.	4.28	0.67	4.22	0.87	4.10	0.89
5. I would like to use an AR app to learn other engineering subjects.	4.16	0.79	4.30	0.77	4.18	0.80
1=Strongly disagree, 2=Disagree, 3=Neither, 4=Agree, 5=Strongly agree						

Table 5-16 and Table 5-17 present the results of sections three and four of the survey for both the experimental and control groups. In both tables, the mean values from questions are shown, where the higher the mean indicates students agreeing with the statement more strongly. In looking at Table 5-16, over the semester, there was not a clear pattern in the

results from the surveys when comparing the experimental and control groups. While on survey two the experimental group responded more strongly to some questions, on survey three the opposite was true. However, in both questions five and six, students in the experimental group responded that they felt more connected to both their peers and the professor in the experimental group, as compared to the control group. This could be due to the increased teamwork and interaction among students when using iStructAR in the experimental classroom. Overall, students did respond that they were more engaged in one class than another, referring to responses on questions eleven and twelve. In looking at Table 5-17, one can see that similar to Table 5-16, student perceptions related to questions fluctuated over the semester. Interestingly, students in the experimental group found structural engineering less interesting than those students in the control group, as shown by question one. This being said, the same students were more excited in the experimental group to take another structural engineering course than those students in the control group. However, these differences are relatively minor. It is worth noting that students in the experimental class did feel more confident in their structural engineering skills than those in the control group, as indicated by responses to questions two and five. While the use of iStructAR may not have changed student's prospective interests, it may have led to an increased understanding of and confidence in topics in students in the experimental group.

Table 5-16. *Section four survey results compiled for experimental and control groups.*

	Survey 1		Survey 2		Survey 3		Average	
4. Please rate your level of agreement with the following items related to your level of engagement in this class.	**E**	**C**	**E**	**C**	**E**	**C**	**E**	**C**
1. I looked forward to going to this class.	4.03	3.92	4.00	3.92	3.78	4.17	3.94	4.00
2. This class was interesting.	4.16	4.25	4.22	4.17	3.88	4.08	4.08	4.17
3. I felt engaged during this class.	4.03	4.00	4.16	3.92	3.88	4.00	4.02	3.97
4. The tasks required of me in this class were valuable to me.	4.06	4.08	4.30	4.08	3.80	4.00	4.05	4.06
5. I felt connected to other students in this class.	4.00	3.50	4.03	3.42	3.98	3.75	4.00	3.56
6. I felt connected to my instructor in this class.	4.03	3.92	3.97	3.92	3.85	3.75	3.95	3.86
7. The information in this class was useful.	4.16	4.33	4.30	4.33	4.08	4.17	4.18	4.28
8. We discussed real-world problems in class.	4.38	4.42	4.24	4.17	3.93	4.08	4.18	4.22
9. We solved open-ended problems in this class.	3.84	4.00	3.97	3.92	3.70	4.00	3.84	3.97
10. I frequently took notes during this class.	3.88	4.00	4.22	4.25	4.00	4.50	4.03	4.25
11. I asked questions during this class.	3.28	3.17	3.24	3.25	3.15	3.33	3.22	3.25
12. I responded to questions in this class	3.50	3.67	3.59	3.50	3.25	3.50	3.45	3.56
1=Strongly disagree, 2=Disagree, 3=Neither, 4=Agree, 5=Strongly agree								

Table 5-17. *Section five survey results compiled for experimental and control groups.*

	Survey 1		Survey 2		Survey 3		Average	
5. Please rate your level of agreement with the following items related to your perceptions of structural engineering.	**E**	**C**	**E**	**C**	**E**	**C**	**E**	**C**
1. Structural engineering is interesting.	4.13	4.33	3.95	4.33	3.82	4.08	4.13	4.25
2. I am confident in my skills related to structural engineering.	4.03	3.50	3.97	3.50	3.69	3.50	4.03	3.50
3. I am excited about becoming an engineer.	4.41	4.33	4.43	4.33	4.15	4.33	4.41	4.33
4. I would be excited to take another structural engineering course.	3.94	3.75	3.81	3.75	3.64	3.42	3.94	3.64
5. I felt intimidated by what was required of me in this course.	3.25	3.08	2.76	3.25	3.23	3.42	3.25	3.25
6. I would be interested in pursuing a career related to structural engineering.	3.69	3.83	3.46	3.92	3.41	3.67	3.69	3.81
1=Strongly disagree, 2=Disagree, 3=Neither, 4=Agree, 5=Strongly agree								

5.6 Conclusion and Future Work

Overall, there was no statistically significant evidence that use of the augmented reality application increased student's test scores, linked to their learning of concepts. However, there were no indications that students were no negatively affected by the use of iStructAR. Rather, there were several indications that students may have found the use of the application helpful in visualizing structural responses to different loading conditions. On average, students were more cognitively engaged in activities when using iStructAR than those students who were taught in a traditional manner. Additionally, students responded positively on surveys given throughout the semester. While data from surveys does not dictate the learning potential associated with a technology, it may help researchers understand what students are excited about, and where they place value in their education.

Amidst the positive potential exhibited by iStructAR throughout the study, there were some drawbacks that presented themselves that should be considered when using the application, or a similar application in the classroom. Similar to findings from Dede and Barab (2009) and Shirazi and Behzadan (2014), the technology provided challenges both in a technical and managerial sense. If using the application, instructors should be prepared to rectify technology issues that may arise, and well as prepare the materials associated with the application's activities. Additionally, the use of iPads was found to cause distraction in the experimental class that may have taken away from some student's learning experience. Instructors may be relied upon more heavily to control a learning environment when this sort of technology is present.

The goal of this study was to implement and asses an augmented reality application in an undergraduate education setting focusing on structural analysis. Findings from the research suggest that although iStructAR may not yet have a statistically significant impact

on the learning of students, it does positively enhance the student learning experience. Specifically, students found that iStructAR helped them to contextualize typical two dimensional stick models taught in structural analysis in a real-world, three dimensional context.

Despite a thorough study, limited numbers of students enrolled in structural analysis did limit the findings of the study. With a larger number of students in the study, there is greater chance that stronger correlations could have presented themselves. Future work will include extending the scope of the study to other universities, in hopes of not only expanding the student population, but comparing study results from student populations with different educational backgrounds.

5.7 References

Adanez, G.P., Velasco, A.D. (2002). Predicting academic success of engineering students in technical drawing from visualization test scores. Journal of Geometry and Graphics, 6 (1) 99-109.

Azuma, Ronald. A Survey of Augmented Reality. Hughes Research Laboratories. Malibu, California. Presence: Teleoperators and Virtual Environments, 6(4), 35-385.

Coladarci, T et al. (2004). Fundamentals of statistical reasoning in education. John Wiley & Sons, Inc.

Connolly, P. et al. (2010). Spatial Ability Testing with Augmented Reality. Purdue University. American Society for Engineering Education.

Dede, C., and Barad, S. (2009). “Emerging technologies for leaning science: A time of rapid advances.” J. Sci. Edu. Technol., 18(4), 301-304.

Dominguez, M. et al. Methogologies and tools to improve spatial ability. Procedia-Social and Behavioral Sciences, 51, 736-744.

Gutiérrez et al. (2010). Design and validation of an augmented book for spatial abilities development in engineering students. Computers and Graphics. 34 (201) 77-91.

Miller C. (1996). A Historical review of applied and theoretical spatial visualization publications in engineering graphics. Engineering Design Graphics Journal 60, (3) 12-33.

Reyes et al. (2016). A mobile augmented reality system to support machinery operations in scholar environments. Computer Applications in Engineering Education, 24(6), 967-981.

Shanbari, H. et al. Using Augmented Reality Video in Enhancing Roof Components Comprehension for Construction Management Students. Engineering, construction, and architectural management, 23(6), 765-781.

Sorby S.A. (1999). Developing 3-D spatial visualization skills. The Engineering Design Graphics Journal, 63 (2), 21-32.

Yuen, S, Yaoyuneyong, G, and Johnson, E. (2011). Augmented Reality: An Overview and Five Directions for AR in Education. Journal of Educational Technology Development and Exchange. Volume 4, Issue 1. 6-2011. 119-140.

CHAPTER 6. GENERAL CONCLUSIONS

Chapter 2 analyzed a deck over backwall detail that removed the expansion joint from the bridge deck, instead placing it on the approach slab. In testing, two difference longitudinal reinforcing options were utilized. Testing and finite element modeling concluded that cutting the top longitudinal before the bridge deck minimizes the stress that the deck experiences from the negative moment of the approach slab. If not cut, stress cannot be released, and cracks may form on the surface of the bridge deck. If a saw cut is made to cut the top reinforcing, special care must be made towards choosing an approach filler material for the cut, one that is able to withstand significant stretching and deformation. Additional conclusions found that cracking could be mitigated by moving the saw cut to the edge of the backwall, rather than at the center. Additionally, the end of the approach slab, regardless of reinforcing option, will experience rotation. While a joint at this location prevents harmful deicing chemicals from leaking and causing damage to the substructure of a bridge, further research should be completed to minimize uneven transition from the pavement to the approach slab at this new joint.

Chapter 3 presents results of a study focused on observing the behavior of walls with vertical holes, in comparison to solid reinforcing concrete walls, in order to assess the performance of a scaled tuned liquid wall damper system. Experimental testing was completed utilizing six scaled walls to obtain failure mode and load in axial compression, strong-axis bending, and weak-axis bending. As expected, those reinforced concrete walls with openings did have an associated strength reduction due to a reduction in material able to contribute to resisting load. However, fortunately, the strength reduction was not drastic enough that would prevent the design of tuned liquid damper systems. In general, the

strength reduction may be accounted for by adding additional reinforcing in bending cases. In both experimental testing and finite element modeling, there were no stress concentrations found around the holes. However, failure modes did vary from typical solid reinforced concrete walls. Failure modes must be taken into consideration if using reinforced concrete walls with openings for a TLWD system. Additional future research is highly suggested to develop the concept of the tuned liquid damper system further. Future research should include focus on multi-loading scenarios, dynamic loading, and investigation of material to construct the holes.

Chapter 4 focused on usability testing to improve the user interface associated with a developed augmented reality application. Ten students interacted with the application via a verbal protocol, and data was gathered through a think-aloud procedure, as well as through survey. Overall, no problems were encountered during usability testing that disabled students from completing assigned tasks. Students utilized all functions of the application in their intended manner. At the end of testing, decided improvements included the addition of a screenshot button, as well as ruler that showed dimensions of the structure. Student interaction with augmentation in the application was positive, met with increased user interest and enjoyment.

Chapter 5 presents the methodology and results of implementing the application into an undergraduate structural analysis classroom. Within the study, one class was taught utilizing the typical lecture-style pedagogy, while the other was taught utilizing the application. Pretest and posttest results from the two classes were compared for three different subject matters within structural analysis. Data collection also included transfer problem set results, in-class observations, and survey results. Overall, there was no

statistically significant evidence that use of the augmented reality application increased student's test scores, linked to the learning of concepts. However, there were no indications that students were negatively affected by the use of the application. Rather, students reported that they found the application helpful in visualizing structural response. Additionally, on average, students were more cognitively engaged in activities when using iStructAR than those students who were taught in a traditional manner. Overall, students responded that they were excited about the prospect of the application, and recommended using it in future classes. Future work will included revising testing devices, as well as utilizing the application in additional structural analysis classes.